

# QUANTIFYING WATER USE OF MATURE PECAN NUT TREES AND ORCHARDS IN SELECTED IRRIGATION AREAS OF THE NORTHERN CAPE

Report to the  
**Water Research Commission**  
and  
**South African Pecan Nut Producers' Association**

by

**NJ Taylor<sup>1</sup>, NS Shongwe<sup>1</sup>, S Kunene<sup>1</sup>, MU Pandor<sup>1</sup>, RM Godfrey<sup>1</sup>, W Rossouw<sup>1</sup>,  
MS Zwane<sup>1</sup>, A Molamu<sup>1</sup>, A Kritzinger<sup>1</sup>, JG Annandale<sup>1</sup>, R Gilfillan<sup>1</sup>, A Clulow<sup>2</sup>,  
CS Everson<sup>1,2</sup> and E Lötze<sup>3</sup>**

<sup>1</sup>Department of Plant and Soil Sciences, University of Pretoria

<sup>2</sup>Discipline of Agrometeorology, School of Agricultural, Earth and Environmental  
Sciences, University of KwaZulu-Natal

<sup>3</sup>AgriTechnovation

**WRC Report No. 2814/1/24**  
**ISBN 978-0-6392-0614-1**

**April 2024**



**Obtainable from**

Water Research Commission

Bloukrans Building, Lynnwood Bridge Office Park

4 Daventry Street

Lynnwood Manor

PRETORIA

[orders@wrc.org.za](mailto:orders@wrc.org.za) or download from [www.wrc.org.za](http://www.wrc.org.za)

The publication of this report emanates from a project entitled *Quantifying water use of mature Pecan Nut trees and orchards in selected irrigation areas of the Northern Cape* (WRC Project No. K5/2814//4)

**DISCLAIMER**

This report has been reviewed by the Water Research Commission (WRC) and approved for publication. Approval does not signify that the contents necessarily reflect the views and policies of the WRC, nor does mention of trade names or commercial products constitute endorsement or recommendation for use.

## **EXECUTIVE SUMMARY**

### **BACKGROUND**

The Pecan Nut industry in South Africa has expanded rapidly in recent years, which is expected to continue in the foreseeable future. Information and knowledge of the water use of Pecan Nut trees and orchards is essential for sustainable development, in particular because of scarce surface and groundwater resources and increasing competition for irrigation water use. The current reality is that no comprehensive knowledge is available on water use of Pecan Nut trees and orchards in different production regions. This applies specifically to the Northern Cape, where large areas of irrigated Pecan Nut orchards are being established. Knowledge about factors governing Pecan Nut crop water use, irrigation requirements and stress resilience is critical to support strategic decision making. This is particularly important for mature trees. Measurement and modelling of water use of Pecan Nut trees and orchards is therefore required, in order to extrapolate water use to production areas outside the Northern Cape. Of critical importance is the quantification of daily and seasonal water use; and identifying critical or water sensitive growth stages. This knowledge must eventually be applied for farming practices such as scheduling of irrigation water; determining the water leaching fraction in soils with high salinity levels; and selecting the most appropriate irrigation method. It will also facilitate decision on whether or not pecans can be planted in a region and how much area can be planted with available water resources.

As a whole, knowledge of the water use of Pecan Nut trees and orchards is required for comparison with water use of competing irrigated crops. This will enable judicious expansion of the irrigated area planted under Pecan Nut orchards. Furthermore, knowledge of the water use of Pecan Nut trees and orchards is required to justify or substantiate applications for water use licences, in order for irrigated production to be undertaken within official water use authorisations. Knowledge of the water productivity and economic water productivity use is also required to motivate periodic review of water use licences for long-term production of Pecan Nuts.

### **AIMS AND OBJECTIVES**

#### **General aim**

To analyse water use, yield and quality of specified cultivars of Pecan Nut trees with standardised tree spacing, canopy cover and zero cover crop between tree rows.

## **Specific objectives**

1. To measure and model Pecan Nut tree water use according to seasonal growth stages for mature Pecan Nut trees and orchards;
2. To determine the influence of water use on quality of nuts within generally accepted quality standards such as nut size, kernel % and pops;
3. To quantify water use efficiency and water use productivity of mature Pecan Nut trees and orchards.

## **SCOPE OF THE PROJECT**

The project encompassed the quantification of transpiration and evapotranspiration in two pecan orchards in the Northern Cape Province, located just outside of the towns of Jan Kempdorp and Groblershoop. Measurements were made for five seasons in Vaalharts and four seasons in Groblershoop. Transpiration data was collected for two cultivars which are widely planted in the region, viz. 'Wichita' and 'Choctaw'. Weather data were collected in conjunction with water use measurements in order to determine the driving variables for pecan water use. Ecophysiological measurements were also performed to ensure the determination of unstressed water use. These data were then used to evaluate water use models for use in pecan orchards and included crop coefficient and canopy conductance approaches. Finally, the water use data, together with yield, was used to derive water productivity and economic water productivity for two orchards. These values were then compared to other commercial crops grown in each region.

The second aspect of the project was to determine the impact of water stress at different phenological stages on yield and quality of pecans. This study was conducted at Innovation Africa@UP, the experimental farm facilities belonging to the University of Pretoria. Trees were subjected to a water deficit stress at different phenological stages and yield and quality was determined at the end of each season. The trial was run for five seasons. Phenological stages where stress was implemented included flowering and nut set, nut sizing, nut filling and shuck dehiscence and these treatments were compared to a well-watered control.



## METHODOLOGY

The study was conducted in two mature pecan orchards in the Northern Cape which contained both 'Wichita' and 'Choctaw' trees. The selected orchards were located 25 km south west of the town of Jan Kempdorp on the Vaalharts irrigation scheme and 32 km North West of the town of Groblershoop along the banks of the Orange River. Groblershoop is hotter and drier than Vaalharts with lower rainfall, with the objective of quantifying water use in two slightly contrasting regions in the Northern Cape. Over the course of the trial the annual average temperature was 18.3°C for Vaalharts and 19.1°C for Groblershoop. Long term average rainfall for Vaalharts is approximately 350 mm and 100 mm for Groblershoop. Water stress measurements were performed in the pecan orchard at Innovation Africa@UP (previously the University of Pretoria's Experimental Farm) in Pretoria. Additional measurements were made in this orchard for model parameterisation due to the proximity of the orchard to the University of Pretoria. Pretoria is cooler (average annual temperature during measurements of 14.4°C) than the Northern Cape and has higher rainfall (approximately 670 mm).

This study encompassed the measurement of modelling of water use of mature pecan orchards and the impact of water stress at different phenological stages on yield and quality of pecan orchards. Measurements were made for 5 years in Vaalharts (2018-2023), 4 years in Groblershoop (2019-2023) and 6 years in Pretoria (2017-2023). Details of these orchards are provided in Table 1. The orchard in Vaalharts was irrigated with 150 L h<sup>-1</sup> macro sprinklers and the orchard in Groblershoop was irrigated with drip irrigation (2 drip lines with drippers spaced 0.6 m apart, with a delivery rate of 3.5 L h<sup>-1</sup>). Irrigation in both these orchards were scheduled with the assistance of capacitance probes and adjusted for weather conditions. The orchard in Pretoria was also drip irrigated (3 drip lines, spaced 0.6 m apart and a delivery rate of 1.6 L h<sup>-1</sup>). Weather variables were measured on hourly and daily time steps at each trial site and included solar radiation, air temperature, relative humidity, windspeed and rainfall. These variables were used to calculate reference evapotranspiration (ET<sub>o</sub>) according to Allen et al. (1998).

Transpiration measurements were made on 'Choctaw' and 'Wichita' trees using the heat ratio method, whilst orchard evapotranspiration (ET) was determined using the Eddy Covariance technique in both orchards. In Vaalharts ET was quantified for 4 years and in Groblershoop for 3 years. Soil evaporation measurements were made using micro-lysimeters during visits to the sites. Additional data collected included leaf area index (LAI), fractional interception of photosynthetically active radiation (PAR), volumetric soil water content, tree water status, gas exchange, stomatal conductance and yield and nut quality.

**Table1 Details of pecan orchards where transpiration and evapotranspiration measurements were performed (T – Transpiration; ET – Evapotranspiration, ET<sub>o</sub> – reference evapotranspiration)**

Orchard	Vaalharts	Grobbershoop	Pretoria
Cultivars and Rootstock	'Choctaw' and 'Wichita' on 'Ukulinga'		'Wichita' and 'Western Schley' on Ukulinga
GPS co-ordinates	28°4'11.01"S, 24°37'54.79"E	28° 40' 7.54"S, 21°48' 29.14"E	
Start	9 September 2018	24 August 2019	1 September 2017
End	11 June 2023	14 June 2023	30 June 2023
Duration (days)	1 737	1 391	2 129
Age (years) <sup>a</sup>	12 (planted 2006)	17 (planted 2002)	11 years (planted 2006)
Planting pattern (m)	10 x 10 m		
Planting density (trees ha <sup>-1</sup> )	100 trees ha <sup>-1</sup>		
Orchard area (ha)	10.37	1.71	3.3
Canopy cover <sup>a</sup>	0.5 ('Choctaw' and 'Wichita')	'Choctaw' – 0.3 'Wichita' – 0.65	0.5
Height (m) <sup>a</sup>	10	11	8 m
ET <sub>o</sub> (mm)*	1410	1 570	1470
Rainfall (mm)*	540	280	760
Irrigation (mm)*	830	1 150	168
Transpiration (mm)*	'Choctaw' – 560 'Wichita' – 560	'Choctaw' – 490 'Wichita' – 620	ND
Evapotranspiration (mm)*	1060	1250	ND

<sup>a</sup>at the start of the trial

\*average for the trial

ND – not determined

Using the transpiration and ET data together with yield and quality, crop water productivity was determined as kg m<sup>-3</sup> for each season. Economic water productivity was determined as profit per m<sup>-3</sup> of water evapotranspired by taking into account production costs using Profarmer (<https://info.profarmer.co.za>). Pecans were compared to other annual crops produced in Vaalharts and raisins in Groblershoop. Evapotranspiration and irrigation requirements for the annual crops were determined using SAPWAT4 and grapevines using previously published crop coefficients.

Attempts to model the water use of pecan orchards included the dual crop coefficient FAO-56 approach and approaches which took into consideration canopy conductance. For the canopy conductance estimate of radiation interception by the trees was required and therefore a canopy radiation interception model was parameterised.

Measurements of the water stress trial took place from the 2017/18 season until the 2022/23 season, totally six seasons, at Innovation Africa@UP (University of Pretoria's experimental farm). Measurements were conducted on 11 year old (planted 2006) 'Wichita' trees, which were drip irrigated and spaced 10 m x 10 m. Stress was implemented during flowering and nut set, nut sizing, nut filling and shuck dehiscence. The treatments were arranged in a randomised complete block design with 4 replicates per treatment and 3 trees per replicate. Flower number, nut set, predawn and midday water potentials, transpiration, photosynthesis, stomatal conductance and canopy cover were determined for each treatment. The ability of remote sensing techniques to detect stress in pecan trees were also evaluated. Yield and quality of the different treatments was determined at the end of each season.

## **RESULTS AND DISCUSSION**

Weather conditions over the course of the trial were typical Vaalharts in 2018/19 and 2019/20 but in 2020/21 and 2021/22 rainfall was almost double the annual average, resulting in much cooler conditions than normal. The project was therefore extended for another year and in 2022/23 conditions were more typical of the region. A similar situation was found in Groblershoop where 2019/20 and 2022/23 were normal years but 2021/22 was a high rainfall year, when there only one day when the maximum daily temperature approached 40°C. Groblershoop was hotter and drier than Vaalharts, with an average reference evapotranspiration (ET<sub>o</sub>) of 1570 mm over the course of the study, as compared to Vaalharts with an average of 1410 mm. The high rainfall in the 2020/21 season could have impacted

yield in the Vaalharts orchard due to very wet soils, while in Groblershoop yield was impacted by hail and late frost in 2020/21 and excessive nut drop in 2021/22.

Annual evapotranspiration (ET) reflected the difference in weather conditions over the course of the study at both study sites, as indicated by  $ET_o$ . In Vaalharts, ET varied between 982 and 1270 mm ( $ET_o$  varied between 1310 and 1570 mm), with an average of 1050 mm. Seasonal transpiration (T) varied between 440 and 630 mm for 'Choctaw' trees and 420 to 700 mm for 'Wichita' trees in Vaalharts. These values closely reflected canopy size as a result of pruning activities and growth of the trees. Over the course of the 5 year study the average seasonal T for both cultivars was 560 mm. Maximum transpiration was 3.6 mm day<sup>-1</sup> (360 L day<sup>-1</sup>) for 'Wichita' trees and 4.2 mm day<sup>-1</sup> (420 L day<sup>-1</sup>) for 'Choctaw' trees.

Evapotranspiration in Groblershoop was on average 200 mm higher than in Vaalharts, with an average of 1250 mm over three seasons, varying from 1220 to 1280 mm ( $ET_o$  varied between 1460 and 1670 mm). The higher ET in Groblershoop than Vaalharts, was also reflected in higher T values for 'Wichita', but not for 'Choctaw'. Average seasonal T for 'Wichita' trees was 620 mm and 490 mm for 'Choctaw'. Transpiration varied between 490 and 810 mm for 'Wichita' trees and 400 and 610 mm for 'Choctaw' trees, once again reflecting canopy size changes as a result of pruning and recovery following pruning. 'Choctaw' trees had a lower canopy cover than the other trees for the majority of the trial. Maximum transpiration was 4.8 mm day<sup>-1</sup> (480 L day<sup>-1</sup>) for 'Wichita' trees and 3.6 mm day<sup>-1</sup> (360 L day<sup>-1</sup>) for 'Choctaw' trees.

An analysis of the response of hourly daytime T to difference weather variables demonstrated that T only increased linearly with an increase in air temperature, solar radiation, vapour pressure deficit (VPD) and  $ET_o$  up to a point and then started to plateau. This suggested some sort of physiological control over T, with stomata closing to limit T under high atmospheric evaporative demands. However, analysis of leaf water potential ( $\Psi_{leaf}$ ) over a number of days with contrasting conditions revealed rather different minimum values, suggesting that pecans have more isohydric than anisohydric behaviour. More data over a wider range of conditions, including drought stress, is needed to draw more definite conclusions. However, based on the responses of T to weather conditions suggests that a simple crop coefficient modelling approach, that is a demand limited model, will not provide good estimates of pecan water use and canopy conductance under varying weather conditions needs to be taken into consideration.

The approach of Allen and Pereira (2009) for determining orchard specific transpiration crop coefficients ( $K_t$ ) was tested in the two pecan orchards in the Northern Cape. Canopy size was estimated from drone images and daily estimates of leaf resistance ( $r_{leaf}$ ) were determined as described by Taylor et al. (2015) for citrus. Leaf resistance varied in a similar pattern across

the two orchards for two seasons and when using a relationship between VPD and  $r_{leaf}$  to derive biweekly  $K_t$ , good fortnightly and monthly estimates of  $T$  were obtained when combined with  $ET_o$ . This approach could therefore be used for planning purposes in orchards with VPD and  $ET_o$  from a weather station and estimates of canopy height and canopy cover.

A second approach for estimating  $T$  was tested, which required estimates of canopy radiation interception and two constants derived from measurements of  $T$  using to derive canopy conductance, radiation interception and VPD (Villalobos et al., 2013). The radiation interception model of Oyarzun et al. (2007) was parameterised for pecan using simple estimates of tree and orchard dimensions. The two constants were derived from measurements in the Pretoria orchard and tested in the Northern Cape orchards. These constants provided good daily and monthly estimates of  $T$  for two seasons in each orchard in the Northern Cape. The good performance of both  $T$  models across regions is encouraging and further testing of the models in different orchards should be carried out to provide final validation of the approaches and the ease with which they can be used.

As expected, evaporation rates were dependent on soil water availability in the top soil layer and energy reaching the soil surface, which was impacted by the canopy cover in the orchard. The FAO-56 approach performed reasonably well in both orchards, but a number of parameters were required in order to model  $E_s$  successfully which limits the ability to employ this model readily in orchards to estimate ET using a dual modelling approach.

The profitability of pecans per  $m^3$  of irrigation water applied explains why plantings are expanding so rapidly in the Northern Cape. In Vaalharts, more than half the scheme is now estimated to be planted to pecans. If only crop water productivity ( $WP_c$ ) or irrigation water productivity ( $WP_i$ ) were considered to determine the productive use of water in both regions and the sustainability of pecan production, pecans would likely be deemed to be unsustainable, with values varying between 0.05 and 0.37  $kg\ m^{-3}$  for  $WP_c$  and 0.01 and 0.77  $kg\ m^{-3}$  for  $WP_i$ . The large range being attributed to large variations in yield from year to year. This is important as this is the metric reported in popular literature for consumers. Whilst more water is required to produce a pecan crop than most other crops (except for lucerne) in Vaalharts, it can largely be attributed to a longer growing season than most other annual crops. However, if one considers summer-winter crop rotations, pecan annual water use is similar to these cropping systems. Concerns regarding the high water use of pecans relative to other crops are therefore not valid, and the total planted area on schemes relative to available water should rather be considered if plantings take place outside of existing allocations. If only the profitability of water evapotranspired or applied is considered, then pecans are the best use of water in both schemes when average or above average rainfall is received, with economic water productivity values ranging between no profit to R21.99  $m^{-3}$  based on evapotranspiration

or no profit to R48.05 m<sup>-3</sup>. However, in drought years when water allocations are restricted the flexibility allowed by annual crop production would be advantageous, in order to make the most of the given allocation. The years it takes from planting to the break-even point also need to be considered for pecans when making comparisons with other crops.

A water deficit stress was successfully implemented in the pecan orchard in Pretoria for three of the six seasons. High rainfall during three seasons prevented a consistent water deficit being achieved during each phenological stage. A decline in photosynthesis and stomatal conductance was noted when predawn leaf water potential fell below -0.45 MPa and midday stem water potential fell below -0.9 MPa. The two most sensitive stages to water stress, in terms of yield and quality, were flowering and nut set and nut filling. Stress during flowering and nut set resulted in increased nut drop and as a result yield was reduced due to fewer nuts. When stress was implemented during nut filling yield was reduced as a result of poorly filled nuts. Stress at both these stages had a significant effect on gross income over the course of the trial. Stress during nut sizing only reduced nut size in two of the six seasons, causing a reduction in gross profit as a result of a smaller nut size and lower prices. Stress during shuck dehiscence tended to increase the percentage of sticktights but this effect was not consistent. Overall, gross profit was reduced when stress was implemented during all four phenological stages, suggesting well-watered conditions should be maintained throughout a season. However, if allocations are reduced some savings could be made during nut sizing and shuck dehiscence with minimal impact on yield and quality. Importantly, care should be taken to avoid water logged conditions at the transition from shell hardening (water stage) to nut filling, as in two seasons significant water stage fruit split reduced yield considerably in the 'Wichita' trees.

Research on detecting water stress in pecan trees using remote sensing tools has proved largely inconclusive. This work began in the high rainfall seasons when there was very little contrast between well-watered and water stressed trees to test correlations between ground measurements and vegetation indices. However, the nature of the water stress response in pecans might not lend itself to detection of stress via VIs. Vegetation indices quantify changes in canopy structure (e.g. wilting) or changes in chlorophyll content, which are linked to water stress in some crops. As pecan leaves do not wilt, it does not seem possible to use VIs which detect structural changes, as with other crops. This, however, needs to be confirmed in a season when a greater level of stress is achieved. Parametrising the CWSI for pecans has also not been successful in the trial. Whilst a lot of progress was made, the parameters required for the accurate estimation of the CWSI could not be accurately estimated. This is a notoriously difficult thing to do and now that we have a much more accurate thermal camera, we are hoping that it will be possible in future, as this may be the most reliable way to detect

water stress in pecan canopies. This work will be ongoing in future projects, as the experimental orchard at Innovation Africa @UP is ideally set up to allow for trees to be stressed at various growth stages, allowing the careful quantification of stress versus a well-watered control.

## **NEW KNOWLEDGE AND INNOVATION**

Increased knowledge on water use of pecan orchards in South Africa in the hotter production regions was required by the pecan industry in South Africa prior to the start of the study, as this is where the majority of pecan orchards are found. Whilst measurements were made in a previous WRC project (Report No. 1770/1/14), there was concern for the extrapolation of modelling exercises to these hotter production regions, where pecan trees are in leaf for longer. Measurements of transpiration, evaporation and evapotranspiration in orchards in the Northern Cape has expanded knowledge on pecan orchard water use and allowed the parameterisation of two water use models, which provided good daily and weekly estimates of pecan water use in two locations, which can be used for tactical irrigation decision making, irrigation planning and irrigation system design purposes. Seasonal estimates of water use can be compared to water availability on a scheme level to assess the area that can realistically be planted to pecans with the available water. Water productivity and economic water productivity was determined for a number of seasons at each location in the Northern Cape. Whilst pecans do not compare favourably with annual crops grown in the region in terms of water productivity, due to low average yields, the economic value of the crop per m<sup>3</sup> of water evapotranspired and applied far exceeds these other crops. This information can be used by pecan producers to justify the water used for pecan production.

Quantitative information on the impact of water stress at different phenological stages on yield and quality of pecan orchards was obtained over six seasons. This long term data set provides key insights into the impact of stress on tree physiology and yield and the importance of making the most of available rainfall during a season.

Although, previously published models have been used to estimate pecan water use, the innovation lies in parameterising the models for pecan. Specific attention was given to models that require inputs easily determined by growers, which will increase the likelihood of these models being used to improve irrigation management. The parameterised canopy radiation interception model for pecans, using data that can be collected with a cell phone or basic drone, could also be used in future to assess pruning practices. These pruning practices could

be key to maintaining smaller canopies which could reduce orchard transpiration and therefore total water use.

## **CAPACITY BUILDING**

There were seven students registered on this project (1 PhD, 5 MSc and 1 BSc (Hons)). Four MSc students (Mr S Kunene, Mr M Zwane, Mr M Pandor and Mr W Rossouw) and the one BSc (Hons) student (Ms A Molamu) have graduated. Funding from this project will be used for the remaining two students to graduate.

Results from the study were also shared via a number of different forums, including presentations at local and international conferences, grower study groups, the SAPPA AGM; and four popular publications in the SA Pecan.

## **CONCLUSIONS**

The study has provided comprehensive measurement of ET for two orchards and T for two cultivars in each orchard for a minimum of four years in each orchard. These two orchards were located in slightly different climatic zones in the Northern Cape Province. As expected, both T and ET were determined by a combination of canopy size and the prevailing weather. Annual ET was higher in Groblershoop than in Vaalharts, due largely to hotter and drier conditions. Both these orchards had higher ET than ET from an orchard in Cullinan (close to Pretoria), quantified in a previous project, which justified the requirement for measurements in this region where the majority of pecan orchards are found in South Africa. Changes in T volumes from season to season and region to region reflected canopy size, emphasising the importance of accurate quantification of canopy size for water use models. As a result, a radiation interception model requiring inputs that can be easily measured was parameterised for pecans. For this model either drone images or a cell phone can be used to capture key inputs. Importantly, T did not increase at the same rate with an increase in atmospheric evaporative demand and as it got hotter and drier T tended to plateau as it got hotter and drier, suggesting that stomatal control over T needs to be considered when modelling T of pecans.

Two models estimating transpiration were successfully tested in pecans and parameters specific to pecans were derived for future use. The crop coefficient approach performed very well on a monthly basis and can be used for planning purposes, whilst the canopy



conductance approach may be better suited to tactical irrigation decision, including weekly scheduling of irrigation. Two evaporation models were also tested and both performed reasonably well in three orchards. The combination of T and E estimates from the two models can be used to derive irrigation requirements.

When comparing water productivity ( $WP_c$ ) of pecans with other annual and perennial crops cultivated in each region, pecan performs poorly, due to relatively low yields and high water use. It was also evident that  $WP_c$  varied considerable from year to year, especially in Groblershoop, and this was attributed to the alternate bearing nature of pecans (especially 'Choctaw) and weather conditions in Groblershoop which caused excessive nut drop at times. However, when comparing economic water productivity ( $EWP_c$ ) with other crops grown in each region it is clearly evident why pecan production has expanded so much in this region. Pecan had much higher values than other crops due to the high value of the harvested nut. Additional research should be conducted to determine  $WP_c$  and  $EWP_c$  over the life time of an orchard to make fair comparisons with other crops.

Although stress could not be implemented during each phenological stage throughout the 6 years of the trial, there was sufficient data to suggest that the most sensitive stages for water stress in terms of yield and quality are flowering and nut set and nut filling. Yield was routinely decreased during both these stages, with quality also compromised during nut filling. In some seasons stress during nut sizing impacted nut size and during shuck dehiscence there was an increase in sticktights. When considering the full duration of the trial, there was an impact of stress at every phenological stage on gross income suggesting that irrigation should be well-managed in pecans throughout a season, with stress avoided at each stage. However, in seasons where water allocations are insufficient to meet the full ET demand on the crop, it may be possible to make some savings during nut sizing and shuck dehiscence without a significant impact on yield and quality.

The detection of spatial water stress in pecans needs much more work. This depends heavily on the prevailing weather conditions in order to achieve stress in the orchard, to be able to create bigger contrasts between well-watered and stressed trees. In addition, a more accurate thermal camera may allow for a more accurate determination of canopy temperatures and therefore stress.

## **RECOMMENDATIONS FOR FUTURE RESEARCH**

The project determined orchard water use and highlighted that canopy size was major determinant of seasonal water use volumes and not yield. Water use in “off years” (low yields) will therefore be the same as “on years” (good yields), if canopy size is similar, resulting in a wide variation in water productivity. In order to improve water productivity across seasons it may be feasible to prune trees to maintain a smaller canopy with similar yield. This needs to be tested to determine how much water can be saved and if more consistent yields can be achieved. This will also allow the testing of the water use models parameterised in this study.

With the increased accessibility of remote sensing tools it will be important to test these tools in pecan for the assessment of plant stress across an orchard. Instead of doing laborious water potential measurements to assess stress, remote sensing tools could be used to assess stress across an entire orchard. This could increase yield per hectare, as well as optimising irrigation scheduling. The testing of various methods to detect stress in pecans needs to be continued, as very little success was achieved in the current study. Using remote sensing to determine spatial and season ET of orchards could also aid in improved water use management within and across orchards in a region. These models need to be tested in pecan orchards against ground-based methods. Data from the current study could be used to do this.

Water productivity and economic water productivity calculations should be performed over the life time of an orchard, as is done for water footprinting analyses to take into account water required before they come into production. This will allow fairer comparisons between crops and allow growers to make more informed decisions on the water cost of growing pecans compared to other crops and the impact pecan production has on water resources on a catchment level. This will allow the assessment of what area can sustainably be planted to pecans in an area. Separate benchmarks for different production regions which differ in climate should be considered, as hotter and drier regions will require more water to produce the same yield as cooler and wetter regions. Future research should focus on ways of normalising water productivity for climate, including rainfall. Assessing the effective use of rainfall to supplement crop water requirements and how much rainfall is actually effective for the crop in a season should also receive more attention in future.

## **GENERAL SUMMARY**

The contract objectives have been met and, in some instances, they have been exceeded. Water use was measured in two orchards in different regions, which fell within the hot Northern

Cape region. Despite weather conditions not being typical of the region for two seasons and low yields in Groblershoop, the extension of the project by an additional year, allowed for one more season of measurements under more typical conditions for the region. Measurements of water use yielded valuable information on the impact of canopy size on transpiration and on evaporation rates. Evaporation rates were also impacted by the wetting pattern of the irrigation system. These measurements facilitated the parameterisation of two transpiration and evaporation models. Seasonal water use, together with yield data and production cost data (Profarmer) allowed for the determination of both water productivity and economic water productivity of two orchards in two locations for a number of seasons.

Six seasons of water stress at different phenological stages were successfully completed in the orchard in Pretoria. Of these six seasons, significant stress was implemented for most phenological stages for three seasons, which yielded valuable insight into the impact of water stress on yield and quality of pecan orchards. Data from this study will help growers manage water during times of reduced allocations, to prevent significant declines in yield and quality, whilst also making water savings. A remote sensing aspect was added to the project to try and detect spatial stress and whilst not providing conclusive results, it has laid the foundation for future work.

## ACKNOWLEDGEMENTS

This project was directed, funded and managed by the Water Research Commission in collaboration with the South African Pecan Nut Producers' Association (SAPPA). The research team is also very grateful for the support and co-operation Marnus Groenewaldt (Groen Boerdery) and Alvin Archer. Without farmers allowing us access to their orchards and providing additional support, this study would not have been possible. This was especially true during COVID-19 lockdown when Alvin Archer charged and changed batteries for us and harvested trees individually for us. We are indebted to these growers for the enormous amount of support they provided throughout the course of the study. We would also like to thank Albert Bouwmeester who allowed us to conduct quality analyses at his processing facility and bought the nuts from Innovation Africa@UP, resulting in income for us to maintain the orchard. A special thanks goes to Hardus du Toit and Ivan Schubach from SAPPA for assisting us throughout the trial when we could not get to the site or when we needed an extra pair of hands or some advice. Dup Haarhoff and Eugene le Roux are also thanked for assistance with soil water content and irrigation data from Groen Boerdery and for access to Profarmer. They also provided excellent advice throughout the study.

The project team would like to thank the Reference Group of the WRC Project for the assistance and the constructive discussions during the duration of the project:

Prof. S Mpandeli	Water Research Commission (Chairman)
Dr L Nhamo	Water Research Commission
Dr SN Hlophe-Ginindza	Water Research Commission
Mr A Archer	South African Pecan Nut Producers Association
Mr A Bouwmeester	South African Pecan Nut Producers Association
Mr A Coetzee	South African Pecan Nut Producers Association
Mr H du Toit	South African Pecan Nut Producers Association
Dr S Dzikiti	University of Stellenbosch
Mr D Haarhoff	GWK
Ms M Kapari	Water Research Commission
Mr E le Roux	GWK
Prof. S Midgley	Department of Agriculture Western Cape
Mr J van Rensburg	South African Pecan Nut Producers Association

# TABLE OF CONTENTS

EXECUTIVE SUMMARY .....	III
ACKNOWLEDGEMENTS .....	XVI
LIST OF FIGURES .....	XX
LIST OF TABLES .....	XXXII
LIST OF ABBREVIATIONS .....	XXXV
1. INTRODUCTION .....	1
1.1 Background .....	1
1.2 Aims and objectives.....	2
1.3 Approach and Scope .....	2
2. LITERATURE REVIEW .....	4
2.1 Phenology and morphology of pecans.....	4
2.1.1 Canopy development and leaf morphology .....	4
2.1.2 Root growth and morphology .....	7
2.1.3 Flowering and flower morphology .....	11
2.1.4 Nut growth and morphology .....	13
2.2 Pecan water use.....	16
2.3 Factors affecting water use in pecans .....	19
2.3.1 Environmental factors .....	20
2.3.2 Management practices.....	20
2.3.3 Tree-related factors.....	21
2.4 Methods of estimating canopy size in orchards .....	24
2.4.1 Aerial and ground-based imagery .....	26
2.4.2 Canopy radiation interception .....	27
2.5 Modelling radiation interception in fruit trees.....	28
2.6 Modelling pecan water use .....	33
2.7 Crop Water productivity and economic crop water productivity of pecans...	38
2.7.1 Definition of crop water productivity and economic crop water productivity .....	38
2.7.2 Previous reports of crop water productivity in pecans .....	38
2.8 The impact of water stress on pecan yield and quality .....	41
3. MATERIALS AND METHODS .....	46

3.1	Water use of pecan orchards.....	46
3.1.1	Site descriptions .....	46
3.1.2	Weather variables.....	53
3.1.3	Transpiration measurements .....	55
3.1.4	Soil evaporation measurements.....	58
3.1.5	Evapotranspiration measurements.....	61
3.1.6	Ecophysiological measurements.....	63
3.1.7	Determination of canopy size.....	63
3.1.8	Irrigation and soil water content .....	65
3.1.9	Crop water productivity and economic water productivity .....	67
3.1.10	Water use modelling .....	68
3.1.11	Statistical analysis of data.....	81
3.2	The impact of water stress on yield and quality of PECAN orchards .....	82
3.2.1	Site description .....	82
3.2.2	Treatments .....	82
3.2.3	Quantification of plant stress.....	84
3.2.4	Nut development.....	86
3.2.5	Yield and quality .....	87
3.2.6	Irrigation and soil water content .....	88
3.2.7	Statistical analysis of data.....	89
3.3	Remote Sensing .....	89
3.3.1	Remote Sensing Data Collection .....	90
3.3.2	Remote Sensing Data Processing .....	93
3.3.3	Field Data Collection.....	98
3.3.4	Water Stress Detection by Vegetation Indices .....	99
3.3.5	Crop Water Stress Index.....	99
4.	RESULTS AND DISCUSSION.....	104
4.1	Pecan water use.....	104
4.1.1	Seasonal weather .....	104
4.1.2	Canopy growth and development.....	112
4.1.3	Transpiration and evapotranspiration rates .....	115
4.1.4	Ecophysiology.....	123
4.1.5	Irrigation and soil water content .....	134
4.1.6	Soil Evaporation.....	142
4.1.7	Crop water productivity .....	146
4.2	Modelling pecan water use .....	155

4.2.1	Parameterisation and validation of a crop coefficient model.....	155
4.2.2	Parameterisation and validation of a radiation interception model.....	165
4.2.3	Parameterisation and validation of a canopy conductance model .....	169
4.3	Conclusions .....	174
4.4	impact of water stress at different phenological stages on yield and quality of pecans.....	176
4.4.1	Weather variables.....	176
4.4.2	Irrigation management.....	179
4.4.3	Canopy development and senescence .....	182
4.4.4	Midday and predawn stem water potential .....	183
4.4.5	Photosynthesis and stomatal conductance .....	189
4.4.6	Flowering and nut set.....	194
4.4.7	Nut growth .....	195
4.4.8	Nut drop.....	197
4.4.9	Yield .....	200
4.4.10	Quality .....	201
4.4.11	Total income as a result of imposing water at key phenological stages...	207
4.4.12	Conclusions .....	208
4.5	Remote Sensing .....	210
4.5.1	Water Stress Detection by Vegetation Indices .....	210
4.5.2	Water Stress Detection by Thermal Remote Sensing .....	214
4.5.3	The Non-Water-Stressed-Baseline .....	215
4.5.4	The Crop Water Stress Index.....	219
4.5.5	Conclusions .....	222
5.	GENERAL DISCUSSION AND CONCLUSIONS.....	224
6.	RECOMMENDATIONS .....	227
	REFERENCES.....	229
	APPENDIX A – CAPACITY BUILDING .....	246
	Degree purposes .....	246
	Non-degree purposes .....	254
	Organisation .....	254
	Community .....	254
	APPENDIX B – KNOWLEDGE DISSEMINATION AND TECHNOLOGY TRANSFER .....	255
	APPENDIX C – DATA STORAGE .....	257

## LIST OF FIGURES

Figure 2.1 A six year old pecan tree with a tree height of 4 m, lateral feeder root growth of 7 m and a root depth of 2 m. In the circle is a representation of the 11 largest lateral roots (Woodroof and Woodroof, 1934).	7
Figure 2.2 Pecan root development in orchards in Hartswater, which have been A) flood irrigated and 2) sprinkler irrigated. Root development in (A) was restricted by a sudden change in texture down the profile. Proliferation of feeder roots in the top 40 cm is evident in these orchards.	9
Figure 2.3 Growth of ten pecan taproots over a 24 hour period when subjected to various temperatures (Woodroof and Woodroof, 1934).	10
Figure 2.4 A) Staminate (catkins) and B) pistillate pecan flowers	11
Figure 2.5 Relative fruit growth rate and average fruit development stages for 'Ideal' and 'Western' pecans in the Mesilla Valley, New Mexico (Herrera, 1990). Dates are for the Northern Hemisphere. Approximate dates (from left to right) for the Southern Hemisphere are November, February and April.	14
Figure 2.6 Developmental stages of pecan nuts (Wells and Conner, 2007)	15
Figure 2.7 Anatomy of a mature pecan nut	16
Figure 2.8 Conceptual model for the behaviour of isohydric versus anisohydric plants by regulating (A) $\Psi_{leaf}$ , (B) productivity, and (C) survival in response to increasing relative changes in the stress level (i.e. decreasing soil water content) (Attia et al., 2015)	22
Figure 2.9 Attenuation of irradiance through a canopy according to Beer's Law (Teh, 2006).	28
Figure 2.10 A schematic diagram showing a rectangular orchard hedgerow that varies in two-dimension (X and Z) (Cohen et al., 1987).	30
Figure 2.11 Schematic representation of fruit tree orchard architecture and dimensions required for the model developed by Oyarzun et al. (2007).	32
Figure 2.12 Relationship between relative crop coefficient ( $K_c/K_{c\ max}$ ) and effective canopy cover (ECC) (Wang et al., 2007c) and B) relative crop coefficient ( $K_c/K_{c\ ref}$ ) and fractional cover ( $f_c$ ) (Samani et al., 2011) for pecan orchards near Las Cruces, New Mexico.	35
Figure 2.13 Daily crop coefficients as a function of thermal time for a 'Western Schley' orchard near Las Cruces, New Mexico (Sammis et al., 2004b).	36
Figure 2.14 Evaluation of the growing degree day GDD- $K_c$ relationship of Sammis et al. (2004b) in different production regions of South Africa, using long term weather data to calculate GDD for the growing season in each location.	37



Figure 2.15 The six stage crop coefficient curve suggested in the study by Ibraimo et al. (2016) illustrating how the curve could be adjusted with visual observations of canopy or nut development for different production regions. ....	37
Figure 2.16 A) Monthly values of plant water use efficiency (WUE) of pecan trees (Biomass/ET) and B) the impact of VPD on monthly measured and predicted water use efficiency (WUE) for pecan trees near Las Cruces in New Mexico (Wang et al., 2007a). ....	40
Figure 2.17 Effect of adequate water during the nut sizing stage. Pecans on the left (A) are from irrigated trees, while those on the right (B) are from non-irrigated trees (Wells, 2016).....	43
Figure 2.18 Relationship of percentage kernel to rainfall during the first 15 days in September (Northern Hemisphere conditions) (Sparks, 1992) .....	44
Figure 3.1 A) The orchard at Groen Boerdery in the 2018/2019 and in B) 2022/2023 seasons. The two sites where sap flow measurements are made are indicated.....	47
Figure 3.2 A) Aerial view of the orchard in May 2021 and B) status of the ground cover between rows in summer of 2023.....	48
Figure 3.3 Google Earth image of the A) Vaalharts and B) Groblershoop orchards showing the position of the orchards relative to the automatic weather stations (AWS). The area surrounding the orchards is also illustrated for the purposes of the Eddy Covariance measurements. ....	49
Figure 3.4 The positioning of the trees used for sap flow measurements in the orchard in Groblershoop. Photo taken in January 2020 .....	51
Figure 3.5 The mixed cultivar pecan orchard close to Groblershoop an aerial view of the orchard and the orchard floor in January 2023.....	51
Figure 3.6 Overview of the Pecan research orchard from 2018 (left) at the start of the trial to 2022 (right). The 10 x 10 m planting used for the water stress measurements is indicated in the yellow block.....	52
Figure 3.7 The automatic weather station installed within 1 km of the trial site in Vaalharts	53
Figure 3.8 The automatic weather station installed within 250 m of the study orchard on the farm close to Groblershoop.....	55
Figure 3.9 A) The sap flow equipment used to measure transpiration, consisting of two T-type thermocouples and a heater probe in the middle. B) Probe placement around the trunk of a pecan tree. C) The shade netting erected around a pecan tree in Groblershoop to shade the sap flow probes.....	57
Figure 3.10 Determination of wounding caused as a result of the insertion of probes in the tree to determine heat pulse velocities and ultimately transpiration. ....	57

Figure 3.11 Position of the micro-lysimeters for Innovation Africa@UP Pretoria. The blue stars represent the position of the line quantum sensors that were permanently installed underneath the canopy. ....	59
Figure 3.12 Position of the micro-lysimeters for the three pecan orchards (A) Groblershoop, and (B) Vaalharts. ....	60
Figure 3.13 A) Position of the Open Path Eddy Covariance system above the tree canopy. B) Position of the Open Path Eddy Covariance (red dot) system in relation to the sap flow measurements in 2022/23 season (stars). ....	61
Figure 3.14 A) Positioning of the Eddy Covariance system in the Groblershoop orchard installed in September 2020. The red arrow indicates the positioning of the tower, whilst the yellow arrows indicate the locations of the transpiration measurements. B) The Eddy covariance tower within the work row. ....	63
Figure 3.15 The grid layout for the determination of fractional interception of PAR, from A) above and B) from under the tree canopy. ....	64
Figure 3.16 A) Piezometer to determine the depth of the water table, B) water meters to determine irrigation volumes and 3) CS616 sensors determining soil water content in the top 20 cm of the soil profile ....	66
Figure 3.17 Positioning of soil water monitoring equipment in the pecan orchards in A) Vaalharts and B) Groblershoop. ....	67
Figure 3.18 Schematic representation of a fruit tree orchard showing model input parameters used in the radiation interception model. The dashed lines show the interaction between solar rays (--) and the trees when: (1) the direct rays of the sun pass unobstructed below the canopy; (2) the direct rays of the sun pass unobstructed through gaps in the canopy, observed as a sun-fleck on the shaded ground area (Cp); and (3) the beam passes by the edge of the canopy, thus casting a shadow. X, Y, and Z show the Cartesian axes Oyarzun et al. (2007) ....	69
Figure 3.19 Orchard layout showing all treatments, blocks and measurements trees, where soil water monitoring equipment (chameleon soil water sensor) is located (the blue blocks) and where the sap flow equipment has been moved to for the 2022/23 season (red outlined blocks). W – Wichita, WS – Western Schley ....	83
Figure 3.20 Plastic sheeting used to eliminate rainfall from stress treatments ....	84
Figure 3.21 Cross-section cut at the mid-point of the nut and perpendicular cut along the longitudinal dimensions of the nut ....	87
Figure 3.22 A) Chameleon soil water sensors buried in the ground. B) Chameleon reader connected to the sensor array with colour display in the well-watered control during the course of the trial ....	89

Figure 3.23 Raster histogram of the simple ratio index (SRI) used to decide on a background-separation threshold value, showing a large background spike and normal distribution for the canopy. The threshold in this case is an SRI value of approximately 5. .	94
Figure 3.24 NDVI Image of pecan orchard showing little differentiation between shadows and the pecan canopy .....	95
Figure 3.25 Simple ratio index (SRI) image of the pecan orchard showing clear differentiation between pecan canopy and the background .....	95
Figure 3.26 Threshold raster created using threshold value of the SRI .....	96
Figure 3.27 Individual canopy polygons created using threshold value of simple ratio index (SRI) .....	96
Figure 3.28 Normalised difference vegetation index (NDVI) orchard image with all non-canopy pixels removed .....	97
Figure 3.29 Grid aligned to individual canopies, used to extract average vegetation indices (VI) and thermal canopy values.....	97
Figure 3.30 Raster histogram of thermal pecan canopy images, showing a normal distribution, used to derive the limits of the crop water stress index (CWSI).....	101
Figure 4.1 Daily values of maximum and minimum temperatures ( $^{\circ}\text{C}$ ), solar radiation ( $\text{MJ m}^{-2} \text{ day}^{-1}$ ), rainfall (mm) and maximum and minimum relative humidity (%) at Groen Boerdery from 9 September 2018 to 31 August 2023.....	105
Figure 4.2 The accumulation of positive chill units for the 2019, 2020, 2021 and 2022 winters at Groen Boerdery outside of Jan Kempdorp. Chill units were calculated from 1 May to 31 August to allow comparisons between seasons. ....	105
Figure 4.3 Daily Reference evapotranspiration (short crop – $\text{ET}_o$ and Tall crop $\text{ET}_r$ ) and vapour pressure deficit (VPD) at Groen Boerdery from 9 September 2018 to 31 August 2023 .....	106
Figure 4.4 Daily values of maximum and minimum temperatures ( $^{\circ}\text{C}$ ), solar radiation ( $\text{MJ m}^{-2} \text{ day}^{-1}$ ), rainfall (mm) and maximum and minimum relative humidity (%) at Groblersshoop from 24 August 2019 to 31 August 2023. ....	108
Figure 4.5 The accumulation of positive chill units for the 2020, 2021 and 2022 winters in Groblersshoop. Chill units were calculated from 1 May to 31 August to allow comparisons between seasons. ....	108
Figure 4.6 Daily Reference evapotranspiration (short crop – $\text{ET}_o$ and Tall crop $\text{ET}_r$ ) and vapour pressure deficit (VPD) at Groblersshoop from 24 August 2019 to 9 February 2023	109
Figure 4.7 The accumulation of growing degree days for the 2019/20 to 2022/23 seasons for A) Groblersshoop, B) Vaalharts and C) Pretoria .....	111
Figure 4.8 Changes in fractional canopy cover in Vaalharts during A) 2018/19, (B) 2019/20, (C), 2020/21, (D) 2021/22 season and (E) 2022/23 season. Fractional canopy cover was	

determined from drone images which were analysed with the Canopeo app. Values were an average of the four trees in each orchard.....	113
Figure 4.9 Changes in fractional canopy cover in Groblershoop orchard during (A) 2019/20 season, (B) 2020/21 season, (C) 2021/22 and D 2022/23 season. Fractional canopy cover was determined from drone images which were analysed with the Canopeo app. Values were an average of the four trees in each orchard. ....	114
Figure 4.10 Changes in fractional intercepted photosynthetically active radiation (FIPAR) determined with a ceptimeter for the two cultivars in Groblershoop during the (A) 2021/22 and (B) 2022/23 seasons, and Vaalharts during the C) 2021/22 and (D) 2022/23 seasons	115
Figure 4.11 Changes in transpiration (T) for 'Choctaw' and 'Wichita' trees in relation to evapotranspiration (ET) and reference evapotranspiration ( $ET_o$ ) over the five seasons from 9 September 2019 to 11 June 2023 in Vaalharts.....	116
Figure 4.12 Transpiration crop coefficients for the five seasons (2018-2023) for 'Wichita' and 'Choctaw' pecan trees at Vaalharts .....	119
Figure 4.13 Changes in transpiration (T) for 'Choctaw' and 'Wichita' trees in relation to evapotranspiration (ET) and reference evapotranspiration ( $ET_o$ ) over four seasons from 24 August 2019 to 14 June 2023 for Groblershoop. ....	120
Figure 4.14 Transpiration crop coefficients for the four seasons (2019-2023) seasons for 'Wichita' and 'Choctaw' pecan trees at Groblershoop .....	122
Figure 4.15 The relationship between transpiration crop coefficients ( $K_t$ ) and canopy size determined by measuring A) fractional interception of PAR by the canopy (FIPAR) and B) canopy cover determined using the Canopeo app ( $fc_{canopeo}$ ) combined with aerial images of the orchard. The relationships were determined using data from both sites in the Northern Cape province.....	123
Figure 4.16 Predawn leaf water potential ( $\psi_{pd}$ ) and midday stem water potential ( $\Psi_{smd}$ ) for Groblershoop during the A) 2021/22 season. and B) 2022/23 seasons. The horizontal solid red line demonstrates the $\Psi_{smd}$ threshold value (-0.90 MPa) for mild stress as outlined by Othman et al. (2014). The dotted red line indicates the threshold for $\psi_{pd}$ that corresponds to the $\Psi_{smd}$ as determined in the stress trial during this study.....	124
Figure 4.17 Predawn leaf water potential ( $\psi_{pd}$ ) and midday stem water potential ( $\Psi_{smd}$ ) for Vaalharts during the A) 2018/19, B 2020/21 and C) 2022/23 season. The horizontal solid red line demonstrates the $\Psi_{smd}$ threshold value (-0.90 MPa) for mild stress as outlined by Othman et al. (2014). The dotted red line indicates the threshold for $\psi_{pd}$ (-0.45 MPa) that corresponds to the $\Psi_{smd}$ as determined in the stress trial during this study. ....	125
Figure 4.18 Response of hourly transpiration of A, C, E, G) 'Wichita' and B, D, E, F)'Choctaw' trees in Groblershoop to hourly A & B) air temperature, C & D) vapour pressure	

deficit, E & F) reference evapotranspiration and G & H) solar radiation. Data was for daylight hours (08:00 to 17:00) from November to April each season.....	127
Figure 4.19 Response of hourly transpiration of A, C, E, G) 'Wichita' and B, D, E, F)'Choctaw' trees in Vaalharts to hourly A & B) air temperature, C & D) vapour pressure deficit, E & F) reference evapotranspiration and G & H) solar radiation. Data was for daylight hours (08:00 to 17:00) from November to April each season.....	128
Figure 4.20 Comparison of diurnal sun leaf water potential collected over the 2020/21 and 2021/22 growing seasons in Groblershoop. ....	130
Figure 4.21 Comparison of daily variation in A) solar radiation, B) air temperature, C) vapour pressure deficit, D) water potential, E) transpiration and F) stomatal conductance in 'Wichita' trees in Groblershoop from 06:00 to 18:00 on 14/12/2021 (black line) and 03/05/2022 (dotted line).....	131
Figure 4.22 Relationship between predawn water potentials and midday sun leaf water potentials. Data from both stressed and non-stressed 'Wichita' trees in Pretoria. The dotted line depicts the 1:1 line.....	132
Figure 4.23 Response of midday stomatal conductance to predawn water potential in 'Wichita' trees in Pretoria at Innovation Africa@UP .....	133
Figure 4.24 Relationship between stomatal conductance and midday sun leaf water potential in 'Wichita' trees in Pretoria at Innovation Africa@UP .....	133
Figure 4.25 Cumulative transpiration of 'Wichita' (Trans. W) and 'Choctaw' (Trans. C) trees, evapotranspiration (ET), reference evapotranspiration (ET <sub>o</sub> ) and rainfall + irrigation (R+I) for the A) 2018/18, B) 2019/20, C) 2020/21, D) 2021/22 and E) 2022/23 seasons in Vaalharts. ....	136
Figure 4.26 Cumulative transpiration of 'Wichita' (Trans. W) and 'Choctaw' (Trans. C) trees, evapotranspiration (ET), reference evapotranspiration (ET <sub>o</sub> ) and rainfall + irrigation (R+I) for the A) 2019/20, B) 2020/21, C) 2021/22 and D) 2022/23 seasons in Groblershoop .....	137
Figure 4.27 Daily profile water content for the root zone (0-75 cm) for the Vaalharts site for the A) 2018/29, B) 2019/20, C) 2020/21 and D) 2021/22 seasons. The solid red line indicates field capacity and the dotted line permanent wilting point, as determined from soil texture and assessing drainage after large rainfall events. Plant available water lies between these two lines. Daily volumetric soil water content was taken at 5:00, when maximum water uptake for the day had taken place. Sensors were removed at the end of the 2021/22 season. ....	138
Figure 4.28 Daily profile water content for the root zone (0-75 cm) for the Groblershoop site for the A) 2019/20, C) 2020/21 and D) 2021/22 seasons. The solid red line indicates field capacity and the dotted line permanent wilting point, as determined from soil texture and drainage following large rainfall events. Plant available water lies between these two lines.	

Daily volumetric soil water content was taken at 18:00, when maximum water uptake for the day had taken place and because the grower irrigated at night. Sensors were removed at the end of the 2021/22 season.....	139
Figure 4.29 Depth of the water table in the pecan orchards in A) Vaalharts in the 2018/19 season, B) Vaalharts and Groblershoop in the 2021/22 season and C) Vaalharts and Groblershoop in the 2022/23 season. Data from 2019-2021 is missing partly due to COVID lockdown restrictions.....	141
Figure 4.30 Spatial and temporal variation of average daily soil evaporation ( $E_s$ ) ( $\text{mm day}^{-1}$ ) from micro-lysimeters throughout the 2022/23 season in the Groblershoop orchard. The fractional cover ( $f_{\text{canopeo}}$ ) is plotted on the secondary y-axis.....	143
Figure 4.31 Spatial and temporal variation of average daily soil evaporation ( $E_s$ ) ( $\text{mm day}^{-1}$ ) from micro-lysimeters in Vaalharts orchard during 2022/23 season. The fractional cover ( $f_{\text{canopeo}}$ ) is plotted on the secondary y-axis. ....	144
Figure 4.32 Daily soil evaporation ( $E_s$ ) estimated using the FAO-56 dual $K_c$ model for the (A) 2022/2023 growing seasons Groblershoop, as affected by changes in atmospheric evaporative demand ( $ET_o$ ), canopy size (estimated-FIPAR) and rainfall and irrigation events .....	145
Figure 4.33 Daily soil evaporation ( $E_s$ ) estimated using the FAO-56 dual $K_c$ model for the (A) 2022/2023 growing seasons Groblershoop, as affected by changes in atmospheric evaporative demand ( $ET_o$ ), canopy size (estimated-FIPAR) and rainfall and irrigation events .....	146
Figure 4.34 Changes in fractional canopy cover in the orchards in Vaalharts (V) and Groblershoop (G) for the 2021/22 season. Fractional canopy cover was determined from drone images which were analysed with the Canopeo app. Values were an average of the four trees in each orchard. ....	156
Figure 4.35 Mean biweekly leaf resistance ( $r_{\text{leaf}}$ ) for the orchard in Vaalharts (V) and Groblershoop (G) determined using the approach of Allen and Pereira (2009). Data was from the 2021/22 season .....	157
Figure 4.36 Fortnightly measured and estimated transpiration crop coefficients ( $K_t$ ) for the A) 'Wichita' trees in Vaalharts, B) 'Choctaw' trees in Vaalharts, C) 'Wichita' trees in Groblershoop and D) 'Choctaw' trees in Groblershoop for the 2021/22 season. ....	158
Figure 4.37 Daily measured and estimated transpiration in A) 'Wichita' and B) 'Choctaw' trees in Vaalharts and C) 'Wichita' and D) 'Choctaw' trees in Groblershoop. Transpiration was estimated using fortnightly estimates $K_t$ derived from average mean leaf resistance ( $r_{\text{leaf}}$ ) for each region. ....	159
Figure 4.38 Summed monthly measured and estimated transpiration in A) 'Wichita' and B) 'Choctaw' trees in Vaalharts and C) 'Wichita' and D) 'Choctaw' trees in Groblershoop fir the	

2021/22 season. Transpiration was estimated using fortnightly estimates $K_t$ derived from average mean leaf resistance ( $r_{leaf}$ ) for each region. Monthly estimates were derived by summing transpiration for each month. ....	160
Figure 4.39 Relationship between fortnightly mean leaf resistance and A) reference evapotranspiration and B) vapour pressure deficit using combined average leaf resistance data from Vaalharts and Groblershoop. ....	161
Figure 4.40 Changes in fractional canopy cover in the orchards in Vaalharts (V) and Groblershoop (G) for the 2022/23 season. Fractional canopy cover was determined from drone images which were analysed with the Canopeo app. Values were an average of the four trees.....	162
Figure 4.41 Estimated mean biweekly leaf resistance ( $r_{leaf}$ ) for the orchard in Vaalharts and Groblershoop in the 2022/23 season determined using the relationship between VPD and $r_{leaf}$ determined in the 2021/22 season. ....	162
Figure 4.42 Fortnightly measured and estimated transpiration crop coefficients ( $K_t$ ) for the A) 'Wichita' trees in Vaalharts, B) 'Choctaw' trees in Vaalharts, C) 'Wichita' trees in Groblershoop and D) 'Choctaw' trees in Groblershoop for the 2022/23 season. ....	163
Figure 4.43 Daily measured and estimated transpiration in A) 'Wichita' and B) 'Choctaw' trees in Vaalharts and C) 'Wichita' and D) 'Choctaw' trees in Groblershoop in the 2022/23 season. Transpiration was estimated using fortnightly estimates $K_t$ derived from average mean leaf resistance determined from a relationship with VPD. ....	164
Figure 4.44 Summed monthly measured and estimated transpiration in A) 'Wichita' and B) 'Choctaw' trees in Vaalharts and C) 'Wichita' and D) 'Choctaw' trees in Groblershoop in the 2022/23. Transpiration was estimated using fortnightly estimates $K_t$ derived from mean leaf resistance ( $r_{leaf}$ ) determined using the relationship with VPD. Monthly estimates were derived by summing transpiration for each month.....	165
Figure 4.45 Seasonal changes in maximum canopy porosity ( $C_p$ ) for the three trial sites measured using A) the VitiCanopy mobile phone application, B) PAR interception sensors and C) the relationship between fractional ground cover measured using Canopeo app ( $f_{c_{canopeo}}$ ) and canopy porosity ( $C_p$ ) measured using VitiCanopy application and PAR sensors (line quantum sensors and a Ceptometer). ....	167
Figure 4.46 Diurnal variation of hourly fractional interception of photosynthetically active radiation (FIPAR) for 'Wichita' trees grown in A, B, C and D) Vaalharts, E, F, G, and H) Groblershoop and I, J, K and L) Innovation Africa @ UP, Pretoria. Data was collected in A, E, and I) September 2021, B, F and J) February 2022, C, G and K) April 2023, and D, H, and L) May 2022. Triangles represent measured PAR interception, and crosses represent estimated PAR interception by the canopies. The Canopy porosity was estimated using equation $y = -0.7928x + 0.9537$ . ....	168

Figure 4.47 Comparison between measured and estimated values of daily fractional interception of PAR for A) 'Wichita' trees in Vaalharts, B) 'Choctaw' trees in Vaalharts, C) 'Wichita' trees in Groblershoop, (D) 'Choctaw' trees in Groblershoop and (E) 'Wichita' trees in Pretoria	169
Figure 4.48 The linear function relating fractional interception of solar radiation (QRsp) divided by canopy conductance (Gc) to vapour pressure deficit (D) to determine the slope and intercept of the curve for use in transpiration modelling. This relationship was determined in the pecan orchard at Innovation Africa@UP.	170
Figure 4.49 Daily measured and estimated transpiration for Wichita' trees in A) 2021/22 and B) 2022/23 seasons and 'Choctaw' trees in the C) 2021/22 and (D) 2022/23 seasons in Groblershoop.	171
Figure 4.50 Daily measured and estimated transpiration for Wichita' trees in A) 2021/22 and B) 2022/23 seasons and 'Choctaw' trees in the C) 2021/22 and (D) 2022/23 seasons in Vaalharts.	172
Figure 4.51 Monthly measured and estimated transpiration for Wichita' trees in A) 2021/22 and B) 2022/23 seasons and 'Choctaw' trees in the C) 2021/22 and (D) 2022/23 seasons in Groblershoop.	173
Figure 4.52 Monthly measured and estimated transpiration for Wichita' trees in A) 2021/22 and B) 2022/23 seasons and 'Choctaw' trees in the C) 2021/22 and (D) 2022/23 seasons in Vaalharts.	173
Figure 4.53 Daily weather variables (1 September to 31 May) on the Hatfield Experimental Farm (Innovation Africa@UP) for the A) 2017/18, B) 2018/19, C) 2019/20, D) 2020/21, E) 2021/22 and F) 2022/23 seasons, indicating each phenological stage. 1 – flowering, 2 – nut sizing, 3 – nut filling, 4 – shuck dehiscence. ET <sub>o</sub> – reference evapotranspiration	178
Figure 4.54 Chill unit accumulation in winter from 2017 to 2022. Chill units were calculated using the positive daily chill unit model of Linsley-Noakes et al. (1995).	179
Figure 4.55 Seasonal rainfall at Innovation Africa@UP for the A) 2020-2021, B) 2021-2022 and C) 2022-2023 growing seasons	180
Figure 4.56 Changes in fractional canopy cover for the various treatments for the A) 2018/2019 season and B) 2019/2020 season	183
Figure 4.57 Midday stem water potential ( $\psi_{smd}$ ) for the six seasons. A) season one (2017/18), B) season two (2018/19), C) season three (2019/20), D) season four (2020/21) E) season five (2021/22) and season six (2022/23). The vertical lines on each figure indicates the different phenological stages (1 – flowering and nut set, 2 – nut sizing, 3 – nut filling and 4 – shuck dehiscence). The horizontal red line demonstrates the stem water potential threshold value (-0.90 MPa) for mild stress as outlined by Othman et al. (2014).	185



Figure 4.58 Predawn leaf water potential ( $\psi_{pd}$ ) for the five seasons. A) season one (2017/18), B) season two (2018/19), C) season three (2019/20), D) season four (2020/21), E) season five (2021/22) and F) season six (2022/23) The vertical lines on each figure indicates the different phenological stages (1 – flowering and nut set, 2 – nut sizing, 3 – nut filling and 4 – shuck dehiscence). The horizontal red line demonstrates the predawn water potential threshold value (-0.45 MPa) for mild stress as determined in this study from the relationship between $\psi_{pd}$ and $\psi_{smd}$ .....	186
Figure 4.59 Relationship between midday stem water ( $\psi_{smd}$ ) and predawn leaf water potential ( $\psi_{pd}$ ) for the six seasons. A) season one (2017/18), B) season two (2018/19), C) season three (2019/20), D) season four (2020/21), E) season five (2021/22) and F) season six (2022/23) .....	188
Figure 4.60 Relationship between midday stem water ( $\psi_{smd}$ ) and predawn leaf water potential ( $\psi_{pd}$ ) for the six seasons combined .....	189
Figure 4.61 Diurnal stomatal conductance ( $g_s$ ) A) before and B) during the water stress and photosynthesis ( $A_n$ ) C) before and D) during the water stress at the flowering and nut set stage. Each value was an average of 4-6 leaves from 4 trees. Mean values with the same letters are not significantly different from each other ( $p > 0.05$ ) .....	190
Figure 4.62 Diurnal stomatal conductance ( $g_s$ ) (a) before and (b) during the water stress and photosynthesis ( $A_n$ ) (c) before and (d) during the water stress at the nut sizing stage. Each value was an average of 4-6 leaves from 4 trees. Mean values with the same letters are not significantly different from each other ( $p > 0.05$ ).....	191
Figure 4.63 Diurnal stomatal conductance ( $g_s$ ) A) before and B) during the water stress and photosynthesis ( $A_n$ ) C) before and D) during the water stress at the nut filling stage. Each value was an average of 4-6 leaves from 4 trees. Mean values with the same letters are not significantly different from each other ( $p > 0.05$ ).....	192
Figure 4.64 Diurnal stomatal conductance ( $g_s$ ) A) before and B) during the water stress and photosynthesis ( $A_n$ ) C) before and D) during the water stress at the shuck dehiscence stage. Each value was an average of 4-6 leaves from 4 trees. Mean values with the same letters are not significantly different from each other ( $p > 0.05$ ).....	193
Figure 4.65 The response of A) stomatal conductance and B) photosynthesis to increasing water stress as indicated by midday stem water potential in pecan trees .....	194
Figure 4.66 The impact of water stress during flowering and nut set stage on number of female flowers per cluster for the A) 2018/2019 season and B) 2019/2020 season. Treatments with the same letter are not significantly different from each other ( $p < 0.05$ ) .	195
Figure 4.67 Nut elongation (length) during the A) 2018/19 season and B) 2019/20 season and nut expansion (diameter) during the C) 2018/19 season, D) 2019/20 season as influenced by water stress during the nut sizing stage.....	196

Figure 4.68 Percentage nut drop in the A) first season (2017/18), B) second season (2018/19), C) third season (2019/20), D) fourth season (2020/21), E) fifth season (2021/22) and F) sixth season (2022/23). Treatments with the same letter are not significantly different from each other ( $p < 0.05$ ).....	198
Figure 4.69 Water stage fruit split in the experimental orchard during the 2020/2021 season. A) Split nuts in the tree, B) split nuts on the tree which have senesced, C and D) nut drop because of water stage fruit split and E) longitudinal section of split nuts.....	199
Figure 4.70 Water stage fruit split in the experimental orchard during the 2021/2022 season. A) Split nuts on the tree, B) split nuts that have fallen off the tree, C) and D) longitudinal section of split nuts .....	199
Figure 4.71 A) Sound and B) unsound kernel during the 2022/23 season. A high percentage of unsound kernel was found during this season in a number of treatments.....	206
Figure 4.72 The relationship between canopy temperature ( $T_c$ ) and midday stem water potential ( $\psi_{\text{midday}}$ ), showing the problems with using leaf temperature alone to detect water stress .....	214
Figure 4.73 Relationship between the difference between canopy and air temperature ( $T_c - T_a$ ) and midday stem water potential ( $\psi_{\text{smd}}$ ), showing that correcting for $T_a$ alone is not sufficient for detecting water stress .....	215
Figure 4.74 Non-water stressed baseline (NWSB) plotted from data collected during the 2020/21 season at the Vaalharts site .....	216
Figure 4.75 Non-water stressed baseline (NWSB) plotted from data collected during the 2021/22 season at the Vaalharts site .....	216
Figure 4.76 Combined non-water stressed baseline (NWSB) from both measurement season .....	217
Figure 4.77 Non-water stressed baseline (NWSB) from the 2020/21 season using only data from the two hours after sunrise and two hours before sunset .....	218
Figure 4.78 Non-water stressed baseline (NWSB) from the 2021/22 season including data from the infrared radiometer detecting the temperature of a bare branch within the canopy (indicated by open circles) .....	219
Figure 4.79 Relationship between the crop water stress index (CWSI) calculated using the non-water stressed baseline (NWSB) and the static Upper Limit for each season, and the midday stem water potential ( $\psi_{\text{smd}}$ ) .....	220
Figure 4.80 Relationship between the crop water stress index (CWSI) with a lower limit found from a wet reference surface and an upper limit of $6^\circ\text{C}$ , and midday stem water potential ( $\psi_{\text{smd}}$ ) .....	221

Figure 4.81 Relationship between the CWSI with a lower limit found from a wet reference surface and an upper limit of 6°C on 13 April 2022, and midday stem water potential ( $\psi_{\text{smd}}$ ) .....	221
Figure 4.82 Relationship between the crop water stress index (CWSI) calculated using the thermal image histogram, and midday stem water potential ( $\psi_{\text{smd}}$ ) .....	222

## LIST OF TABLES

Table 2.1 Evapotranspiration of pecan orchards reported in literature. $f_c$ is fractional canopy cover; ET is evapotranspiration and T is transpiration. All data indicates seasonal ET, unless otherwise specified. ....	18
Table 2.2 Measured monthly crop coefficients for the reference pecan orchard ( $K_{c-ref}$ ) given by Samani et al. (2011) for New Mexico conditions, which have been offset by 6 months to adjust for the seasons in the southern hemisphere .....	34
Table 2.3 Effect of the timing of water deficit on nut shape and size (Adapted from Sparks (2006)). To adjust to Southern Hemisphere conditions June is December, July is January and August is February, all fall within the nut sizing period .....	43
Table 3.1 Details of the mixed pecan cultivar orchards in Vaalharts and Groblershoop in the Northern Cape. W = Wichita and C = Choctaw .....	48
Table 3.2 Values used to parameterize the FAO-56 dual crop coefficient model in order to estimate soil evaporation coefficient in Groblershoop and Vaalharts.....	80
Table 3.3 Wavelength bands available from the Micasense Altum Multispectral and thermal sensor with band centres and bandwidth ( <a href="https://support.micasense.com/hc/en-us/articles/360010025413-Altum-Integration-Guide#h.5ow085yb2oll">https://support.micasense.com/hc/en-us/articles/360010025413-Altum-Integration-Guide#h.5ow085yb2oll</a> ).....	91
Table 3.4 UAV data collection flights, and available plant water stress measurements. Rows highlighted in grey indicate the days selected for data analysis.....	92
Table 3.5 Vegetation Indices created using the multispectral images of the UP Pecan orchard .....	93
Table 3.6 Methods used to calculate the CWSI.....	103
Table 4.1 Seasonal weather averages for Vaalharts (September to June when the trees are in leaf).....	107
Table 4.2 Seasonal weather data for Groblershoop (September to June when the trees were in leaf).....	110
Table 4.3 Average, maximum and total seasonal transpiration, reference evapotranspiration and evapotranspiration for the 'Choctaw' and 'Wichita' trees in Vaalharts .....	117
Table 4.4 Average, maximum and total seasonal transpiration, reference evapotranspiration and evapotranspiration for the 'Choctaw' and 'Wichita' trees in Groblershoop.....	121
Table 4.5 Crop water productivity ( $WP_T$ ) and economic water productivity ( $EWP_T$ ) for the 'Choctaw' and 'Wichita' trees in an orchard in Vaalharts for the 2018/19, 2019/20, 2020/21, 2021/22 and 2022/23 seasons, based on transpiration values. Yield was adjusted to 4% moisture content. ....	148
Table 4.6 Crop water productivity ( $WP_T$ ) and economic water productivity ( $EWP_T$ ) for the 'Choctaw' and 'Wichita' trees in an orchard in Groblershoop for the 2019/20, 2020/21,	

2021/22 and 2022/23 seasons, based on transpiration volumes. Yield was adjusted to 4% moisture content. ....	149
Table 4.7 Reference evaporation, evapotranspiration and water productivity indicators for the pecan orchard in Vaalharts (1 September to 30 June growing season).....	151
Table 4.8 Reference evaporation, evapotranspiration and water productivity indicators for the pecan orchard in Groblershoop (1 September to 30 June growing season) .....	152
Table 4.9 Average evapotranspiration ( $ET_c$ ), average yields and average irrigation requirements for the predominant crops in Vaalharts and Groblershoop. Average yields for raisin grapes are from the 2020/21 and 2021/22 season based on estimates from Raisins South Africa. Data for 2023 is not currently available. ....	152
Table 4.10 Total gross income, production costs, water productivity and economic crop water productivity for the predominant crops in Vaalharts and Groblershoop, considering crop evapotranspiration and irrigation requirements. No 2022/23 production figures were available for raisin grapes. ....	153
Table 4.11 Modelling statistics for the estimation of transpiration in the orchards in Vaalharts and Groblershoop for the 2021/22 season .....	160
Table 4.12 Modelling statistics for the estimation of transpiration in the orchards in Vaalharts and Groblershoop for the 2022/23 season .....	165
Table 4.13 Modelling statistics for the estimation of daily fractional interception of photosynthetically active radiation (FIPAR) in Vaalharts and Groblershoop orchards .....	169
Table 4.14 Seasonal water application; Irrigation and rainfall water applied at the different phenological stages as water stress was implemented for five seasons. Season one (2017/2018), season two (2018/2019), season three (2019/2020), season four (2020/2021), season five (2021/2022), and season six (2022/23). ND-not determined .....	181
Table 4.15 Average in shell yield for the different stress treatments in the 2017/18 season, 2018/19 season, 2019/20 season, 2020/21 season, 2021/22 and 2022/23 season. Yield was adjusted to 4% moisture content. Treatments with the same letter are not significantly different from each other ( $p < 0.05$ ).....	201
Table 4.16 Quality parameters including number of nuts $kg^{-1}$ , percent kernel, m and wafers/air pockets percentage of pecan trees for the fully irrigated control and water stressed treatments in the 2017/18 season .....	202
Table 4.17 Quality parameters including average nut diameter, number of nuts $kg^{-1}$ , percent kernel, unsound kernel (percentage pops), wafers/air pockets percentage and percent stick tights of pecan trees for the fully irrigated control and water stressed treatment in the 2018/19 season .....	202
Table 4.18 Quality parameters including average nut diameter, number of nuts $kg^{-1}$ , percent kernel, unsound kernel (percentage pops), wafers/air pockets percentage and percent stick	

tights of pecan trees for the fully irrigated control and water stressed treatments in the 2019/20 season .....	203
Table 4.19 Quality parameters including number of nuts kg <sup>-1</sup> , percent kernel, percent unsound kernel or pops and wafers/air pockets percentage of pecan trees for the fully irrigated control and water stressed treatments in the 2020/21 season .....	204
Table 4.20 Quality parameters including number of nuts kg <sup>-1</sup> , percent kernel, moisture percentage and wafers/air pockets percentage of pecan trees for the fully irrigated control and water stressed treatments in the 2021/22 season .....	205
Table 4.21 Quality parameters including number of nuts kg <sup>-1</sup> , percent kernel, and wafers/air pockets percentage of pecan trees for the fully irrigated control and water stressed treatments in the 2022/23 season .....	206
Table 4.22 Total income received as a result of imposing water stress at different phenological stages. ....	207
Table 4.23 Relationships between vegetation indices (VIs) and midday stem water potential ( $\psi_{smd}$ ) collected during the 2020/21 and 2021/22 seasons, stomatal conductance ( $g_s$ ) collected during the 2020/2021 season and $\psi_{smd}$ collected on 24 February 2022.....	211
Table 5.1 Summary of tree water use of the orchards in the Northern Cape. T – transpiration, ET – evapotranspiration, $WP_c$ – crop water productivity, EWP – economic water productivity .....	225

## LIST OF ABBREVIATIONS

AE	application efficiency
AWS	automatic weather station
B	height of insertion of lowest branches
C	soil parameter for stage II of evaporation
CRM	coefficient of residual mass
CWSI	crop water stress index
D	Willmot index of agreement
De	cumulative depth of evaporation
EC	eddy covariance
ECC	effective canopy cover
$E_i$	estimated value
$EWP_c$	economic water productivity ( $R\ m^{-3}$ )
$EWP_i$	Irrigation economic water productivity ( $R\ m^{-3}$ )
$EWP_T$	economic water productivity based on transpiration ( $R\ m^{-3}$ )
Ex	distance between trees in a row (m)
Ey	distance between rows of trees (m)
FAO	Food and Agriculture Organization of The United Nations
FC	field capacity
GDD	growing degree days
GPS	global positioning system
HPV	heat pulse velocity
HWR	height to width ratio
$I_i$	depth of irrigation
IRGA	infrared gas analyser
MAE	mean absolute error
MCARI	modified chlorophyll absorption in reflectance index
ML	micro-lysimeter
ND	not determined
NDVI	Normalised difference vegetation index
NIR	near infrared
NWSB	non-water stressed baseline
OPEC	open path eddy covariance
$O_i$	measured value
OSAVI	optimised soil adjusted vegetation index

PCU	positive chill unit
PFTE	polytetrafluoroethylene
$P_i$	precipitation
PWP	permanent wilting point
$R^2$	coefficient of determination
RCBD	randomised complete block design
RDVI	renormalised difference vegetation index
ReNDVI	red edge normalised difference vegetation index
ReSR	red edge simple ratio
REW	readily available water
RGB	red green blue
$RH_{\min}$	minimum relative humidity (%)
RMSE	root of the mean square error
$RO_i$	run-off
SAPPA	South African Pecan Nut Producers' Association
SPAC	soil-plant-atmosphere-continuum
SRI	simple ratio index
TCARI	transformed chlorophyll absorption ratio
TEW	total evaporable water
$T_{ew}$	depth of transpiration from the exposed and wetted fraction of the soil surface
VI	vegetation index
VPD	vapour Pressure Deficit (kPa)
W	Wichita
$WP_c$	crop water productivity ( $\text{kg m}^{-3}$ )
$WP_i$	irrigation water productivity ( $\text{R m}^{-3}$ )
$WP_T$	crop water productivity based on irrigation ( $\text{kg m}^{-3}$ )
WRC	Water Research Commission
WS	Western Schley
WUE	water use efficiency
$W_x$	canopy width perpendicular to the row direction
$W_y$	canopy width along the row direction
<b>Symbol</b>	<b>Description and units</b>
$A_n$	photosynthesis ( $\mu\text{mol m}^{-2} \text{s}^{-1}$ )
$A_{ML}$	area of microlysimeter



$c_w$	specific heat capacity of the wood matrix ( $\text{J kg}^{-1}^\circ \text{C}^{-1}$ )
$c_s$	specific heat capacity of the sap ( $\text{J kg}^{-1}^\circ \text{C}^{-1}$ )
$C_p$	specific heat capacity of air ( $\text{J kg}^{-1} \text{K}^{-1}$ )
$C_p$	canopy porosity (unitless)
$d$	zero plane displacement (m)
$E_s$	evaporation from the orchard floor (mm)
$ET$	evapotranspiration (mm or $\text{m}^3$ )
$ET_o$	reference evapotranspiration (mm)
$f_c$	observed fraction of soil covered by vegetation seen from directly above
$f_{\text{canopeo}}$	fractional cover determined using the Canopeo app
$f_{\text{ceff}}$	effective fraction of ground covered or shaded by vegetation near solar noon
$f_{\text{DIPAR}}$	daily fractional interception of photosynthetically active radiation
$f_{\text{ew}}$	fraction of soil that is wetted and exposed to solar radiation
$f_{\text{IPAR}}$	fraction of intercepted photosynthetically active radiation
$F_r$	adjustment factor relative to stomatal control
$f_w$	fraction of soil wet by irrigation
$G$	soil heat flux ( $\text{W m}^{-2}$ )
$g_a$	aerodynamic conductance ( $\text{m s}^{-1}$ )
$g_s$	stomatal conductance ( $\text{mol m}^{-2} \text{s}^{-1}$ )
$g_{\text{smd}}$	midday stomatal conductance ( $\text{mol m}^{-2} \text{s}^{-1}$ )
$G_c$	canopy conductance ( $\text{m s}^{-1}$ )
$G_t$	total hydraulic conductance within a tree
$h_{\text{canopy}}$	tree height (m)
$H$	sensible heat ( $\text{W m}^{-2}$ )
$I$	solar radiation below the canopy ( $\mu\text{mol m}^{-2} \text{s}^{-1}$ )
$I_o$	solar radiation above the canopy ( $\mu\text{mol m}^{-2} \text{s}^{-1}$ )
$k$	extinction coefficient
$k_w$	thermal diffusivity of green (fresh) wood ( $\text{cm}^2 \text{s}^{-1}$ )
$K_c$	crop coefficient
$K_{\text{cb}}$	basal crop coefficient
$K_{\text{c-ref}}$	crop coefficient of a well-managed mature pecan orchard
$K_{\text{c max}}$	largest $K_c$ value that can be sustained by the crop
$K_{\text{t full}}$	transpiration crop coefficients for fully grown orchard
$K_d$	canopy density coefficient

$K_e$	soil evaporation coefficient
$K_t$	transpiration crop coefficient
$K_r$	evaporation reduction coefficient
$L$	average width of wetted area
$LAD$	leaf area density ( $m^3 m^{-3}$ )
$LAI$	leaf area index ( $m^2 m^{-2}$ )
$LE$	latent energy ( $W m^{-2}$ )
$LL$	lower limit ( $T_c - T_a$ ) of the crop water stress index
$m_c$	moisture content of sapwood sample (%)
$M_L$	parameter that simulates the physical limits imposed on water flux through the plant root, stem and leaf systems
$M_{ML}$	mass of microlysimeter
$P$	precipitation
$P_a$	atmospheric pressure (Pa)
$PAR$	photosynthetically active radiation ( $\mu mol s^{-1}$ )
$QR_{sp}$	fractional interception of daily total solar radiation
$RH_{min}$	minimum relative humidity (%)
$R_l$	Fraction of daily radiation reaching the soil surface
$r_{leaf}$	mean leaf resistance ( $s m^{-1}$ )
$r_s$	mean surface resistance ( $s m^{-1}$ )
$R_n$	net radiation ( $W m^{-2}$ or $MJ m^{-2} day^{-1}$ )
$R_s$	solar radiation ( $W m^{-2}$ or $MJ m^{-2} day^{-1}$ )
$R_{so}$	solar radiation under clear sky conditions ( $MJ m^{-2} day^{-1}$ )
$R_{sp}$	daily total solar radiation ( $J m^{-2} day^{-1}$ )
$S^2$	sum of squares
$SFD$	sap flux density ( $m^3 m^{-2} h^{-1}$ )
$t$	time (days)
$T_a$	air temperature ( $^{\circ}C$ )
$T_c$	canopy temperature ( $^{\circ}C$ )
$T_{dry}$	warmest pixel ( $^{\circ}C$ )
$T_{leaf}$	leaf surface temperature ( $^{\circ}C$ )
$T_{max}$	maximum daily temperature ( $^{\circ}C$ )
$T_{min}$	minimum daily temperature ( $^{\circ}C$ )
$T_{wet}$	coolest pixel ( $^{\circ}C$ )
$\Psi_{leaf}$	leaf water potential (MPa)
$\Psi_{pd}$	pre-dawn leaf water potential (MPa)

$\psi_s$	soil water potential (MPa)
$\psi_{sm}$	midday sun leaf water potential (MPa)
$\psi_{smd}$	stem water potential (MPa)
$u_2$	wind speed at 2 m height ( $\text{m s}^{-1}$ )
UL	upper limit ( $T_c - T_a$ ) of the crop water stress index
$v_1$	increase in temperature of upper thermocouple after the heat pulse is released ( $^{\circ}\text{C}$ )
$v_2$	increase in temperature of the lower thermocouple after the heat pulse is released ( $^{\circ}\text{C}$ )
$V_c$	corrected heat pulse velocity ( $\text{cm h}^{-1}$ )
$V_h$	heat pulse velocity ( $\text{cm h}^{-1}$ )
$\text{VPD}_{\text{air}}$	air vapour pressure deficit (kPa)
$\text{VPD}_{\text{leaf}}$	leaf to air vapour pressure deficit (kPa)
$V_s$	sap velocity ( $\text{cm h}^{-1}$ )
$V_w$	volume of wood sample ( $\text{cm}^3$ )
w	wounding width (cm)
X	distance between the heater and the upper and lower thermocouple (cm)
$Z_e$	thickness of the topsoil layer from which evaporation occurs
$\Delta$	slope of the saturation vapour pressure vs air temperature curve ( $\text{kPa K}^{-1}$ )
$\Delta T$	temperature difference
$\Delta T_o$	temperature difference during a period of zero flow
$\rho_a$	density of dry air ( $\text{kg m}^{-3}$ )
$\rho_b$	basic density of wood ( $\text{g cm}^{-3}$ )
$\rho_s$	density of water ( $\text{kg m}^{-3}$ )
$\gamma$	psychrometric constant ( $\text{kPa K}^{-1}$ )
$\lambda$	the latent heat of vaporization ( $\text{J kg}^{-1}$ )
$\eta$	mean angle of the sun above the horizon
$\theta$	soil water content
$\phi$	latitude (radians)
$\delta$	solar declination (radians)
$\tau_f$	solar radiation passing between canopies
$\tau_c$	solar radiation traversing through canopies
$\phi_r$	row azimuth

This page was intentionally left blank

# **1. INTRODUCTION**

## **1.1 BACKGROUND**

The Pecan Nut industry in South Africa has expanded rapidly in recent years, which is expected to continue in the foreseeable future. Information and knowledge of the water use of Pecan Nut trees and orchards is essential for sustainable development, in particular because of scarce surface and groundwater resources and increasing competition for irrigation water use. The current reality is that no comprehensive knowledge is available on water use of Pecan Nut trees and orchards in different production regions. This applies specifically to the Northern Cape, where large areas of irrigated Pecan Nut orchards are being established. Measurement and modelling of water use of Pecan Nut trees and orchards is therefore required, in order to extrapolate water use to production areas outside the Northern Cape. Knowledge of the water use of Pecan Nut trees is important for water management, in particular during the mature growth phases of the orchard. Knowledge must be obtained of the total and seasonal water use; and identifying critical or water sensitive growth stages. This knowledge must eventually be applied for farming practices such as scheduling of irrigation water; determining the water leaching fraction in soils with high salinity levels; and selecting the appropriate irrigation method. It will also facilitate decision on whether or not pecans can be planted in a region and how much area can be planted with available water resources.

As a whole, knowledge of the water use of Pecan Nut trees and orchards is required for comparison with water use of competing irrigated crops. This will enable judicious expansion of the irrigated area planted under Pecan Nut orchards. Furthermore, knowledge of the water use of Pecan Nut trees and orchards is required to justify or substantiate applications for water use licences, in order for irrigated production to be undertaken within official water use authorisations. Knowledge of the efficiency and productivity of water use is also required to motivate periodic review of water use licences for long-term production of Pecan Nuts.

Research questions for this study therefore included

- What is the maximum unstressed water use of mature pecan orchards in the Northern Cape Province of South Africa?
- What is the partitioning of water use between tree transpiration and evaporation from the soil orchards?
- What is the crop water productivity and economic water productivity of well managed mature pecan orchards?

- What is the best approach to model water use of pecan, which allows the estimation of pecan orchard water use in the hotter western regions of South Africa, where pecans are extensively grown?
- How does water stress at different phenological stages impact yield and quality of pecan orchards?

## **1.2 AIMS AND OBJECTIVES**

### **General aim**

To analyse water use, yield and quality of specified cultivars of Pecan Nut trees with standardised tree spacing, canopy cover and zero cover crop between tree rows.

### **Specific objectives**

1. To measure and model Pecan Nut tree water use according to seasonal growth stages for mature Pecan Nut trees and orchards;
2. To determine the influence of water use on quality of nuts within generally accepted quality standards such as nut size, kernel % and pops;
3. To quantify water use efficiency and water use productivity of mature Pecan Nut trees and orchards.

## **1.3 APPROACH AND SCOPE**

The project encompassed the quantification of transpiration and evapotranspiration in two pecan orchards in the Northern Cape Province, located just outside of the towns of Jan Kempdorp on the Vaalharts irrigation scheme and Groblershoop. Measurements were made for five seasons in Vaalharts and four seasons in Groblershoop. Transpiration data was collected for two cultivars which are widely planted in the region, viz. 'Wichita' and 'Choctaw'. Weather data were collected in conjunction with water use measurements in order to determine the driving variables for pecan water use. Ecophysiological and soil water content measurements were also performed to ensure the determination of unstressed water use. These data were then used to evaluate water use models for use in pecan orchards and included crop coefficient and canopy conductance approaches. A radiation interception model was also successfully parameterised for pecan orchards. Finally, the water use data, together

with yield, was used to derive water productivity and economic water productivity for two orchards across all season. These values were then compared to other commercial crops grown in each region.

The second aspect of the project was to determine the impact of water stress at different phenological stages on yield and quality of pecans. This study was conducted at Innovation Africa@UP, the experimental farm facilities belonging to the University of Pretoria. Trees were subjected to a water deficit stress at different phenological stages and yield and quality was determined at the end of each season. Additional measurements of predawn leaf water potential, midday stem water potential, photosynthesis and stomatal conductance were performed to assess the level of stress within the orchard. The trial was run for six seasons. Phenological stages where stress was implemented included flowering and nut set, nut sizing, nut filling and shuck dehiscence and these treatments were compared to a well-watered control. A remote sensing aspect was added to this project for the final three years to try and detect spatial stress in the orchard. This included correlating vegetation indices with ground measurements and trying to parameterise the crop water stress index for pecans using a number of different methods.

## **2. LITERATURE REVIEW**

### **2.1 PHENOLOGY AND MORPHOLOGY OF PECANS**

#### **2.1.1 CANOPY DEVELOPMENT AND LEAF MORPHOLOGY**

Canopy development is dependent on several exogenous and endogenous factors. Exogenous factors include the interaction between heat and chilling requirements that allows bud break and normal growth to occur (Sparks, 1993). Once chilling has been achieved, the heat requirement is set, with an inverse relationship existing between the heat requirement and chill unit accumulation. Bud break will therefore be delayed if the tree receives insufficient chilling hours and there is a cool spring (Smith et al., 1992, Sparks, 1993). Insufficient chill can also result in variable bud break (Sparks, 1993). The chilling requirement varies considerably with cultivars and chill units should be calculated for each area in which pecans are to be cultivated, in order to select the most appropriate cultivars (Kuden et al., 2013). Chill units can be calculated by various models, and care should be taken to use the most appropriate model for the conditions and to make sure of the model when assessing the chill units required by a cultivar (Linsley-Noakes et al., 1995, Weinberger, 1950). Andales et al. (2006) also used thermal time in his model of pecan development to determine the length of different growth stages, but these parameters may not necessarily hold true in areas outside of where the model was calibrated. Temperature may also play a role in the rate of leaf senescence at the end of the season. Miyamoto (1983) observed that defoliation of 'Western' started when temperatures dropped to -4°C or below for a period of a few days. Production areas which do not experience a sudden freeze may therefore have longer growing seasons. Water stress during canopy development is also likely to result in smaller leaves and a smaller canopy than unstressed trees.

Endogenous factors largely reflect the deciduous nature of pecan trees, which means that there is new canopy growth in spring, which serves as a strong sink during this phase of leaf and shoot expansion (Andales et al., 2006). In autumn following harvest the tree stores large amounts of carbohydrates in preparation for foliation and fruit set events the following season (Wood et al., 2003). The tree relies heavily on the stored carbohydrate reserves because the photosynthetic capacity of the young soft flush leaves are not able to meet the demand of the growing tree. During this stage of leaf expansion the leaf is a net importer of carbohydrates, up until leaf expansion decreases as the leaf nears maximum size and becomes a net exporter of carbohydrates (Loescher et al., 1990). Flowering and fruit set coincides with the spring



flush, which further stresses the need for stored carbohydrate reserves to ensure good fruit set and therefore yield (Wood et al., 2003).

Optimal canopy development is required to increase the fractional canopy cover (fraction of ground covered by vegetation) in order to utilize the maximum amount of available sunlight (Jennings et al., 1999). Leaves which expand rapidly will be able to maximise photosynthesis and reach maturity at an earlier stage (Loescher et al., 1990). The canopy can be regarded as a complex solar harvesting system that uses the process of photosynthesis to convert photosynthetically active radiation (PAR), water and carbon dioxide (CO<sub>2</sub>) into carbon sugars used in vegetative and reproductive development (Lambers et al., 2008a). Canopy morphology impacts the amount of PAR intercepted through the effective arrangement of the leaves (Terashima and Hikosaka, 1995). Different pecan cultivars have diverse morphological traits, which impacts canopy structure, shape and size and therefore PAR interception and management practices (Wood, 1996).

Cultural practices can be used to optimize the pecan canopy for maximum light interception and to ease management practices such as harvesting and chemical spraying (Andales et al., 2006). Pruning is an important practice that can improve light interception, yield and nut quality, especially as pecan trees are shade intolerant and can become unproductive when subjected to overcrowding (Lombardini, 2006, Andersen and Crocker, 2004). It can be done manually or mechanically and between 10-130 kg tree<sup>-1</sup> dry mass can be removed depending on the severity of the shading (Andales et al., 2006).

The shape of pecan canopies can be divided into three classes: full ellipse (greatest width at midcrown), semi-ellipse (greatest width at end of crown) or cylindrical, with each form occupying a certain volume as determined by the cultivar and prevailing management practices (Wood, 1996). Mature cultivars containing the *aperirecto* form (limb ratio <0.65) will consist of canopies that are widest at the bottom of the crown (semi-ellipse form), whereas cultivars containing the *clistoforticat* form will have the greatest width at the mid-canopy or higher (Wood, 1996, Sparks, 2005). The *clistoforticat* form that exhibits a full ellipse is inferior to the *aperirecto* form that has a semi-ellipse form. This is due to the shading effect on the lower limbs of the *clistoforticat* form causing shade-induced crown form changes, resulting in a vase-like appearance, with flattened crown tops as the tree matures (Wood, 1996, Wood, 1995a). The *aperirecto* form will be exposed to maximum sunlight, without the over shading effect of top crown growth, and is preferred for increased nut production and quality (Lombardini, 2006).

Canopy height and width varies considerably between different cultivars and cultivars can range between 6 m to 15 m in height and 5 m to 12 m in width. Wood (1996) identified five crown height and four crown width categories, where 80% of tested cultivars were slightly taller than their width and only 17% were twice as long as their width. This is an important consideration as tree height will influence the geometry and planting density of the orchard, as adequate open space is needed between orchard rows and between trees in a row to prevent over shading.

Canopy and structural compositions determine how effectively the leaves can utilise PAR, water and nutrients to assimilate carbon (Ackerly et al., 2000). Pecan trees have compound leaves that vary between cultivars in midrib and palisade tissue thickness (Nemati, 1968). According to Chortyk et al. (1995), pecan leaves contain a cuticle that changes in chemical composition as the leaves mature. Leaf structure can be quite complex when considering stomatal characteristics, epidermal cell density and the number of trichomes on each leaf. The leaf characteristics are important in determining the regulation of water loss and the leaf level water use efficiency ( $WUE_{\text{Leaf}}$ ) defined as the ratio of leaf transpiration to photosynthesis (Sagaram et al., 2007).

Pecan leaves only have stomata on the abaxial side of the leaves, at densities of 363-463 stomata  $\text{mm}^{-2}$  (Sagaram et al., 2007). The stomata vary in shape and size between cultivars and within a cultivar, with an uneven distribution on the leaf surface (Nemati, 1968). In a study on three pecan cultivars Sagaram et al. (2007) found that stomatal densities differed according to the cultivar, but appeared to remain constant within a cultivar despite different growing locations. Stomatal density is important as it can influence the trees ability to tolerate abiotic stress, such as water stress (Jarvis and Davies, 1998), and unfavourable temperatures (Kleinhenz et al., 1995). However, in pecan trees stomatal density will not show any change in succeeding generations, as it is not a plastic trait within pecan (Sagaram et al., 2007). Therefore the stomatal density of the cultivar is dependent on the long term climatic conditions where the cultivar originated. Epidermal cell density is similar to stomatal density as it differs between cultivars, but not within a cultivar at different locations. According to a study done by Sagaram et al. (2007), both the number and type of trichomes differed between cultivars and within cultivars at different locations. Three different types of trichomes have been observed on immature pecan trees, which are awnlike hairs, concave peltate and vesiculare trichomes (Grauke et al., 1987). Sagaram et al. (2007) attributed this difference within a cultivar at different locations to abiotic factors, especially solar radiation and elevation. Therefore, the type of trichomes found on a cultivar are dependent on the prevailing environmental conditions.

### 2.1.2 ROOT GROWTH AND MORPHOLOGY

Plant roots are the major organ responsible for water and nutrient uptake, making them an important plant part. A thorough understanding of the root structure and function is necessary to guide crop management practices and optimise nutrient and water allocation according to root growth patterns and distribution. Pecan trees establish a taproot system with weak laterals before top growth occurs, therefore for at least the first four years of seedling growth the root system will be a preferential sink as it expands substantially (Sparks, 2005, Woodroof and Woodroof, 1934). After the fourth year the canopy and roots occupy roughly the same volume, in their respective environments, but canopy growth exceeds root growth from this period onwards and little root growth occurs deeper into the soil from this point onwards, as seen in Figure 2.1 (Woodroof and Woodroof, 1934). This allows for increased horizontal root growth, which facilitates both water and nutrient uptake and is considered a survival adaptation.

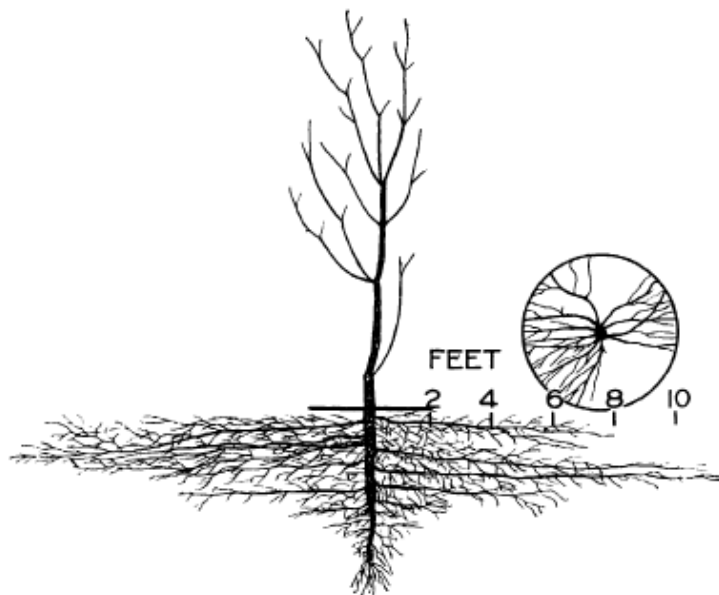


**Figure 2.1 A six year old pecan tree with a tree height of 4 m, lateral feeder root growth of 7 m and a root depth of 2 m. In the circle is a representation of the 11 largest lateral roots (Woodroof and Woodroof, 1934).**

The inability to be flexible in generating a lateral root system during seedling development is considered an adaptive trait (Sparks, 2005). which suggests tight developmental control of the tree and increases the possibility of the taproot reaching greater depths (Sparks, 2005). Pecan trees have a taproot systems that can reach great depths of up to 7 m, depending on the soil depth and draining patterns (Alben, 1955). Lateral roots will develop perpendicular to the taproot and parallel to the soil surface. The lateral roots play a key role in plant anchoring, nutrient allocation, water uptake and can extend to lengths twice as wide as the canopy

(Sparks, 2005). Fibrous roots develop from lateral roots, commonly referred to “humus strivers” or “feeder roots”, that grow to the soil surface and spread out horizontally upon reaching the surface (Lyr and Hoffmann, 1967, Woodroof and Woodroof, 1934). The growth of these roots are inhibited by drought, freezing or cultivation (Lyr and Hoffmann, 1967, Woodroof and Woodroof, 1934). The functional role of fibrous roots are the uptake of water and nutrients from soils to supply the demand of the developing canopy, that can lead to the conversion of the juvenile stage to the reproductive stage (Sparks, 2005). Over prolonged periods the feeder roots will grow into a short lived, high density mat that increases the volume from which water and nutrient uptake can occur. The large soil volume, which is occupied by the roots, is important to meet the water requirements of the large canopy. Deeper roots are also proposed to play an important role in water uptake (Sparks, 2005).

Pecans typically have a differential root flush pattern throughout a single production season. These root flushes occur just before spring shoot growth occurs. According to White Jr and Edwards (1978) root growth starts in the upper humus layer, as the soil temperature and moisture content are still optimal in this zone. As the season progresses, and soil temperature and water drainage increases, root growth in the top layer ceases and root growth commences deeper in the soil. During the growing season, the rate of root growth declines as kernel development commences (White Jr and Edwards, 1978). The roots grow less vigorously and start to branch. These roots are sensitive to adverse environmental conditions, such as temperature, water stress, lack of nutrients, but have the ability to continue growth once favourable conditions arise, allowing multiple growth cycles during the year (Woodroof and Woodroof, 1934). Importantly, similar work has not been done in South Africa, where soil temperatures and soil water content during winter are typically not limiting to root development. A discrepancy between apple root growth in the Northern Hemisphere and South Africa has been observed by Dr Elmi Lötze (pers. comm.).



**Figure 2.2 Pecan root development in orchards in Hartswater, which have been A) flood irrigated and 2) sprinkler irrigated. Root development in (A) was restricted by a sudden change in texture down the profile. Proliferation of feeder roots in the top 40 cm is evident in these orchards.**

Woodroof and Woodroof (1934) found the optimal soil temperature for root growth ranges between 21°C and 36°C, reaching a peak at 29°C, whilst too high temperatures (>45°C) or too low temperatures (<2°C) significantly reduced root growth (Figure 2.3). The resulting reduced root growth as a result of adverse temperatures cannot be explained by a single process and is rather attributed to various changes in the root, such as respiration rate or enzyme inhibition (Kaspar and Bland, 1992, Pregitzer et al., 2000, Kozlowski, 1992). High soil temperatures are linked to higher soil evaporation rates, resulting in water stress conditions that could lead to reduced root growth (Hargreaves and Samani, 1985). Pecan root growth is also associated with water availability, as root growth has been observed to cease under water limiting soil conditions and commence again when the soil water content reaches favourable levels (Woodroof and Woodroof, 1934, Sparks, 2005). Robinson (1994) reported similar results for root growth and proliferation occurring towards nutrient rich zones. Sparks (2005) proposed that differential functions for roots exist, with roots in the humus-topsoil layer mainly responsible for nutrient uptake, whilst deeper roots play a more important role in water uptake.

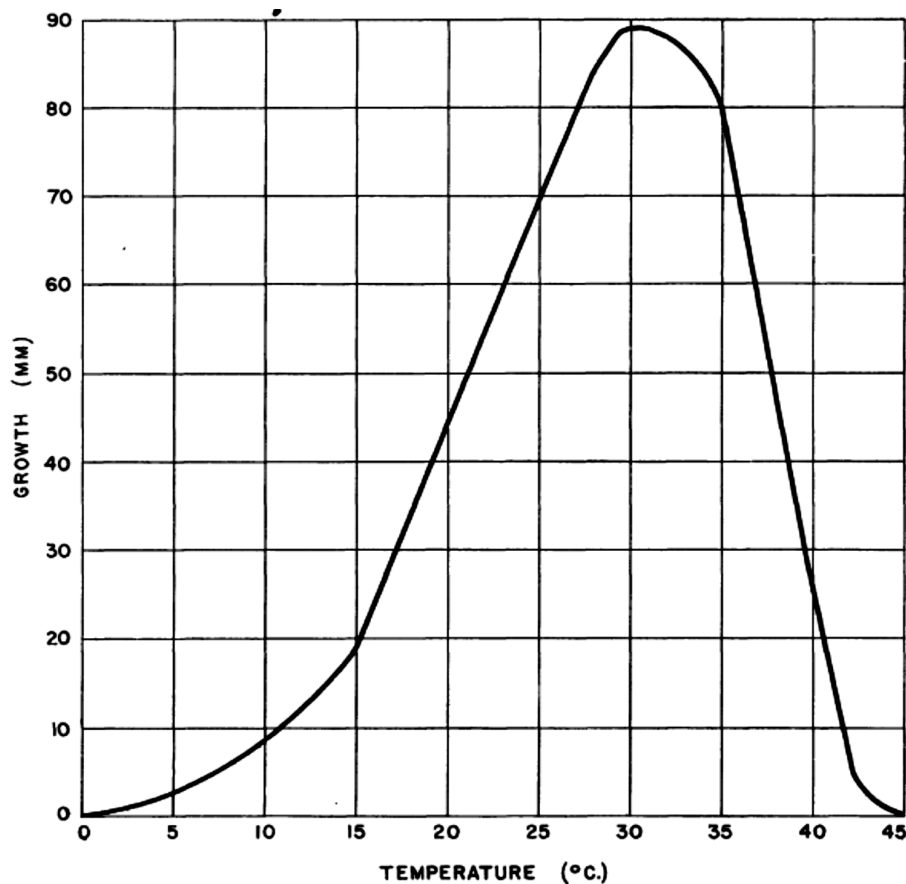


**Figure 2.3 Growth of ten pecan taproots over a 24 hour period when subjected to various temperatures (Woodroof and Woodroof, 1934).**

The root area capable of taking up water and nutrients is important when considering appropriate water and nutrient application zones. Pecan trees usually contain mycorrhizal fungi on the small roots, but these associations are seldom found on large roots (Woodroof and Woodroof, 1934, Sparks, 2005). The roots do not have root hairs, therefore mycorrhizal fungi play a pivotal role in nutrient uptake (Woodroof and Woodroof, 1934, Simard and Durall, 2004), as a healthy symbiotic relationship between the fibrous root system and the mycorrhizal fungi ensures sufficient nutrient uptake. The mycorrhizal roots come at an energy expense to the tree, as respiration rates of the fungi are high. These roots are therefore a strong sink and the mycorrhizal fungus can account for up to 25% of the CO<sub>2</sub> respired by mycorrhizal roots (Kozlowski, 1992). The fine roots also have a high mortality rate during periods of drought, which will regrow once favourable conditions arise (Woodroof and Woodroof, 1934). The energy cost linked to the growth, elongation, thickening and mycorrhizal metabolism of roots severely impacts stored carbohydrate reserves.

These fine roots contribute to the tree's total carbon and nutrient sink, whilst playing an important role in nutrient uptake aiding in tree health. The large taproot, with the lateral and



fibrous system, contributes to starch deposition (Loescher et al., 1990). The root system is the main storage organ for non-structural carbohydrates, as it contains the highest concentration of stored carbohydrates, especially in the secondary xylem tissue (Loescher et al., 1990, Woodroof and Woodroof, 1934). Factors governing the use of these stored root reserves for initiating root growth are complex and variable. Such regulating factors are the status of bud dormancy of shoots, hormonal growth regulator availability, as well as the number of chill units received, days until bud break and the root growth potential (Lacointe, 2000, Kozlowski, 1992, Loescher et al., 1990, Kuden et al., 2013).

### 2.1.3 FLOWERING AND FLOWER MORPHOLOGY

Several types of inflorescences, which are closely related to each other, exist within the *Juglandaceae* family. The exhibited traits can be traced back to a common ancestor that displayed panicle characteristics (Manning, 1938). Pecan flowers are monoecious and develop separate staminate and pistillate flowers (Figure 2.4) (Wood, 2000). Female flowers are typically wind pollination, with cross-pollination required for good fruit set.

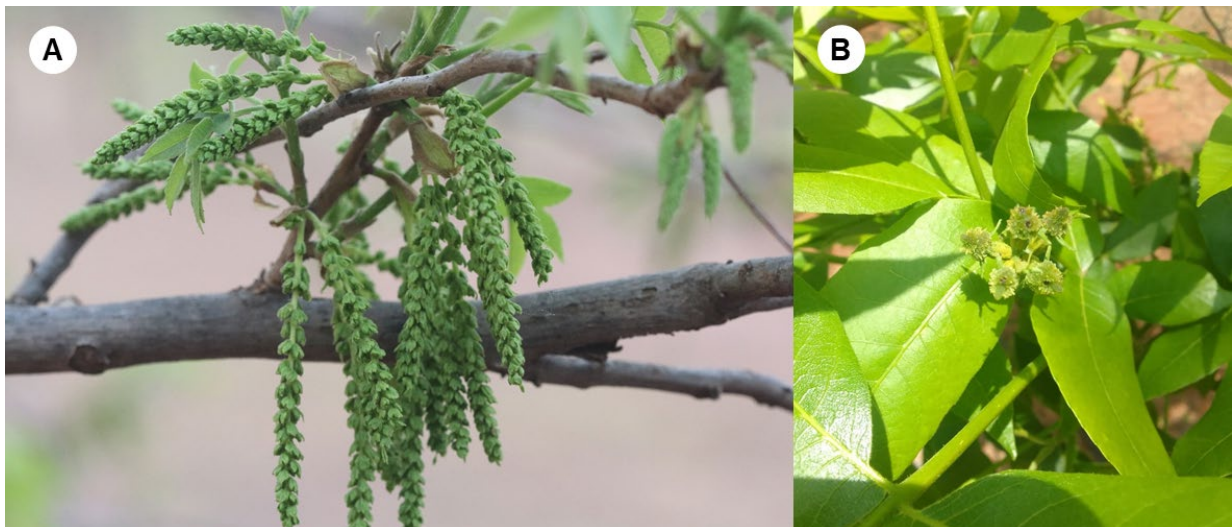


**Figure 2.4 A) Staminate (catkins) and B) pistillate pecan flowers**

Staminate flowers, known collectively as catkins, are located on the base of new shoots borne on the previous season's wood (Figure 2.4A) (Manning, 1938). Catkins typically contain between 100 and 400 individual staminate flowers (Wood, 2000). The pecan does, however, differ from the normal interpretation of staminate flowers, which are described as possessing an unlobed bract and two bracteoles, which cover the anther from three sides, as the pecan tree possesses only tepalled staminate flowers, characterized by a single bract, rounded floral

apex, two lateral bracteoles and three to ten stamens. These staminate flowers vary in length according to cultivar and can be classified into two groups (Manning, 1940, Manning, 1938). The first group has short, thick, compact catkins, with short floral bracts, whilst the second group characteristically have narrow, thin catkins with elongated bracts. The development of new staminate flowers is the same for protogynous and protrandous cultivars, with differences only occurring in the size of the catkin, the length of the bracts and the occurrence of stamen and anther differentiation (Yates and Sparks, 1994).

Protogynous (Type II) and protrandous (Type I) cultivars differ in time of pollen shed and anther receptivity, according to five stages described by Yates and Sparks (1992). In protogynous cultivars female flowers mature before pollen shed, whilst in protrandous cultivars pollen is shed before the female flowers are mature (Wood et al., 1997). There is no difference in the type of pollen between protogynous and protrandous cultivars. Pecan pollen grains vary in size between 43-53  $\mu\text{m}$  and are generally spherical in shape, containing three germ pores. Pollen can travel great distances of up to 2 km to pollinate the female flower (Sparks, 2005). It is important to plant both protogynous and protrandous pecan cultivars that are complementary, in order to ensure sufficient cross pollination occurs (Wood, 2000). In the case of self-pollination, pecans produce low quality nuts and periods of severe fruit drop may occur (Sparks, 2005, Wood, 2000). Protogynous cultivars need to produce sufficient number of pistillate flowers in order to achieve optimal pollination from the protrandous cultivars.

Pistillate inflorescences consist of ten or more individual flowers 5.5 mm to 8 mm in length protruding alongside a central axis, which are borne at the tip of the current season's growth (Figure 2.4B) (Woodroof and Woodroof, 1926). It contains a floral envelope and a pistil, with an absent style, and receptive stigma that varies in shape and colour, according to different cultivars and developmental stages (Woodroof and Woodroof, 1926). The floral envelope contains an anterior bract, two lateral bracteoles and a posterior sepal (Manning, 1940, Shuhart, 1927). Pistillate flowers normally develop on the terminal ends of the branch, but have the ability to be produced on lateral buds if abnormal conditions arise, such as severe frost (Shuhart, 1927, Woodroof and Woodroof, 1926). Shuhart (1927) and Woodroof and Woodroof (1926) described four different types of terminal buds, from which three types are false terminal bearers suited for reproductive pistillate flower development and one is a true terminal bud that has the capacity to bear if unfavourable conditions arise. Regardless of conditions, flower drop occurs where undeveloped terminal flowers, which fail to pollinate, are dropped, leaving a small distinctive scar (Woodroof and Woodroof, 1926). Aborting flowers can be identified by a 65%, 55% and 30% decrease in flower diameter, length and weight relative to non-aborting flowers, as well as a less extended integument (Yates and Sparks,



1994). The location of pistillate and staminate flowers on the tree is important to consider when pruning and tree training practices are implemented, as it will influence fruit set and subsequent nut growth and yield.

#### **2.1.4 NUT GROWTH AND MORPHOLOGY**

Pecans are typically alternate bearers, which is strongly, but not solely, regulated by endogenous factors. Currently there are two hypotheses that explain alternate bearing: 1) the level of accumulated carbohydrate reserves during the dormant season for subsequent fruit and canopy development and 2) carbohydrate reserves in combination with phytohormone levels (Loescher et al., 1990, Wood et al., 2002, Wood, 1995a). The 'on' and 'off' years in the alternate bearing cycle influence the number of flowers produced, which determine the bearing intensity.

The amount of stored carbohydrates and cultivar type both influence the amount of fruit drop that occurs throughout the season. Three waves of fruit drop occur in pecans. The first wave of flower drop occurs in November as a result of insufficient pollination and poor differentiation of the pistillate flowers and can account for 80% of the flowers failing to reach maturity (Isbell, 1928, Woodroof, 1926). The second drop occurs after pollination and can be attributed to two factors; 1) insufficient fertilization and 2) poor endosperm development, which accounts for up to 70% of nut drop depending on the cultivar (Sparks, 2005, Woodroof, 1926, Sparks and Heath, 1972). The third wave of nut drop occurs during the summer as a result of fruit abortion, competition determined by source-sink relationships, disease and pest damage or any unfavourable environmental conditions sufficient enough to induce injury, e.g. water stress (Sparks and Heath, 1972, Woodroof et al., 1928).

Unfavourable conditions vary in their impact on nut growth, as it depends on the timing of these events and the stage of nut development. Pecan nut size is influenced during the early and middle parts of the growing season and nut filling is most affected during the last period of the growing season (Woodroof and Woodroof, 1927). These periods are divided into two phases, which correlates to specific nut growth stages. Phase I is endosperm development and phase II is embryo growth (Figure 2.5) (Herrera, 1990). The different stages of nut development are presented in Figure 2.6. Phase I, which encompasses the period of pistillate receptivity until endosperm development and can be influenced by; unfavourable temperatures that prevent sufficient pollination from occurring, insufficient accumulation of heat units, nutritional deficiencies and water stress (Sparks, 2005, Finch and Van Horn, 1936,

Herrera, 1990). During phase II, that is characterized by nut filling, the tree is most vulnerable to nutrient and water stress that can impact nut filling quite severely (Finch and Van Horn, 1936, Woodroof et al., 1928). During the critical stage of nut filling the nutritional and water status of the tree should be optimal to ensure adequate nut size and even nut filling.

The nut filling stage is the period in which embryo growth occurs, filling the cavity first proximally and then laterally and can be divided into three separate periods according to the rate of mass increase during development (Herrera, 1990). The first stage starts at full bloom up until 40 days after bloom (DAB), and during this phase nut growth occurs slowly (Finch and Van Horn, 1936). The second stage starts 40 DAB and continues until 150 DAB and is characterized by a rapid increase in nut growth, as a result of the hull, shell and kernel gaining size and mass (Finch and Van Horn, 1936). The third and last stage starts 150 DAB and continues until 180 DAB. During this stage the nut decreases in mass because outer hull dehydration commences and the husk hardens off (Finch and Van Horn, 1936).

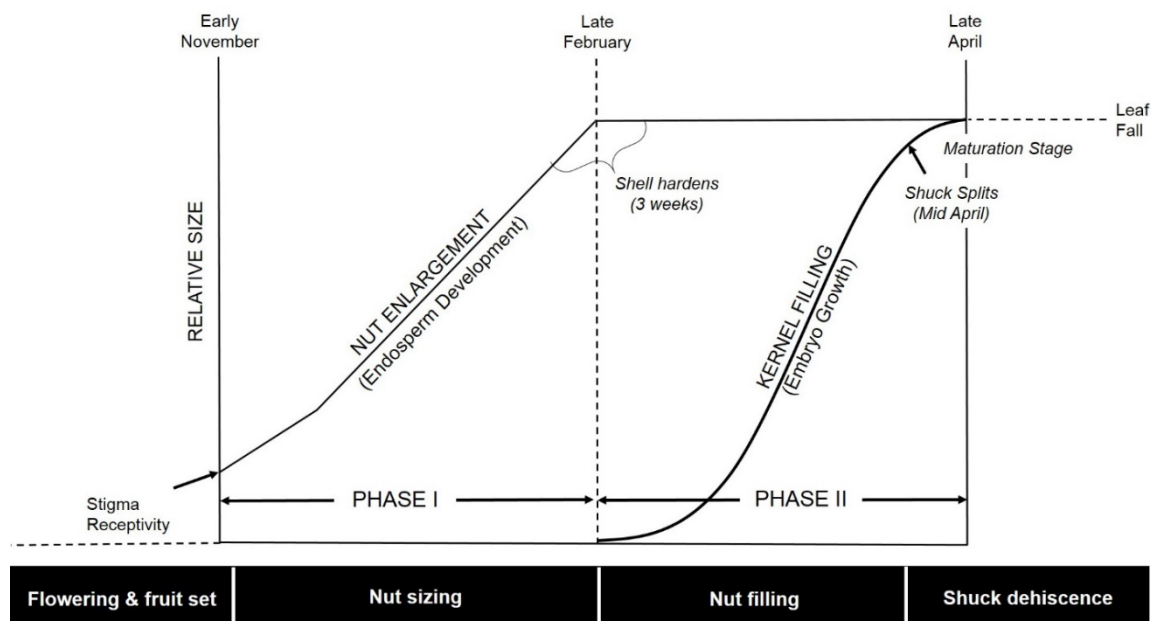


**Figure 2.5 Relative fruit growth rate and average fruit development stages for 'Ideal' and 'Western' pecans in the Mesilla Valley, New Mexico (Herrera, 1990). Dates are for the Northern Hemisphere. Approximate dates (from left to right) for the Southern Hemisphere are November, February and April.**

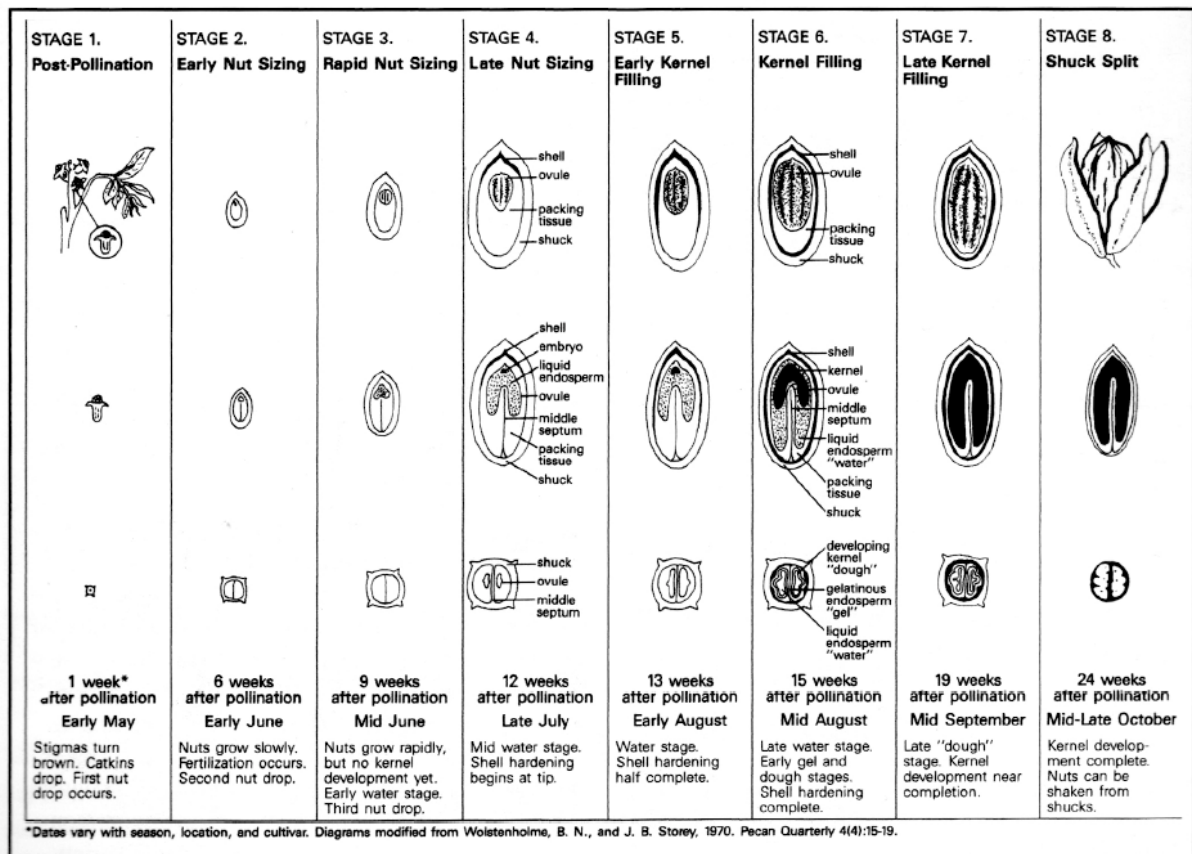


**Figure 2.6 Developmental stages of pecan nuts (Wells and Conner, 2007)**

The harvestable pecan nut consists of four distinctive components, which include the hull, shell, packing tissue and middle septum (Figure 2.7) (Sparks, 2002). The hull is a modified calyx that increases in size, thickness and tannin formation during development (Woodroof and Woodroof, 1927). The hull encloses the entire nut until maturity is reached and the dehydrated hull bursts open exposing the shell to the environment. The shell is the ovarian wall that increases in size and thickness up until shell hardening commences (Finch and Van Horn, 1936, Woodroof and Woodroof, 1927). Shell hardening occurs from the apex to the base of the nut in the three weeks just prior to maturity (Woodroof and Woodroof, 1927). Underneath the shell, the ovarian cavity is split in two by the middle septum. The middle septum consists of two types of tissue that splits the cotyledons of the kernel from the base to the apex of the septum (Woodroof and Woodroof, 1927). The middle septum contains an array of complex vascular bundles that protrude into the tissue of the cotyledons (Finch and Van Horn, 1936). The kernel fills all the available space between the middle septum and serves as the economically valuable component of the pecan nut. According to Woodroof and Woodroof (1927), the pecan kernel increases in dry matter and oil percentage as a result of carbohydrate transformation that occurs as the nut reaches maturity. Oil is a lipid compound and requires large amounts of energy to synthesize (De Vries, 1975). It is therefore important to maintain

high levels of carbohydrate reserves during the nut growth and oil accumulation periods to achieve optimal yield and quality (Sparks, 2005).



**Figure 2.7 Anatomy of a mature pecan nut**

## **2.2 PECAN WATER USE**

Crop water use or evapotranspiration (ET) is the combined water loss in vapour form by a crop through evaporation from the soil ( $E_s$ ) and through plant transpiration (T) (Allen et al., 1998). In most agricultural fields such as orchards, T may include evaporation from both the crop of interest and a cover crop (Ferreira et al., 2012). In commercial agricultural systems, T losses are deemed beneficial as they are directly involved in plant productivity whilst  $E_s$  losses are considered non-beneficial. This implies that accurate quantification of both components of ET is important to develop and/or adopt strategies that maximise T and minimise  $E_s$  (Jovanovic et al., 2020). As the primary user of water worldwide, adopting such strategies in irrigated crops is mandatory, especially under the current global water scarcity and the increasing pressure for agricultural sectors to implement on-farm water management practices to ensure that the needs of all users can be met. Although having been explored primarily, under the rubric of the Food and Agriculture Organization (FAO) guidelines, accurate estimates of ET in commercial orchards are still the subject of many studies (Kool et al., 2014). There are still gaps in the knowledge of practical illustrated guides for farmers detailing factors impacting T and  $E_s$  from orchards, how to make general information specific to their location and possible ways of making water savings during a production season. This is not surprising as orchards resemble a complex system with different management practices such as pruning and training, irrigation and planting densities. Nonetheless, sustainable irrigation management requires accurate quantitative information on evapotranspiration (ET), the second largest water balance component in orchards (Villalobos et al., 2013).

In terms of measuring and estimating water use, pecans (*Carya illinoensis*) share difficulties with most orchards. Firstly, they are grown in different parts of the world with contrasting climatic conditions (i.e. the United States of America, Mexico, China, Australia, Israel, and South Africa). This means water use models need to be comprehensively tested and universal parameterization of simple semi-empiric models such as those proposed by Samani et al. (2011) may need to be adjusted to local conditions (Ibraimo et al. (2016). Secondly, there is still a need to understand the physiological control of transpiration by pecan trees (Gutschick and Sheng, 2013). It has been demonstrated that under conditions of high atmospheric demand (particularly as the vapour pressure deficit (VPD) surpasses 1.4 kPa), pecan T does not increase at the same rate as the VPD increases (Ibraimo, 2018). However, Andersen and Brodbeck (1988a) reported an increase in T under conditions of high atmospheric demand. The authors attributed this to the fact that pecan trees evolved an efficient water transport system in their native natural floodplain habitat. This threshold-type of relationship suggests that there may be some physiological control that could be linked to the hydraulic capacity of the tree.

Another challenge is the use of the canopy conductance ( $G_c$ ) for estimating T of pecan trees. Differences in stomatal conductance due to leaf age which ultimately translates to a possible season  $G_c$  variation has been reported by Andersen and Brodbeck (1988a). Although this has been acknowledged by Gutschick and Sheng (2013) and Ibraimo (2018), the seasonal dynamics and magnitude of leaf conductance and ultimately  $G_c$  in pecan trees remain unclear.

Lastly, pecan orchards represent heterogeneous systems that are characterised by trees in rows interspaced with bare ground and are sometimes frequently irrigated (Abudu et al., 2016, Ibraimo, 2018, Samani and Bawazir, 2015, Sammis et al., 2004b, Samani et al., 2009, Wang et al., 2007c). This means that the two components of ET (T and  $E_s$ ) are equally important., Therefore, to provide accurate water use estimates,  $E_s$  and T should be measured or estimated separately. Different studies on pecan water use have been conducted and the published data for pecan in different growing regions of the world are summarized in Table 2.1

**Table 2.1 Evapotranspiration of pecan orchards reported in literature.  $f_c$  is fractional canopy cover; ET is evapotranspiration and T is transpiration. All data indicates seasonal ET, unless otherwise specified.**

Reference	Tree age (years)	Canopy size ( $F_c\%$ )	ET or T (mm)	Measurement method	Irrigation method	Climate
Miyamoto (1990)	5		ET = 530	Soil water balance	Flood	Arid, desert
	15		ET = 920	Soil water balance	Flood	Arid, desert
	25		ET = 1160	Soil water balance	Flood	Arid, desert
Bawazir and King (2004)	40-65		ET = 1479	Eddy covariance	Flood	Arid, desert
Sammis et al. (2004b)	30	65-70	ET = 1420	Eddy covariance	Flood	Arid, desert
Wang et al. (2007c)	2-35 (16 orchards)	3-70%	*ET=0.55-8.4 mm day <sup>-1</sup>	Eddy covariance and Remote sensing	Flood	Arid, desert
Samani et al. (2009)		2.5-80	ET = 413-1095	Remote sensing	Flood	Arid, desert
Ibraimo et al. (2016)	36		ET=985 T= 888	Sap flow and modelled E	Micro-sprinkler	Semi-arid, subtropical
	37		ET= 1050 T= 861	Sap flow and modelled E	Micro-sprinkler	Semi-arid, subtropical

From the data in Table 2.1 it is evident that pecans have a high seasonal water use with ET ranging between 920-1479 mm for a season for mature trees. When commenting on the water use of different orchards, Wang et al. (2007c) indicated that pecan trees have higher levels of ET than most crops. However, considerable differences have been observed (Table 1), These differences may be due to various factors including tree age, atmospheric evaporative demand and canopy size among other factors (Miyamoto, 1983, Wang et al., 2007c). The influence of the canopy size can be observed from the study by Miyamoto (1990) (Table 1) where water use varied according to the different canopy size classes, with the young orchard (5 years old) have the smallest value of 530 mm, whilst the orchard with 15 year old trees had a value of 920 mm and the matured orchard (25 years) showed the highest seasonal value of 1160 mm.

Whilst the cited studies in Table 1 have provided the combined quantification of  $ET_c$ ,  $E_s$  can also be the major component of ET, but there is little quantitative information on the separate measurement or assessment of the  $E_s$  component. Often,  $E_s$  is quantified as a residual from ET and T. However, when obtained as a residual of the two components, the resultant  $E_s$  is not solely from the soil but also from other surfaces such as bodies of water and evaporation

from underground cover (Kool et al., 2014). Although the processes occur simultaneously,  $T$  is disconnected from the soil's physical conditions related to  $E_s$ . Under non-limiting soil water conditions, pecan  $E_s$  varies due to spatiotemporal soil water content, canopy structure (shape and size), and weather conditions (particularly the atmospheric evaporative demand) (Ibraimo, 2018). These factors have a direct influence on the fraction of wetted area and the degree of shading, which ultimately influence the rate of evaporation through the limitation of the two stages of  $E_s$ . Despite the interlinking of these factors, a study by Ibraimo (2018) indicated that the canopy size was the overriding factor controlling  $E_s$  of young pecan trees grown under different densities (10 m x 10 m and 5 m x 10 m). The low-density orchard showed a seasonal value of 336 mm or 80% of ET, whilst the high-density orchard recorded a seasonal value of 273 mm or 70% of ET. Since the trees were grown in the same orchard (under the same orchard management practices: irrigation, pruning strategies, and orchard floor management), the spatial variation in  $E_s$  of the trees was attributed to the differences in the canopy size, i.e. the effective fractional cover ( $f_{c\text{ eff}}$ ) between the trees. Accurate measurements of changes in canopy size are important for  $E_s$  quantification.

## 2.3 FACTORS AFFECTING WATER USE IN PECANS

Under adequate soil water conditions, the factors that influence pecan water use ( $T$  and  $E_s$ ) can be broadly categorized under (1) environmental factors, i.e. air temperature ( $T_a$ ), solar radiation ( $R_s$ ) and VPD, (2) tree related factors such as hydraulic dynamics to water flow, physiological conductances, canopy structure (i.e. size, shape) (3) management practices (pruning, irrigation practices, orchard floor management) and (4) soil characteristics (Wang et al., 2007c). Whilst both the magnitude of  $T$  and  $E_s$  can be influenced by atmospheric conditions, the rate at which  $E_s$  occurs is further determined by the availability of water in the surface soil and the effect of shading by canopies whilst the rate of  $T$  is additionally governed by the physiological characteristics of the trees. Commenting on the understanding of water use in pecan orchards Deb et al. (2012) highlighted that for plant water status indicators to be used for irrigation scheduling, there is a need for a complete understating of the variation of soil water content (in root-zone), distribution of plant roots, careful monitoring of plant growth characteristics and the atmospheric evaporative demand.

### **2.3.1 ENVIRONMENTAL FACTORS**

Transpiration in pecans species varies diurnally and seasonally in response to environmental factors. The fluctuation of these factors directly influences the atmospheric evaporative demand and ultimately the rate of T. Under non-limiting soil water conditions, pecans transpiration exhibits a linear relationship with the atmospheric demand, i.e. reference evapotranspiration ( $ET_o$ ) and vapour pressure deficit (VPD), until it reaches a plateau (at  $4 \text{ mm day}^{-1}$   $ET_o$ , VPD 1.4 kPa and  $R_s = 21 \text{ MJ m}^{-2} \text{ day}^{-1}$ ). Beyond that point the rate of increase of T with increasing VPD begins to decline, most likely as a result of stomatal closure. This suggests that perhaps T in pecans is supply-limited (Ibraimo, 2018). The effects of air temperature have an indirect effect on ET through interaction with other factors such as atmospheric demand. It also plays a major role in canopy development, phenological stages and ultimately the length of the season. Generally, in woody plants, the influence that  $E_s$  is linearly dependent on the energy available and water gradients in the soil until the soil is dry enough to reduce the soil hydraulic conductivity (Bonachela et al., 1999, Bonachela et al., 2001, Ibraimo, 2018, Paço et al., 2012, Villalobos et al., 2000, Zhao et al., 2013, Allen et al., 1998). The evaporation of water from soil is a physical process, governed mostly by atmospheric conditions, the availability of water in the surface soil and the effect of shading by canopies.

### **2.3.2 MANAGEMENT PRACTICES**

Different crop management has been used to manipulate beneficial and non-beneficial crop water use to cope with conditions of water scarcity (Jovanovic et al., 2020). Orchard management practices such as pruning and training, among others, have a major influence on the water use of orchard tree crops. Canopy size reduction practices, such as pruning, largely contribute to a reduction in water use, particularly T of orchard trees (Ferreles et al., 2012). Pecan orchards are pruned for various reasons, such as rejuvenating old trees, controlling disease, to facilitate harvesting and to allow solar radiation penetration in the inner canopy (Andales et al., 2006). This results in decreased leaf area and canopy solar radiation interception, which ultimately reduces T and increases  $E_s$ . Often, a reduction in T usually translates to an unwanted reduction in crop yield, hence, water savings that logically target the reduction of the non-beneficial water use ( $E_s$ ) are important. These include the use of mulch, localized irrigation systems and cover crop. However, there is a debate that the cover crops could also significantly contribute to an increased orchard water use (Ntshidi et al., 2021).



### 2.3.3 TREE-RELATED FACTORS

#### 2.3.3.1 Hydraulic flow resistances

Transpiration in trees is controlled by the atmospheric evaporative demand and limited by stomatal conductance ( $g_s$ ) which is regulated, to a certain extent, by water availability (Mirfenderesgi et al., 2016). This process is depended on the well-coordinated hydraulic architecture of the tree which determines the water uptake and transport through total (soil-to-leaf) hydraulic conductance ( $G_t$ ) within the tree (Meinzer, 2002). The total hydraulic conductance can be viewed as a measure of the ability of the soil to supply water to the transpiring leaves (Hubbard et al., 2001). Assuming a lack of significant water storage, a valid assumption in some crops (Cohen et al., 1983),  $G_t$  can be calculated using equation 1 which states that under steady-state water flow conditions,  $G_t$  is described by the relationship between  $T$  and the water potential difference between the roots ( $\Psi_{root}$ ) and the leaves ( $\Psi_{leaf}$ ) (Alarcón et al., 2003, Meinzer, 2002). The 'steady state' condition means that the water uptake by the roots must be equal to the water loss by leaf transpiration. Therefore,  $G_t$  can be calculated as:

$$G_t = T / (\Psi_{root} - \Psi_{leaf}) \quad (1)$$

Mathematically, equation 1 means that 'under non-limiting soil water conditions with negligible soil to root resistance (the inverse of conductance) for water flow, the efficiency of water transport to leaves may be explained by measuring the response of  $\Psi_{leaf}$ . So, under high evaporative demand, a small decrease in  $\Psi_{leaf}$  would indicate a low resistance or a high conductance which indicates an efficient water transport system in the tree (Blackman et al., 2019).

However, the use of equation 1 is an oversimplification of water transport in some trees. Studies have shown that plants have an internal water storage pool, hence they violate the 'steady state flow' (Blackman et al., 2019, Lambers et al., 2008b, Moreshet and Green, 1984, Steppe, 2004). As a result, a modification of the Ohms law analogy had been proposed which includes a dynamic water flow and further introduced the electric-equivalent capacitors concept (Mirfenderesgi et al., 2016). This allows the water flow into a part of the SPAC ( $F_{in}$ ) to be different from the water flow going out ( $F_{out}$ ). At this point, the water flow in xylem vessels can be compared with the flow in cylindrical pipes whereby the amount of water that can move through the xylem per unit time is proportional to the fourth power of the radius of the pipe (i.e.

xylem) (Lambers et al., 2008b). Hence, any evolutionary change in vessel diameter in the xylem will alter or modify the hydraulic traits of the tree (Steppe, 2004).

Although the influence of  $G_t$  on  $T$  has been well documented, there is still uncertainty on the partitioning or the location of the greatest hydraulic resistance (Williams et al., 2001). However, studies have shown that it varies greatly with crops and species (Alarcón et al., 2003, Cohen et al., 1983, Moreshet and Green, 1984, Nardini and Tyree, 1999, Rodríguez-Gamir et al., 2010, Tyree et al., 1998). Understanding the dynamics of  $G_t$  in plants is important for plant-dependent irrigation control, especially in the context of isohydric (water conservers) and anisohydric (water spenders) responses to soil water deficits (Sperry et al., 2008, Steppe et al., 2008) (Figure 2.8). This is particularly important as global water supplies are limited and commercial growers need to apply water during the most sensitive periods to stress.

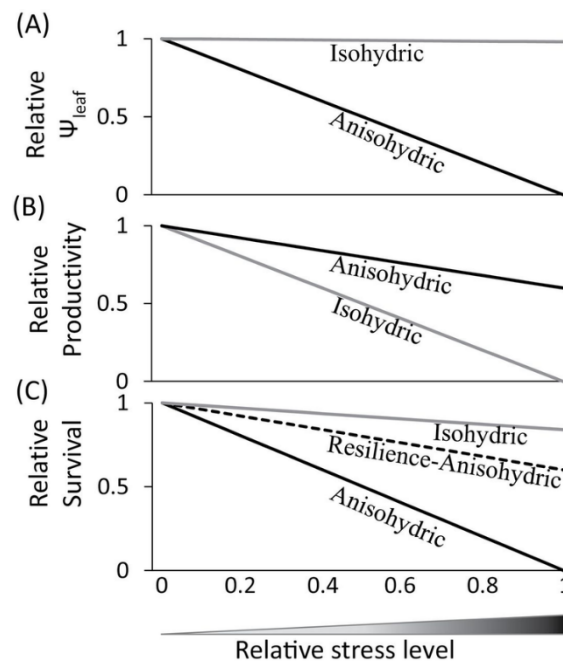


**Figure 2.8 Conceptual model for the behaviour of isohydric versus anisohydric plants by regulating (A)  $\Psi_{\text{leaf}}$ , (B) productivity, and (C) survival in response to increasing relative changes in the stress level (i.e. decreasing soil water content) (Attia et al., 2015)**

In pecan trees, the ability to transport water remains unclear. Early studies (Anderson and Brodbeck 1988, Wolstenholme 1979) reported that pecans have efficient water transport, with the trees having their stomates opened even under high evaporative demand and having midday water potentials of -1.9 MPa. The same sentiments were shared by Steinberg et al. (1990), during a study aimed at characterizing the water transport system in young pecan trees. The authors observed a  $\Psi_{\text{leaf}}$  of -2.0 MPa without any changes in transpiration rate, high

hydraulic conductance and low capacitance (i.e. no significant lag along the transpiration stream). This allowed them to conclude that when compared to other woody species, pecan trees have effective water transport. Ibraimo (2018) observed that under high evaporative demand especially as the vapour pressure deficit (VPD) reaches 1.4 kPa,  $T$  reaches a threshold point. Suggesting that under high atmospheric demand, there is an imbalance between the demand and the supply of water to the transpiring leaves. Since the rate of supply depends on the hydraulic capacity of the xylem pathway, the study by Ibraimo (2018) suggests that there may be some physiological control that could be linked to the hydraulic capacity of the tree. Such behaviour has been observed in citrus species (Cohen et al., 1983) although the absolute threshold values were lower than the ones observed in pecan trees. The physiological control of transpiration in citrus was attributed to high resistance to water flow found in the roots-to-stem pathway, which was linked to the root anatomy of the trees. Smit et al. (2020), observed a strong stomatal control in macadamia nut trees which was attributed to hydraulic limitation that exists in the stem to leaf pathway. However, there are no studies that have been conducted to quantify the dynamics and the possible location of the hydraulic limitations that have been suggested by the findings of Ibraimo (2018). Schultz (2003) suggested that the inability to supply sufficient water to the leaves is a result of hydraulic limitations of the xylem. Furthermore, it is still unclear if pecan trees are isohydric or anisohydric or if they have a dynamic water management strategy, i.e. they can shift from isohydric-like behaviour to anisohydric-like behaviour in response to changing environmental conditions and possibly due to fruit load (Sade and Moshelion, 2014). However, it is acknowledged that they are well adapted to different growing conditions especially semiarid and arid climatic regions.

#### *2.3.3.2 Canopy size and phenological stages*

The size of the canopy is one of the major factors resulting in differences in water use and its partitioning in orchard fruit trees such as pecans. Generally, under standard conditions mature orchards have higher water requirements compared to young or immature orchards (Sammis et al., 2004a, Sammis et al., 2004b). Therefore, for basic irrigation infrastructure planning, pecan growers should consider the rapid increase in water use from planting to maturity (Sammis et al., 2004a). Given the importance of the size of the canopy in relation to water use of crops, growers must be equipped with a reliable and cost-effective method for quantifying/ and or estimating the temporal and spatial changes in canopy size (Rosell and Sanz, 2012). The significance of canopy size in determining tree water use in orchard crops was demonstrated in several studies using different measures of canopy size, i.e. leaf area density (LAD) (Testi et al., 2006, Orgaz et al., 2006), leaf area (Angelocci et al., 2004, Castel, 2000),

shaded area (Williams et al., 2003, Ayars et al., 2003, Goodwin et al., 2006, Green et al., 2003), interception of radiation by the canopy (Consoli et al., 2006, Williams and Ayars, 2005a, Espadafor et al., 2015) and canopy cover (Samani et al., 2011). Although different canopy size descriptors were used, the authors highlighted the characterization of canopy size as an important variable in measuring and/or modelling water fluxes. Similar observations were made by Ibraimo (2018) in pecans, but unlike the studies mentioned above, Ibraimo (2018) did not evaluate the direct relationship between the canopy size and water use but concluded that canopy size is one of the major determinants of transpiration in pecan orchards. A study by Abudu et al. (2016) on pecan water use indicated that despite other factors such as the differences in plant physiology and the atmospheric evaporative demand contributing to the differences in water-use rates, the canopy size and its management were the dominant factors.

Pecan trees are deciduous, and canopy changes throughout the season are usually characterised by rapid growth during the start of the season until midseason and then plateau, followed by senescence at the end of the season (Sammis et al., 2004a). This trend is also observed in transpiration of pecan trees, indicating the need to adjust transpiration of these trees to canopy size. Apart from the work of Samani et al. (2011), there have been no attempts to study the relationship between canopy size and  $K_c$ . Somewhat surprisingly, considering the importance of the canopy size in relation to orchard water use, simple, readily applicable, and cost-effective methods for quantifying canopy size in orchards remain a challenge, as frequently either expensive and/or complex approaches are used (Dong et al., 2020). Oftentimes canopy size in orchards is measured using commercial light sensors. Light sensors are based on monitoring the light-shadow windows of a tree on the ground or the gap fraction within the canopy (Giuliani et al., 2000). For a heterogeneous canopy such as the one found in pecan orchards this implies that several measurements should be made to account for the temporal and spatial variability within the canopy making the measurement time consuming and expensive to be performed in all possible conditions. This is a major drawback because a precise estimation of the canopy size at any specific growth or production cycle in pecan orchards may help to establish accurate adjustments of irrigation in relation to crop water use.

## **2.4 METHODS OF ESTIMATING CANOPY SIZE IN ORCHARDS**

Different approaches have been used to measure or estimate canopy size in orchards. This includes direct measurements such as the use of manual tape measure methods and destructive sampling (Ouyang et al., 2020). Canopy structural parameters can also be

indirectly obtained by analysis of light penetration in the canopy using commercial sensors such as ceptometer (Anthony and Minas, 2021). Most recently, ground-based and aerial image analysis techniques using high tech-sensors and mobile applications that are capable of making field measurements have been used to obtain different canopy sizes measures such as leaf area index (LAI), canopy dimensions (height and widths) and canopy volume among others (Gautam et al., 2021).

Although the use of canopy light sensors to estimate canopy size is usually characterised by high cost, time-consuming, and sometimes requires expertise to interpret results, they remain one of the widely used techniques in crops particularly orchard crops (Rosell and Sanz, 2012). The wide use can be attributed to the fact that canopy radiation interception is related to crop growth (photosynthesis and transpiration), a subject of interest to many agricultural scientists (Westling et al., 2018). Generally, the relationship between canopy size and water use occurs due to the interception of solar radiation. In addition, the recent exploitation of water use models as a solution to eliminating the problems associated with water use measurements in complex stands (i.e. orchards and forests) automatically guarantees the interest in radiation interception models, which are often incorporated in water use models (Sinoquet et al., 2001). Also a study by Sammis et al. (2004a) indicated that for young pecan trees, water use was proportional to the amount of solar radiation intercepted by the canopy. Furthermore, canopies in orchard trees are constantly pruned mainly to favour the entry of light through the canopy (GarcíaOrtiz et al., 2008) hence, the use of light interception seems reasonable in comparison to other canopy size estimates such as the canopy volume which is a crude estimate of the canopy size because several assumptions are made about the canopy shape (Puppo et al., 2019). These often lack the accurate characterisation of the canopy elements that influence transpiration. On the other hand, canopy size measures such as the leaf area index (LAI) and the canopy density (the amount of leaf area per canopy volume) are not easy to obtain (Andújar et al., 2019). This implies that a thorough investigation of the dynamics of canopy light or radiation interception in orchard crops is both relevant and important in water use studies.

Equally important, and widely adopted canopy size estimating technique is the use of aerial and ground-based image analysis (Tu et al., 2019). Assessing spatial and temporal variability of orchard crops for agricultural management requires intensive and periodical information gathering from the orchards. The use of drones that are equipped with standard red, green, blue (RGB), multispectral and thermal cameras to acquire high-resolution aerial images that can be used for monitoring crop health, crop yield and canopy properties provide an effective tool for growers and farm managers for such assessment (Parker et al., 2020). Multi-spectral

imagery acquired from an unmanned aerial system has been demonstrated as an accurate and efficient platform for measuring various tree structural attributes, but research in complex horticultural environments such as pecans trees has been limited. Advances have come from the use of different remote sensing techniques and aerial images especially from unnamed ariel vehicle (UAV).

#### **2.4.1 AERIAL AND GROUND-BASED IMAGERY**

Unmanned Aerial Vehicles (UAVs) or drones are remotely controlled small aircraft that can take ariel geo-referenced and high-resolution crop images using a Global Positioning System (GPS) and specialised thermal and multispectral sensors (Nhamo et al., 2020). Drone ariel images can provide a low-cost generation of three-dimensional geomatic products such as point clouds and two-dimensional composite maps such as Digital Surface Models (DSMs) using photogrammetry software such as Pix4D mapper. These have laid a good foundation for canopy information measurements in orchards. As a developing tool, UAV-based images have been used to generate non-destructive measurement of canopy structural features in orchards such as size, volume, projected ground cover, height, canopy dimensions.

UAV measurement technology is highly efficient and non-destructive and is suitable for large-scale measurement of information about orchards and field crops. Compared with the ground measurement method, this technology is more suitable for applications in large, modern precision agricultural production management.

Geometric features such as canopy projected area, length and canopy width can be automatically calculated from the created orthophotograph mosaics using any open source geographic information system software such as QGIS and ArcGIS among others (Torres-Sánchez et al., 2018). Apart from assessing canopy growth, UAV-based image technology can be used for crop management practices such as pruning (Jiménez-Brenes et al., 2017). Alternatively, canopy structural parameters can be estimated using ground-based images, which have recently become obtainable using smartphones application that can take upward-looking imagery and can offer an objective and accurate solution to the measurement of canopy parameters such as plant leaf area index, canopy cover, canopy volume and canopy porosity (Ouyang et al., 2020). Among these, is the use of VitiCanopy app, which is cable of of estimating canopy porosity.

## **2.4.2 CANOPY RADIATION INTERCEPTION**

Radiation interception by the crop canopy affects all components of canopy microclimate including the partitioning of evapotranspiration (ET) between evaporation directly from the soil (E) and T. This is more so because the fraction of solar radiation intercepted by the canopy is the parameter that accounts for the influence of canopy size in T, one of the key determinants of water use in pecans and orchard tree crops in general (Wang and Wang, 2017, Wang et al., 2007b). The light distribution within crop canopies is dependent upon the features of plant canopy architecture, such as leaf number, leaf size, shape, curvature, and leaf inclination and azimuth, which is highly spatiotemporally variable.

Canopy radiation interception by crops has been studied for several reasons: (1) to estimate photosynthetic rates and biomass production (Monteith, 1977), (2) to estimate crop water use from the amount of solar energy available to drive evapotranspiration (Annandale et al., 2004), and (3) to estimate canopy structural characteristics, such as canopy size (canopy density, LAI) and shape (Giuliani et al., 2000). Canopy radiation interception is quantified by computing the differences between incoming radiation at the top of the canopy and the bottom of the canopy. Measurements of radiation interception in homogenous canopies are easier compared to those in heterogeneous stands, such as orchard canopies (Mariscal et al., 2000). In orchard canopies, diurnal fractional radiation interception of a given tree, or an orchard, will vary depending on the time of the day, row orientation, slope and aspect, time of year and the canopy size. Hence, accurate measurements of radiation interception in orchards require that measurements be integrated over time and space (in case of two or three-dimensional crops) (Wünsche et al., 1995). Direct measurements are usually taken using hand-held solar radiation sensors (such as a ceptometer) or sensors that can be installed beneath the canopy, such as tube-solarimeters and line quantum sensors (Johnson et al., 2010). These sensors are normally installed in a square grid to capture the variation beneath the canopy and in the alley; or, in terms of the ceptometer, the sensors are moved quickly to various grid positions and repeated readings are made over time. This is time-consuming, and accurate measurements can be limited by the number of available sensors (Zarate-Valdez et al., 2015). In addition, making such measurements in large fields in a short time is difficult. As a result, the use of radiation interception models capable of estimating radiation distribution within a canopy of any form using canopy characteristics (shape, size, and dimensions) is often used (Rojo et al., 2014). When leaves are not on the tree, the branches intercept 14% of the solar radiation.

## 2.5 MODELLING RADIATION INTERCEPTION IN FRUIT TREES

The use of radiation interception models as a measure of canopy density in crops was initiated by Monsi and Saeki (1953). These authors introduced the concept of Beer's Law, which relates the attenuation or the extinction of solar radiation to the properties of the material through which the solar radiation is traversing. Ideally, the law states that the extinction of solar radiation is an exponential function of the path length through the medium (equation 2) (Figure 2.9). In plant canopies, this implies that the canopy acts as a turbid homogeneous medium, and as the solar beams pass through the canopy, it will decay exponentially with the cumulative leaf area index (LAI) as one moves deeper into a canopy (Teh, 2006). Therefore, the amount of solar radiation below any homogeneous canopy is given by:

$$I = I_0 \exp(-kL) \quad (2)$$

Where  $I$  is the amount of direct solar radiation below the canopy,  $I_0$  is the amount of solar radiation above the canopy,  $k$  is the extinction or attenuation coefficient, and  $L$  is the cumulative LAI.

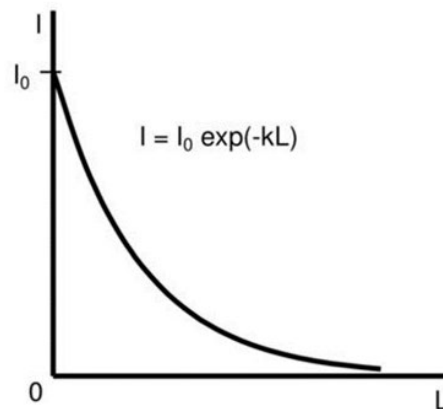


**Figure 2.9 Attenuation of irradiance through a canopy according to Beer's Law (Teh, 2006).**

Equation 2 is valid for canopies that are uniformly distributed and continuous. In discontinuous canopies such as orchards and isolated trees (i.e. young trees), the amount of intercepted radiation will be overestimated since it violates two assumptions (that the leaf area is randomly distributed and that the canopy is continuous) and the error is directly proportional to the discontinuity of the canopy (Teh, 2006). To account for radiation interception in such canopies, Jackson and Palmer (1979) developed a simple geometric model capable of estimating solar radiation interception in discontinuous canopies. The authors suggested that solar radiation



distribution in canopies be explained in terms of transmission or interception. In discontinuous canopies, such as orchards, this is explained using two components: (1) the solar radiation that passes between the canopy ( $\tau_f$ ) and (2) the solar radiation that traverses through the canopy ( $\tau_c$ ), which is therefore attenuated. The value of  $\tau_f$  is dependent on solar altitude and azimuth and is therefore greatly influenced by time of day, time of the year, row orientation, and latitude, whilst  $\tau_c$  depends on the leaf area and its arrangement within the canopy. To calculate the solar radiation transmitted in discontinuous canopies ( $\tau_d$ ) the authors used the sum of the two components as:

$$\tau_d = \tau_f + \tau_c \quad (3)$$

Then solar radiation interception in fractional terms is therefore calculated as:

$$fIPAR = 1 - \tau_d \quad (4)$$

And the maximum interception value by an orchard of any form will be:

$$fIPAR_{max} = 1 - \tau_f \quad (5)$$

For a hedgerow of a defined profile,  $\tau_f$  integrated over the desired period can be calculated from the trigonometrical relationships between cast shadow length, solar altitude and azimuth and the diffuse solar radiation distribution from an overcast sky (Cain, 1972; Jackson and Palmer, 1972). The calculation of  $\tau_c$  requires information about the canopy structure (amount of leaf area and its arrangement) through which the solar beam must pass to reach the ground. Under uniform or homogenous plant canopies, such as wheat, the total interception in the field can be easily obtained using equation 2 multiplied by the area of interest. In orchard systems, (as indicated by equation 3), solar radiation interception will depend on the canopy geometry, the angle of the sun, the azimuth, and the structural change of the canopy during growth. Ideally, an efficient model in hedgerow crops should be based on estimating parameters of the area covered by the canopies and should include the development of the canopy from early stages to continuous and/or discontinuous matured canopies (Oyarzun et al., 2007). For continuous canopies (hedgerows), two-dimensional models are more suitable since the canopy exhibits only one horizontal discontinuity, which means it is continuous along the rows, as shown in Figure 2.10 (Cohen et al., 1987). In addition, some authors have considered the importance of the competition from neighbouring trees when estimating radiation interception in hedgerows. This is important with tall trees, closely spaced, at low sun angles (Annandale et al., 2004)

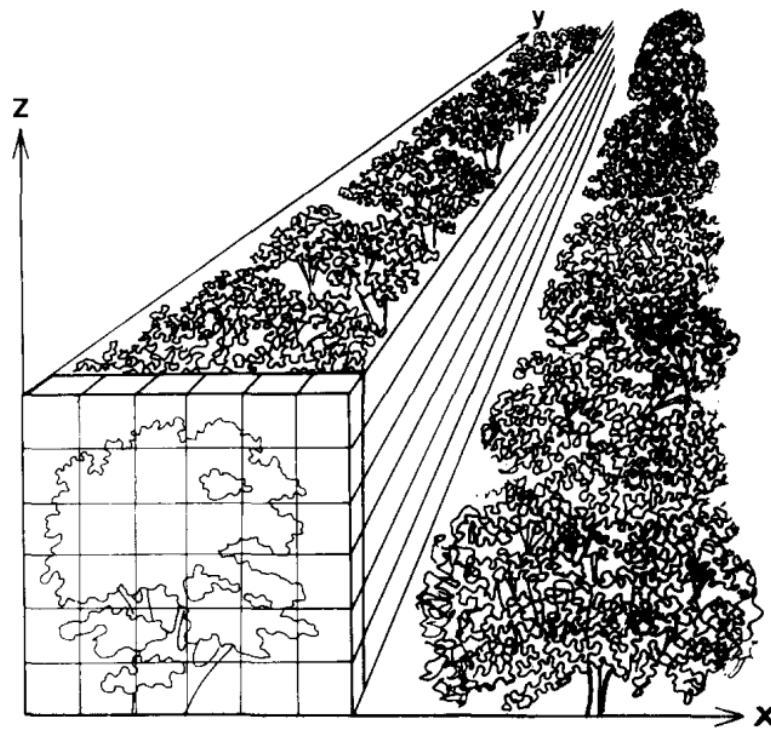


**Figure 2.10 A schematic diagram showing a rectangular orchard hedgerow that varies in two-dimension (X and Z) (Cohen et al., 1987).**

Solar radiation dynamics in orchards can vary in three dimensions, i.e. isolated trees or young orchards, hence under such conditions, a three-dimensional model can be more suitable for estimating radiation interception. (Abraha and Savage, 2010, Sinoquet et al., 2001), where the canopies exhibit discontinuity in and along the row and between rows, and radiation transmission within the canopy varies in the X-Y-Z axes. Describing the canopy structure in three-dimensional space gives a better representation of real canopies. In addition, three-dimensional models are flexible, as they can also downgrade to a two-dimensional model when the canopy forms a hedgerow and reduce to a one-dimensional model when the plants grow and cover the ground uniformly. However, such models may require many input parameters, which are sometimes difficult to obtain (Abraha and Savage, 2010).

Different canopy shapes have been used to develop radiation interception models, such as ellipsoids (Abraha and Savage, 2010, Annandale et al., 2004, Wang and Jarvis, 1990), spheres (Rubke, 2015), and rectangles (Oyarzun et al., 2007). Often an ellipsoidal shape is used because of its flexibility and suitability for most tree canopies. A simple and flexible two-dimensional geometric model based on the early works by Charles-Edwards and Thornley (1973) was developed and validated by Annandale et al. (2004) for different canopy characteristics (canopy size and leaf area density) in different crops (citrus, peach, and *Leucaena*). The model was developed to study the spatial distribution of shadows projected

on the ground by tree canopies. Solar radiation interception was computed by considering, the solar beam that passes through the canopy ( $\tau_c$  in equation 3), the solar beam that passes through the gaps, therefore un-intercepted by the canopy ( $\tau_f$  in equation 3) and the extent of competition from neighbouring trees.

Deviating from the ellipsoidal shapes, Cohen et al. (1987) used a prismatic shape for shamouti orange hedgerows. This is a much simpler geometric shape compared to the use of ellipsoids, however, the model required LAD as an input parameter, which was determined using a direct method (metal frames), which can be tedious and destructive. The interest of the current study is the work by Oyarzun et al. (2007) who expanded the model of Cohen et al. (1987) and developed a model capable of estimating radiation interception in both young and hedgerow orchards, i.e. a three-dimensional model. This model can estimate radiation interception of fruit trees using simple canopy dimensions (canopy diameters, tree height, bare-stem height) and canopy porosity (Figure 2.11). The model calculates radiation interception based on the geometric relationship of the shadow cast by the trees (assumed to be prismatic shaped) on the ground. The flexibility (used in matured and young orchards) coupled with the easily-obtainable input parameters, makes model parameterisation easier and broadens its application as an agricultural tool for orchard management practices, such as pruning effects and orchard designs (Campos et al., 2017). Its major drawback is the estimation of canopy porosity in the shaded area cast by the trees on the ground, a parameter of interest in the current study. Several studies in fruit trees (Ibraimo, 2018, Marsal et al., 2013, Oyarzun et al., 2007) have highlighted that it is the most important parameter that is not easy to obtain. It is often estimated using subjective methods that are associated with errors since sun flecks contain full and partially lit areas on the ground (Abraha and Savage 2010). Therefore, the accuracy of the model depends on the accurate estimation of this parameter of the canopy and the parametrisation thereof.

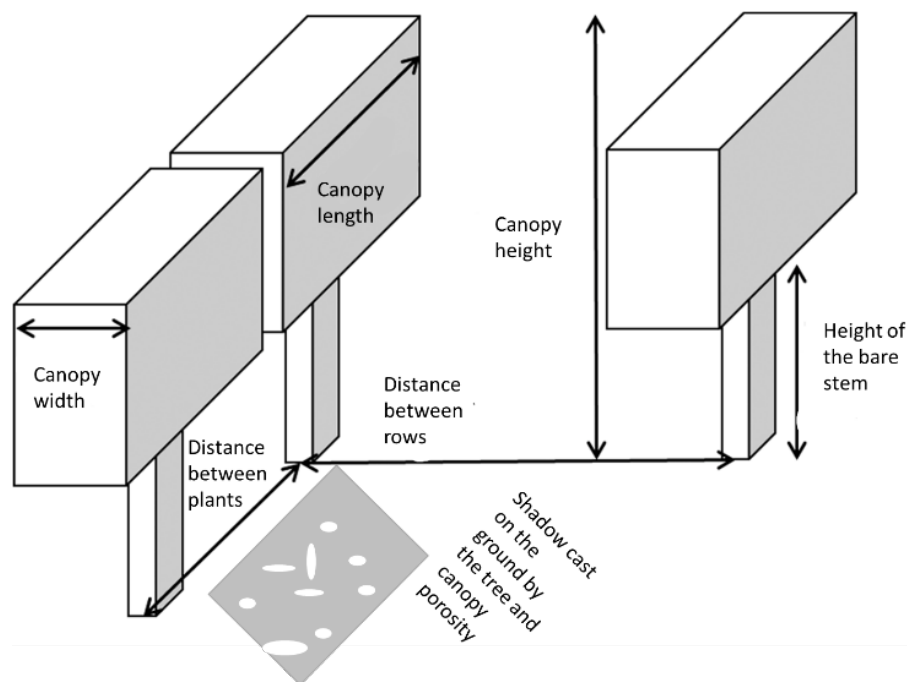


**Figure 2.11 Schematic representation of fruit tree orchard architecture and dimensions required for the model developed by Oyarzun et al. (2007).**

As a result, accurate estimation of the fraction of intercepted solar radiation will help to adjust  $T$  for different canopy sizes and probably answer the question; “based on canopy size and local conditions how much water pecan trees use over a given period, i.e. a month and/or over a season”? A simple general model for estimating intercepted solar radiation in different orchards has been suggested by Oyarzun et al. (2007) and has been used in water use modelling (Ibraimo, 2018, Marsal et al., 2013, Testi et al., 2006) due to easily obtainable input parameters. While coupling the model to existing water use models has indicated successful results, a major challenge has been estimating the canopy porosity, a key parameter in the model. This parameter represents the amount of radiation transmitted by the canopy (Oyarzun et al., 2007), and per a given canopy it can vary spatially and temporarily with the increase in leaf area, orchard management practises such as pruning and possibly with yield. An interesting and yet not well-explored approach to estimating the model parameters particularly the canopy porosity is the use of drone-based ariel images and/or mobile applications such as VitiCanopy (De Bei et al., 2016), GLAMA (Tichý, 2016) and Canopeo (Patrignani and Ochsner, 2015).

## 2.6 MODELLING PECAN WATER USE

Due to the large variation in water use volumes for pecans, reported in Chapter 3, and the high cost of doing measurements, it is important to try and model water use in order to extrapolate measured values to a wide range of conditions. A number of different models have been used for estimating pecan water use, which vary in complexity and detail (Miyamoto, 1983, Allen et al., 1998, Annandale et al., 1999, Andales et al., 2006, Wang et al., 2007c, Samani et al., 2011, Sammis et al., 2013). Complex, detailed models may be more explanatory and more accurately transferred to different situations, but they usually require a number of inputs which may not be practical or easy to obtain in field situations (Annandale et al., 1999; Andales et al., 2006). Simple crop models, on the other hand, are usually more empirical, based on robust relationships between plant behaviour and key environmental variables, but only tend to apply within their calibration range. They therefore do not always apply outside the area in which the relationships were developed. However, due to their limited input requirements, they are often more easily adopted by farmers. The FAO-56 model (Allen et al., 1998) and the pecan monthly water use simulator (Samani et al., 2011) are two such models, in which crop ET is calculated from meteorological data and single crop coefficients ( $K_c$ ), where the  $K_c$  is defined as the ratio of ET to  $ET_0$ . The major limitation of using empirical approaches to estimate water use of orchards is that crop coefficients vary between orchards, with midseason  $K_c$  values for mature pecan orchards of between 1.1 and 1.39 reported in the arid New Mexico climate (Miyamoto, 1983; Sammis et al., 2004). Various modelling approaches, both generic and pecan-specific, have been developed to adjust crop coefficients to specific climatic conditions and orchard management practices using weather variables, thermal time, crop height, fractional canopy cover and the degree of stomatal control on crop water use (Miyamoto, 1983, Allen et al., 1998, Sammis et al., 2004b, Wang et al., 2007c, Allen and Pereira, 2009, Samani et al., 2011, Taylor et al., 2015). Whilst FAO-56 provides a simple, generic procedure for adjusting  $K_c$  values for climate using wind speed, minimum relative humidity and crop height (Allen et al., 1998), pecan-specific water use models have focused on adjusting  $K_c$  values of pecans according to fractional canopy cover and thermal time (Wang et al., 2007b; Samani et al., 2011). Similar simple relationships between  $K_c$  and fractional canopy cover (estimated as fraction of midday radiation intercepted by the canopy) have been established for other deciduous crops, including peaches and grapes (Johnson et al., 2000, Johnson et al., 2002, Williams and Ayars, 2005b, Goodwin et al., 2006, Marsal et al., 2014). Unfortunately, these empirical modelling approaches are seldom evaluated in production regions other than where they were developed, which differ in both climate and irrigation system employed. Thus, they often contain artefacts of the local growing conditions, making

them less transferable to areas with very different conditions, with consequent impacts on irrigation water management and planning.

The crop coefficient modelling approach has most often been used for pecans, with orchard specific  $K_c$  values determined using canopy cover (Figure 2.12) (Samani et al., 2011, Wang et al., 2007c). Whilst Wang et al. (2007b) developed their relationship from six orchards (Figure 2.12A), Samani et al. (2011) used 279 orchards to develop their relationship (Figure 2.12B). The  $K_{c-ref}$  values used to adjust  $K_c$  values (equation [6]) were derived from a well-managed mature pecan orchard and are given in Table 2.2

$$K_c = (0.6035f_{c\ eff} + 0.4808)K_{c-ref} \quad (6)$$

**Table 2.2: Measured monthly crop coefficients for the reference pecan orchard ( $K_{c-ref}$ ) given by Samani et al. (2011) for New Mexico conditions, which have been offset by 6 months to adjust for the seasons in the southern hemisphere**

	Month								
	Sep	Oct	Nov	Dec	Jan	Feb	Mar	Apr	May
$K_{c-ref}$	0.39	0.59	0.87	1.02	1.04	1.24	1.26	0.84	0.39

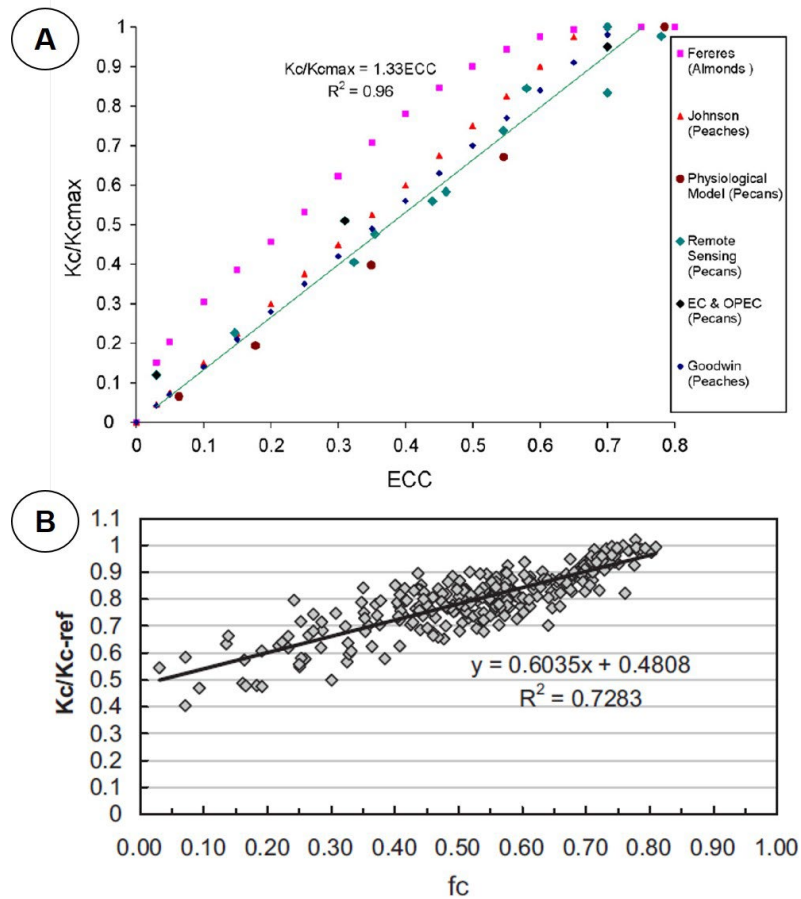


**Figure 2.12: Relationship between relative crop coefficient ( $K_c/K_{c\ max}$ ) and effective canopy cover (ECC) (Wang et al., 2007c) and B) relative crop coefficient ( $K_c/K_{c\ ref}$ ) and fractional cover ( $f_c$ ) (Samani et al., 2011) for pecan orchards near Las Cruces, New Mexico.**

Samani et al. (2011) suggested that the  $K_{c-ref}$  values in Table 2.2 should be adjusted for local conditions. One way to do this is to use the growing degree day (GDD)- $K_c$  relationship determined by Sammis et al. (2004) (Figure 2.13).

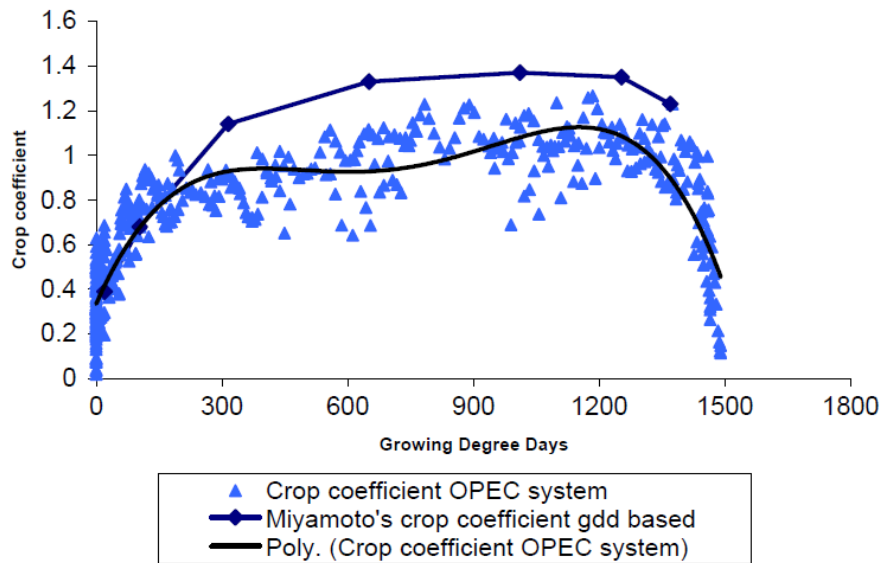


**Figure 2.13: Daily crop coefficients as a function of thermal time for a 'Western Schley' orchard near Las Cruces, New Mexico(Sammis et al., 2004b).**

In the paper published by Ibraimo et al. (2016), based on data obtained during a previous WRC project, the approach of Samani et al. (2011) showed very good promise in estimating monthly water use of pecans, provided the  $K_{c-ref}$  values were adjusted for local conditions using GDD- $K_c$  relationship developed by Sammis et al. (2004). However, attempts to extend this equation to some of the hotter production regions in South Africa failed due to the much higher GDD during the growing season in these areas (Figure 2.14). It was therefore suggested that visual observations of canopy development be used to adjust the six stage crop coefficient curve derived during the study (Figure 2.15). The possibility of using visual cues to adjust the length of the various stages needs to be determined in the current study. In addition, it may also be necessary to develop a dual crop coefficient approach, which models transpiration and soil evaporation separately. This may aid in improving daily or weekly estimates of ET.



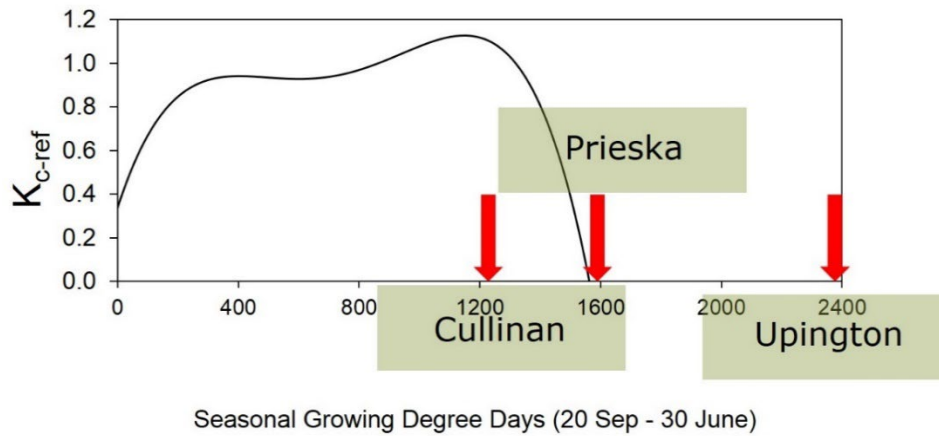


**Figure 2.14: Evaluation of the growing degree day GDD- $K_c$  relationship of Sammis et al. (2004b) in different production regions of South Africa, using long term weather data to calculate GDD for the growing season in each location**

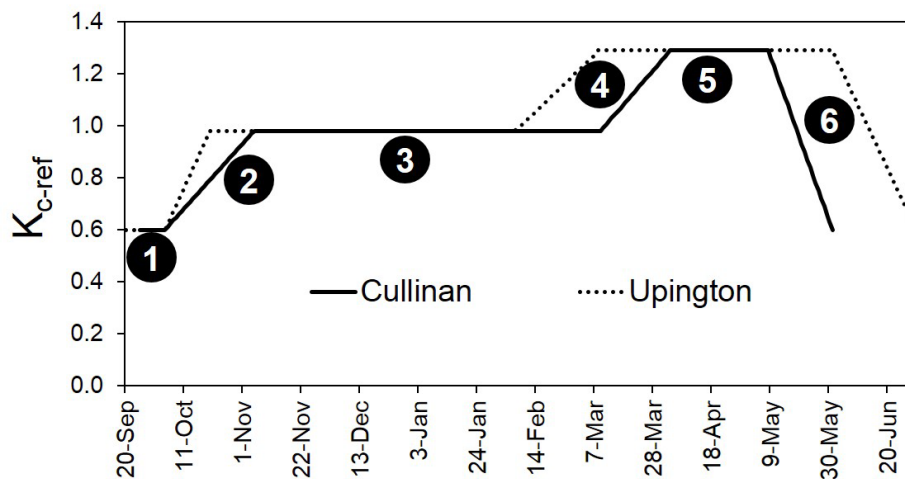


**Figure 2.15: The six stage crop coefficient curve suggested in the study by Ibraimo et al. (2016) illustrating how the curve could be adjusted with visual observations of canopy or nut development for different production regions.**

## 2.7 CROP WATER PRODUCTIVITY AND ECONOMIC CROP WATER PRODUCTIVITY OF PECANS

### 2.7.1 DEFINITION OF CROP WATER PRODUCTIVITY AND ECONOMIC CROP WATER PRODUCTIVITY

Fernández et al. (2020) recently attempted to establish some consensus regarding the definition and suitability of different indicators. Due to the clarity provided by these authors, it was decided to use the water use indicators in this study. Crop water productivity based on  $ET_c$  ( $WP_c$ ,  $\text{kg m}^{-3}$ ) or crop water productivity based on  $T$  ( $WP_T$ ) and irrigation water productivity ( $WP_I$ ,  $\text{kg m}^{-3}$ ) are calculated as:

$$WP_c = \frac{yield}{ET_c} \quad \text{or} \quad WP_T = \frac{yield}{T} \quad \text{or} \quad WP_I = \frac{yield}{IWU} \quad (7)$$

Where  $IWU$  is volume of irrigation water applied. Economic crop water productivity ( $EWP_c$ ,  $\text{R m}^{-3}$ ) and economic irrigation water productivity ( $EWP_I$ ,  $\text{R m}^{-3}$ ) are calculated using the net margin as:

$$EWP_c = \frac{profit}{ET_c} \quad \text{or} \quad EWP_I = \frac{profit}{IWU} \quad (8)$$

### 2.7.2 PREVIOUS REPORTS OF CROP WATER PRODUCTIVITY IN PECANS

As previously stated, pecans require a large amount of water, greater than that of other row crops, with  $ET$  exceeding 1000 mm for the growing season for mature pecan trees (Miyamoto, 1983, Sammis et al., 2004b, Bawazir and King, 2004, Samani et al., 2009, Ibraimo et al., 2016). This poses a problem in a semi-arid country, such as South-Africa, which is characterized by sporadic and unpredictable rainfall patterns. Therefore, the need exists to conceptualize the  $WP$  of pecan trees in order to utilize the allocated water as efficiently as possible and to allow the benchmarking of growers. Economic water productivity calculations are very important for a crop such as pecan, as yields are low ( $1.5\text{--}4 \text{ t ha}^{-1}$ , the nut is rich in oil, low in water content and has a thick, protective shell) and water use is quite high, which means that  $WP$  is very low compared to other fruit tree crops, such as apples and citrus. However, when the economic value of the crop is taken into account it may compare much more favourably to these crops. It is also important to note that  $WP$  and  $EWP$  will also vary from season to season as a result of the alternate bearing nature of the crop, where a year of good yields (“on year”) will typically be followed by a season with lower yields (“off year”). Prices for nuts also vary from year to year depending on the market. Therefore,  $WP$  and  $EWP$  measurements in orchards should be performed for a minimum of two years. When

considering a WP for pecans it is also important to consider the entire life time of an orchard, as pecans take 5-6 years to come into production and during this time water is still required without any economic benefit.

Water productivity figures for mature pecan orchards were comparable for New Mexico/Texas and Cullinan in South Africa, varying between  $0.15 \text{ kg m}^{-3}$  to  $0.31 \text{ kg m}^{-3}$  (Miyamoto, 1990, Ibraimo et al., 2016, Sammis et al., 2004b). Miyamoto (1983) suggested WP (yield/ET) of 'Western' pecans in the El Paso Valley in Texas to be approximately  $0.25 \text{ kg m}^{-3}$  in a wet year and between  $0.27$  and  $0.303 \text{ kg m}^{-3}$  in a moist year. Unfortunately, this author did not define what was meant by a wet and moist year. In a two year study, Sammis et al. (2004b) found a WP of  $0.18 \text{ kg m}^{-3}$  in an "off year" and  $0.31 \text{ kg m}^{-3}$  in an "on year" near Las Cruces, whilst Wang et al. (2007a) working in the same area and with the same cultivar ('Western Schley') reported an average WP of  $0.149 \text{ kg m}^{-3}$  in an "off year" and  $0.262 \text{ kg m}^{-3}$  in an "on year" over a 5 year period. In the three year study in Cullinan WP was  $0.15 \text{ kg m}^{-3}$  in an "off year" and  $0.26 \text{ kg m}^{-3}$  in an "on year" for 'Choctaw'. Water productivity needs to be determined for the hotter and drier production regions of South Africa, where higher yields are obtained, but where water use may also be higher. This is important as it may not be fair to benchmark growers in drier and hotter regions against growers in cooler and more humid environments. More water will be needed to produce a crop in areas with higher evaporative demand. There are no reports of EWP for pecans. This will also vary from year to year based on supply and demand pricing of nuts in "on" and "off" years.

Wang et al. (2007a) attempted to estimate plant water use efficiency (WUE) based on ET per unit of dry mass produced over the course of a season, determined using a physiological model for estimating biomass accumulation of the whole tree. This provides some useful insights into how WUE differs during different phenological stages and how it is influenced by VPD (Figure 2.16). Water use efficiency was high at the start and end of the season due mainly to low ET fluxes as a result of low VPD (Figure 2.16A). This influence is clearly illustrated in Figure 2.16B. One might have also expected lower WUE near the end of the season during nut filling, as this is a very energy expensive process. These authors also estimated that 25-35% of the total seasonal tree growth was in the roots, which represents a significant sink for carbohydrates. Dry matter allocation to the nuts was 13.8% in an "on year" and 8.0% in an "off year".

When taking into account the value of water use efficient crops, it is important to consider the value of irrigation water used, as well as its application method (Ward and Michelsen, 2002). Water increases in value in semi-arid regions with low availability, therefore timely and

judicious water application is necessary in order to ensure optimum efficiency or optimum application efficiency (AE), which is defined as the ratio of the volume of water used by the crop to the amount of irrigation water applied (Kruse, 1978). The AE is dependent on the type of irrigation system used for a specific crop. For example pecans exhibited a higher AE for flood irrigation (89%) compared to other crops (50-73%) (Al-Jamal et al., 2001, Oster et al., 1986). This can be attributed to pecans widespread root system that occupies a larger surface area, combined with the trees ability to absorb and use large amounts of water. However, findings by Othman et al. (2014) suggest that pecans suffer water stress at the end of a drying down cycle for flood irrigation, which reduces photosynthesis and may impact yield. Flood irrigation may therefore not be the most appropriate irrigation system for minimising stress in pecan orchards.

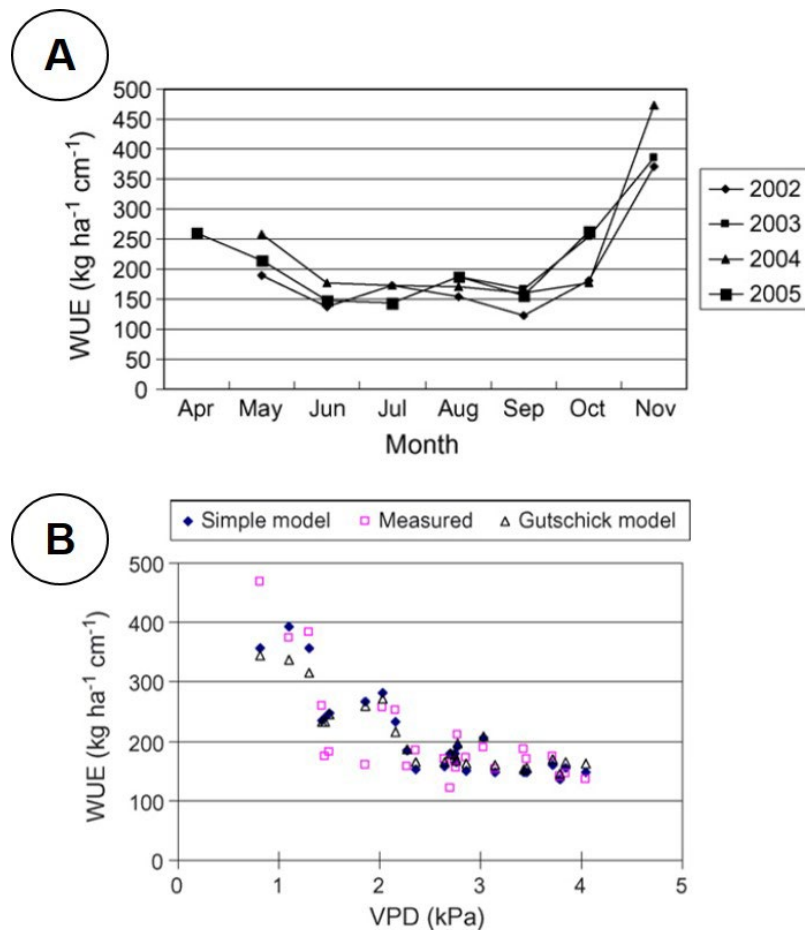


**Figure 2.16 A) Monthly values of plant water use efficiency (WUE) of pecan trees (Biomass/ET) and B) the impact of VPD on monthly measured and predicted water use efficiency (WUE) for pecan trees near Las Cruces in New Mexico (Wang et al., 2007a).**

Areas characterized by low rainfall events require supplemental irrigation to meet the crops high water demand. It is therefore essential to define the irrigation water productivity ( $WP_i$ ) which is the ratio between the harvested crop yield and the seasonal water applied (this could also be calculated using irrigation + rainfall) ( $\text{kg ha}^{-1} \text{ mm}^{-1}$ ) (Howell, 1994). Irrigation water productivity is affected by a wide range of factors which include; soil characteristics, type of crop, cultural and management practices, canopy interception and drainage water loss (Sammis et al., 2004b). It would be beneficial for the farmer to increase  $WP_i$  as this will lead to increased profits. It can be accomplished through the timing of irrigation application by using various methods of irrigation scheduling, such as measuring soil water potential or plant measurements, such as the water stress index (Sammis et al., 2004b, Garrot et al., 1993). Irrigation water productivity is higher for irrigation systems that have less surface evaporation, created by the wetting pattern of the irrigation system, therefore surface and subsurface systems have higher  $WP_i$  ( $0.0235\text{-}0.127 \text{ t ha}^{-1} \text{ mm}^{-1}$  and  $0.0283\text{-}0.227 \text{ t ha}^{-1} \text{ mm}^{-1}$  respectively) than micro-sprinklers or furrow irrigation ( $0.0044\text{-}0.0659 \text{ t ha}^{-1} \text{ mm}^{-1}$  and  $0.0086\text{-}0.056 \text{ t ha}^{-1} \text{ mm}^{-1}$  respectively) (Sammis, 1980). Irrigation water productivity of pecans is also highly dependable on its alternate bearing cycle, where it increases in “on” years, because of higher yields per amount of water used, and decreases in “off” years, because of lower yields for the same amount of water used during “on” years (Sammis et al., 2004b). Pecan  $WP_i$  was estimated at  $0.0016 \text{ t ha}^{-1} \text{ mm}^{-1}$  on average and is quite low when compared to other crops (Sammis et al., 2004b).

## **2.8 THE IMPACT OF WATER STRESS ON PECAN YIELD AND QUALITY**





Water stress, in general, is a major problem in agriculture and the ability to withstand or counteract water stress is of major economic importance. Water stress has a negative effect on all aspects of plant growth and development with plant responses to water stress being complex, involving adaptive changes and/or deleterious effects (Chaves et al., 2002, Shao et al., 2008). Usually tolerance to water stress involves subtle changes in cellular biochemistry (Shao et al., 2008). Plant responses to water stress include, reduced root length, reduced shoot growth, smaller leaf areas, reduced plant biomass accumulation, altered nutrient uptake and distribution, leaf abscission, lower yield, smaller fruit size and reduced photosynthesis. In some instances, water stress can result in an increase in root growth to enable roots to penetrate deeper into the soil to extract water from deeper soil layers (Chaves et al., 2002). Vegetative and fruit growth in fruit trees are sensitive to water stress (Mahhou et al., 2005). Plant physiological processes, such as photosynthesis and transpiration, depend on the rapidity, severity and duration of the drought event.

Water stress has profound effects on plant physiology in general, and will therefore impact pecan productivity and growth. Pecans responses to water stress varies according to the tree age, soil type and weather conditions. Mature pecan leaves do not wilt and therefore do not exhibit any visible signs of water stress until leaf or fruit drop (Miyamoto, 1983). Wells and Harrison (2010) mentioned that excessive water stress causes the tree to shed leaves and drop nuts or only moderately fill the nuts. Prior to shell hardening, water stress is more likely to result in leaf abscission than nut abscission (Wells and Harrison, 2010).

The need exists to produce pecans under non-stressed conditions to obtain good yields of good quality nuts (Kilby, 1980). If pecan trees are subjected to significant water stress, detrimental effects can occur, as yield can be reduced by 24%, nut mass by 8% and trunk growth by up to 27% (Garrot et al., 1993). Moderate to low water stress conditions can adversely affect shoot growth, nut development, nut filling, shuck opening and increased nut drop (Zertuche, 1982, Finch and Van Horn, 1936, Sparks, 1989). Good irrigation management from the start of the season will result in good strong vegetative growth, needed to support the developing nuts and to replenish stored reserves at the end of the season (Wells, 2016).

The period when water stress occurs causes variable results in terms of nut quality and yield (Figure 2.5). The common visible effects of prolonged drought during flowering and nut set are excessive nut drop and “shell hardening” of small nuts (Wells, 2016). Even though the flowering and nut set stage does not have a critical requirement for water, the nut sizing period, entailing nut elongation and expansion, is dependent on available soil water, as water stress during this stage leads to smaller nuts of decreased volume that causes the cavity to be filled more rapidly (Figure 2.17) (Sparks, 2001). The nut filling period is crucial to obtain nuts of good quality (>48% fill) and is most vulnerable to water stress conditions (Sparks, 2005, Sparks, 2002). Whilst smaller nuts will be filled more rapidly, larger nuts run the risk of insufficient fill (<48%) (Sparks, 2001). Deficit irrigation has been used as a method to regulate nut size to ensure proper nut filling, by applying less water during nut sizing to get nuts with a small volume, and subsequently increasing irrigation during the nut filling stage to obtain better kernel development (Table 2.3) (Sparks, 2001, Sparks et al., 1995). Smaller pecan nuts usually have a better taste than larger nuts and obtain quality standards more readily as a result of more intact kernels, or whole halves that are easily obtained during nut filling of smaller nuts (Sparks, 2005, Sparks, 2002). However, in South Africa better prices are obtained for large nuts and nut size is therefore a quality parameter. Small nuts, caused by water stress during the nut sizing phase may lead to water stage fruit split in many varieties, resulting from a sudden influx of water during the nut filling stage.

**Table 2.3**Effect of the timing of water deficit on nut shape and size (Adapted from Sparks (2006)). To adjust to Southern Hemisphere conditions June is December, July is January and August is February, all fall within the nut sizing period

Nut Profile	Nut Size and Shape	Water Deficit Timing
	Normal	No Water Deficit
	Reduced size; normal shape	Throughout Season
	Reduced size; round shape	June to July 15
	Slightly reduced size; obovate shape	July 25 to August 15

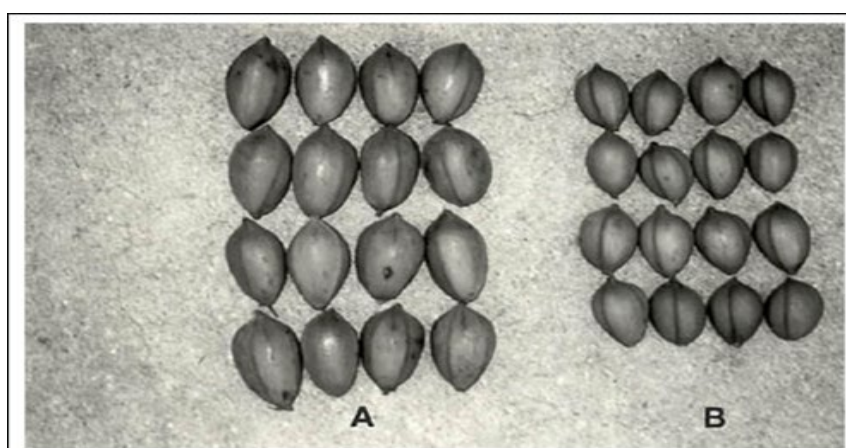


**Figure 2.17** Effect of adequate water during the nut sizing stage. Pecans on the left (A) are from irrigated trees, while those on the right (B) are from non-irrigated trees (Wells, 2016)

The nut filling stage occurs from about the middle of February to the first week of April in South Africa, depending on variety. The most critical period for water use is often during the first two weeks of March. Lack of sufficient irrigation or rainfall during the nut filling stage will lead to poorly filled nuts, which will result in poor nut quality (Figure 2.18).

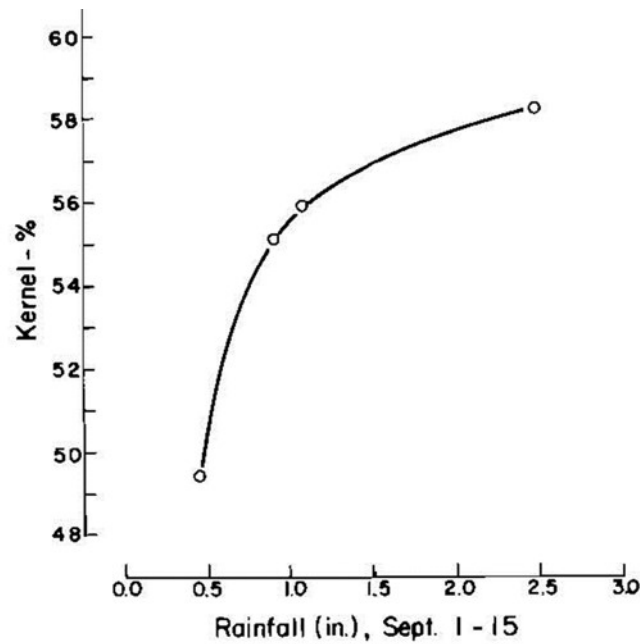


**Figure 2.18 Relationship of percentage kernel to rainfall during the first 15 days in September (Northern Hemisphere conditions) (Sparks, 1992)**

Water stress after nut filling results in delayed shuck split, thereby increasing the percentage of stick tights or pops (nuts with unopened shucks). These nuts are usually characterized first by black markings on the shuck and later the entire shuck turns black as they approach maturity. Pecans that are damaged in this manner typically have poorly filled kernels and the abscission layers at the shuck sutures do not develop. As a result, the shuck does not open and sticks tightly to the nut. These pecans are hard to shake off the tree and the meat percentage is low, about 10-30 percent (Sparks, 2006).

Identifying water sensitive and non-sensitive phenological stages is therefore critical for managing irrigation in times when water allocations are reduced below the full evapotranspiration requirements of an orchard. It can also allow water savings during a season, which can potentially be used to expand the planted area of pecans or for other crops and increase profitability. This study, therefore, aimed to determine the most sensitive growth stages to water stress in pecan, when yield and quality is negatively impacted. This will help farmers manage their irrigation water, by allocating sufficient water to the most sensitive phenological stages and making savings during less sensitive stages under conditions where their annual water allocation may be reduced due to water scarce conditions. Furthermore, it aimed to determine the point at which pecan trees start experiencing water stress by assessing photosynthesis in stressed and control trees relative to both predawn and midday



stem water potentials. This will help guide judicial irrigation scheduling in pecan orchards in future, which will allow increased water use efficiency in the industry.

The early detection of plant water stress across a whole farm is critical for avoiding any yield reduction in individual trees which would impact overall farm yield and profitability. This is a key aim in precision agriculture. Assessing individual trees with ground-based measurements is difficult and time consuming. However, advancements in unmanned aerial vehicle (UAV) technology and improvements in sensing technology, have allowed the assessment of plant parameters, including plant stress, over large area. The most appropriate method to detect plant stress in different species needs to be carefully assessed relative to ground based tree measurements of stress. As a result, a remote sensing component was added to the water stress study, as we had the ideal situation to assess various methods for determining plant stress through remote sensing in pecans.

### 3. MATERIALS AND METHODS

#### 3.1 WATER USE OF PECAN ORCHARDS

##### 3.1.1 SITE DESCRIPTIONS

###### 3.1.1.1 *Vaalharts*

The trial site in Vaalharts was situated approximately 25 km South West of Jan Kempdorp, Northern Cape (GPS-Coordinates: 28°4'11.01"S, 24°37'54.79"E) (Figure 3.2) on a 12 year old mixed cultivar pecan orchard (at the start of the trial, planted in 2006) of roughly 10.37 ha (1037 trees). The orchard consisted of 40 rows of full bearing, irrigated pecan trees (cultivars include 'Wichita', 'Choctaw', 'Navaho' and 'Western Schley' all grafted on 'Ukulinga' rootstocks) planted at an industry standard of 10 m x 10 m spacing, totalling 100 trees ha<sup>-1</sup> (Figure 3.1). Sap flow equipment was installed in eight trees in the orchard, separated into two sites. Initially, at site A, tree 1 and 2 were 'Choctaw' trees and tree 3 and 4 were 'Wichita'. At site B tree 1 and 4 were 'Choctaw' trees and tree 2 and 3 were 'Wichita' trees. In October 2022 the sap flow systems were moved to new trees. At site A and B trees 1 and 4 were 'Choctaw' and trees 2 and 3 were 'Wichita'. Trees were planted in a North West-South East orientation (51° W of N). Trees were pruned on a 4 year cycle according to industry standards, with a mechanical hedger to provide uniformity. Trees were irrigated by means of one 150 L h<sup>-1</sup> Mamkad 16 sprinkler (NaanDanJain Irrigation) per tree, with a wetted diameter of 6.5 m. Irrigation was scheduled according to a cycle determined by readings from an Aquacheck probe installed between a pecan tree and a macro-sprinkler in the orchard. The details of the pecan orchard in this study are provided in Table 3.1. In this particular trial site weeds are used as a cover crop (Figure 3.2). Weed growth is not promoted, but rather mowed to a manageable height throughout the season. This is a changing trend in orchards in this region to facilitate mechanical harvesting. Pruning is done on a 4 year cycle, where one side of the canopy is pruned on every second row in year 1. In year 2 one side of the canopy in the rows skipped in the previous year are pruned. In year 3 the other side of the trees pruned in year 1 are pruned and finally in year 4 the other side of the trees pruned in year 2 are pruned. A google Earth image showing the positioning of the AWS relative to the orchard is provided in Figure 3.3.

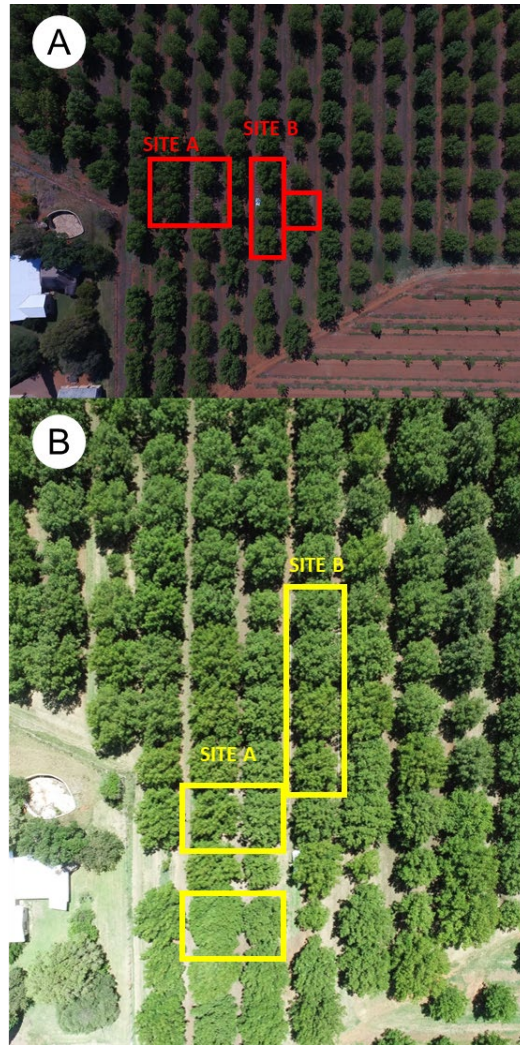


**Figure 3.1A) The orchard at Groen Boerdery in the 2018/2019 and in B) 2022/2023 seasons. The two sites where sap flow measurements are made are indicated.**



**Figure 3.2 Location of the experimental orchards in South Africa**

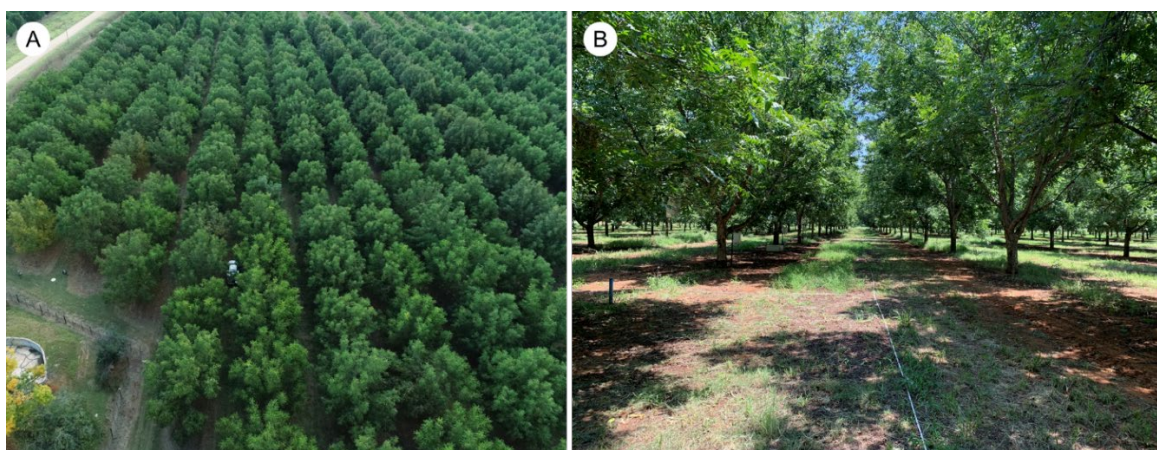


**Figure 3.3 A) Aerial view of the orchard in May 2021 and B) status of the ground cover between rows in summer of 2023**

**Table 3.1 Details of the mixed pecan cultivar orchards in Vaalharts and Groblershoop in the Northern Cape. W = Wichita and C = Choctaw**

Orchard Reference	Vaalharts	Groblershoop
Cultivar	'Wichita' and 'Choctaw'	'Wichita' and 'Choctaw'
Rootstock	'Ukulinga'	'Ukulinga'
Planting date	2006 (12 years at start)	2002 (17 years at start)
Orchard block area	10.37 ha	1.71 ha
GPS co-ordinates	28°4'11.01"S, 24°37'54.79"E	28° 40' 7.54"S, 21°48' 29.14"E
Tree spacing	10 m x 10 m (100 m <sup>2</sup> )	10 m x 10 m (100 m <sup>2</sup> )
Row orientation	North West-South East (51° West of North)	North West-South East (35° West of North)
Irrigation – Type – Delivery rate – Wetted diameter	Microsprinkler 150 L h <sup>-1</sup> 6.5 m full surface	Drip 3.5 L h <sup>-1</sup> 2 drip lines, drippers spaced 0.6 m apart (33 drippers per tree 115 L h <sup>-1</sup> )
Canopy dimension at start of study	Height – 10 m Width – 5.7 m Breadth – 6 m	Height – 11 m Width – 9 m (W), 4 m (C) Breadth – 9 m (W), 8 m (C)
Max. canopy cover	Wichita and Choctaw ~ 0.50	Wichita ~0.65 Choctaw ~0.30
Leaf area index – orchard	Wichita ~ 3.10 m <sup>2</sup> m <sup>-2</sup> Choctaw ~ 2.90 m <sup>2</sup> m <sup>-2</sup>	Wichita ~ 2.45 m <sup>2</sup> m <sup>-2</sup> Choctaw ~ 2.10 m <sup>2</sup> m <sup>-2</sup>
Pruning strategy	4 year cycle	4 year cycle
No of experimental trees	8	8



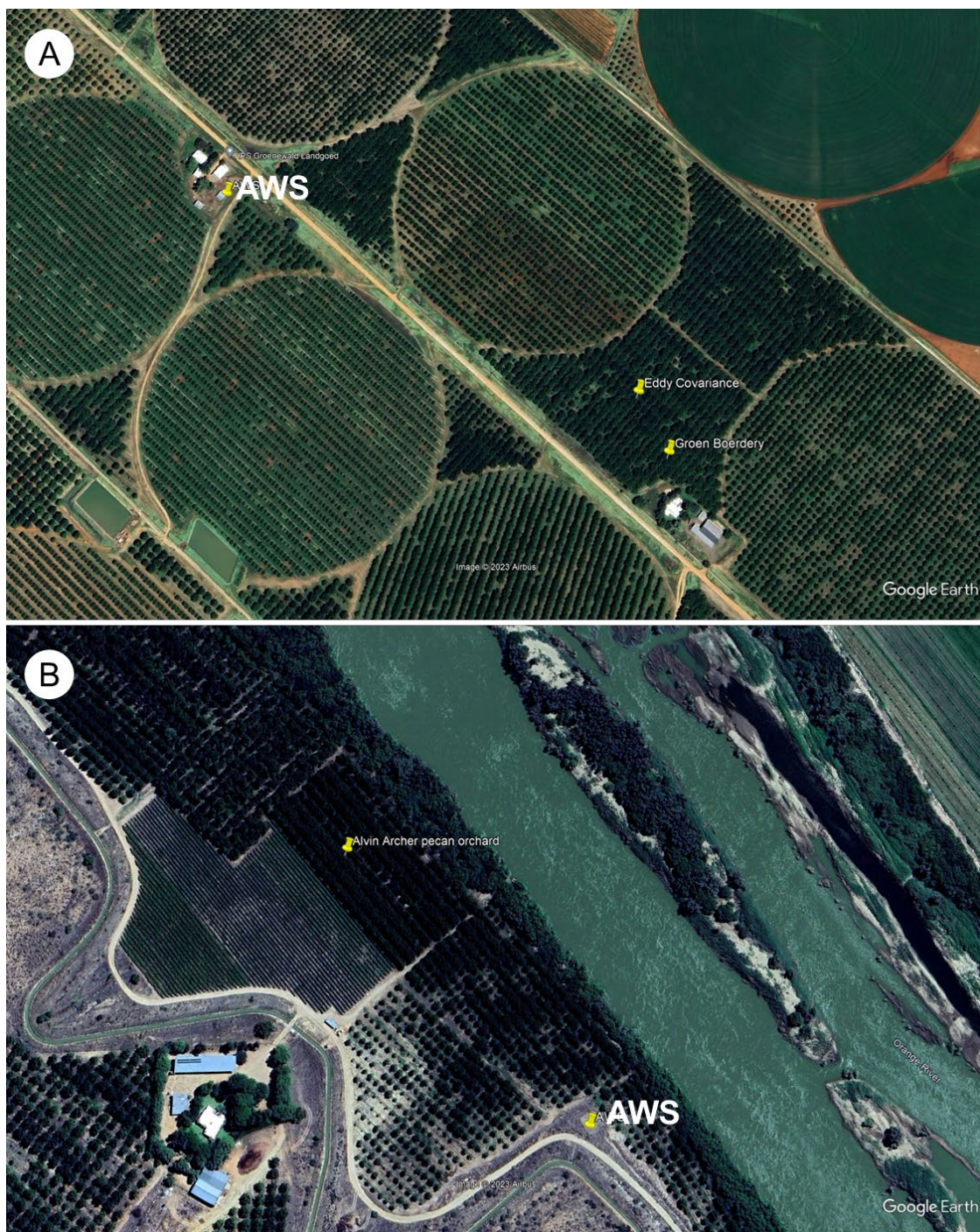


**Figure 3.4 Google Earth image of the A) Vaalharts and B) Groblershoop orchards showing the position of the orchards relative to the automatic weather stations (AWS). The area surrounding the orchards is also illustrated for the purposes of the Eddy Covariance measurements.**

### 3.1.1.2 Groblershoop

The trial site was situated in between Groblershoop and Grootdrink in the Northern Cape Province (GPS-Coordinates: 28° 40' 7.54"S, 21°48' 29.14"E) (Figure 3.2) in a 17 year old (at the start of the trial, planted August 2002) mixed cultivar pecan orchard of 1.71 ha (171 trees) (Figure 3.4). The orchard consisted of 9 rows of full bearing, irrigated pecan trees (cultivars include 'Wichita', 'Choctaw', 'Navaho' and 'Mohawk' all grafted on 'Ukulinga' rootstocks) planted at an industry standard of 10 m x 10 m spacing, totalling 100 trees ha<sup>-1</sup>. Sap flow equipment was installed in eight trees in the orchard, separated into two sites. At site A there were four 'Wichita' trees that were installed with a heat pulse velocity (HPV) system. At site B four 'Choctaw' trees were installed with a HPV system (Figure 3.4 and Figure 3.5). Trees were planted in a North West-South East orientation (51° W of N). Trees were pruned on a 4 year cycle according to industry standards, with a mechanical hedger to provide uniformity. Trees were irrigated by means of two drip lines, with 0.6 m in between drippers and a delivery rate of 3.5 L h<sup>-1</sup> (approximately 116 L h<sup>-1</sup> tree<sup>-1</sup>). Typically, irrigation took place every second night during the peak of the season for 11 hours. Adjustments were made according to capacitance probe readings. The inter-row is kept clean through chemical weed control. Details of the pecan orchard in this study are provided in Table 3.1.

The orchard is mechanically pruned and every year every fourth row is hedge pruned. The vertical cut is made 2 m from the stem at a 30 to 45° angle (depending on the equipment available) at a height of 9-10 m. There are nine rows in the orchard and the pruning strategy is as follows, rows 1, 5 and 9 were pruned in 2017, rows 4 and 8 were pruned in 2018 and rows 3 ('Choctaw' row with measurement trees) and 7 were pruned in 2019. Rows 2 ('Wichita' row with measurement trees) and 6 were pruned in 2020. In 2021 the pruning cycling started again with rows 1, 5 and 9. In 2022 rows 4 and 8 were pruned.



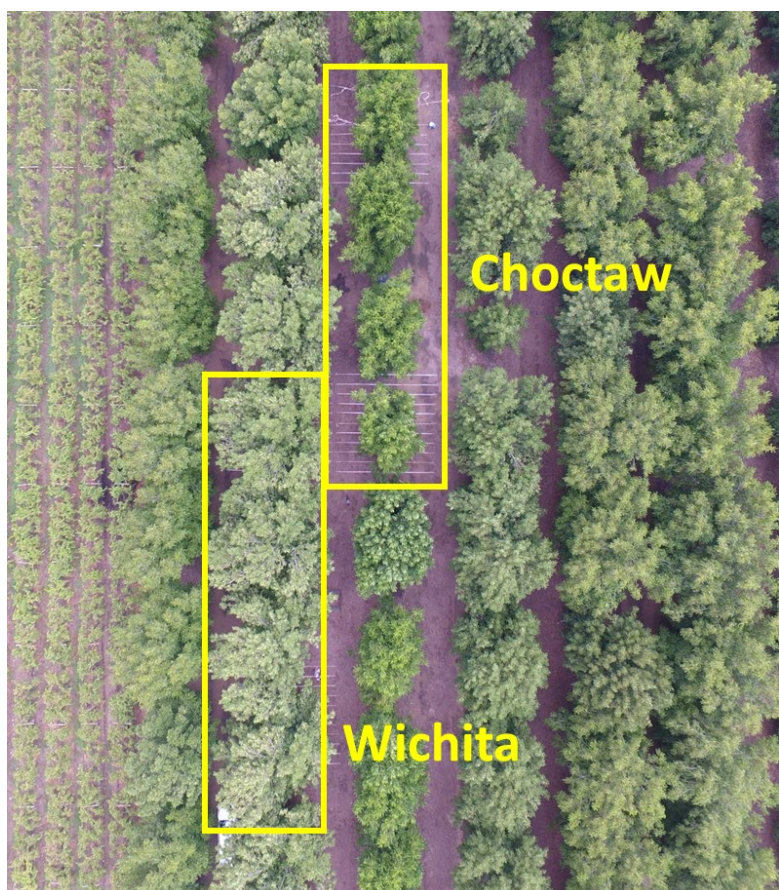


**Figure 3.5** The positioning of the trees used for sap flow measurements in the orchard in Groblershoop. Photo taken in January 2020



**Figure 3.6** The mixed cultivar pecan orchard close to Groblershoop an aerial view of the orchard and the orchard floor in January 2023



### 3.1.1.3 Innovation Africa @UP

The pecan orchard at Innovation Africa@UP (formerly the Experimental farm) was used to parameterise the radiation interception model, the conductance model of Villalobos et al. (2013) and the FAO-56 evaporation model (Allen et al., 1998). Data from this orchard was also used to determine the environmental and physiological control of transpiration. The orchard (25°4'55.85" S, 28°15'3.88" E, 1372 altitude) (Figure 3.2) is in the country's summer rainfall region, characterized by high intensity and short duration rainfall events, with sunny periods in between rains. Weather data (rainfall, relative humidity, solar radiation, vapor pressure deficit, and air temperature) was collected by an automatic weather station situated 230 m from the pecan orchard. The pecan research orchard was 3 ha in size (Figure 3.6) with mixed varieties on 'Ukulinga' rootstocks, however, the focus was on 'Wichita' trees for measurements. The trees were planted in a north-south orientation at two planting densities, i.e. 10 x 10 m and 5 x 10 m. For the experimental purposes, the 10 x 10 m planting density was used since it is the recommended planting density for commercial production (DAFF, 2006). The soil type in the orchard was a clay loam (45% Sand, 36% clay and 19% silt). The orchard was irrigated using pressure compensated drippers. Emitters were spaced 0.6 m apart and each emitter delivered 1.6 L.h<sup>-1</sup>. Three dripper lines were laid parallel to each other, with the middle dripper under the trees and the other two on either side of the trees, 1 m away from the tree trunk. Each tree was fertilized with LAN, superphosphate, potassium chloride, and zinc at the beginning of each season. The trees were pruned before the start of each season to a modified central leader.

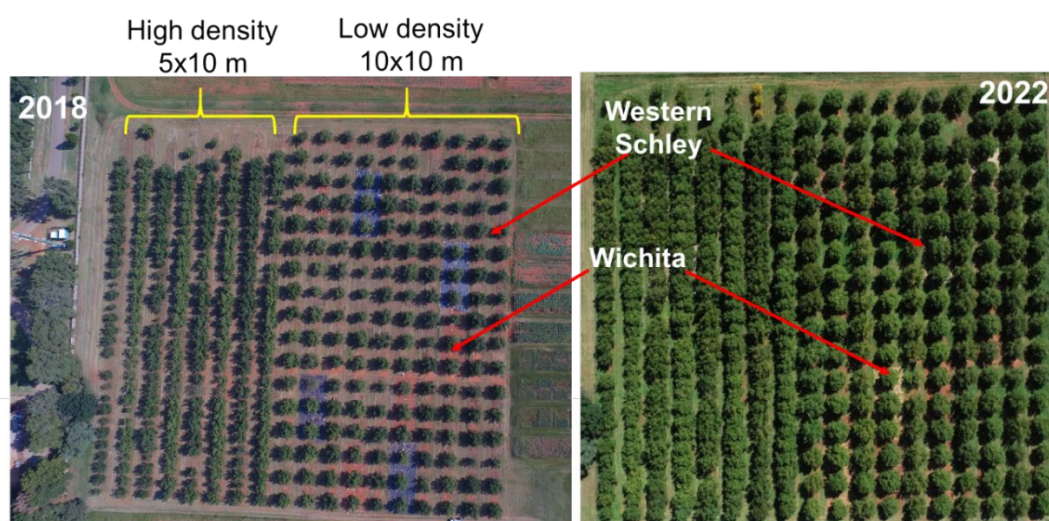


**Figure 3.7 Overview of the Pecan research orchard from 2018 (left) at the start of the trial to 2022 (right). The 10 x 10 m planting used for the water stress measurements is indicated in the yellow block**



### 3.1.2 WEATHER VARIABLES

#### 3.1.2.1 Vaalharts

Weather data was obtained from an Automatic Weather Station coupled to a CR1000 data logger (Campbell Scientific Inc. Logan, Utah, USA) connected to a modem. The weather station was installed within 1 km of the orchard, to the North-west. It was placed within a fenced area for security reasons (Figure 3.3 and Figure 3.7). The variables measured included solar radiation (LI-200S, Li-Cor, Lincoln, Nebraska, USA), temperature and relative humidity (HMP50, Vaisala Oyj, Vantaa, Finland), wind speed (cup anemometer, RM Young, Traverse City, Michigan, USA), and rainfall (TE525 tipping bucket rain gauge, Texas Electronics, Dallas, Texas, USA). Sensors were positioned according to FAO-56 for calculating reference evapotranspiration ( $ET_o$ ) (Allen et al., 1998). Quality of the data was assessed according to Allen (2008) Solar radiation was adjusted based on calibration with an Eppley standard precision pyranometer (The Eppley Laboratory Inc, Rhode Island, USAs). The weather station was surrounding by irrigated agriculture and therefore estimates of  $ET_o$  were likely to be accurate. Positive daily chill units were calculated according to Linsley-Noakes et al. (1995).



**Figure 3.8** The automatic weather station installed within 1 km of the trial site in Vaalharts

Thermal time was calculated using daily minimum and maximum temperatures and a base temperature for pecans of 15.5°C (Miyamoto, 1983) as follows

$$GDD = \frac{T_{max} + T_{min}}{2} - 15.5 \quad (9)$$

### 3.1.2.2 Groblershoop

Weather data was collected from an Automatic Weather Station (ClimaVue 50 (METER, Pullman WA, USA) attached to a CR300 datalogger (Campbell Scientific Inc. Logan, Utah, USA)) (Figure 3.3 and Figure 3.8 ). The weather station was situated 250 m from the orchard with irrigated agriculture to the north, east and west of the AWS. An open area is situated to the south. Due to the presence of irrigated agriculture,  $ET_o$  was likely to be well estimated. The variables measured included solar radiation, temperature, relative humidity, windspeed and rainfall, which were all measured by the ClimaVue 50, mounted at 2 m from the ground over a dry grass surface. Sensors were positioned according to FAO-56 for calculating reference evapotranspiration (Allen et al., 1998). Quality of the data was assessed according to Allen (2008). An adjustment was made to solar radiation adjustment which was underestimated. An additional rain gauge was placed close to the orchard in August 2021 due to faults with the rain measurements at the AWS. Overestimation of wind speed was noted in the summer of 2022/23, which were checked against windspeed from the Eddy Covariance tower. A calibration of the AWS was performed in February 2023 and windspeed was adjusted accordingly.



**Figure 3.9 The automatic weather station installed within 250 m of the study orchard on the farm close to Groblershoop**

### **3.1.3 TRANSPIRATION MEASUREMENTS**

In order to measure transpiration a heat pulse velocity (HPV) method was used, more specifically the heat ratio method (Burgess et al., 2001). This method is appropriate for pecan trees, and was used previously in pecan trees in South Africa (Ibraimo et al., 2016). Measurements were made on four ‘Choctaw’ trees and four ‘Wichita’ trees at each site. To ensure that good transpiration data was obtained, the sap flow systems in Vaalharts were moved from the initial trees (used at the beginning of the trial) to new trees in September 2022. Measurements were conducted in the same trees in Groblershoop for the duration of the trial.

Four heat pulse probe sets were used for each tree (each consisting of a heater probe inserted into a 2.5 mm brass collar and two type-T copper-constantan thermocouples embedded in 2 mm outside-diameter PTFE tubing, placed equidistantly up and down stream of the heater probe at a distance of 0.475 cm) (Figure 3.9). In order to account for the radial variation in sap flux within the conducting sapwood, thermocouples were inserted at varying depths to account for radial variation in the stem in each tree trunk, at 0.5 m above the soil surface and were equally spaced and randomly arranged around the trunk. The heat pulse velocity ( $V_h$ ) in  $\text{cm h}^{-1}$  for each probe set was calculated following Marshall (1958) as:

$$V_h = \frac{k_w}{x} \ln\left(\frac{v_1}{v_2}\right) * 3600 \quad (10)$$

where  $k_w$  is the thermal diffusivity of green (fresh) wood (assigned a value of  $2.5 \times 10^{-3} \text{ cm}^2 \text{ s}^{-1}$  (Marshall 1958)),  $x$  is distance in cm between the heater and either the upper or lower thermocouple,  $v_1$  and  $v_2$  are the maximum increases in temperature after the heat pulse is released (from initial temperatures) as measured by the upstream and downstream thermocouples and 3600 converts seconds to hours. Heat pulse velocities were measured and logged on an hourly basis using a CR1000 data logger and an AM16/32B multiplexer (Campbell Scientific Ltd, Logan, Utah, USA). Wounding corrections were performed by using wounding coefficients  $b$ ,  $c$ , and  $d$  obtained from a numerical model developed by Burgess et al. (2001) using the following equation:

$$V_c = bV_h + cV_h^2 + dV_h^3 \quad (11)$$

where  $V_c$  is the corrected heat pulse velocity. The functions describing the correction coefficients in relation to wound width ( $w$ ) were as follows:

$$b = 6.6155w^2 + 3.332w + 0.9236 \quad (12)$$

$$c = -0.149w^2 + 0.0381w - 0.0036 \quad (13)$$

$$d = 0.0335w^2 - 0.0095w + 0.0008 \quad (14)$$

The wound width was assessed through visual inspection and subsequent measurement of the outer diameter of the wound (Figure 3.10). The presence of heartwood was determined by taking wood cores with an incremental borer. These core samples were stained using safranin, with unstained areas being marked as non-conducting wood. Other wood characteristics, including sapwood moisture content ( $m_c$ ) and density ( $\rho_b$ ) were determined from additional core samples taken during the measurement period. These were determined for 'Wichita' and 'Choctaw' trees for both a number of times over the course of the study.



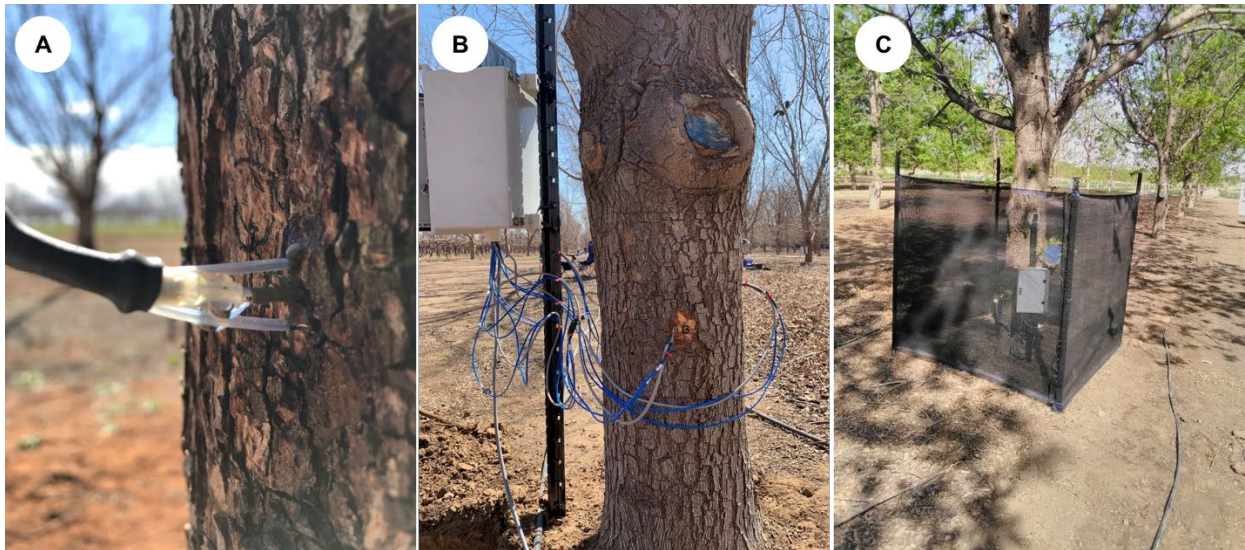


**Figure 3.10** A) The sap flow equipment used to measure transpiration, consisting of two T-type thermocouples and a heater probe in the middle. B) Probe placement around the trunk of a pecan tree. C) The shade netting erected around a pecan tree in Groblershoop to shade the sap flow probes.



**Figure 3.11** Determination of wounding caused as a result of the insertion of probes in the tree to determine heat pulse velocities and ultimately transpiration.

### 3.1.4 SOIL EVAPORATION MEASUREMENTS

Soil evaporation ( $E_s$ ) measurements were carried out with 18 micro-lysimeters in Pretoria (Figure 3.11) and 22 micro-lysimeters (ML) in Vaalharts and Groblersshoop (Figure 3.12) and. In each location, one of the four trees equipped with sap flow measurement instruments was utilized for  $E_s$  measurements. Orchards in Pretoria and Groblersshoop were drip irrigated (three drip lines per row, drippers spaced 0.6 m apart, with a delivery rate of  $1.6 \text{ L h}^{-1}$ , and two drip lines per row, drippers spaced 0.6 m apart, with a delivery rate of  $3.5 \text{ L h}^{-1}$  and a wetting diameter of 1.5 m respectively), whilst the orchard in Vaalharts was irrigated with one macro sprinkler per tree ( $150 \text{ L h}^{-1}$ ). The placement of the micro-lysimeters was designed to account for spatial variations in both water distribution and shading within the allocated tree area. The total area covered by the micro-lysimeters was divided into four zones: Zone 1 – sunny and wet, Zone 2 – shaded and wet, Zone 3 – sunny and dry, and Zone 4 – shaded and dry. In the drip irrigated orchards, Zone 1 was situated outside the canopy zone near the drippers, Zone 2 was positioned beneath the canopy and adjacent to the drippers, Zone 3 was located outside the canopy, and Zone 4 was positioned beneath the canopy but outside the radius of the wetted area. In Pretoria, four micro-lysimeters (4, 9, 10 and 15) were installed under sunny and wet area, five were placed under shaded and wetted area (11, 12, 17, 13 and 18), three were located under sunny and dry area (1, 2 and 5) and four were located under shade and dry area (Figure 3.11).

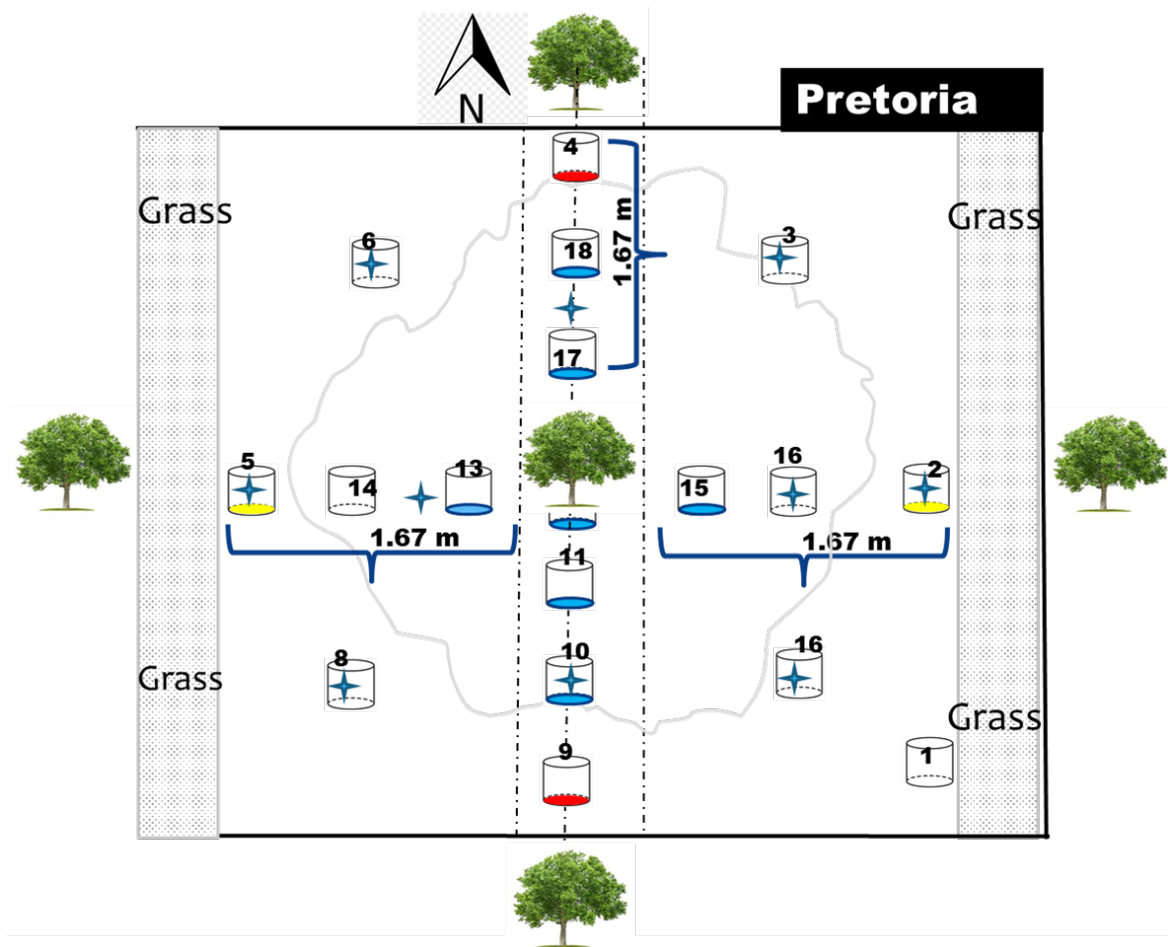


**Figure 3.12 Position of the micro-lysimeters for Innovation Africa@UP Pretoria. The blue stars represent the position of the line quantum sensors that were permanently installed underneath the canopy.**

The arrangement of micro-lysimeters in the drip-irrigated orchard in Groblershoop closely resembled the setup in Pretoria, with the majority of micro-lysimeters placed in both wet and dry areas, as well as shaded areas. In contrast, a distinct configuration was employed in the Vaalharts orchard, given that the orchard was under full surface irrigation.

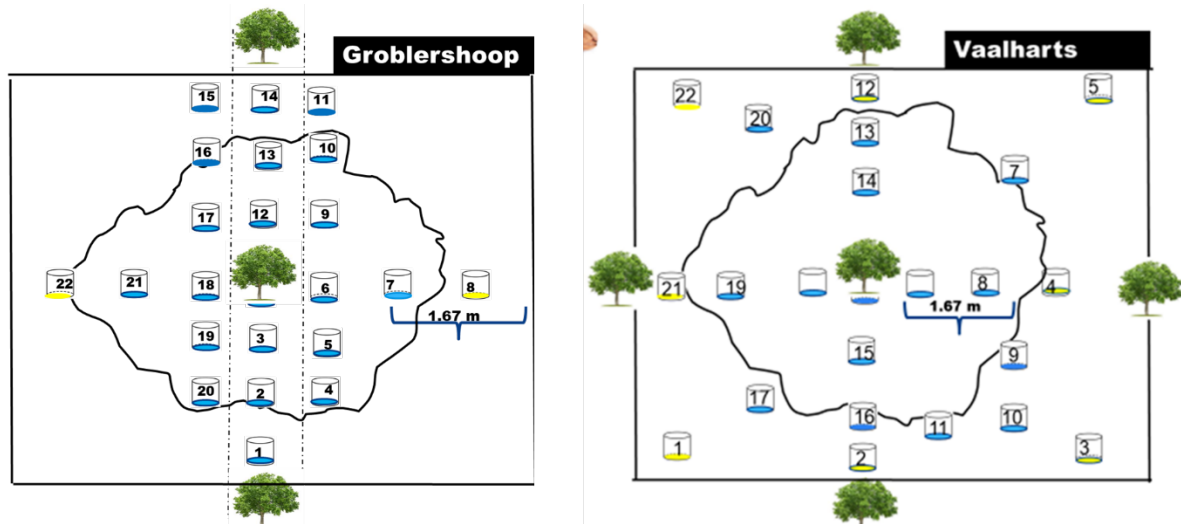


**Figure 3.13 Position of the micro-lysimeters for the three pecan orchards (A) Groblershoop, and (B) Vaalharts.**

The micro-lysimeters were 2 mm thick, and 140 mm deep with an internal diameter of 85 mm. Each micro-lysimeter had an external ring that was permanently installed throughout the measurement period. Undisturbed soil cores were sampled according to the procedure by Daamen et al. (1993) and the rate of  $E_s$  was calculated according to Flumignan et al. (2012) as:

$$E_{ML} = \frac{\Delta M_{ML}}{A_{ML}} + P \quad (15)$$

Where  $\Delta M_{ML}$  is the micro-lysimeter variation in mass (kg),  $A_{ML}$  is the micro-lysimeter surface area and  $P$  is precipitation in mm. Total evaporation is determined based on a weighted area that each micro-lysimeters represents within the area occupied by a tree.

To account for the influence of the canopy size, its variable positional shadings along the days and seasons, we conducted evaporation measurements simultaneously with diurnal FIPAR measurements. The details of the FIPAR measurement procedure are provided in section 3.1.7.



### 3.1.5 EVAPOTRANSPIRATION MEASUREMENTS

#### 3.1.5.1 Vaalharts

An extended Open Path Eddy Covariance (OPEC) system (Campbell Scientific Inc., Logan, UT, USA) was installed within 500 m of the North-East edge of the orchard at a height of 1.2 m above the 8 m trees (Figure 3.13). Micrometeorological variables measured included latent heat ( $\lambda E$ ), sensible heat ( $H$ ) and soil heat fluxes ( $G$ ). These measurements started in April 2019 and continued until the end of the trial in June 2023

The OPEC system consisted of a CR3000 datalogger and IRGASON open-path analyser and sonic anemometer (Campbell Scientific Inc., Logan, Utah, USA), which was mounted on a lattice mast. Air temperature and humidity were measured using a HygroClip2 HC2-S(3) thermohygrometer probe (Rotronic Instruments, Bassersdorf, Switzerland). Net radiation ( $R_n$ ) was measured using an NR-Lite net radiometer (Model 240-110 NR-Lite, Kipp & Zonen, Delft, Netherlands) 9.2 m above ground. Four soil heat flux plates (model HFT-S, REBS, Seattle, Washington, USA) were used to measure soil heat flux ( $G$ ) at a depth of 80 mm under the trees and between the rows, and four TCAV-L soil temperature averaging probes (Campbell Scientific Inc., Logan, Utah, USA) at depths of 20 and 60 mm were used to calculate the heat stored above the plates. Heat flux plates were placed under a tree and in the middle of the work row to account for variation in solar radiation distribution on the orchard floor throughout the day.

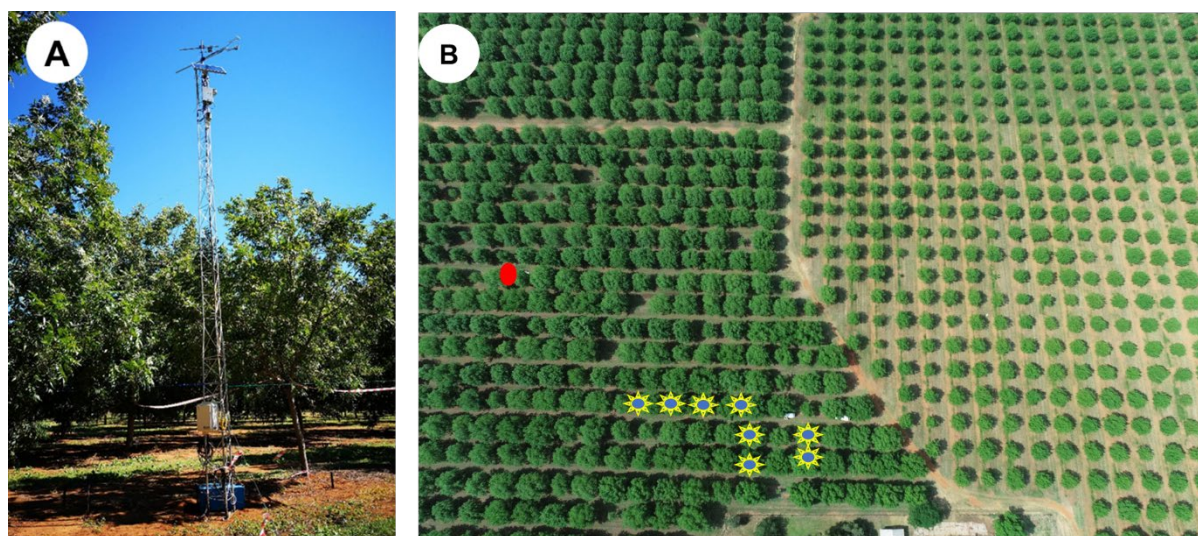


**Figure 3.14 A) Position of the Open Path Eddy Covariance system above the tree canopy. B) Position of the Open Path Eddy Covariance (red dot) system in relation to the sap flow measurements in 2022/23 season (stars).**

Volumetric water content in the first 60 mm of the soil surface was measured using two time-domain reflectometry sensors (CS616, Campbell Scientific Inc., Logan UT, USA). These sensors were connected to a CR3000 datalogger (Campbell Scientific Inc., Logan, UT, USA) and measurements were performed at 10 Hz frequency and averages obtained every 30 minutes. The EasyFlux<sup>TM</sup>-DL software applied the most common open-path EC corrections to fluxes.

Two infrared thermometers (model SI-121-SS, Apogee Instruments, INC., Logan, Utah, USA) were installed in February 2020 to monitor canopy temperature. They were positioned close to the top of the mast, with one facing the closest tree to the south east of the mast and the other to a tree in the neighbouring row to the west of the tower.

### *3.1.5.2 Groblershoop*

An eddy covariance system was installed in the orchard in Groblershoop on 15 September 2020 and will remain in the orchard until the end of the measurements in June 2023. The system was mounted on a pneumatic mast at approximately 15.5 m from the soil surface and approximately 2 m above the canopy (Figure 3.14). Micrometeorological variables measured included latent heat ( $\lambda E$ ), sensible heat ( $H$ ) and soil heat fluxes ( $G$ ). The system consisted of a CSAT3 3-D sonic anemometer and EC150 infrared gas analyser (Campbell Scientific Inc., Logan, UT, USA). Air temperature and humidity were measured using a HMP45C probe (Vaisala Oyj, Helsinki, Finland). Net radiation ( $R_n$ ) was measured using an NR-Lite net radiometer (Model 240-110 NR-Lite, Kipp & Zonen, Delft, Netherlands) 15.5 m above the ground. Four soil heat flux plates (model HFT-S, REBS, Seattle, Washington, USA) were used to measure soil heat flux ( $G$ ) at a depth of 80 mm under the trees and between the rows, and four TCAV-L soil temperature averaging probes (Campbell Scientific Inc., Logan, Utah, USA) at depths of 20 and 60 mm were used to calculate the heat stored above the plates. Heat flux plates were placed under a tree and within the middle of the row to account for variation in solar radiation distribution on the orchard floor throughout the day. Volumetric water content in the first 60 mm of the soil surface was measured using two time-domain reflectometer sensors (CS616, Campbell Scientific Inc., Logan UT, USA). These sensors were connected to the CR3000 datalogger (Campbell Scientific Inc., Logan, UT, USA) and measurements were performed at 10 Hz frequency and averages obtained every 30 minutes. The EasyFlux<sup>TM</sup>-DL software applied the most common open-path EC corrections to fluxes.



**Figure 3.15 A) Positioning of the Eddy Covariance system in the Groblershoop orchard installed in September 2020. The red arrow indicates the positioning of the tower, whilst the yellow arrows indicate the locations of the transpiration measurements. B) The Eddy covariance tower within the work row.**

### 3.1.6 ECOPHYSIOLOGICAL MEASUREMENTS

To determine if the trees were experiencing any water stress during the measurement period, predawn leaf water potential ( $\Psi_{pd}$ ) and stem water potential ( $\Psi_{smd}$ ) measurements were made every 4-6 weeks with a Model 600 Scholander pressure chamber (PMS Instrument Company, Albany, USA). Measurements of  $\Psi_{pd}$  were conducted before sunrise. For  $\Psi_{smd}$ , leaves were enclosed in foil covered plastic bags at least 30 min prior to measurements. Midday stem water potential below -0.9 MPa, were considered to represent unstressed conditions (Othman et al., 2014), whilst the threshold for  $\Psi_{pd}$  was -0.42 MPa. For these measurements three leaves per tree were measured and all trees instrumented with sap flow equipment were measured. For hydraulic conductance estimates and to determine if pecans tend to be more isohydric or anisohydric in their water use behaviour, leaf water water potential of three sun and three shade leaves were measured throughout the day at 2 h intervals. Stomatal conductance ( $g_s$ ) was measured using an LI-600 leaf porometer/fluorometer (LiCor Lincoln, Nebraska, USA)

### 3.1.7 DETERMINATION OF CANOPY SIZE

In order to understand the drivers of tree transpiration various canopy size measures (such as leaf area index (LAI), fractional ground cover (fc) and fractional interception of photosynthetically active radiation (FIPAR)) were determined at regular intervals throughout the study apart from during the COVID-19 lockdown. Measurements were taken on at least



two of the four trees per cultivar in the first three years and then on all four trees per cultivar the last two years of the study. Canopy cover measurements were obtained from drone-based images at each trial site. The images were used to estimate fractional ground cover referred to as ( $f_{c_{canopeo}}$ ) hereafter using Canopeo® image analysis tool in Matlab (Mathworks, Inc., Natick, MA) (Patrignani and Ochsner, 2015). The FIPAR was measured using an AccuPAR LP-80 ceptometer (Decagon Devices, Pullman, WA, USA). Measurements were taken under cloudless, full-sun conditions on a predetermined 1 m x 1 m grid, starting from the stem and stretching across the row and between the rows. Above canopy measurements were taken outside the orchard (Figure 3.15). Additional diurnal FIPAR measurements were determined to account for the dynamics of PAR interception in the orchard over a day. One tree per site at each study site was selected for the diurnal measurements. Hourly FIPAR was calculated from measured PAR transmittance using equation [16] (Palmer, 1977). Daily fractional interception of PAR was then computed by integrating the hourly measurements throughout the measurement hours.

$$FIPAR = \left(1 - \frac{PAR_b}{PAR_a}\right) \quad (16)$$



**Figure 3.16 The grid layout for the determination of fractional interception of PAR, from A) above and B) from under the tree canopy.**

Leaf area index measurements were taken using LAI-2200C Plant Canopy Analyser (Li-Cor Biosciences, Lincoln, Nebraska, USA) under diffuse light conditions. Measurements were taken at dawn or, when possible, during overcast conditions to avoid direct sunlight. The

instrument was programmed to take eighteen measurements per tree: two readings above the canopy (referred to as  $LAI_{ab}$ ) and sixteen readings below the canopy (referred to as  $LAI_b$ ). All the above-canopy readings were taken in an open area adjacent to the orchard, both prior to and following the collection of below-canopy measurements. Below-canopy measurements were taken within the tree rows and directly beneath the canopy, utilizing a 90° view cap on the optical sensor to restrict measurements to the tree row while keeping the operator out of the sensor's field of view. The measurements taken across the row were evenly spaced and maintained at the same height, as recommended by Welles and Norman (1991).

### **3.1.8 IRRIGATION AND SOIL WATER CONTENT**

Volumetric soil water content was determined at three positions in both orchards using TEROS-10 sensors (formerly GS-1, METER Group, Pullman, Washington, USA) which were placed at various depths down the soil profile. In Vaalharts, TEROS-10 sensors were placed at three different positions perpendicular to the row at tree 2 site B. These positions were within the row (halfway between the tree and the micro-sprinkler), at the edge of the canopy (2.7 m from the tree row) and in the middle of the row (5 m from the tree row). At each position, five GS-1 sensors were placed at 30, 40, 60, 90 and 120 cm from the soil surface. These sensors were removed at the start of the 2022/23 season, as sufficient data had been collected. Volumetric water content across a work row in the top 20 cm was determined using five CS616 sensors, placed perpendicular to the tree row midway between the tree and the micro-sprinkler. The sensors were placed at the tree row (0 cm) and then 1.25 m, 2.50 m, 3.75 m and 5.00 m from the tree row

In Groblershoop, TEROS-10 sensors were placed within the row (between the two drip lines), underneath a drip line (2.0 m from the tree row) and in the middle of the row (5 m from the tree row). At each of the three positions, five Teros-10 were placed at different depths of 30, 40, 60, 90 and 120 cm from the soil surface. This was in the row of 'Choctaw' trees. These sensors were also removed at the start of the 2022/23 season, as sufficient data had been collected. Five CS616 water content reflectometers were placed close to the 'Wichita' tree row in the top 20 cm (Figure 3.16). Sensors were placed at 0 m, 1.0 m, 2.0 m, 3.0 m and 5.0 m from the centre of the tree row, which corresponded to the wetting pattern of the drip irrigation and to account for zones shaded by the trees and wet by the irrigation.

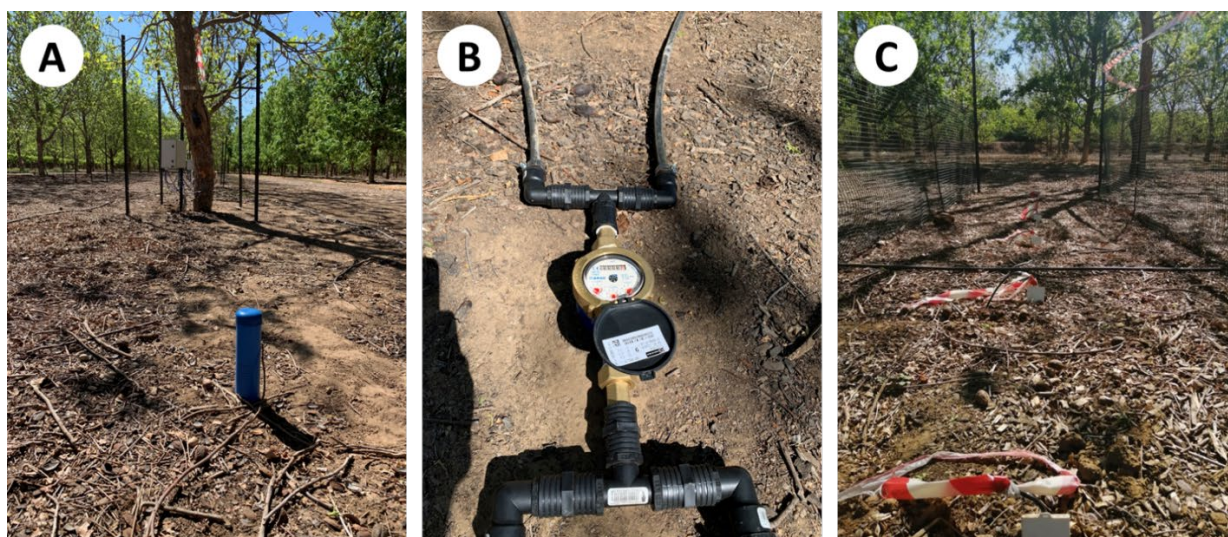


**Figure 3.17 A) Piezometer to determine the depth of the water table, B) water meters to determine irrigation volumes and 3) CS616 sensors determining soil water content in the top 20 cm of the soil profile**

Irrigation events were measured at each site with flow meters installed upstream of each respective study site (Figure 3.16B). The water meters were read during each visit to the orchard and volumes applied per tree calculated from the readings for a season. A METER PS-1 Irrigation Pressure Switch (METER Group, Pullman, Washington, USA) was plumbed into a line in Groblershoop to determine irrigation run times. This was connected to an EM50 logger (METER Group, Pullman, Washington, USA).

In water use experiments it is important to measure all inputs of water into the system that might affect total tree water use. The failure to measure all the water inputs into the system can result in an underestimation of actual tree water use. To account for periodic water table fluctuations, a piezometer was installed at a depth of 2.5 m depth (Figure 3.16A). The piezometer was installed in the centre of the trial site to account for a larger measurement area. The positioning of the irrigation and soil water monitoring equipment in both orchards is provided in Figure 3.17.



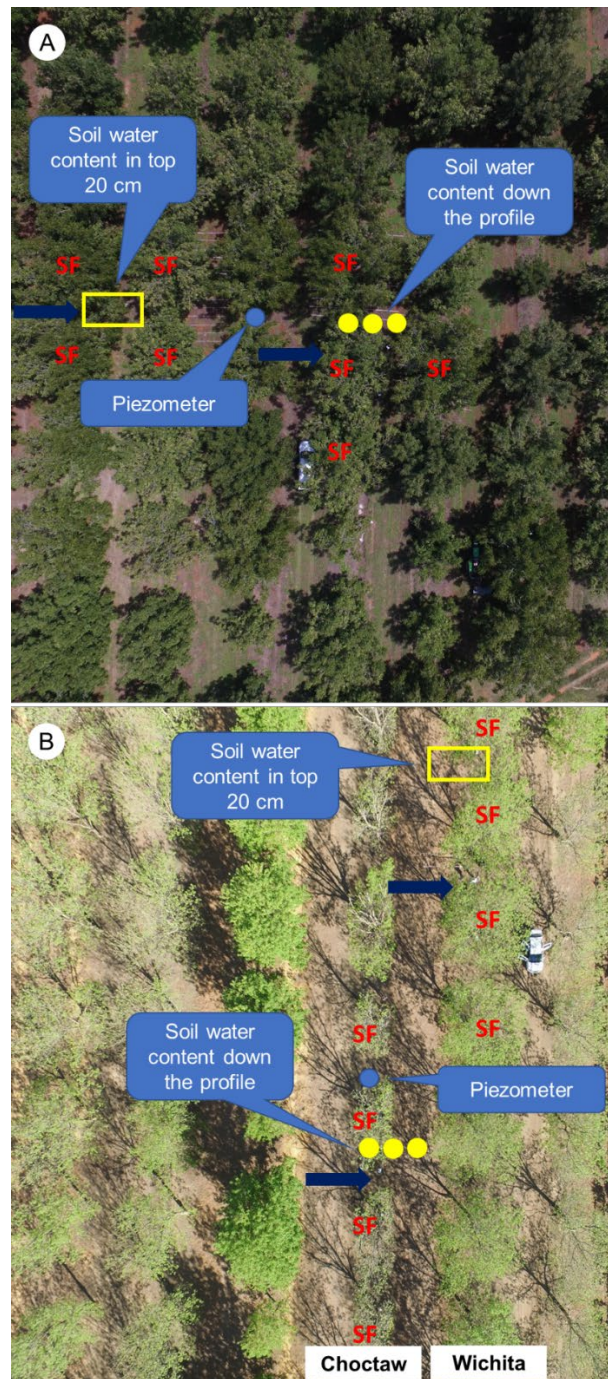


**Figure 3.18 Positioning of soil water monitoring equipment in the pecan orchards in A) Vaalharts and B) Groblershoop.**

### 3.1.9 CROP WATER PRODUCTIVITY AND ECONOMIC WATER PRODUCTIVITY

Yield for the whole orchard was obtained for each farm and for the individual trees instrumented with sap flow equipment. Quality assessments were performed by local processors, who also provided the price per kg, which allowed the estimation of gross profit

per ha. Crop budgets for pecans and annual crops were obtained via GWK's (local co-operative) Profarmer programme for each season (<https://info.profarmer.co.za>). Average yields for annual crops were also taken from Profarmer. Crop budgets for raisin grapes were obtained from Raisins South Africa Kostegids 2022 (<https://raisinsa.co.za/>).

SAPWAT4 (Van Heerden and Walker, 2016), which follows the FAO-56 approach, was used to estimate average ET for annual crops grown in the Vaalharts region and raisin grapes in the Groblershoop region. This method is widely used in South Africa to estimate crop water and irrigation requirements, including by the government. Long term weather data (1950-1998) for the region was used to estimate an average ET for maize, cotton, lucerne, wheat and groundnuts. In the simulation the annual crops were irrigated with a centre pivot and the soil chosen was a sandy loam, which represents the majority of soils in the region. Both microsprinkler and drip irrigation were considered for raisin grapes, with a sandy loam soil.

Water use indicators as defined by Fernández et al. (2020) were used in this study. Crop water productivity based on  $ET_c$  ( $WP_c$ ,  $kg\ m^{-3}$ ) or crop water productivity based on T ( $WP_T$ ) and irrigation water productivity ( $WP_I$ ,  $kg\ m^{-3}$ ) were calculated as:

$$WP_c = \frac{yield}{ET_c} \quad \text{or} \quad WP_T = \frac{yield}{T} \quad \text{or} \quad WP_I = \frac{yield}{IWU} \quad (17)$$

Where IWU is volume of irrigation water applied. Economic crop water productivity ( $EWP_c$ ,  $R\ m^{-3}$ ) and economic irrigation water productivity ( $EWP_I$ ,  $R\ m^{-3}$ ) are calculated using the net margin as:

$$EWP_c = \frac{profit}{ET_c} \quad \text{or} \quad EWP_I = \frac{profit}{IWU} \quad (18)$$

Profit was calculated by subtracting total production costs from the gross profit per ha, based on commodity prices for each season from Profarmer.

### 3.1.10 WATER USE MODELLING

#### 3.1.10.1 *Radiation interception modelling*

The fraction of intercepted photosynthetically active radiation (FIPAR) by the pecan trees was estimated using the model of Oyarzun et al. (2007). The model estimates FIPAR of an orchard based on the fraction of the ground surface that is shaded by the orchard trees at any given



time. This is obtained based on geometric relationships of the size of the shadow cast by the trees, the orchard configuration, and the canopy porosity ( $C_p$ ), which represents the transmitted light within the canopy gaps and is observable as sun-flecks within the shadow area cast by the trees on the ground (Figure 3.18). The model considers that  $C_p$  varies during the day following the sun elevation, with minimum values of  $C_p$  at sunrise and sunset and maximum values at solar noon. Input parameters required by the model include: the canopy width, both perpendicular to the row direction ( $W_x$ ) and along the row direction ( $W_y$ ), the maximum canopy height measured from the ground, ( $H$ ), the height of the insertion of the lower branches ( $B$ ) referred to as bare stem height hereafter, and  $C_p$ . The beam and the diffuse radiation are considered separately since the penetration of direct beam and diffuse radiation into the canopy is different (Weiss and Norman 1985). In addition, the model requires the distance between trees within and between rows ( $E_x$  and  $E_y$ ), and the row azimuth ( $\phi_r$ ). Figure 3.18 shows a schematic representation of the canopy dimensions and orchard configuration input parameters of the model.

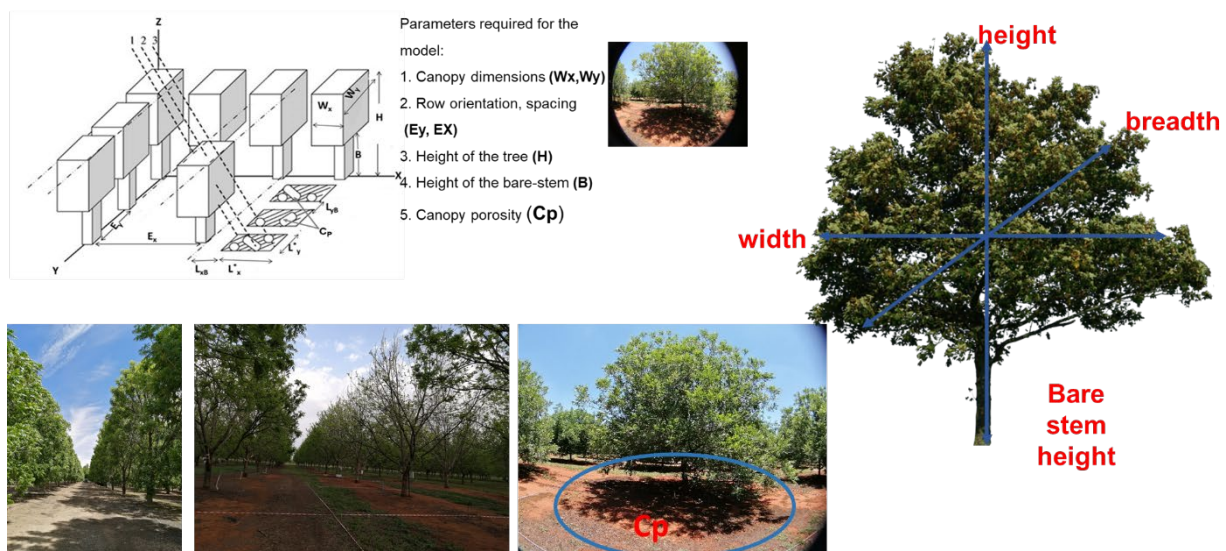


**Figure 3.19 Schematic representation of a fruit tree orchard showing model input parameters used in the radiation interception model. The dashed lines show the interaction between solar rays (--) and the trees when: (1) the direct rays of the sun pass unobstructed below the canopy; (2) the direct rays of the sun pass unobstructed through gaps in the canopy, observed as a sun-fleck on the shaded ground area ( $C_p$ ); and (3) the beam passes by the edge of the canopy, thus casting a shadow. X, Y, and Z show the Cartesian axes Oyarzun et al. (2007)**

## Modelling intercepted photosynthetically active radiation in row crops

### Location of the sun

First the incident incoming daily and hourly solar radiation (partitioned into diffuse and direct radiation) prior to interaction with vegetation or soil was determined. This depended on

geographical location, weather patterns, and time of year. A detailed description of how to compute the incoming daily and hourly solar radiation are given in Oyarzun et al. (2007) and Campbell and Norman (1998). The current section will focus on the computation of intercepted radiation based on the shadow of the tree canopies.

### **Computation of the intercepted beam and diffuse radiation based on the shadow cast on the ground**

In discontinuous stands, the length of the shadow cast on the ground is defined in two directions; (1) the length perpendicular to the rows ( $L_x$ ) and (2) the length along the row direction ( $L_y$ ). The two lengths were computed from the canopy height, solar zenith and azimuth angle following the procedure by Cohen et al. (1997) as:

$$L_x = H[\tan(\theta) \sin(\phi_s - \phi_r)] \quad (19)$$

$$L_y = H[\tan(\theta) \cos(\phi_s - \phi_r)] \quad (20)$$

Where ( $\theta$ ) is zenith angle and is the azimuth angle ( $\phi_s$ )

Equations [19] and [20] assume that the tree canopy extends completely to the floor. However, this rarely happens in orchard trees. Therefore, the length of the blank shadow perpendicular ( $L_{x,B}$ ) and along the rows ( $L_{y,B}$ ) must be calculated to adjust for the bare stem that has no effect on the shadow cast on the orchard floor (Oyarzun et al., 2007). The two shadow lengths were calculated as:

$$L_{x,B} = B[\tan(\theta) \sin(\phi_s - \phi_r)] \quad (21)$$

$$L_{y,B} = B[\tan(\theta) \cos(\phi_s - \phi_r)] \quad (22)$$

In addition, equations [21] and [22] do not account for the slope effect on the shadow cast on the orchard floor. Thus, a correction factor ( $\sigma$ ) which accounts for the combined effect of sun position, the slope, and the aspect of the slope on the shadow length must be computed. This factor considers that the length of the shadow cast on a sloped surface could be greater or smaller than the shadow cast on a horizontal plane. The value of  $\sigma$  was estimated using equation [23].

$$\sigma = \begin{cases} \cos \rho, & [45^\circ < (\phi_s - \phi_p) < 135^\circ] \\ \frac{1}{\cos \rho}, & [225^\circ < (\phi_s - \phi_p) < 315^\circ] \\ 1, & \text{otherwise} \end{cases} \quad (23)$$

The effective shadow length cast by the trees on the sloped surface in a perpendicular direction to the row ( $L_x^*$ ) and along the row direction ( $L_y^*$ ) was determined as:

$$L_x^* = (L_x - L_{x,B})\sigma \quad (24)$$

$$L_y^* = (L_y - L_{y,B})\sigma \quad (25)$$

### The fraction of the shaded orchard floor

According to Oyarzun et al. (2007), the fraction of the orchard floor that is shaded at any given time is given as:

$$f_{sh} = \frac{[(L_x^* + W_x)W_y + (L_y^* + W_y)W_x - (W_x W_y)]}{(E_x E_y)} \quad (26)$$

This value corresponds to the fraction of beam intercepted by black canopies without considering the effects of  $C_p$  or scattering. When the sun is directly overhead (zero zenith angle),  $f_{sh}$  is equivalent to the fraction of the orchard floor occupied by the trees. Conversely, when the shadow is large enough to extend beyond several adjacent rows, the value of  $f_{sh}$  could mathematically be higher than one, so it is limited to one (Oyarzun et al., 2007).

The fraction of hourly and daily intercepted radiation was calculated by considering the beam and the diffuse radiation components. The model assumes that the fraction of hourly and daily intercepted diffuse radiation is the same, and the value of the fraction of intercepted daily diffuse radiation depends on the daily average effective orchard diffuse transmittance ( $\tau_{b,h}$ ).

The fraction of intercepted beam on an orchard basis for each hour ( $f_{b,h}$ ) was calculated as:

$$f_{b,h} = f_{sh}(1 - C_p^*) \quad (27)$$

Where  $C_p^*$  is the effective canopy porosity, calculated from the  $C_p$  and the canopy absorptivity coefficient ( $\alpha$ ),  $\alpha$  was assumed to be 0.85 in the PAR range (Schultz 1996) and 0.5 for  $S_g$ .

Therefore, the value of  $C_p^*$  was given by:

$$C_p^* = \exp[\ln(C_p)\sqrt{\alpha}] \quad (28)$$

The hourly beam transmittance on an orchard basis was obtained as:

$$\tau_{b,h} = (1 - f_{b,h}) \quad (29)$$

and the daily average effective diffuse transmittance on an orchard basis ( $\tau_{d,D}$ ) was then obtained numerically after (Campbell and Norman, 2012) and modified as:

$$\tau_{d,D} = 2 \sum_{h=t_{sr}+1}^{h=t_{ss}} \tau_{b,h} \cos(\theta_h) \sin(\theta_h) d\theta_{h-(h-1)} \quad (30)$$

Where  $t_{sr}$  is the time of sunrise and is the time of sunset  $t_{ss}$

Then, the diffuse radiation interception fraction for the orchard was determined as:

$$f_{d,D} = 1 - \tau_{d,D} \quad (31)$$

Finally, the estimated hourly values of PAR interception  $fIPAR_h$  was calculated as:

$$FIPAR_h = f_{b,h}F_{PARb,h} + F_{d,D}F_{PARd,h} \quad (32)$$

The computation of daily PAR interception  $fDIPAR$  was obtained by integrating the estimated hourly intercepted PAR as:

$$fDIPAR = \frac{\int_{h=t_{sr}+1}^{h=t_{ss}} (fIPAR_h * PAR_h) dh}{\int_{h=t_{sr}+1}^{h=t_{ss}} PAR_h dh} \quad (33)$$

Where  $PAR_h$  is the hourly incoming PAR, obtained as

$$PAR_h = \frac{S_{g,h}^* F_{PAR}}{S_g} \quad (34)$$

and  $F_{PAR,h}/S_g$  is the fraction of global solar radiation that corresponds to the PAR wavelength range, which was assumed to be 0.50 in an energy-based context ( $W m^{-2}$ ) (Rohrig et al., 1994; Spitters et al., 1984; Wang et al., 2002).

## Field measurements

Canopy dimensions and canopy architecture measurements were obtained concurrently with the FIPAR measurements. Canopy dimensions (H, W<sub>x</sub>, W<sub>y</sub>,) were estimated using a tape measure and QGIS V 2.2.0 (® Free Software Foundation, Inc., Boston USA) package. The canopy porosity was estimated using the VitiCanopy® application installed on an Android mobile phone equipped with an external fisheye lens. Row orientation and the aspect were measured with a compass, which was corrected for magnetic declination so that row orientation was relative to true north. Location data (altitude, latitude, longitude and standard meridian) were determined using Google Earth. The slope was determined with an inclinometer, whilst daily global solar radiation (S<sub>g</sub>, D, in MJ m<sup>-2</sup>d<sup>-1</sup>) was obtained from the automatic weather stations installed on the farms.

### 3.1.10.2 Crop coefficient approach

The strict definition of a basal crop coefficient (K<sub>cb</sub>) includes some evaporation when the soil surface is dry (Allen et al., 1998) and as direct measurements of *T* were made using a sap flow method in this trial, transpiration crop coefficients (K<sub>t</sub>) were derived instead of K<sub>cb</sub>, as proposed by Villalobos et al. (2013). Daily K<sub>t</sub> values were calculated by dividing measurements of *T* by daily ET<sub>o</sub> as follows:

$$K_t = \frac{T}{ET_o} \quad (35)$$

Estimates of K<sub>t</sub> were calculated according to the procedure outlined by Allen and Pereira (2009), where K<sub>t</sub> during conditions of nearly full ground cover (K<sub>t full</sub>) is multiplied with a density coefficient (K<sub>d</sub>), which is linked to the abundance of vegetation present, and is presented as follows:

$$K_t = K_{t \text{ full}} \times K_d \quad (36)$$

Daily values of K<sub>d</sub> were calculated in accordance with Allen and Pereira (2009) as:

$$K_d = \min \left( 1, M_L f_{c \text{ eff}}, f_{c \text{ eff}}^{\left( \frac{1}{1+h} \right)} \right) \quad (37)$$

where  $f_{c \text{ eff}}$  is the effective fraction of ground covered or shaded by vegetation [0.01-1] near solar noon,  $M_L$  is a multiplier on  $f_{c \text{ eff}}$  describing the effect of canopy density on shading and on maximum relative evapotranspiration per fraction of ground shaded [1.5-2.0], with a value of 1.5 chosen for pecan and  $h$  is tree height.

The effective fraction of ground covered ( $f_{c \text{ eff}}$ ) was calculated as according to Allen et al. (1998) for a hedgerow planting as follows:

$$f_{c \text{ eff}} = f_c \left[ 1 + \frac{HWR}{\tan(\eta)} \right] \leq 1 \quad (38)$$

where  $f_c$  is the observed fraction of soil surface that is covered by vegetation as seen from directly overhead and HWR is the height to width ratio.  $f_{c \text{ eff}}$  is usually calculated at solar noon, such that  $\tan(\eta)$  is the mean angle of the sun,  $\eta$ , above the horizon during the period of maximum evapotranspiration, which is calculated as

$$\eta = \arcsin [\sin(\varphi) \sin(\delta) + \cos(\varphi) \cos(\delta)] \quad (39)$$

where  $\varphi$  is latitude and  $\delta$  is solar declination in radians.

The HWR was calculated as

$$HWR = \frac{h_{canopy}(\cos(\Gamma))}{width} \quad (40)$$

Where  $\Gamma$  is the angle of the plant row from an east-west direction in radians and width is the mean width of the canopy.

In accordance with Allen and Pereira (2009),  $K_{t \text{ full}}$  can be approximated, for large stand size (greater than about 500 m<sup>2</sup>), as a function of mean plant height ( $h$ , m) and adjusted for climate using wind speed ( $u_2$ , m s<sup>-1</sup>), percentage minimum relative humidity ( $RH_{\min}$ ), and the degree of stomatal control on  $T$  relative to most agricultural crops ( $F_r$ , unitless), as follows:

$$K_{t \text{ full}} = F_r \left( \min(1.0 + 0.1h, 1.20) + [0.04(u_2 - 2) - 0.004(RH_{\min} - 45)] \left(\frac{h}{3}\right)^{0.3} \right) \quad (41)$$

where  $F_r$  [0-1] is a relative adjustment factor for stomatal control and was calculated as follows:

$$F_r \approx \frac{\Delta + \gamma(1 + 0.34u_2)}{\Delta + \gamma \left( 1 + 0.34u_2 \frac{r_{\text{leaf}}}{100} \right)} \quad (42)$$

where  $r_{\text{leaf}}$  is the mean leaf resistance (s m<sup>-1</sup>);  $\Delta$  is the slope of the saturation vapour pressure versus air temperature curve (kPa °C<sup>-1</sup>) and  $\gamma$  is the psychrometric constant (kPa °C<sup>-1</sup>).  $r_{\text{leaf}}$  for most agricultural crops under full cover conditions (when the LAI exceeds 3.0 m<sup>2</sup> m<sup>-2</sup>) is 100 s m<sup>-1</sup> (Allen and Pereira 2009). No values of  $r_{\text{leaf}}$  have been proposed for pecan.  $r_{\text{leaf}}$  for each orchard was estimated by inverting Equation [42], after solving for  $F_r$  by inverting Equation [41], using known daily values of  $K_{t \text{ full}}$ .  $K_{t \text{ full}}$  values were calculated using measured daily  $K_t$  and  $K_d$  estimated from measured data. These  $r_{\text{leaf}}$  values were subsequently used to estimate  $F_r$  for independent seasons of measurements using Equation [41] in order to estimate  $K_t$  and  $T$  values for model validation purposes.

Taylor et al. (2015), demonstrated that the use of a single value of  $r_{\text{leaf}}$  in the estimation of crop coefficients was not appropriate for estimating water use of citrus and suggested that the use of monthly estimates of  $r_{\text{leaf}}$  might provide more accurate estimations of water use in citrus. Various methods of estimating  $r_{\text{leaf}}$  for the accurate determination of  $K_t$  values for the pecan orchards was therefore attempted and tested.

### 3.1.10.3 Transpiration modelling

The canopy conductance model of Villalobos et al. (2013) was used to estimate calculated transpiration estimates (mm day<sup>-1</sup>) from the estimated FIPAR (section 3.1.10.1) and daytime vapour pressure deficit (VPD).

The model estimates  $T$  (mm day<sup>-1</sup>) as a function of FIPAR of the canopy (dimensionless), daily total solar radiation ( $R_{sp}$ , J m<sup>-2</sup> day<sup>-1</sup>) and vapour pressure deficit (VPD, kPa) as follows:

$$T = 37.08 \times 10^{-3} \frac{(FIPAR)R_{sp}}{a + bVPD} \frac{VPD}{P_a} \quad (43)$$

where the coefficient  $37.08 \times 10^{-3}$  is used to convert the units to mm day<sup>-1</sup>;  $a$  ( $\mu\text{E mol}^{-1}$ ),  $P_a$  is atmospheric pressure in kPa and  $b$  ( $\mu\text{E mol}^{-1} \text{ kPa}^{-1}$ ) are the intercept and slope of the linear function relating  $(FIPAR \cdot R_{sp})/G_c$  to VPD. Daytime mean values of canopy conductance ( $G_c$ , mm day<sup>-1</sup>) were calculated by the inversion of the imposed evaporation equation from measured transpiration as follows:

$$G_c = \frac{TP_a}{VPD} \quad (44)$$

The model was calibrated and validated with different  $T$  datasets obtained from all the orchards under study. A threshold VPD value of less than 0.2 kPa was used to eliminate errors associated with extremely low VPD values on  $G_c$  as suggested by Phillips and Oren (1998). This value was selected after observing large errors in computed  $G_c$  when  $T$  and/or VPD had very low values. In addition, data during rainy days were excluded from  $T$  estimation since sap flow is reduced in wet canopies (Villalobos et al., 2006).

#### 3.1.10.4 *Evaporation modelling*

Two contrasting models were used to estimate evaporation ( $E_s$ ) below the canopy (1) the modified model of Bonachela et al. (2001) following the procedure by Tezza et al. (2019) and the FAO-56 approach (Allen et al., 1998). The former calculates  $E_s$  based on the two-stage evaporation: stage 1 (energy limiting) and stage 2 (falling stage). During stage 1,  $E_s$  is calculated as the sum of the equilibrium evaporation at the soil surface and an aerodynamic term derived from the Penman-Monteith equation, whilst in stage 2,  $E_s$  is obtained as a function of time following the procedure by Ritchie (1972). Details of the original model can be obtained from Bonachela et al. (1999) and the subsequent study by Bonachela et al. (2001). The current description will focus on the adjustments that were made to improve the estimation of  $E_s$ . For estimating  $E_s$  during stage 1 equation [45] was used

$$E_{s1} = \left[ \frac{\Delta}{(\Delta + \gamma)} \right] R_n \times a + \left[ \frac{\gamma}{(\Delta + \gamma)} \right] VPD \cdot 2.7 (1 + u_2/100) \quad (45)$$



where  $E_{s1}$  is soil evaporation during the energy-limiting stage ( $\text{mm day}^{-1}$ ),  $\Delta$  is the slope of the vapour pressure curve ( $\text{kPa } ^\circ\text{C}^{-1}$ ),  $\gamma$  is psychrometric constant ( $\text{kPa } ^\circ\text{C}^{-1}$ ),  $R_n$  is net radiation ( $\text{mm day}^{-1}$ ),  $a$  is the PAR transmissivity (estimated using the FIPAR model), VPD is the vapour pressure deficit (kPa), and  $u_2$  is the wind speed at 2 m height ( $\text{km day}^{-1}$ ). To adjust for the shape of the wetted area and its arrangement in a long row the wind speed function in equation [46]  $(2.7 (1 + u_2/100))$  can be obtained using the one presented for elongated water bodies as:

$$f(u_2) = (2.33 + 1.65 u_2)L^{-0.1} \quad (46)$$

Where  $u_2$  is the wind speed at 2 m height ( $\text{m s}^{-1}$ ) and  $L$  is the average width of the water surface.

We also tested an equation by Tezza et al. (2019) which simply calculates  $E_{s1}$  as

$$E_{s1} = ET_0 K_x \left(1 - \frac{R_i}{100}\right) \quad (47)$$

Where  $1 - \left(R_i/100\right)$  is the fraction of daily radiation reaching the surface, which was estimated using the FIPAR model.

Estimation of the falling stage  $E_{s1}$  for a complete drying cycle was according to Ritchie (1972) as :

$$E_{s2} = C \left(t^{0.5} - (t - 1)^{0.5}\right) \quad (48)$$

where  $E_{s2}$  is daily soil evaporation during the falling rate stage ( $\text{mm day}^{-1}$ ),  $t$  is time (days) elapsed from the day following rain, and  $C$  is a soil parameter ( $\text{mm day}^{-0.5}$ ). since  $E_s$  in wet soils is strongly related to the soil parameter  $U$  and  $C$  (from Ritchie equation) were obtained by adding, in the original equation, a time-dependence function (time since last irrigation,  $t$ ), as in Equation [46] (the wind speed function) in the original equation with a best-fit exponent. Since measurements for a complete dry cycle were not possible this optimisation gave us an alternative opportunity to access the empirical approach compared to the predefined parameters by Ritchie (1972).

The FAO-56 approach is also based on the two-stage method, however, the evaporation coefficient ( $K_e$ ) assumes an evaporation decay function that is based on the relative amount of water remaining in an evaporation layer (Allen et al., 1998, Allen et al., 2005). Evaporation is divided into two stages that characterize the form or nature of control on the evaporation process and rate (Ritchie, 1972). During stage 1,  $E_s$  is controlled by weather variables. During

this stage, the soil surface is sufficiently wet so that water is transported to the surface at least at a rate equal to the evaporation potential (the topsoil is assumed to be at field capacity), and therefore the evaporation rate is limited by energy availability (Allen et al., 2005). At this stage, the amount of water evaporated is related to the hydraulic conductivity and water-holding capacity of the soil, evaporative demand, and depth of the wetting event. During stage 2 evaporation,  $E_s$  is controlled by water availability. At this point, the surface soil water content has decreased to where the hydraulic capacity of the soil is unable to allow water loss (Tezza et al., 2019). The evaporation rate during stage 2 progressively decreases and ends when the total amount of water that can be evaporated from the topsoil is depleted. The FAO-56 procedure for calculating  $E_s$

$$E_s = E_s = ET_0 K_e \quad (49)$$

Whereby the soil evaporation coefficient was determined as described by the FAO-56 dual crop coefficient approach (equation 49) (Allen et al., 2005, Allen et al., 1998);

$$K_e = K_r(K_{c \max} - K_{cb}) \leq f_{ew} K_{c \max} \quad (50)$$

Where  $K_r$  is a dimensionless evaporation reduction coefficient that depends on the cumulative depth of water evaporation from the surface,  $K_{c \max}$  is the largest value a crop coefficient can sustain, as it is energetically unfavourable to maintain a  $K_c$  above 1.4 (Allen et al., 1998), following rain or irrigation,  $K_{cb}$  is the basal crop coefficient which follows the same assumption as Taylor et al. (2015) whereby  $K_{cb}$  is presumed equal to the transpiration crop coefficient ( $K_t$ ) because sap flow was used to estimate transpiration and  $K_{cb}$  includes some background evaporation from a dry soil, and lastly  $f_{ew}$  is the fraction of soil that is wetted and receives solar radiation.  $K_{c \max}$  was set at 1.4 as the maximum values observed at the trial site varied between 1.35 and 1.4, with an added 0.05 which is an empirical coefficient which accounts for any increase in  $K_t$  as a result of surface wetting (Allen et al., 2005).

During a complete drying cycle, following rain or irrigation, the soil evaporation reduction can be calculated as (Allen et al., 1998).

$$TEW = (\theta_{FC} - 0.5\theta_{PWP})Z_e \quad (51)$$

Where TEW is total evaporable water (mm),  $\theta_{FC}$  the volumetric soil water content at field capacity conditions, the modelling procedure assumes topsoil  $\theta_{FC}$  conditions following a large wetting event (rainfall amount should be larger than  $0.2 \times ET_0$  to be considered as a large

wetting event (Allen et al., 1998)),  $\Theta_{PWP}$  is the volumetric soil content at permanent wilting point, it is assumed that after a rainfall event the soil is allowed to dry to a point that is halfway between oven dry conditions (complete absence of water) and wilting point,  $Z_e$  represent the thickness of the topsoil layer from which evaporation occurs, according to procedure  $Z_e$  should be selected that it is representative of  $E_s$  values over complete drying cycles through model calibration using  $E_s$  measurements. In this study  $Z_e$  values were fixed at 150 mm for the sandy loam soils in Vaalharts and Groblershoop. The soil water content at  $\Theta_{FC}$  was calculated as  $0.214 \text{ m}^3\text{m}^{-3}$  and the  $\Theta_{PWP}$  at  $0.09 \text{ m}^3\text{m}^{-3}$  with the procedure described by Saxton et al. (1986) which considers soil texture and composition. Parameters for calculation are provided in Table 3.2.

The subsequent calculated value of TEW was used to calculate the reduction cycle of soil evaporation that occurs in two different stages (Allen et al., 1998). Stage 1 occurs after a rainfall or irrigation event, at the onset of the drying cycle, when the soil is at field capacity conditions. At this stage the assumption is made that the soil surface is wet resulting in evaporation to occur at a maximum rate from the exposed soil ( $K_r = 1$ ) with the only imposed limitation being the availability of energy at the soil surface. At the conclusion of stage 1 the cumulative depth of evaporation, termed  $D_e$ , has reached its maximum without restriction, regarded as the readily evaporable water (REW), which was taken as 10 mm in this study (Allen et al., 1998). As the process of evaporation proceeds further, stage 2 ensues, during which less water is available for evaporation. Consequently, there is a reduction in  $E_s$  (evaporative demand) relative to the total residual water content in the topsoil, as described by Equation [52] (Allen et al., 1998);

$$K_r = \frac{TEW - D_{e,i-1}}{TEW - REW} \text{ where } D_{e,i-1} < REW \quad (52)$$

Where  $D_{e,i-1}$  is the cumulative depth of evaporation after a large wetting event at the end of day<sub>*i-1*</sub> (mm), which is determined by a daily water balance computation for the topsoil layer using equation [53] (Allen et al., 1998);

$$D_{e,i} = D_{e,i-1} + (P_i - RO_i) + \frac{I_i}{f_w} - \frac{E_{s,i}}{f_{ew}} - T_{ew,i} - DP_{e,i} \quad (53)$$

Where  $D_{e,i}$  represents the cumulative depth of evaporation following a substantial wetting event at the end of day *i* (mm) and  $D_{e,i-1}$  is the cumulative depth of the previous day,  $P_i$  is the effective rainfall on day *i* (mm),  $RO_i$  is the runoff that occurs after a precipitation event on day

$i$  (mm),  $I_i$  is the depth of irrigation on day  $i$  (mm),  $E_{s,i}$  is the amount of evaporation occurring on day  $i$  (mm),  $T_{ew,i}$  is the depth of transpiration from the exposed and wetted fraction of the soil surface layer on day  $i$  (mm),  $DP_{e,i}$  is the deep percolation loss from the topsoil if the soil exceeds field capacity conditions on day  $i$  (mm),  $f_w$  is the fraction of the soil surface wetted by irrigation (ranges between 0.01 and 1), where  $f_{ew}$  is the exposed and wetted soil fraction (ranges between 0.01 and 1). In this study  $Ro_i$  was assumed to be zero because the effective precipitation events causing runoff likely replenished the topsoil's water content to field capacity conditions. Also,  $T_{ew,i}$  was presumed to be negligible since the transpiration from the layer where evaporation occurs is minimal in deep-rooted crops like pecan (Allen et al., 1998). The soil surface receiving both irrigation and precipitation ( $f_{ew}$ ) was defined as  $f_i - f_{c\ eff}$  where  $f_{c\ eff}$  is the fraction of soil surface covered by vegetation at solar noon, and  $f_r$  represents the fraction of the wetted soil surface, always taken as 1 regardless of ground cover type (Allen et al., 2005, Allen et al., 1998). The  $f_{ew}$  and  $f_w$  was calculated from Equation [54] and Equation [55] as:

$$f_{ew} = \min (1 - f_{c\ eff}, 1) \quad (54)$$

$$f_w = \min (1 - f_{c\ eff}, f_w) \quad (55)$$

As pecans are deep rooted crops, all the available soil water in  $f_{ew}$  and  $f_w$  is assumed to be available for  $E_s$  with very little of the water contributing to the transpiration deeming it negligible (Allen et al., 2005). The maximum of  $K_c$  can therefore not exceed  $f_w K_{c\ max}$  (Allen et al., 1998). The subsequent value is then compared against  $K_e$  to ensure it is less than the imposed upper limit.

**Table 3.2 Values used to parameterize the FAO-56 dual crop coefficient model in order to estimate soil evaporation coefficient in Groblershoop and Vaalharts**

Parameters	Vaalharts	Groblershoop
Soil surface layer depth ( $Z_e$ ) (m)	0.15	0.15
$\Theta_{FC}$ ( $m^3m^{-3}$ )	0.214	0.214
$\Theta_{PWP}$ ( $m^3m^{-3}$ )	0.09	0.09
Surface area wetted by irrigation ( $m^2$ )	84.94	76.94
Fraction of surface area wetted by irrigation	0.849	0.56
$K_{c\ max}$	1.4	1.4
Fraction of soil surface covered by the canopy	0.14-0.97	0.26-0.90

### 3.1.11 STATISTICAL ANALYSIS OF DATA

Model performance was evaluated using the Willmott index of agreement (D), mean absolute error (MAE), root mean square error (RMSE), the coefficient of residual mass (CRM) and the coefficient of determination ( $R^2$ ). The index of agreement is a measure of the degree to which the model predictions (observed vs. estimated) are accurate (Willmott, 1981), whilst MAE, RMSE and CRM are residual based measures that give a quantitative estimate of the deviation of the modelled outcome from the observed data set (Bellocchi et al., 2011, Abraha and Savage, 2010). The coefficient of determination ( $R^2$ ) is a correlation measure which describes the goodness-of-fit of a model. According to Bellocchi et al. (2011),  $R^2$  and D values range between 0 and 1, which demonstrates the worst and best model performance values respectively. MAE varies between zero and infinity, with zero indicating best model performance values. Acceptable values for these statistical indices are:  $R^2$  and D should be greater than 0.8 and MAE (expressed as a percentage) should be less than 20%. The CRM optimum value is zero, with positive and negative values indicate underestimation and overestimation of the model, respectively. The algorithms for computing the statistical indices are given below

$$RMSE = \sqrt{\frac{\sum_{i=1}^n (P_i - O_i)^2}{n}} \quad (56)$$

$$MAE = \frac{\left(\frac{1}{n}\right) \sum_{i=1}^n |P_i - O_i|}{O} * 100 \quad (57)$$

$$D = 1 - \frac{\sum_{i=1}^n (P_i - O_i)^2}{\sum_{i=1}^n (|P_i - O_i| + |O_i - O|)^2} \quad (58)$$

$$CRM = 1 - \frac{\sum_{i=1}^n O_i - \sum_{i=1}^n P_i}{\sum_{i=1}^n O_i} \quad (59)$$

Where  $P_i$  and  $O_i$  are the estimated and measured values for each model,  $n$  is the number of observations (pairs of data both estimated and measured values), and  $O$  is the mean of the measured values.

## **3.2 THE IMPACT OF WATER STRESS ON YIELD AND QUALITY OF PECAN ORCHARDS**

### **3.2.1 SITE DESCRIPTION**

The experiment was conducted at the University of Pretoria's Experimental Farm, Innovation Africa@UP, South Africa (25°4'55.85" S, 28°15'3.88" E, 1372 altitude) from September 2017 and has run for five seasons to date. Details of the orchard are provided in section 3.1.1.3.

### **3.2.2 TREATMENTS**

The experiment is laid out in a random complete block design (RCBD) with each treatment replicated four times (Figure 3.19). There are five treatments, including a well-watered control (treatment one). Treatment two, three, four, and five trees are where stress is imposed at flowering and nut set, nut sizing, nut filling and hardening and shuck split (maturity). Stress was implemented by irrigation withdrawal to a specific treatment and covering the soil with black plastic on the area allocated to the three trees in a replicate to eliminate rainfall (Figure 3.20). The plastic was only applied to the low-density block (10 x 10 m) and irrigation was scheduled according to the control of the low-density block. The stress levels were kept within limits, as outlined by Othman et al. (2014). In a study in New Mexico, Othman et al. (2014) established midday stem water potential thresholds for irrigating pecans for conditions in New Mexico; -0.40 and -0.85 MPa for well-watered trees, moderately stressed between -0.90 to -1.45 MPa and severely stressed between -1.5 and -2.0 MPa. During stress periods, midday stem water potential was maintained between -0.90 to -1.45 MPa for moderate stress, thereby avoiding severe stress. This was also monitored by taking weekly predawn water potentials. When water potential dropped below the acceptable limits, the trees were irrigated to slightly refill the profile and alleviate some of the stress.

All measurements were taken in relation to the control (treatment one) at all the phenological growth stages. After the completion of each phenological stage, the stressed trees were irrigated back to field capacity, which differed slightly from the irrigation for the control. The period of stress recovery was monitored through the assessment of pre-dawn leaf water potentials and midday stem water potentials and/or stomatal conductance measurements.

10 x 10									
	1	2	3	4	5	6	7	8	9
1	W	WS	W	WS	W	WS	W	WS	W
2	W	WS	1 W	WS	4 W	WS	3 W	WS	5 W
3	W	WS	W	WS	W	WS	W	WS	W
4	W	WS	W	WS	W	WS	W	WS	W
5	W	WS	2 W	WS	3 W	WS	5 W	WS	4 W
6	W	WS	W	WS	W	WS	W	WS	W
7	W	WS	W	WS	W	WS	W	WS	W
8	W	WS	3 W	WS	1 W	WS	1 W	WS	2 W
9	W	WS	W	WS	W	WS	W	WS	W
10	W	WS	W	WS	W	WS	W	WS	W
11	W	WS	4 W	WS	5 W	WS	2 W	WS	1 W
12	W	WS	W	WS	W	WS	W	WS	W
13	W	WS	W	WS	W	WS	W	WS	W
14	W	WS	5 W	WS	2 W	WS	4 W	WS	3 W
15	W	WS	W	WS	W	WS	W	WS	W
16	W	WS	W		W	WS	W	WS	W

**Figure 3.20 Orchard layout showing all treatments, blocks and measurements trees, where soil water monitoring equipment (chameleon soil water sensor) is located (the blue blocks) and where the sap flow equipment has been moved to for the 2022/23 season (red outlined blocks). W – Wichita, WS – Western Schley**



**Figure 3.21 Plastic sheeting used to eliminate rainfall from stress treatments**

### **3.2.3 QUANTIFICATION OF PLANT STRESS**

#### **3.2.3.1 Midday and predawn stem water potential**

Water stress was assessed through the measurements of midday leaf water potential ( $\Psi_{\text{smd}}$ ) on the middle tree of the experimental trees in all treatments and replications every 5-6 days using a Scholander type pressure chamber (Model 3005, Soil moisture Equipment Co., Santa Barbara, CA). Pre-dawn leaf water potential ( $\Psi_{\text{pd}}$ ) was determined on eight leaves from each measurement tree, with measurements taking place prior to sunrise. For  $\Psi_{\text{smd}}$ , leaf samples were selected from the inside of the canopy only, enclosed in a plastic bag and were covered with aluminium foil for a period of 30-60 minutes. This was to allow the leaves to equilibrate to the water potential of the stem before water potential was determined (Scholander et al., 1965). For diurnal leaf water potentials differences between well-watered and water stressed treatments were determined by selecting sunlit leaves and shaded leaves under the canopy at hourly intervals from 07:00 am to 05:00 pm. Two shaded leaves were selected from the inside of the canopy as close to the trunk as possible, and four from each of the cardinal points on the outside the canopy. The purpose of these measurements were to evaluate plant water status and then use this measure to determine if the plant is experiencing water stress, since leaf water potential measures the integrated effect of soil, plant, and atmospheric conditions on water availability within the plant itself.



### 3.2.3.2 Fractional canopy cover

Canopy cover was determined by measuring fractional interception of (PAR) using a Decagon AccuPAR LP-80 ceptometer (Decagon Devices, Pullman, WA, USA). Sampling of PAR below the canopy was conducted across and within the row (covering the total area allocated to one tree) at pre-determined 1 m intervals, whilst a full sun reading was taken in an open area next to the orchard. Measurements were taken weekly on one experimental tree in all blocks, in the 2018/19 and 2019/20 seasons (middle tree of all treatments) during canopy growth at the beginning of the season and during the end of the season as the leaves senesced (Mid-April to May). In the middle of the season, measurements were taken at two to three-week intervals. A Phantom 3 drone, fitted with a RGB camera, was also flown 15 m above the canopy to take photographs of the experimental trees at the same height (the middle tree of all treatments in all blocks) at midday on a weekly basis during canopy development and end of the season as leaf senescence began. In the middle of the season, it was flown every two to three weeks.

These measurements were then used to determine canopy cover by analysing the images using the Canopeo application in MATLAB R2017a software (Patrignani and Ochsner, 2015). As defined by Liang et al. (2012), canopeo is an automatic colour threshold (ACT) image analysis tool developed in the Matlab programming language (Mathworks, Inc., Natick, MA) using colour values in the red-green-blue (RGB) system. Canopeo analyses and classifies all pixels in the image (Liang et al., 2012).

### 3.2.3.3 Gas exchange

Measurements of leaf gas exchange were performed in the 2018/19 season and included net CO<sub>2</sub> assimilation rate ( $A$ ), stomatal conductance ( $g_s$ ), and intercellular CO<sub>2</sub> concentration ( $C_i$ ), which were measured using an infra-red gas analyser (IRGA) (Model: LI-6400 XT, LI-COR, Lincoln, Nebraska, USA). Sensors inside the cuvette monitored leaf surface temperature ( $T_{\text{leaf}}$ ) and leaf-to-air vapour pressure deficit ( $VPD_{\text{leaf}}$ ). Measurements of  $A$  and  $g_s$  were performed on the third fully expanded leaf from the apex of each shoot for each water stress treatment and the well-watered control every 5-6 days to assess the impact of water stress on gas exchange. For the diurnal spot measurements of leaf gas exchange, measurements were made on four leaves on the outside of the canopy at the four cardinal points on one tree per treatment and per block. Chamber CO<sub>2</sub> concentration was maintained at 400  $\mu\text{mol mol}^{-1}$ , the flow rate was 400  $\mu\text{mol s}^{-1}$ , PAR inside the chamber was maintained between 1500-2000

$\mu\text{mol m}^{-2} \text{ s}^{-1}$  (LI-6400 XT LED light source), and RH was maintained at more than 50% (to prevent stomatal oscillations).

Additional measurements of  $g_s$  were performed using an AP4 porometer (Delta-T Devices Ltd, Cambridge, United Kingdom). Six leaves were selected from one experimental tree per replicate block, with four sunlit leaves and two shaded leaves under the canopy measured at midday on a weekly basis. Diurnal measurements were conducted when there was a difference in pre-dawn leaf water potentials between the well-watered control and water stressed treatments.

### **3.2.4 NUT DEVELOPMENT**

Nut growth was assessed from flowering and nut set to shuck dehiscence or the maturity stage. Nut set was determined by labelling three clusters per tree in all the treatments. The number of flowers per cluster were counted soon after the female flowers were visible and the number of nuts set per cluster was recorded. The number of nuts remaining on the tree were recorded on a weekly basis and was used to determine nut drop during the trial. The increase in nut size (length and diameter) was measured from nut set to final nut size (when no further increases nut size was recorded) on weekly basis using Vernier calipers (GripsWorks, Arnold, Missouri, USA) on the marked clusters per experimental tree whilst attached to the tree.

For nut development, three nuts on each treatment were harvested every two weeks. A cross section cut at the mid-point of the nut was made on two nuts and a perpendicular cut was made on one nut (Figure 3.21). The nuts were dissected with a sharp knife in the first half of the growing season. Later in the season, as the shell hardened, nuts were sectioned with a saw. Stages that were analysed included kernel deposition (dough), ovary wall (shell) lignification, cotyledon thickening (nut filling) and fruit maturity, as judged by involucre (hull) dehiscence. This was used to classify nut development, that is, how the nuts develop in response to water stress treatments as compared to the well-watered control and to determine the different phenological stages.



**Figure 3.22 Cross-section cut at the mid-point of the nut and perpendicular cut along the longitudinal dimensions of the nut**

### **3.2.5 YIELD AND QUALITY**

At the end of the season, nuts were harvested from each experimental tree in each of the four replications using a mechanical shaker for the second and third season, whilst in the first season they were harvested by hand. All nuts were collected on the floor after shaking the trees to determine sound kernel % and unsound kernel % (including pops). Sub-samples of 1 kg were randomly taken from each crate of the different treatments. Nut quality parameters that were assessed included wet in shell mass, dry in shell mass, average size distribution and shape. The nuts were then cracked for the analysis of total kernel %, kernel colour, shell thickness, moisture content and storage stability at a local processor in Cullinan (Elansdraai Pecan Growers). The nut size was determined as the number of nuts per kg and using Vernier calipers (GripsWorks, Arnold, Missouri, USA). Kernel shell-out percentage was calculated from the total nut and kernel mass after drying. Kernel moisture content was determined by drying a 5 g ground nut samples per treatment in a moisture content analyser (MB23 Food Moisture Analyser Ohaus).

### 3.2.6 IRRIGATION AND SOIL WATER CONTENT

The volume of applied irrigation was recorded using water meters (Multi Jet Water Meter w/o EV ARAD) plumbed into the irrigation at the at the start of the drip line for each treatment replicate in block 1. These meters were read following each irrigation event. Soil water matric potential measurements were made using Chameleon soil water sensors (Virtual Irrigation Academy, [www.via.farm](http://www.via.farm)) (Figure 3.22A). The Chameleon sensor estimates soil water content by displaying colours which correspond to a certain range of soil water tension (Figure 3.22B). These colours are displayed by a hand-held portable reader, which is connected to the sensor array. The chameleon has three sensors in one sensor array which are installed at different depths in the soil profile. In this study these depths were 20 cm, 40 cm, 60 cm, 80 cm, 100 cm and 120 cm. The colours displayed can be blue (wet), green (moist) or red (dry). When the light is blue, it means that the soil matric potential is between approximately 0 and -20 kPa (wet). Typically, under these conditions water is moving in the soil and leaching is possible. At approximately -20 kPa to -40 kPa the colour changes to a green (intermediate), which means the water is still readily available to the plant, but unlikely to be moving in the soil hence leaching cannot occur. The red colour indicates a decline of soil water potential, above -40 kPa (dry) and this means the plant struggles to extract water, thus water stress will occur in plants and could result in a yield penalty. However, when the soil becomes too dry the chameleon lights are not turned on and they are considered grey. This indicates severe soil water deficit. The sensors were installed in all treatments under the drippers.

In this trial chameleon readings were taken one to three times a week. The reason for this was to schedule irrigation in the control and to manage the level of stress in the other treatments and to ensure that the soil water was being depleted in the water stressed treatments. The non-stressed treatments were irrigated when one of the top layers (20 and 40 cm) turned red in the control treatments, whilst in the stressed treatments, the two top layers were kept red and irrigation was only performed if one of the layers turned grey. This data was used in conjunction with  $\Psi_{smd}$ , that is, maintaining a value between -0.40 and -0.85 MPa in the control and -0.90 to -1.45 MPa in the stressed treatments. When the values dropped beyond the minimum threshold (-1.45 MPa), the trees were irrigated.

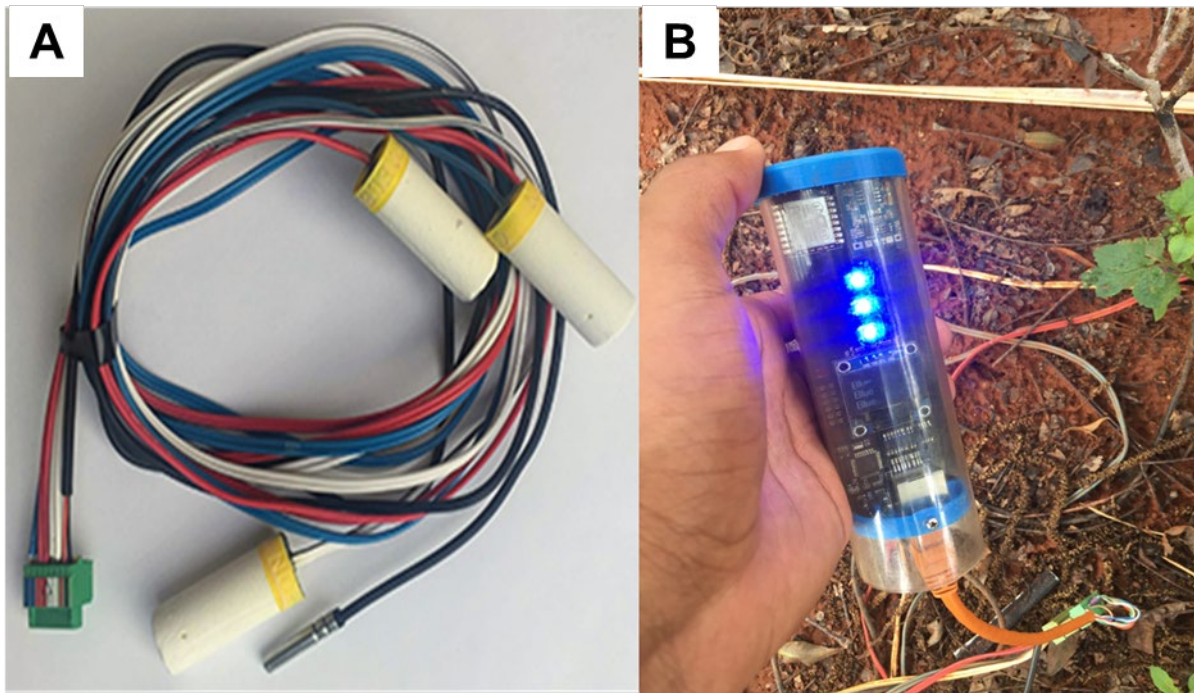


**Figure 3.23 A) Chameleon soil water sensors buried in the ground. B) Chameleon reader connected to the sensor array with colour display in the well-watered control during the course of the trial**

### 3.2.7 STATISTICAL ANALYSIS OF DATA

Excel statistical analysis were used to determine statistical differences between stomatal conductance, photosynthesis and yield (flower set, nut drop) and quality (average nut size, number of nuts  $\text{kg}^{-1}$ , kernel %, moisture %, unsound kernel %, waifer/air pockets % and stick tights) of the water stressed treatments relative to the well-watered treatment. The differences between treatment means were determined using the F test and T test mean separation. The significance levels were  $p < 0.05$  (or 95% confidence level).

## 3.3 REMOTE SENSING

The study was carried out at two sites, the water stress trial in the pecan orchard on the University of Pretoria's Experimental farm (Innovation Africa@UP) and the second being the instrumented pecan water use trial site at the Groen Boerdery Pecan orchard on the Vaalharts Irrigation Scheme. Fertiliser was not applied timeously in the 2020-2021 season in the UP pecan orchard, and the essential micronutrient for pecans, zinc, was not applied. Many trees showed a variety of obvious deficiency symptoms as a result. Fertiliser was applied on time at

the start of the 2021-2022 season, with zinc applied directly to the soil as a drench. No deficiency symptoms were observed, and the trees appeared healthy throughout the season.

Hourly meteorological data (rainfall, air temperature, relative humidity, VPD, wind speed and solar radiation) was available from a weather station situated 230 m from the UP orchard. A second weather station, measuring air temperature, relative humidity, wind speed and solar radiation was installed inside the high-density section of the orchard at the end of November 2021 to be able to obtain higher resolution weather data (20 minutes), and due to concerns about the accuracy of the main weather station. Radiation data from this weather station was not used because it was partly shaded by the canopy.

The study site on the Vaalharts irrigation scheme (28°4'11.01"S, 24°37'54.79"E) has an average annual rainfall of 590 mm and is situated in a 16-year-old 10.37 ha mixed cultivar orchard planted at a 10 x 10 m spacing. In the four seasons on measurement average annual rainfall has been 650 mm on the farm. In February 2020, two SI-121-SS infrared radiometers (Apogee Instruments, North Logan, Utah, USA) were installed on the tower facing the top of two tree canopies. One was directed to the tree to the southeast of the tower and the other towards a tree in the next row to the west of the tower. Canopy temperature data from the IR radiometer facing the southeast during the 2021/2022 season was found to be much higher than the other radiometer, and much higher than the leaf temperature could plausibly be expected to be. Upon further investigation, it was observed that a leafless branch was within the field of view of the thermometer, the temperature readings were then not from leaves, but rather bare bark.

### **3.3.1 REMOTE SENSING DATA COLLECTION**

A UAV was available from the beginning of February 2021. The platform was a DJI Matrice M200 (SZ DJI Technology Co., Ltd. Shenzhen, Guangdong, China) with a Micasense Altum Multispectral and Thermal Sensor attached (Micasense, Inc., Seattle, WA, USA). The device has a sensor for each of the five wavelength bands: Blue, Green, Red, Red-edge and Near Infrared, the centre and band width of each band is presented in Table 3.3. A radiometric thermal band is also available.

The thermal and multispectral bands are synchronised and captured simultaneously. The Altum sensor was radiometrically calibrated using a Calibration Panel before each flight. Thirteen flights were conducted between February and April 2021, when the leaves on the

trees began to senesce. Flying resumed at the end of September 2021 with bud break and continued until senescence began in April 2022, 26 flights were conducted during this season. Images captured before full canopy cover was achieved were not used in the water stress detection section of this study. Trees were in full leaf by the end of October, when plant-based water stress measurements began. While an attempt was made to fly weekly, this was not always possible due to the availability of the UAV operator, as well as the weather conditions. Table 3.4 gives all dates and times that flights were conducted, with the field water stress data available for each date. Dates where collected data was used is highlighted in grey (Table 3.4), 6 images were used from the second half of the 2020/2021 season, and 10 images were used from the 2021/2022 season.

**Table 3.3. Wavelength bands available from the Micasense Altum Multispectral and thermal sensor with band centres and bandwidth**  
(<https://support.micasense.com/hc/en-us/articles/360010025413-Altum-Integration-Guide#h.5ow085yb2oll>)

Band	Centre	Band width
Blue	475 nm	32 nm
Green	560 nm	27 nm
Red	668 nm	14 nm
Red-edge	717 nm	12 nm
Near-Infrared	840 nm	57 nm
Thermal	11 $\mu$ m	6 $\mu$ m

The data from a number of flights were not included in the final data due to complete cloud cover or uneven cloud cover, causing the orchard to be partially shaded. It was found to be exceptionally difficult to separate canopies from the background of images collected on cloudy days, data from these images could also not be confidently compared with the rest of the data collected on sunny days, as observed by Gago et al. (2015).

Flight paths were planned on the DJI ground-station to cover the entire orchard, with about 10 m on each side as a buffer. A flight height of 40 m, with an image overlap of 70% was chosen. Days with clear skies were chosen for the weekly flights where possible, some flights did take place on overcast days, and there were several weeks, in both seasons, where no flight took place due to prolonged inclement weather, primarily in December and January. It was found early on that data from flights on cloudy days were significantly more difficult to process and could often not be used. Ideally flights should have been conducted at solar noon, although this was not possible on most days.

**Table 3.4 UAV data collection flights, and available plant water stress measurements. Rows highlighted in grey indicate the days selected for data analysis**

Date	$\Psi_{smd}$	$g_s$	Flight Start Time
10-Feb-21	Yes	Yes	10:39
17-Feb-21	Yes	Yes	10:58
02-Mar-21	Yes	Yes	11:42
04-Mar-21	Yes	Yes	11:27
10-Mar-21	Yes	Yes	10:41
19-Mar-21	Yes	Yes	10:21
07-Apr-21	Yes	Yes	10:57
14-Apr-21	Yes	Yes	10:44
29-Sep-21	Yes	No	10:35
06-Oct-21	No	No	10:30
13-Oct-21	No	No	10:43
18-Oct-21	No	No	10:29
29-Oct-21	Yes	No	10:23
09-Nov-21	Yes	No	10:50
11-Nov-21	No	No	10:43
17-Nov-21	Yes	No	10:39
24-Nov-21	Yes	No	10:41
07-Dec-21	Yes	No	10:31
17-Dec-21	No	No	10:56
28-Dec-21	No	No	10:59
03-Jan-22	No	No	10:41
05-Jan-22	No	No	10:31
22-Jan-22	Yes	No	10:19
26-Jan-22	Yes	No	10:32
09-Feb-22	Yes	No	10:45
23-Feb-22	No	No	10:39
24-Feb-22	Yes	No	10:35
03-Mar-22	Yes	No	10:33
10-Mar-22	Yes	No	10:59
14-Mar-22	Yes	No	10:55
24-Mar-22	Yes	No	10:45
06-Apr-22	No	No	11:45
13-Apr-22	Yes	No	10:42
21-Apr-22	Yes	No	10:43



### 3.3.2 REMOTE SENSING DATA PROCESSING

Raw multispectral images from the Altum sensor were stitched into orthophotos using Pix4D fields. All geometric and radiometric correction was completed automatically by the orthomosaicing software using the metadata collected from the calibration panel image, and data from the radiation sensor installed at the top of the UAV. The application produced five separate orthophotos for each of the available bands. Further processing was performed in QGIS. The first step was to create composite Vegetation Index (VI) images, using the available bands. Details of the VIs used are included in Table 3.5.

**Table 3.5 Vegetation Indices created using the multispectral images of the UP Pecan orchard**

Name	Abbreviation	Formula (Band)
Normalised Difference Vegetation Index	NDVI	$\frac{NIR - Red}{NIR + Red}$
Simple Ratio Index	SRI	$NIR/Red$
Red-edge Simple Ratio	ReSR	$Red-edge/Red$
Red-edge NDVI (Red-edge Index )	ReNDVI	$\frac{NIR - Rededge}{NIR + Rededge}$
Green NDVI		$\frac{NIR - Green}{NIR + Green}$
Renormalized Difference Vegetation Index	RDVI	$\frac{NIR - Red}{\sqrt{NIR + Red}}$
Optimized Soil Adjusted Vegetation Index	OSAVI	$(1 + 0.16) \frac{NIR - Red}{NIR + Red + 0.16}$
Transformed Chlorophyll Absorption Ratio	TCARI	$3((RE-Red)-0.2(RE-Green)) \left( \frac{Re}{Red} \right)$
Modified Chlorophyll Absorption in Reflectance Index	MCARI	$((RE-Red)-0.2(RE-Green)) \left( \frac{Re}{Red} \right)$
MCARI 1	MCARI 1	$1.2(2.5(NIR-Red) - 1.3(NIR-Green))$

An unsupervised classification into 10 classes was then performed on the SRI using the in-built facility in QGIS. The insights from this process and the SRI raster histogram were used to choose a threshold value to separate pecan tree canopies from the soil and interrow vegetation. The SRI raster histogram for the orchard shows two distinct frequency spikes, a larger spike representing the background, which is the larger part of the image, and a smaller

normal curve being the pecan canopy. The value at the upper edge of the background curve was used as the threshold value and was found to be satisfactory at separating out the background. A sample of the SRI histogram is given in Figure 3.23.

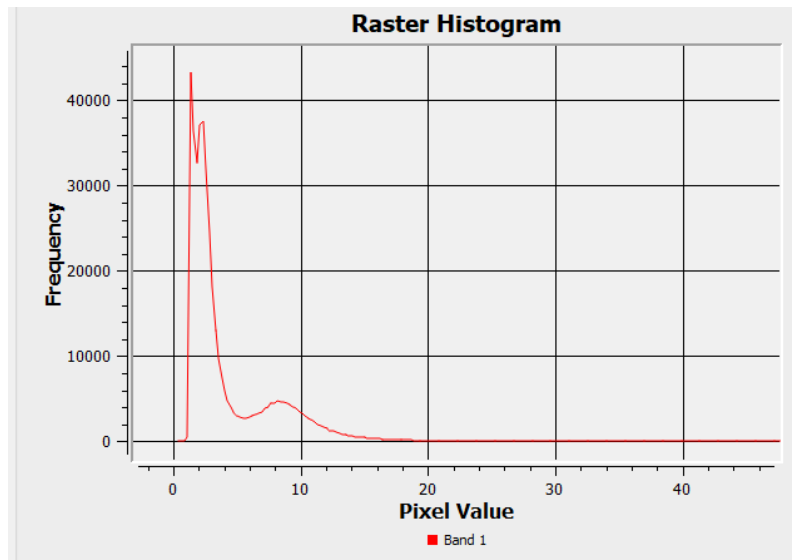


**Figure 3.24 Raster histogram of the simple ratio index (SRI) used to decide on a background-separation threshold value, showing a large background spike and normal distribution for the canopy. The threshold in this case is an SRI value of approximately 5.**

At first, this process was followed for all VIs, however, it quickly became apparent that certain VIs were better at separating out pecan canopies than others. Many of the VIs placed the cover crop in the same class as the tree canopies, due to highlighting specific reflectance properties by design. Several of the VIs, including NDVI (Figure 3.24), had a very small range of values between bare soil and the pecan canopy, making the selection of a threshold value tediously sensitive. Some of the VIs also could not differentiate between shadows and pecan canopy, with shadowed background and lit pecan canopy having the same value. This was a problem as many flights were conducted before the sun was directly overhead. The best and most practical of the VIs for separating pecan canopies was found to be the Simple Ratio Index (SRI), (Figure 3.25), having both a simple formula ( $\text{NIR}/\text{Red}$ ), and a large range of values between bare soil and pecan tree canopies. This gave a large margin of error when selecting the threshold value without fear of leaving out a large amount of canopy or including the background. However, even this VI performed poorly when the data was collected under overcast conditions or the interrow vegetation was too tall.

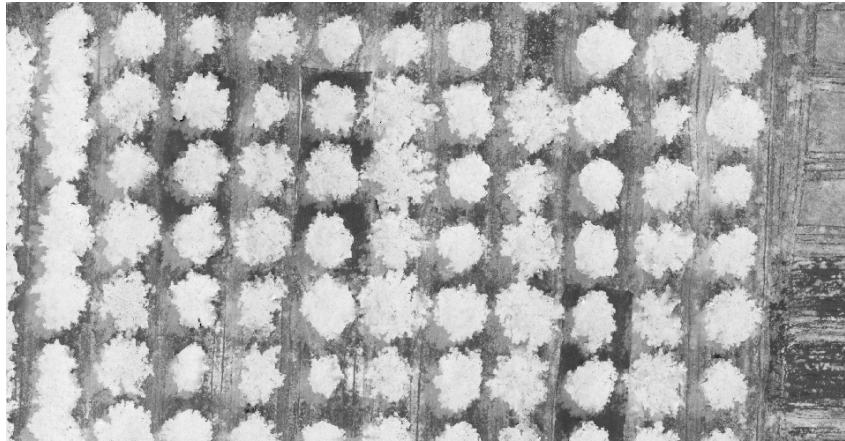


**Figure 3.25 NDVI Image of pecan orchard showing little differentiation between shadows and the pecan canopy**

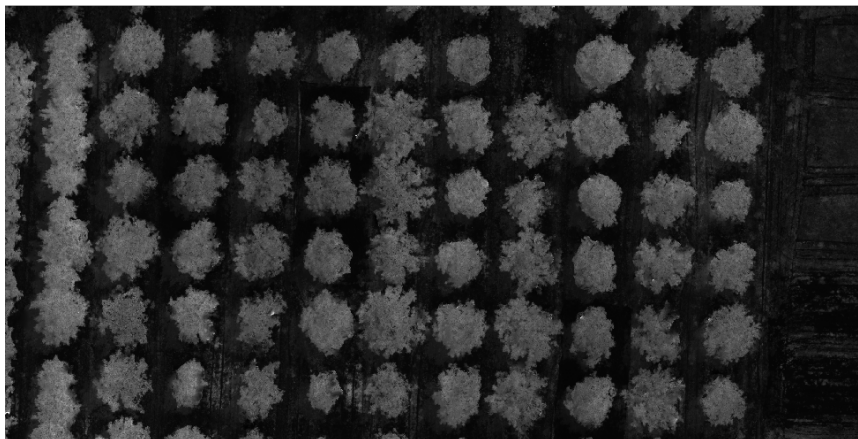


**Figure 3.26 Simple ratio index (SRI) image of the pecan orchard showing clear differentiation between pecan canopy and the background**

Once a threshold value was chosen, a threshold raster was created (Figure 3.26). This is an image where all pixels have a value of either 0 or 1 (that is, black and white). All pixels that were above the threshold value (i.e. the canopy) in the VI are designated 1, while all others are 0. This can be used directly to find canopy area by imposing a vector grid that corresponds to the tree spacing on the image and finding the percentage of each block that is covered by pecan canopy. By dividing the VIs by the threshold image, new VI layers are created that include only the canopies, with all else removed or “cut out”. However, this is a tedious way of extracting data from the VIs, as only one VI layer can be processed at a time, though it can be a visually appealing way to display the VI when overlain on an RGB image of the orchard.

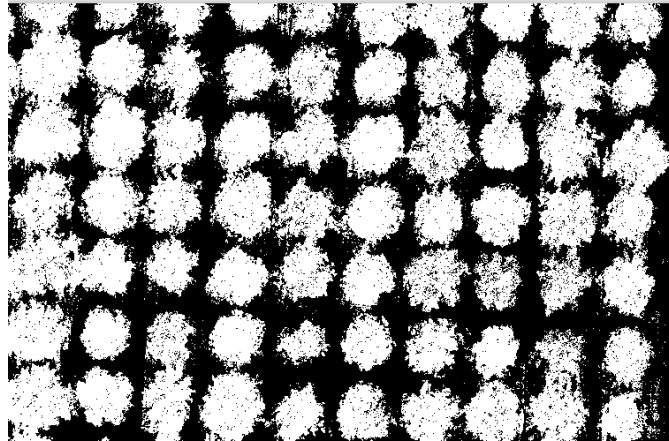


**Figure 3.27 Threshold raster created using threshold value of the SRI**

The method used to extract the VI values of the canopies in the 2020-2021 season, and the early part of the 2021-2022 season was to create a vector layer containing polygons corresponding to the “1” values on the threshold image. Therefore, each polygon covers one pecan canopy (Figure 3.27). The polygons were used to visually validate the threshold value by ensuring that each polygon corresponded well to the canopy it represented. If the polygons included parts of the background, or removed parts of the canopy, a new threshold value was chosen to create a new threshold raster, and the process was repeated until the polygons satisfactorily represented the tree canopies.



**Figure 3.28 Individual canopy polygons created using threshold value of simple ratio index (SRI)**

Since the canopy of the low-density orchard had only just started to close, this method could be used successfully to derive data from individual canopies. Some work was required to

separate polygons where trees canopies has started to overlap or where the cover crop was too tall. Many of the weekly polygon layers also needed to have their geometries fixed to ensure the coordinate integrity of the images. By the middle of the 2021-2022 season, a large proportion of the canopies started to overlap, likely due to the correct nutrition available to the trees in this season and due to the lack of pruning in the orchard. As a result, the canopy polygon method of extracting canopy VI and thermal values became impractical.. For the remainder of the trial, the threshold raster images were used to create canopy only images of each VI image (Figure 3.28).

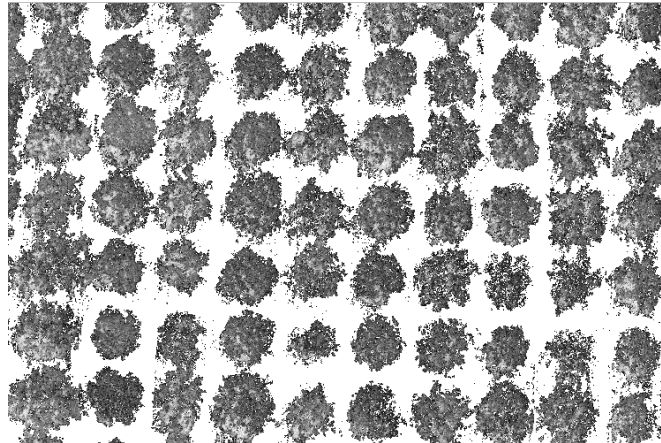


**Figure 3.29 Normalised difference vegetation index (NDVI) orchard image with all non-canopy pixels removed**

A grid polygon layer was then aligned to the canopies (Figure 3.29). Due to the orchard not being planted in completed straight rows, some trees violated the 10 x 10 m spacing. Some trees at the edges of the orchard did not, therefore, align with the grid. Since the VI image contained nothing besides pecan canopy, most grid blocks contained only data from a single canopy and empty space. Blocks that contained parts of other tree canopies were removed.

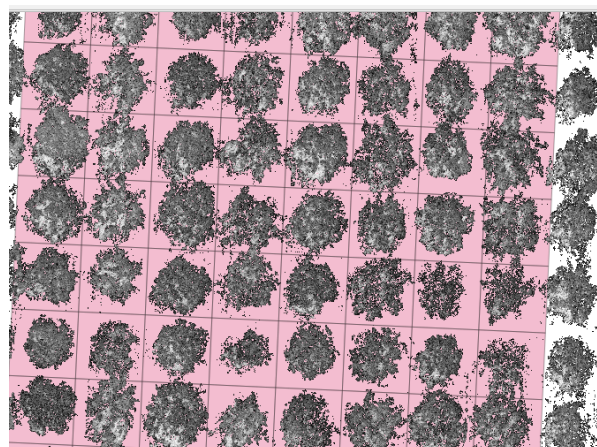


**Figure 3.30 Grid aligned to individual canopies, used to extract average vegetation indices (VI) and thermal canopy values**

The average VI value of each canopy was found using the “Raster Statistics for Polygons” function in QGIS, with the polygon layer as the specifying grid for the earlier images and the aligned grid for the later images, and all the VI layers as the inputs. In this way all the VI layers could be processed at once with a single shapefile layer (.shp). The output was a single new shapefile layer with the VI value of each tree for each VI listed in the Attribute Table of this new layer in QGIS. Each tree on the original shapefile layer was previously given a label as a new attribute, this carried over to the output shapefile to allow identification of individual trees. The attribute table of the output shapefile was copied to a Microsoft Excel spreadsheet (Microsoft Corporation, Redmond, WA, USA), where the labels, which corresponded to the water stress trial tree identification, allowed VI and thermal data to be matched with individual canopies.

The thermal layer captured by the Micasense Altum was also processed using Pix4D. Pixels values of thermal image corresponded to degrees Celsius. The average temperature of each canopy was extracted using the same process, threshold image and polygons as for the VIs.

Each weeks’ image was processed separately from beginning to end (separating canopies using VIs to creating polygons), threshold images and polygon layers were not carried over from one set of images to the next. Using ground control points would have made this process easier as the process location of these points could have allowed the same polygon layer to be used for each image. This process of creating a threshold raster would, however, still need to be conducted several times during each season to account for canopy growth and the effects of the crop load on the canopy structure.

### **3.3.3 FIELD DATA COLLECTION**

Field data was collected from the trees of the UP pecan water stress trial on the same days as the remote sensing data was collected. To assess the water stress status of the trees and provide a possible reference point for the remote sensing data, both  $\Psi_{smd}$  and stomatal conductance ( $g_s$ ) at midday were measured. Measurement trees during the first season of data collection were the well-watered control, and the current stress treatment trees of the water stress trial (these trees change with each phenological stage) to provide a range of stress values. During the second season, because a second operator was available to collect  $\Psi_{smd}$ , the centre tree of every treatment and biological repeat were measured for  $\Psi_{smd}$  within approximately an hour. Midday SWP was collected by covering three leaves on each tree with a foil bag half an hour before measurement. Measurements were conducted with a Scholander



type pressure chamber (PMS Model 600, PMS instrument company, Albany, OR, USA). Stomatal conductance was measured on five leaves of each tree using the LI-600 combination porometer/fluorometer (LICOR, Lincoln, NE, USA) during the first measurement season only, as it was decided at the start of the second season to collect  $\Psi_{smd}$  data of all treatment trees in the orchard. Had  $g_s$  been measured as well, the time difference between the first and last measurement would have been large enough for environmental conditions to change significantly, preventing direct comparison of measurements. It was not always possible to collect accurate  $T_{leaf}$  with the LI-600 due to changes in the sun angle during the period it took to measure all trees. The field data was then correlated against the average VI value of each of the measurement trees. The field data was also used to validate the thermal indices.

### 3.3.4 WATER STRESS DETECTION BY VEGETATION INDICES

The VI values for each canopy were plotted against the corresponding average  $\Psi_{smd}$  and  $g_s$  for that tree. Separate plots were created for each measurement season, due to the differences in the nutritional status of the trees between the two seasons. All data from all measurement dates were plotted together, to give only two plots in total for each VI, one for each season. The 2020-2021 plot only included data collected between February 2021 and April 2021 as the UAV only became available in February. The correlation coefficient ( $R^2$ ) of the plots were used to determine whether a relationship exists between each VI and  $\Psi_{smd}$ . During the first measurement season,  $g_s$  was plotted against the VIs in addition to  $\Psi_{smd}$ .

### 3.3.5 CROP WATER STRESS INDEX

Since leaf temperature ( $T_c$ ) is dependent on both air temperature ( $T_a$ ) and vapour pressure deficit (VPD), in addition to the level of water stress, there can be no meaningful direct relationship between canopy temperature and water status of the tree when compared over different days. The crop water stress index (CWSI) was therefore developed (Jackson et al., 1981). This index uses the difference between the canopy and air temperature adjusted for VPD using the following formula:

$$CWSI = \frac{(T_c - T_a) - (T_c - T_a)_{LL}}{(T_c - T_a)_{UL} - (T_c - T_a)_{LL}} \quad (60)$$

The lower limit (LL) is the difference between canopy and air temperature of a canopy transpiring at the maximum rate over the range of VPD conditions. The upper limit (UL) is the

difference between canopy and air temperature when no transpiration takes place. It should be a constant value across all atmospheric conditions.

#### *3.3.5.1 Finding the lower limit of the CWSI*

The measured non-water-stressed-baseline was created using hourly canopy temperature data from the tower mounted IR radiometers in the Vaalharts orchard study site, and air temperature and VPD data from the nearby weather station. Only canopy temperatures between the start of October and the end of March were used during both seasons of measurement, to ensure that data was collected only from trees in full leaf, and no soil or other background temperature was included. It was assumed that due to good farm management and measurements of  $\Psi_{pd}$  every 4-6 weeks that the trees were not water stressed. A plot using only data collected between 11:00 and 14:00 was created. This was to comply with best practice mentioned in the literature to remove error caused by dramatic changes in sun angle (Testi et al., 2008, Garrot et al., 1993). This ensured that the pattern of sunlight incident on the canopy within the footprint of the IR radiometers remained relatively constant. Hourly  $T_c$  points where rainfall was recorded were removed. The equation of the linear regression line of each season's plot was taken as the NWSB for that season. The NWSB of each season was used individually to calculate the CWSI for that season; and tested against the field measured water stress data. A combined NWSB using data from both seasons was also tested by comparing the CWSI against the plant stress data. This was to determine if accuracy was improved when considering the unique conditions of the season or if including as much variation as possible through combining the data of two seasons would yield better results.

The lower limit of the CWSI was found by using the temperature ( $T_{wet}$ ) of an artificial reference surface placed just outside the UP pecan orchard within the UAV flight path. The wet reference surface consisted of a thin polystyrene sheet, covered in white cloth, floating in a pan of water. The cloth wicks water from the tray as water evaporates from the cloth. The temperature value extracted from the thermal image of the cloth covered board was taken as  $T_{wet}$  on the day. The  $T_a$  component of the lower limit value was obtained from the second automatic weather station placed in the orchard which logged data every 20 minutes.

The statistical histogram of the thermal raster image was also used to determine  $T_{wet}$ . As with the reference surface method, the process was conducted separately for each thermal image. These values were taken as the edges of the normal distribution of the thermal images which contained only pecan canopies, with the background removed, to prevent wet soil or free water



temperatures being used. An example of the thermal histogram is shown in Figure 3.30.  $T_a$  was taken from the orchard weather station inside the orchard.

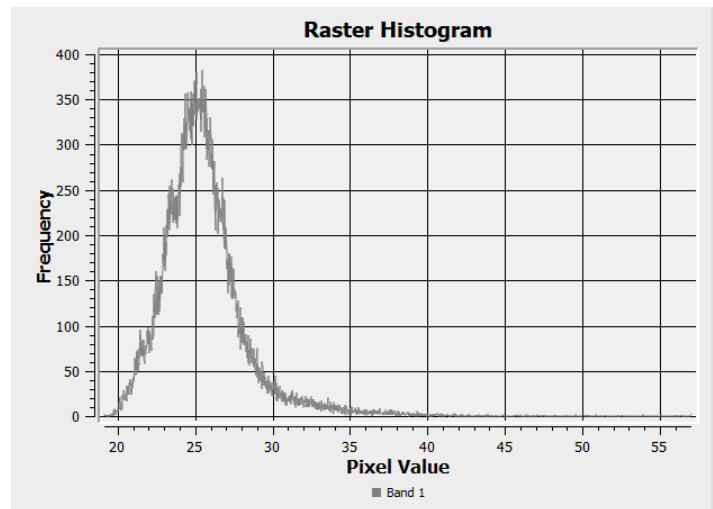


**Figure 3.31 Raster histogram of thermal pecan canopy images, showing a normal distribution, used to derive the limits of the crop water stress index (CWSI)**

#### 3.3.5.2 Finding the Upper Limit of the CWSI

The UL, or  $(T_c - T_a)_{UL}$  is a constant value across the VPD range representing the difference between canopy and air temperature at which no transpiration takes place. This value is temperature dependent, but it is not critical to account for this as long as actual  $T_c - T_a$  of the crop falls below this value. Several methods were attempted to find the UL, including the negative VPD method (Idso, 1982), the artificial reference surface method (Maes et al., 2016), the stressed canopy method (Sammis et al., 1988), and the thermal histogram method (Bian et al., 2019).

The negative VPD method used the NWSB created using data from the IR radiometers at the Vaalharts study site. The upper limit equation from the NWSB requires the  $T_c - T_a$  intercept of the NWSB and the saturated vapour pressure at air temperature, and  $T_a$  plus the intercept, which is negative. Two approaches can be used to find the upper limit on a particular day when the CWSI will be calculated. Either the actual air temperature on the day can be used, or an arbitrary high temperature can be used to derive a static upper limit that will be applied as a constant value. Both approaches were considered. The CWSI was calculated using the NWSB upper limit calculated using the temperature on the day, and 50°C was chosen as the arbitrary temperature for a constant upper limit. This value was chosen as it is sufficiently high to encompass the highest air temperatures experienced in Pretoria, while still being a realistic temperature.

An attempt was also made to calculate the upper limit using a highly stressed pecan canopy, that has stopped transpiring. In August 2021, six trees in the high-density part of the orchard were selected, and the ground was covered with plastic to exclude rain. Irrigation was completely withheld. These trees are not part of the water stress trial, but they were included in the flight path of the weekly flights so that thermal data was available from them. However, due to the high rainfall experienced during the season, the required level of stress was not achieved at any point during the season (see section 3.4 for  $\Psi_{pd}$  and  $\Psi_{smd}$ ).

Trees in the high-density orchard section were also used for destructive upper limit measurements. This entailed severing a leafy branch at the terminal point of the previous year's growth during the hottest part of the day, to ensure that transpiration stopped as fast as possible. The branch was then hung back in the canopy in the approximate original position using heavy duty adhesive tape, to simulate the effects of all other environmental conditions on the leaves. Two cut branches were used on each measurement day. The LI-600 porometer was used to measure the  $g_s$  and leaf temperature of three leaflets on separate leaves on each branch at 10-minute intervals, starting immediately after the branch was cut, until two successive  $g_s$  measurements of zero were recorded. The temperature of the leaflets at this point were taken as an approximation of the temperature of non-transpiring leaves ( $T_{dry}$ ). It, however, quickly became apparent that the measured  $g_s$  and  $T_a$  values of the individual leaflets showed extreme variation, likely due to the position in the canopy and the differences in behaviour of sun and shade leaves. Because only individual leaflets were measured, this variation could not be confidently combined into a single  $T_{dry}$  value for each branch on each measurement day. It was also found that the sun's angle changed significantly during the period from branch cutting to zero  $g_s$ , this resulted in part of a severed branch or the whole branch becoming completely shaded before transpiration stopped. Using the  $T_{dry}$  from these branches would not accurately consider the effect of direct solar radiation on the temperature of the non-transpiring leaf. A handheld IR thermometer would likely have yielded a better result by aggregating the temperature of the entire severed branch, including the tiny environmental variations experienced by each individual leaflet.

The raster histogram method was used on each thermal image to calculate the upper limit as well, by finding  $T_{dry}$  and using  $T_a$  from the weather station. The method used was identical to that used to find  $T_{wet}$ , except that the maximum normally distributed thermal pixel value was used instead of the minimum.

The published upper limit for pecans was also tested. The values found by Sammis (1988) using the severed branch method and a handheld IR thermometer was  $(T_c - T_a)_{UL}$  equals 6°C

for a branch fully exposed to the sun, and 4 °C for a branch tied back into a closed canopy. Since it has become common to use 6°C as an arbitrary upper limit (Baluja, 2012), and the canopies in the UP pecan water stress trial orchard had just begun to close,  $(T_c - T_a)_{UL} = 6^\circ\text{C}$  was used to calculate the CWSI.

### 3.3.5.3 Testing the CWSI

The CWSI was calculated for each day where both thermal data and field data was available. The CWSI was then plotted against  $\Psi_{smd}$  for both seasons and  $g_s$  for the first measurement season. All data collected during each season was plotted separately, a combined plot of both seasons data was also created. This gave one  $\Psi_{smd}$  vs CWSI plot for each season, a  $g_s$  vs CWSI plot for the 2020-2021 season and a combined  $\Psi_{smd}$  plot. These plots were created for each of the methods used to calculate the CWSI. The combinations of the lower and upper limits used to calculate the CWSI are summarised in Table 5.

**Table 3.6 Methods used to calculate the CWSI**

Lower Limit	Upper Limit
NWSB	$(T_c - T_a)_{UL} = +6^\circ\text{C}$
$T_{wet}$ from Artificial Reference Surface, $T_a$ from weather station	$(T_c - T_a)_{UL} = +6^\circ\text{C}$
$T_{wet}$ = coolest pixel, $T_a$ from weather station	$T_{dry}$ = warmest pixel, $T_a$ from weather station

The correlation coefficients ( $r^2$ ) of the plots were used to determine whether a relationship exists between the CWSI and the field measurements of stress. Analysis of Variance (ANOVA) was used to determine whether the relationships between the CWSI and tree water stress was significant at a five percent confidence interval ( $p < 0.05$ ).

## **4. RESULTS AND DISCUSSION**

### **4.1 PECAN WATER USE**

#### **4.1.1 SEASONAL WEATHER**

##### *4.1.1.1 Vaalharts*

Data from the AWS was generally good throughout the duration of the trial (Figure 4.1), apart from missing solar radiation from 9 September to 26 October 2018, when solar radiation ( $R_s$ ) was calculated from minimum and maximum temperatures according to the procedure outlined in FAO-56 (Allen et al., 1998). Solar radiation followed a typical seasonal pattern, with highest values in summer and lowest values in winter. Over the course of the five seasons there were very few cloudy days, with only 147 days with  $R_s < 13 \text{ MJ m}^{-2} \text{ day}^{-1}$ . A large number of cloudy days occurred in 2020/21, 2021/22 and 2022/23 seasons during December and January due to high rainfall experienced in the region during these months. The maximum temperature for the 2018/19 season was  $40.28^\circ\text{C}$ ,  $39.43^\circ\text{C}$  in the 2019/20 season,  $38.86^\circ\text{C}$  in the 2020/21 season,  $39.5^\circ\text{C}$  in the 2021/22 season and  $40.26^\circ\text{C}$  in the 2022/23 season. In the five seasons there were 274 days where the maximum temperature exceeded  $35^\circ\text{C}$ . The 2020 and 2021 winters were colder than the 2019 and 2022, with temperatures dropping to  $-8.03^\circ\text{C}$  in 2020 and  $-8.4^\circ\text{C}$  in 2021. In total there were 180 days below  $0^\circ\text{C}$  over the five seasons. A minimum temperature of  $-4.08^\circ\text{C}$  was recorded in 2019. Although a minimum temperature of  $-4.8^\circ\text{C}$  was recorded in 2022, the season was observed to be colder than the three previous seasons in terms of chill accumulation. This was reflected in the calculation of Daily Positive Chill Units (PCU), where 563 units were accumulated in 2022 (1 May to 31 September), whilst 525 units were accumulated in 2020 and 489 in 2021. In 2019 only 348 PCU were recorded (Figure 4.2).

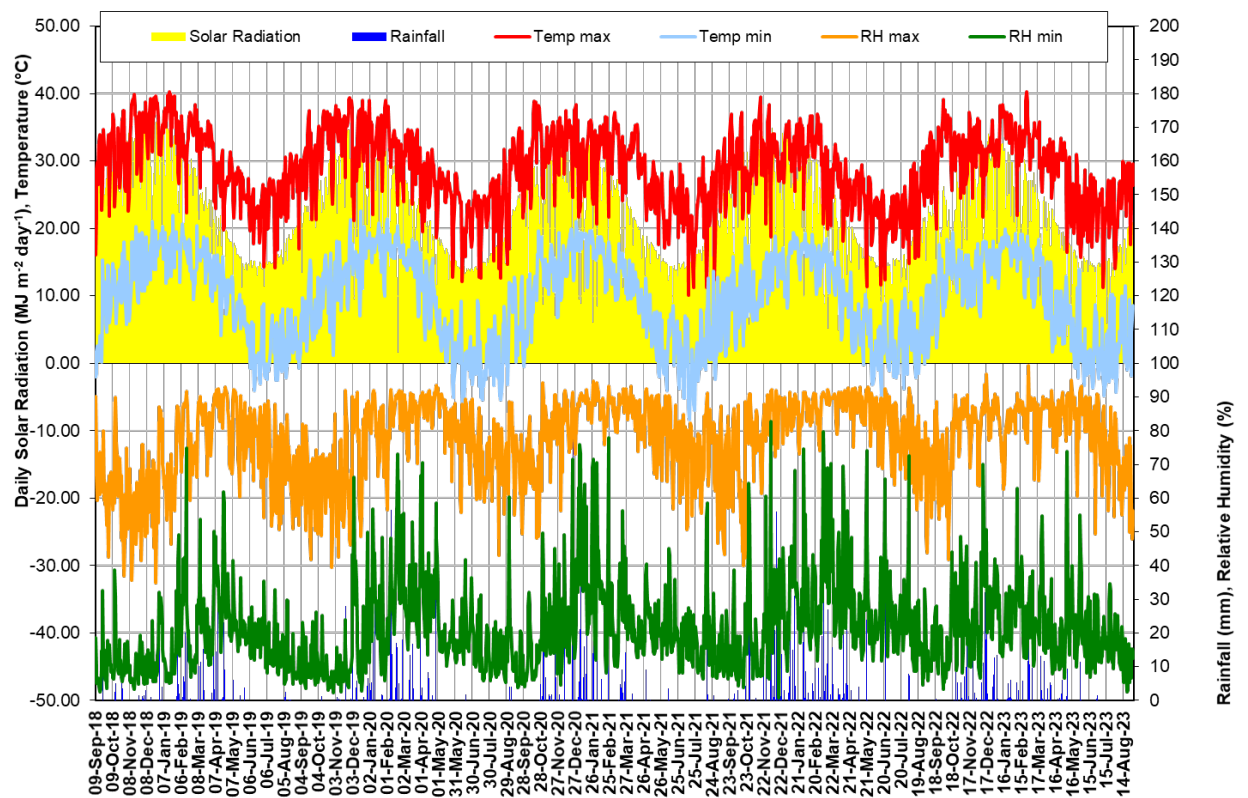


**Figure 4.1** Daily values of maximum and minimum temperatures (°C), solar radiation ( $\text{MJ m}^{-2} \text{ day}^{-1}$ ), rainfall (mm) and maximum and minimum relative humidity (%) at Groen Boerdery from 9 September 2018 to 31 August 2023

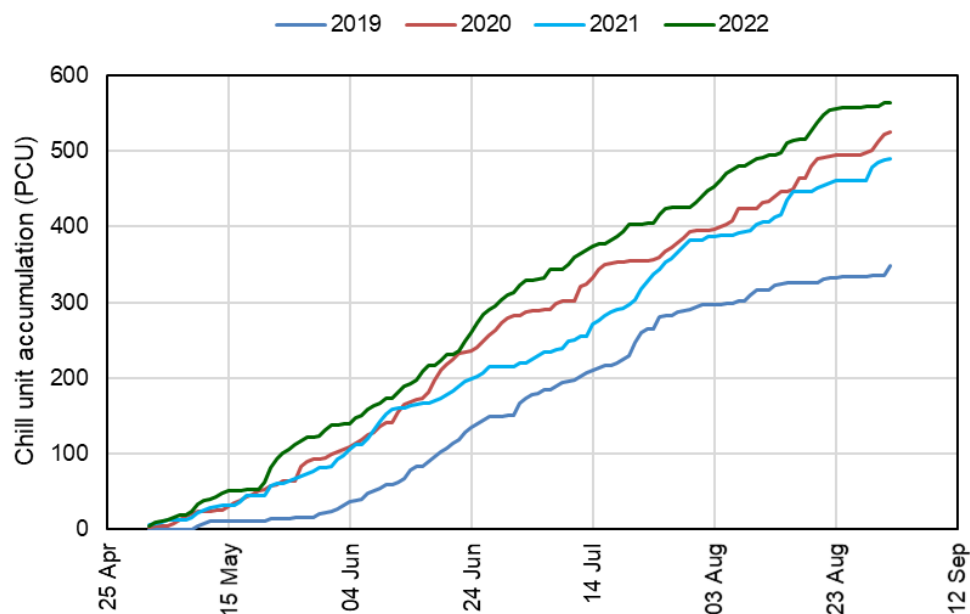


**Figure 4.2** The accumulation of positive chill units for the 2019, 2020, 2021 and 2022 winters at Groen Boerdery outside of Jan Kempdorp. Chill units were calculated from 1 May to 31 August to allow comparisons between seasons.

Reference evapotranspiration and VPD followed a typical seasonal pattern, with highest values in summer and lowest values in winter (Figure 4.3). In 2018/19  $ET_o$  varied between 1.12 and 10.07 mm day<sup>-1</sup> (average = 4.92 mm day<sup>-1</sup>), with VPD varying between 0.42 and 4.05 kPa (average = 2.06 kPa). In 2019/20  $ET_o$  varied between 0.86 and 9.63 mm day<sup>-1</sup> (average = 4.50 mm day<sup>-1</sup>), with VPD varying between 0.40 and 3.82 kPa (average = 1.87 kPa). In 2020/21  $ET_o$  varied between 1.33 and 7.83 mm day<sup>-1</sup> (average = 4.08 mm day<sup>-1</sup>), with VPD varying between 0.36 and 3.56 kPa (average = 1.72). In 2021/22  $ET_o$  varied between 0.89 and 8.03 mm day<sup>-1</sup> (average = 4.33 mm day<sup>-1</sup>), with VPD varying between 0.21 and 3.48 kPa (average = 1.64 kPa). In 2022/23  $ET_o$  varied between 1.01 and 7.21 mm day<sup>-1</sup> (average = 4.57 mm day<sup>-1</sup>), with VPD varying between 0.31 and 3.54 kPa (average = 1.87 kPa). The 2020/21, 2021/22 and 2022/23 seasons were slightly cooler than the 2019/20 season, which was in turn cooler than the 2018/19 season. Total annual  $ET_o$  in 2018/19 (September to August) was 1756 mm, in 2019/20 it was 1645 mm and in 2020/21 it was 1495 mm. The 2021/22 season was cooler than the previous three seasons with a total  $ET_o$  of 1458 mm, with a slight increase in 2022/23 to 1487 mm.

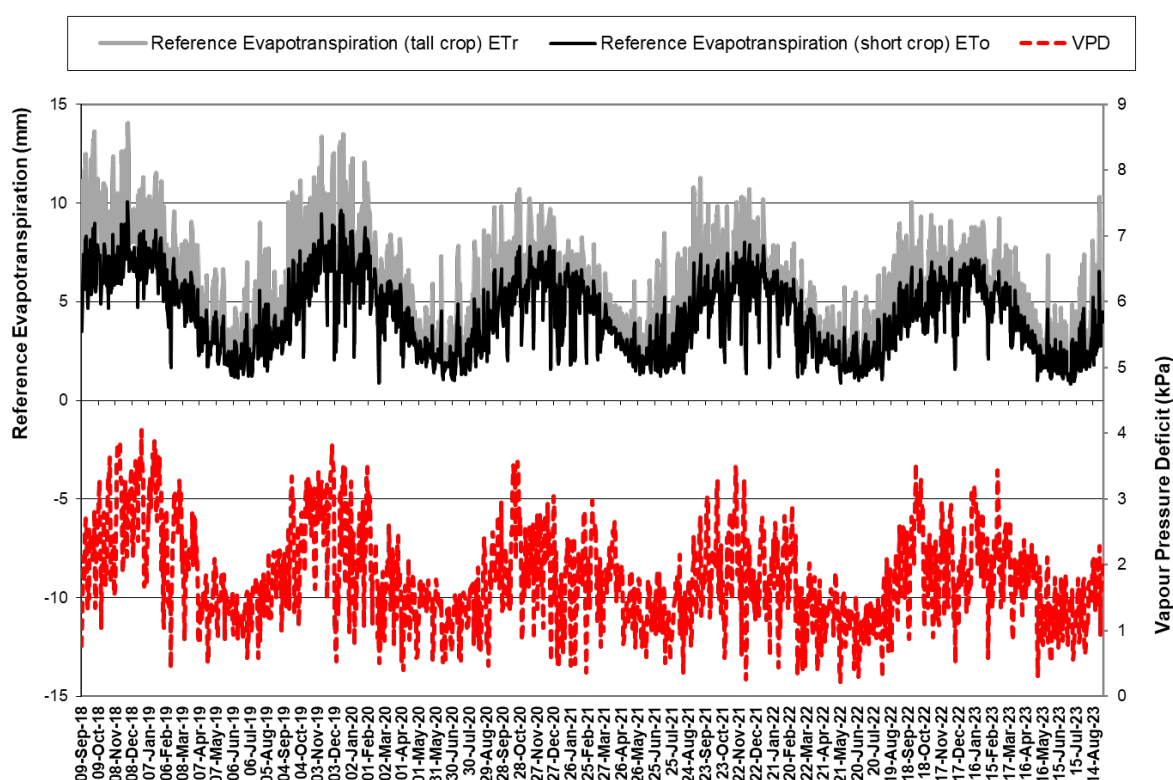


**Figure 4.3 Daily Reference evapotranspiration (short crop –  $ET_o$  and Tall crop  $ET_r$ ) and vapour pressure deficit (VPD) at Groen Boerdery from 9 September 2018 to 31 August 2023**

When comparing daily averages and seasonal totals (September to June when the trees are in leaf), it is also evident that each season has become progressively cooler, with increased rainfall from 2018/19 to 2021/22 (Table 4.1). The 2020/21 and 2021/22 were particularly wet with 644 mm recorded in the 2020/21 season and 796 mm in the 2021/22 season. This was also associated with reduced solar radiation during this period, particularly in January 2021. In the 2022/23 season rainfall was 449 mm which is more typical for the region.

**Table 4.1 Seasonal weather averages for Vaalharts (September to June when the trees are in leaf)**

Season	Avg Daily Temperature (°C)	Avg. Daily VPD (kPa)	Total Rainfall (mm)	Total ET <sub>o</sub> (mm)
2018/19	19.86	2.09	359	1570
2019/20	18.42	1.86	473	1480
2020/21	17.93	1.72	644	1320
2021/22	18.41	1.64	796	1312
2022/23	19.62	1.87	449	1325

#### 4.1.1.2 Groblershoop

Data from the AWS was generally good throughout the duration of the trial (Figure 4.4), apart from an overestimation of rainfall as a result of the rain gauge often becoming blocked. Rainfall data was obtained from Alvin Archer, which included the major rainfall events on the farm for 2019-2021. From September 2021 rainfall data was recorded using a tipping bucket rain gauge next to the orchard. Solar radiation followed a typical seasonal pattern, with highest values in summer and lowest values in winter. Over the course of the three seasons there were very few cloudy days, with only 132 days with  $R_s < 13 \text{ MJ m}^{-2} \text{ day}^{-1}$ . The maximum temperature for the measurement period was 43.1°C which was recorded in the 2019/20 season. The maximum temperature in the 2020/21 season was 41.8°C, 39.9°C in the 2021/22 season and 42.9°C in the 2022/23 season. In the four seasons there were 414 days where the maximum temperature exceeded 35°C and 55 days when the maximum temperature exceeded 40°C. The lowest temperature recorded was -7°C in July and there were 185 days over four seasons that had a minimum temperature below 0°C. During the 2020 winter 446 PCUs were accumulated, whilst in the winter of 2021 424 PCU were accumulated (Figure 4.5). The highest PCU's were accumulated in 2022 with 549 PCU. Chill unit accumulation was lower in Groblershoop than Vaalharts in both seasons.

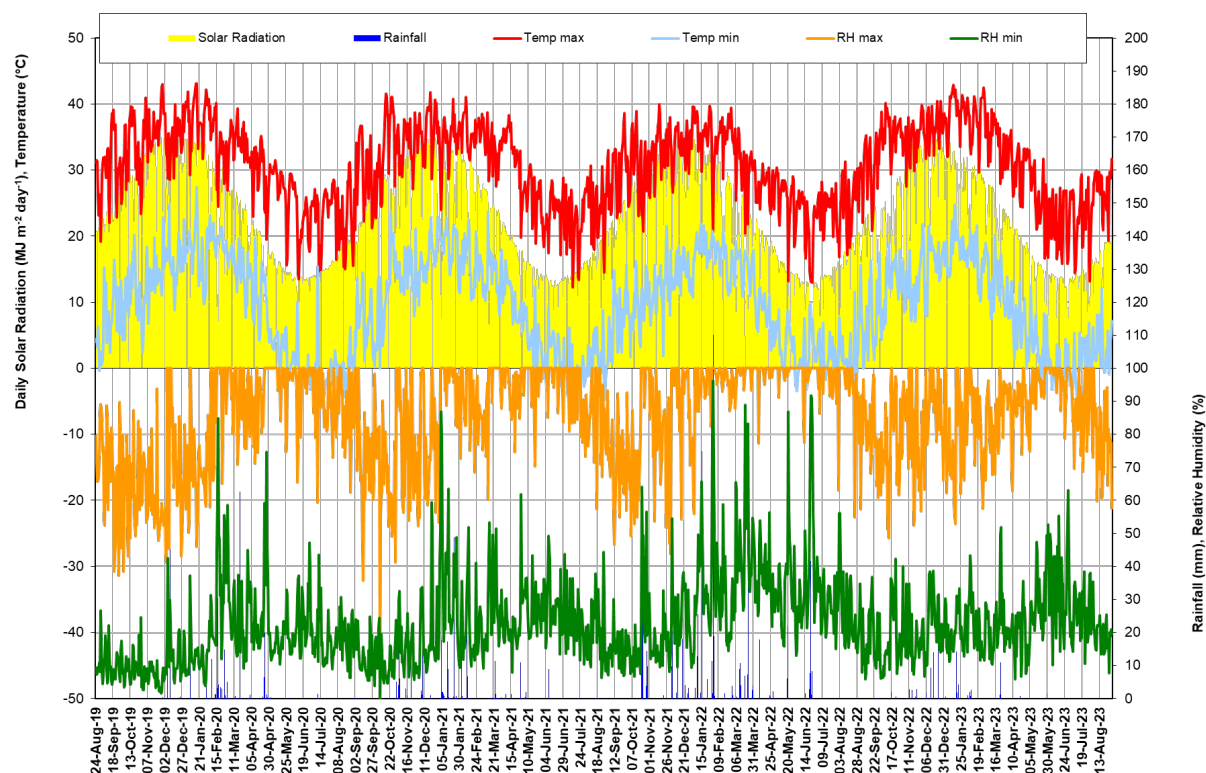


**Figure 4.4** Daily values of maximum and minimum temperatures ( $^{\circ}\text{C}$ ), solar radiation ( $\text{MJ m}^{-2} \text{ day}^{-1}$ ), rainfall (mm) and maximum and minimum relative humidity (%) at Groblershoop from 24 August 2019 to 31 August 2023.

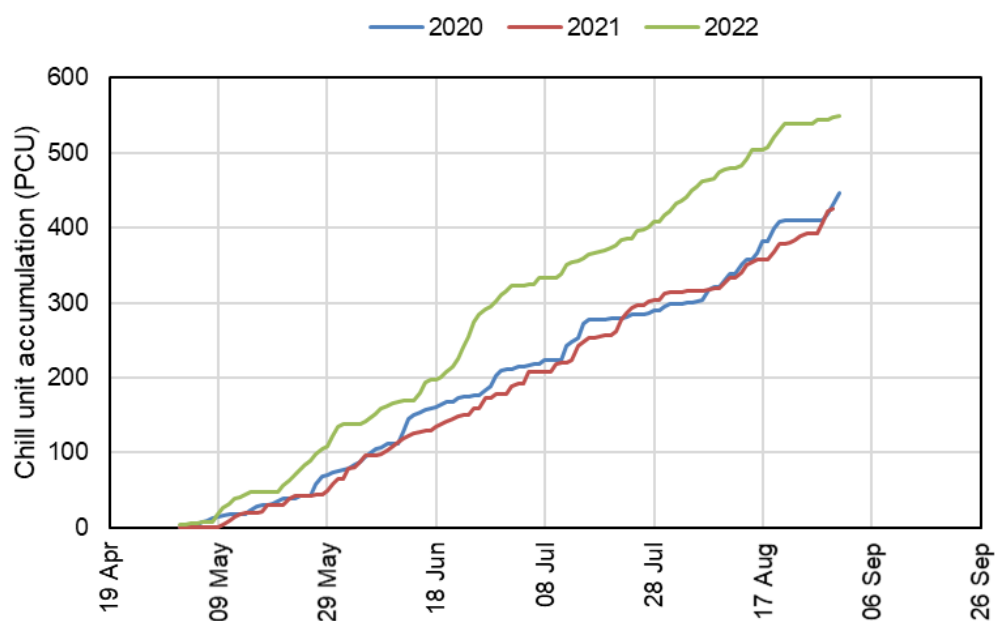


**Figure 4.5** The accumulation of positive chill units for the 2020, 2021 and 2022 winters in Groblershoop. Chill units were calculated from 1 May to 31 August to allow comparisons between seasons.



Reference evapotranspiration and VPD followed a typical seasonal pattern, with highest values in summer and lowest values in winter (Figure 4.6). In the 2019/20 season  $ET_o$  varied between 1.45 and 11.52 mm day<sup>-1</sup> (average = 5.51 mm day<sup>-1</sup>), with VPD varying between 0.23 and 4.76 kPa (average = 2.28 kPa). In the 2020/21 season  $ET_o$  varied between 1.30 and 8.87 mm day<sup>-1</sup> (average = 5.17 mm day<sup>-1</sup>), with VPD varying between 0.20 and 4.25 kPa (average = 2.06 kPa). In the 2021/22 season  $ET_o$  varied between 0.66 and 9.55 mm day<sup>-1</sup> (average = 4.81 mm day<sup>-1</sup>), with VPD varying between 0.05 and 3.43 kPa (average = 1.70 kPa). In the 2022/23 season  $ET_o$  varied between 1.14 and 8.40 mm day<sup>-1</sup> (average = 5.22 mm day<sup>-1</sup>), with VPD varying between 0.35 and 4.05 kPa (average = 2.17 kPa). Total annual  $ET_o$  (September to August) was 1862 mm in the 2019/20 season, 1739 mm in the 2020/21 season, 1642 mm in the 2021/22 season and 1814 mm in the 2022/23 season. This indicates that the first and last seasons were the hottest and driest, which were typical of the region. Fairly high rainfall and cooler conditions for the region were experienced in the 2021/22 season. In all four seasons,  $ET_o$  was higher in Groblershoop than Vaalharts,

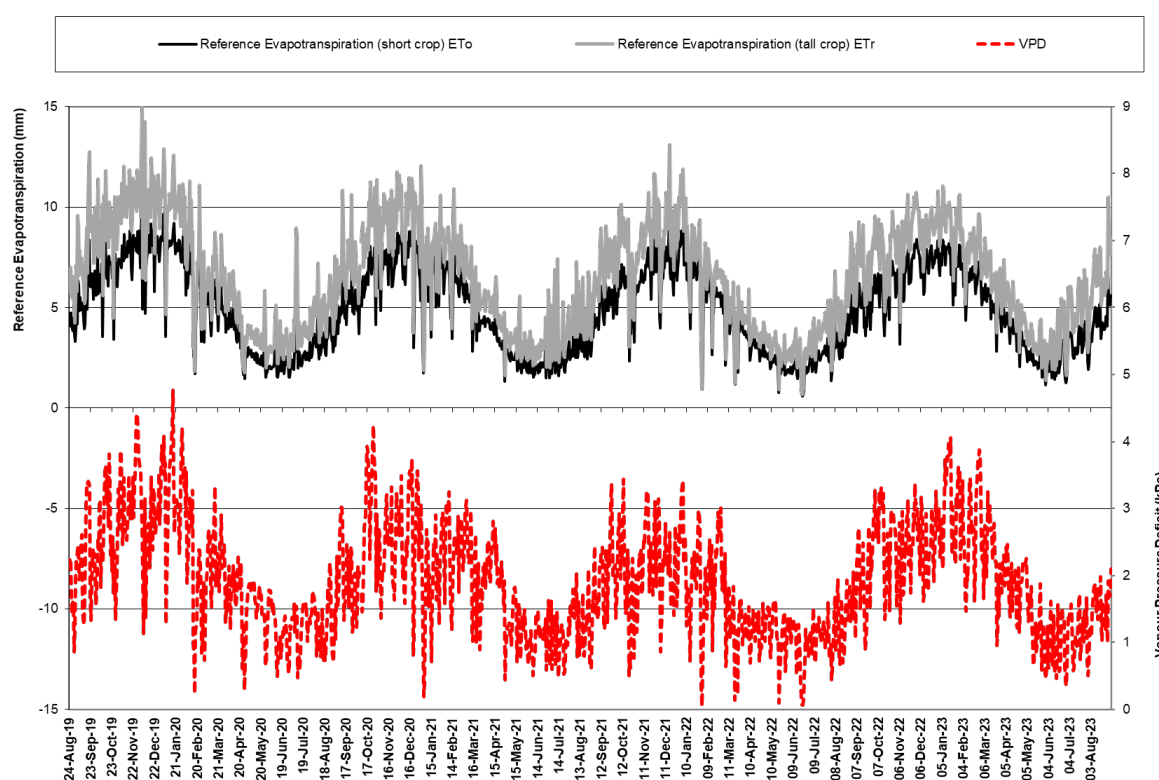


**Figure 4.6 Daily Reference evapotranspiration (short crop –  $ET_o$  and Tall crop  $ET_r$ ) and vapour pressure deficit (VPD) at Groblershoop from 24 August 2019 to 9 February 2023**

When comparing daily averages and seasonal totals (September to June when the trees are in leaf), it is also evident that the 2020/21 and 2021/22 seasons were cooler than the 2019/20

and 2022/23 season, which is illustrated by lower  $ET_o$  (Table 4.2). Rainfall was fairly low except for the 2021/22 when more than 650 mm was recorded for the season, which far exceeds the annual average.

**Table 4.2 Seasonal weather data for Groblershoop (September to June when the trees were in leaf)**

Season	Avg Daily Temperature (°C)	Avg. Daily VPD (kPa)	Total Rainfall (mm)	Total $ET_o$ (mm)
<b>2019/20</b>	21.32	2.27	170*	1673
<b>2020/21</b>	21.03	2.06	180*	1561
<b>2021/22</b>	19.48	1.66	658	1457
<b>2022/23</b>	20.97	2.17	98	1580

\*Rainfall estimated by Alvin Archer from rain gauge on the farm

#### *4.1.1.3 Thermal time comparison of regions*

The calculation of thermal time, calculated as growing degree days (GDD), allowed comparison of regions and seasons and provided an indication of how canopy development could have been impacted in each season (Figure 4.7). It is evident that for all four seasons Groblershoop was hotter than Vaalharts, which in turn was hotter than Pretoria. It was also clear that 2021/22 was a much cooler season at all three locations. On average over the four seasons 1985 GDD was accumulated in Groblershoop, 1654 in Vaalharts and 1212 in Pretoria.

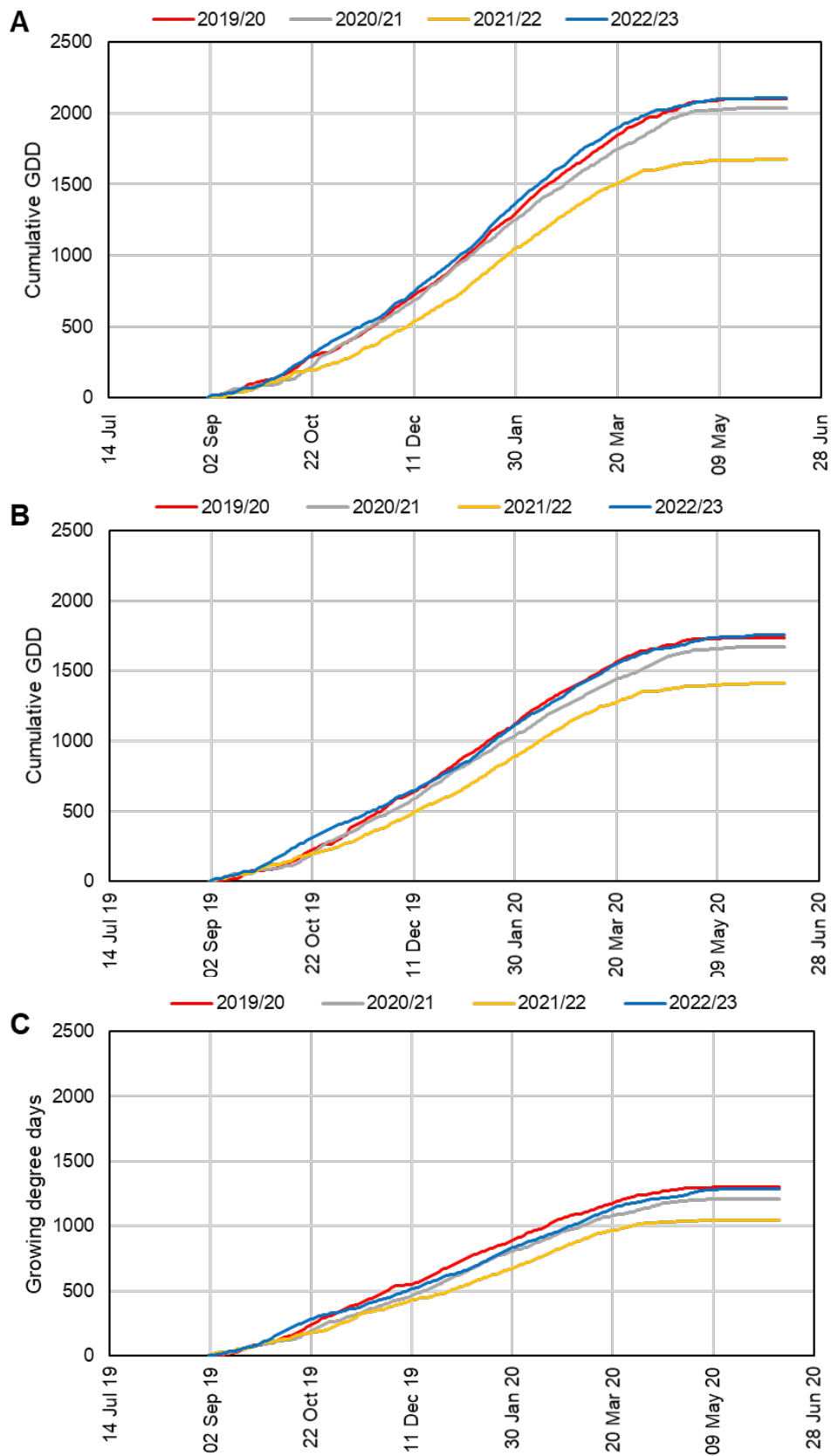


**Figure 4.7** The accumulation of growing degree days for the 2019/20 to 2022/23 seasons for A) Groblershoop, B) Vaalharts and C) Pretoria

## **4.1.2 CANOPY GROWTH AND DEVELOPMENT**

### **4.1.2.1 Vaalharts**

The seasonal pattern of fractional canopy cover was consistent between the years particularly during the 2018/2019, 2021/2022 and 2022/23 seasons (Figure 4.8). This is characterised by an initial rapid increase in canopy size at the beginning of the season for approximately 6-7 weeks from budbreak, after which the increase in canopy size reaches a plateau. Maximum canopy size is reached in mid-December to mid-February, with a steady decline in canopy cover starting in mid-April, marking the start of the senescence stage. Canopy cover declined rapidly in May with leaf fall. However, errors in canopy cover estimates occurred in the 2020/2021 season and part of the 2019/2020 season, which were due to, in large part, to the extrapolation of fractional cover during this period was extrapolated from measurements at Innovation Africa@UP data, through the generation of canopy growth curves. This was necessary due to the COVID-19 travel restrictions during this time which meant it was not possible to cross provincial boundaries. There was also a noticeable difference in canopy cover which was not consistent between years. This was not surprising because of the pruning cycle as described in section 3.1.1. During the 2018/2019 season the 'Choctaw' trees had a maximum canopy cover of 0.6, indicating that they were slightly smaller than the 'Wichita' trees. This size difference between the two cultivars became apparent when comparing their maximum canopy cover values across different years. Specifically, the 'Choctaw' trees maintained a consistent maximum canopy cover of 0.6 in the 2018/2019 season, which continued to a value of 0.64 in the 2019/2020 season but slightly decreased to 0.62 in the 2020/2021 season due to pruning. Subsequently, in the 2021/2022 season, these trees reached a maximum canopy cover of approximately 0.74, further increasing to 0.82 in the 2022/2023 season. In contrast, the 'Wichita' trees exhibited a maximum canopy cover of 0.66 during the 2018/2019 season, which remained relatively stable in the following season, 2019/2020. However, there was a significant increase in the subsequent seasons, reaching maximum values of 0.8 and 0.9 for the 2021/2022 and 2022/2023 seasons, respectively

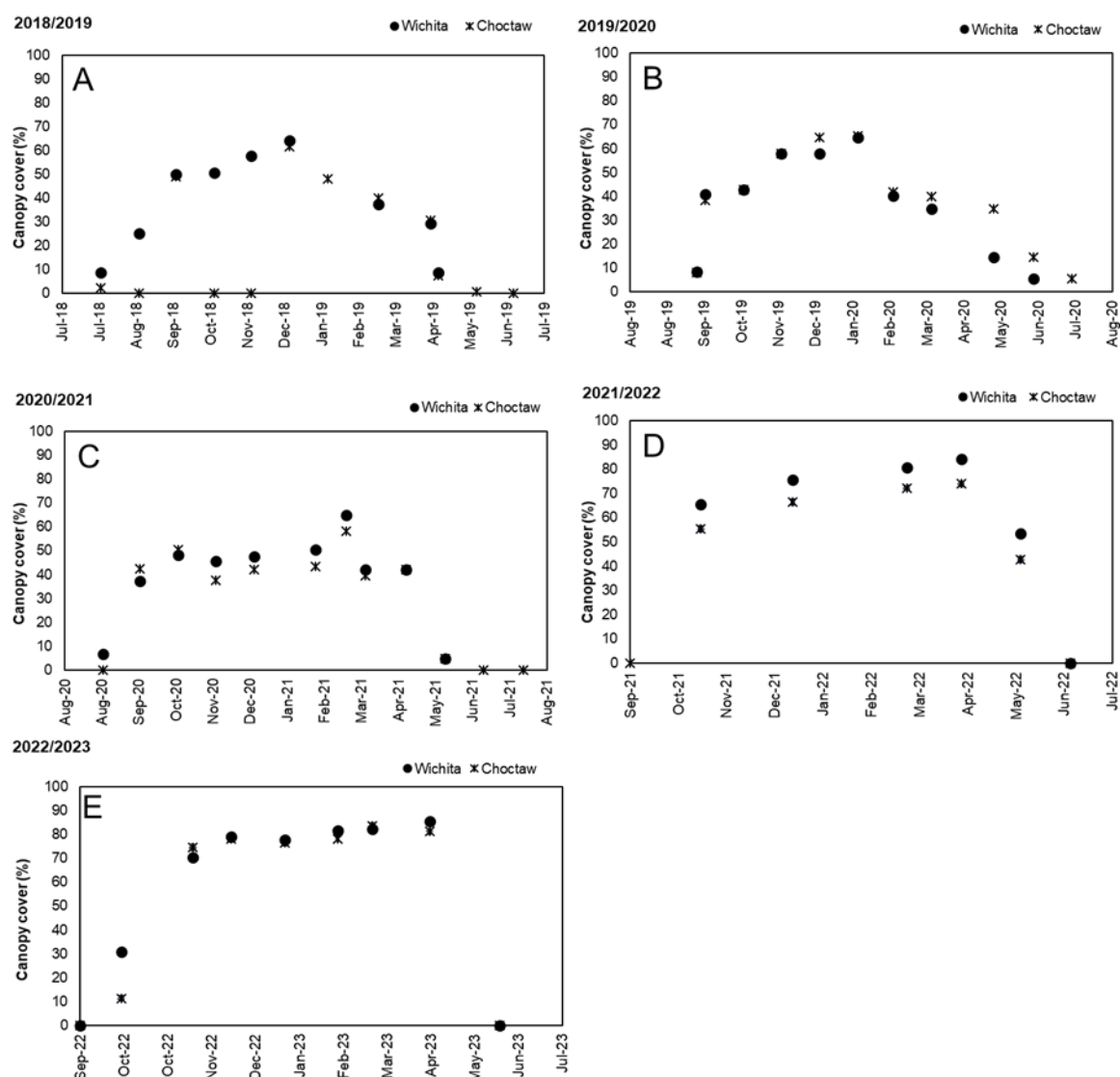


**Figure 4.8** Changes in fractional canopy cover in Vaalharts during A) 2018/19, (B) 2019/20, (C), 2020/21, (D) 2021/22 season and (E) 2022/23 season. Fractional canopy cover was determined from drone images which were analysed with the Canopeo app. Values were an average of the four trees in each orchard.

#### 4.1.2.2 Groblershoop

The seasonal pattern in canopy cover for the past four seasons (2019/2020, 2020/2021, 2021/2022 and 2022/2023) was similar to that observed in Vaalharts with marked differences in canopy size between the two cultivars (Figure 4.9). The 'Wichita' trees in Groblershoop consistently had a bigger canopy than the 'Choctaw' trees. The exception occurred in the 2022/2023 season where both cultivars recorded a maximum canopy cover of 0.84. Over the course of the study there was steady increase in canopy cover from the maximum canopy cover of 0.63 in the first two seasons (2019/2020 and 2020/2021) for 'Wichita' and a maximum

cover of 0.55 for the 'Choctaw' trees. The trees showed a significant increase in canopy size in the next three seasons with a maximum canopy cover of 0.84 and 0.78 for 'Wichita' and 'Choctaw' respectively. This reflects the 4 year pruning cycle in the orchard.

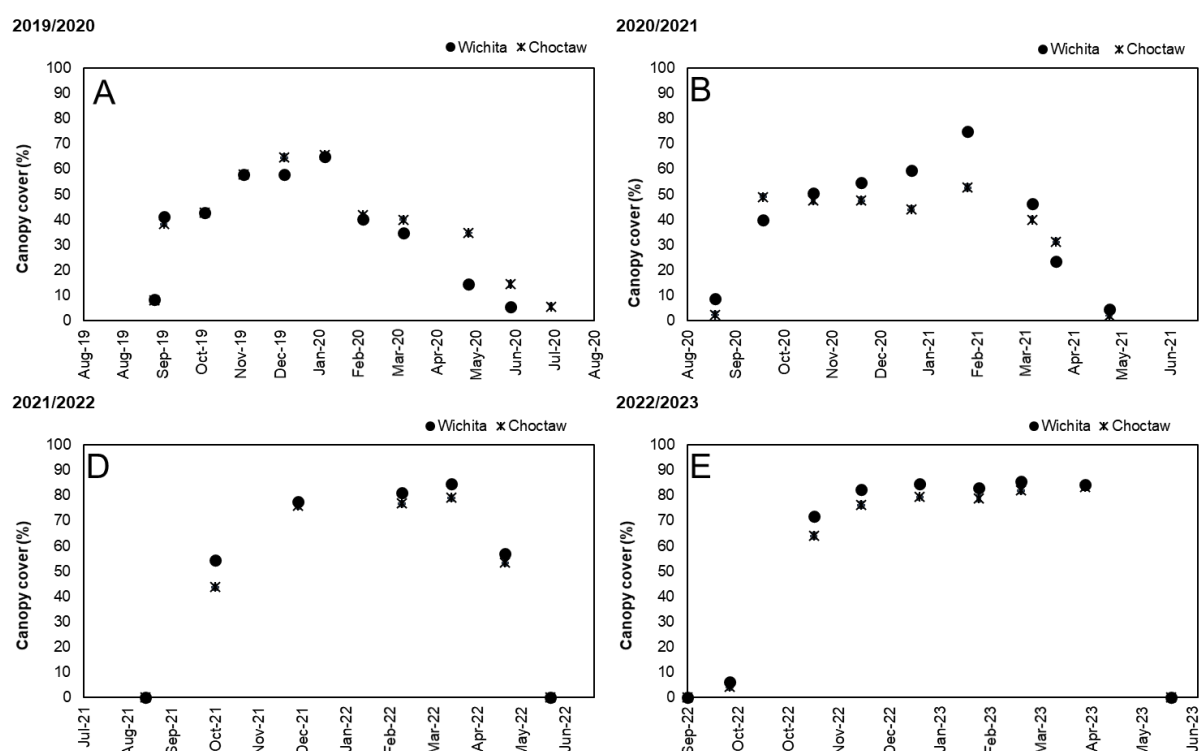


**Figure 4.9** Changes in fractional canopy cover in Groblershoop orchard during (A) 2019/20 season, (B) 2020/21 season, (C) 2021/22 and D 2022/23 season. Fractional canopy cover was determined from drone images which were analysed with the Canopeo app. Values were an average of the four trees in each orchard.

#### 4.1.2.3 Fractional interception of PAR

In line with the observed seasonal trends in canopy cover for both cultivars, the measured FIPAR not only exhibited a similar seasonal pattern across the seasons but also highlighted differences between the cultivars in terms of canopy size. Specifically, the 'Wichita' trees appeared to be slightly larger than the 'Choctaw' trees at both sites (Figure 4.10). Over the preceding two seasons, FIPAR values for 'Choctaw' ranged from a minimum of 0.04 to a maximum of 0.77, while 'Wichita' recorded a maximum value of 0.86 in the 2021/2022 season and ranged between 0.06 and a maximum of 0.79 in the 2022/2023 season in Vaalharts. In Groblershoop, during the 2021/2022 season, FIPAR values were observed to be in the range of 0.03 to 0.9 for 'Wichita' and 0 to 0.86 for 'Choctaw'. During the 2022/2023 season, 'Wichita' trees reached a maximum FIPAR value of 0.9, while 'Choctaw' trees achieved a maximum value of 0.87.

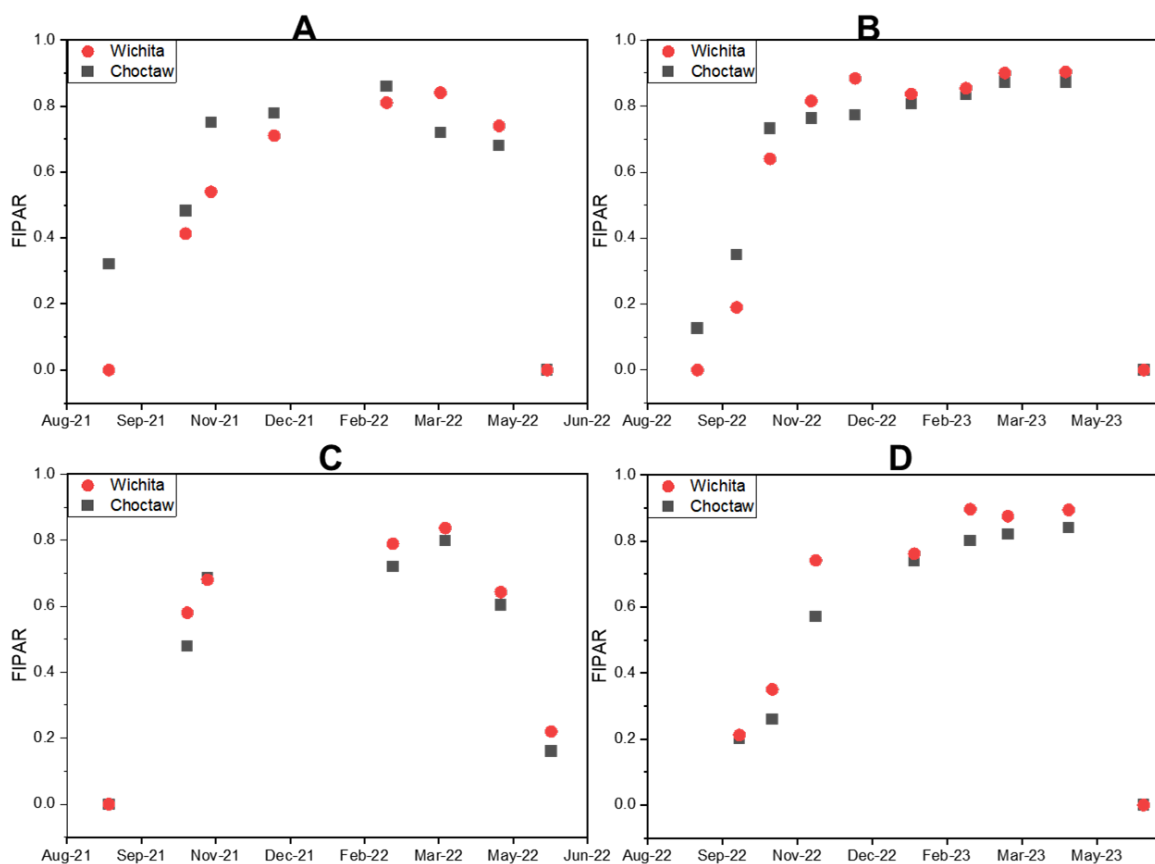


**Figure 4.10** Changes in fractional intercepted photosynthetically active radiation (FIPAR) determined with a ceptimeter for the two cultivars in Groblershoop during the (A) 2021/22 and (B) 2022/23 seasons, and Vaalharts during the C) 2021/22 and (D) 2022/23 seasons.

### 4.1.3 TRANSPIRATION AND EVAPOTRANSPIRATION RATES

#### 4.1.3.1 Vaalharts

In all five seasons, tree transpiration followed the pattern typical for deciduous tree crops, characterized by a rapid increase at the start of the season, reaching a maximum between December and March and then declining from May, when leaf senescence starts, until the end of the season (Figure 4.11). This closely mirrors canopy development of the pecan trees (Figure 4.8 and Figure 4.10). The variation in transpiration rate throughout the season can be explained by changes in canopy cover and  $ET_0$ , where maximum transpiration rates occurred during periods of highest canopy cover and the hottest months (Figure 4.11). Despite, the similar seasonal pattern observed in 2020/21, there was a noticeable decline in transpiration rates during this season compared to the 2018/19 and 2019/20 seasons which reflects the

lower evaporative demand in 2020/21 season when compared to the two previous seasons (Figure 4.11). It also reflects a lightly lower canopy cover in the 2020/21 season as a result of pruning practices. Transpiration increased again in 2021/22 reflecting an increase in canopy cover of the trees, as seasonal  $ET_o$  was very similar to the previous season.

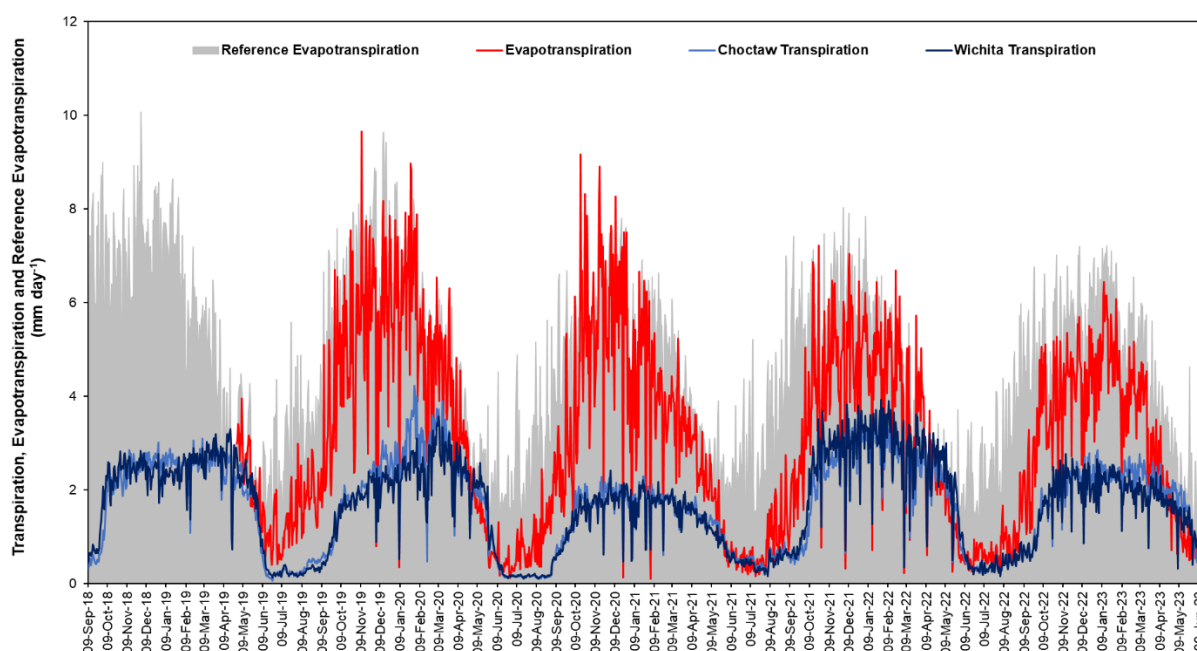


**Figure 4.11 Changes in transpiration (T) for ‘Choctaw’ and ‘Wichita’ trees in relation to evapotranspiration (ET) and reference evapotranspiration ( $ET_o$ ) over the five seasons from 9 September 2019 to 11 June 2023 in Vaalharts.**

Total volume of water transpired by ‘Wichita’ and ‘Choctaw’ trees differed over the five seasons as a result of changing weather conditions and size of the canopy, due to canopy growth and pruning practices (Table 4.3). The difference between the two cultivars in each season varied between 20 and 50 mm, except for the 2021/22 season when ‘Wichita’ trees transpired 70 mm more than ‘Choctaw’. The maximum daily transpiration over five seasons for the ‘Wichita’ trees was  $392 \text{ L tree}^{-1} \text{ day}^{-1}$  ( $3.92 \text{ mm day}^{-1}$ ), whilst for the ‘Choctaw’ trees the maximum transpiration rate was  $423 \text{ L tree}^{-1} \text{ day}^{-1}$  ( $4.23 \text{ mm day}^{-1}$ ). Average transpiration for the middle of the season (November to April) was  $230 \text{ L day}^{-1}$  ( $2.30 \text{ mm day}^{-1}$ ) for the ‘Wichita’ trees, whilst average transpiration for the ‘Choctaw’ trees for this period was  $240 \text{ L day}^{-1}$  ( $2.40 \text{ mm day}^{-1}$ ).

Evapotranspiration measurements began at the end of April 2019 and ended in June 2023. Over this period ET varied between 0.1 and  $9.65 \text{ mm day}^{-1}$ , with an average of  $3.0 \text{ mm day}^{-1}$ .



across the entire measurement period. From October to February average ET was 5.00 mm day<sup>-1</sup>, whilst in the hottest time of the year (December to end of February) ET averaged 5.30 mm day<sup>-1</sup> (Table 4.3).

**Table 4.3 Average, maximum and total seasonal transpiration, reference evapotranspiration and evapotranspiration for the 'Choctaw' and 'Wichita' trees in Vaalharts**

	<b>Choctaw</b>	<b>Wichita</b>
Spring (avg. T mm day <sup>-1</sup> )	1.57	1.63
Summer (avg. T mm day <sup>-1</sup> )	2.47	2.35
Autumn (avg. T mm day <sup>-1</sup> )	2.07	2.12
Max. transpiration (mm day <sup>-1</sup> / L day <sup>-1</sup> )	4.23 / 423	3.92/ 392
Avg. transpiration (Nov-Apr mm day <sup>-1</sup> / L day <sup>-1</sup> )	2.40/240	2.30/230
Seasonal transpiration 2018/19 (Sept-May, mm)	600	625
Seasonal transpiration 2019/20 (Sept-May, mm)	610	560
Seasonal transpiration 2020/21 (Sept-May, mm)	440	420
Seasonal transpiration 2021/22 (Sept-May, mm)	630	700
Seasonal transpiration 2022/23 (Sept-May, mm)	540	500
Seasonal reference evapotranspiration (Sept-June, mm) 2018/19	1570	
Seasonal reference evapotranspiration (Sept-June, mm) 2019/20	1480	
Seasonal reference evapotranspiration (Sept-June, mm) 2020/21	1350	
Seasonal reference evapotranspiration (Sept-June, mm) 2021/22	1310	
Seasonal reference evapotranspiration (Sept-June, mm) 2022/23	1330	
Annual evapotranspiration (September to August) 2019/20	1270	
Annual evapotranspiration (September to August) 2020/21	1120	
Annual evapotranspiration (September to August) 2021/22	1050	
Annual evapotranspiration (September to August) 2022/23	930* (982 until 31 Aug using avg. K <sub>c</sub> )	

\*Measurements were terminated on 11 June 2023

There was a significant difference between ET and T for most of the measurement period (except in autumn for all four seasons) suggesting that evaporation (evaporation from the soil and transpiration of the understorey vegetation) is significant in this orchard, especially when the trees are still coming into leaf. This is not unexpected due to the large area wet by the irrigation. In addition, for two seasons (2020/21 and 2021/22) there was high rainfall, which would have resulted in high evaporation rates from the orchard floor and from tree canopies, which intercepted rain. Annual evapotranspiration from September to August for the 2019/20 season was 1265 mm, 1120 mm for the 2020/21 season, and 1050 for the 2021/22 season (Table 4.3). Measurements were terminated on 11 June 2023 and from September up to this date 930 mm was measured for the 2022/23 season.

Transpiration crop coefficients ( $K_t$ ) followed a 6 stage crop coefficient curve in all five seasons as reported for pecan trees in Cullinan (Ibraimo et al., 2016) and in New Mexico (Sammis et al., 2004a) (Figure 4.12). A peak in  $K_t$  values was found from March to May, which is associated with a flush of leaves and nut filling. Throughout the five seasons,  $K_t$  values were very similar for the 'Choctaw' trees and 'Wichita' trees. Slight differences could be correlated with differences in canopy size over the five seasons. During the late spring and summer period (November to March) the average  $K_t$  for the 'Wichita' trees was 0.30, whilst it was 0.32 for the same period for the 'Choctaw' trees. An increase in  $K_t$  values were observed April and May in all the seasons. During this period  $ET_o$  declined at a faster rate than T resulting in the observed increase in  $K_t$ . This increase was irrespective of the cultivar, season, and production region. The fact that the increase in transpiration at the end of the season, relative to  $ET_o$  is consistent through the different seasons and across the different production regions, suggests that this could be related to the physiology of the trees, as this period is associated with nut filling, an extremely energy expensive process. Andersen and Brodbeck (1988b) found that older pecan leaves have less stomatal control over transpiration, which could explain why higher transpiration rates were found relative to  $ET_o$  later in the season.

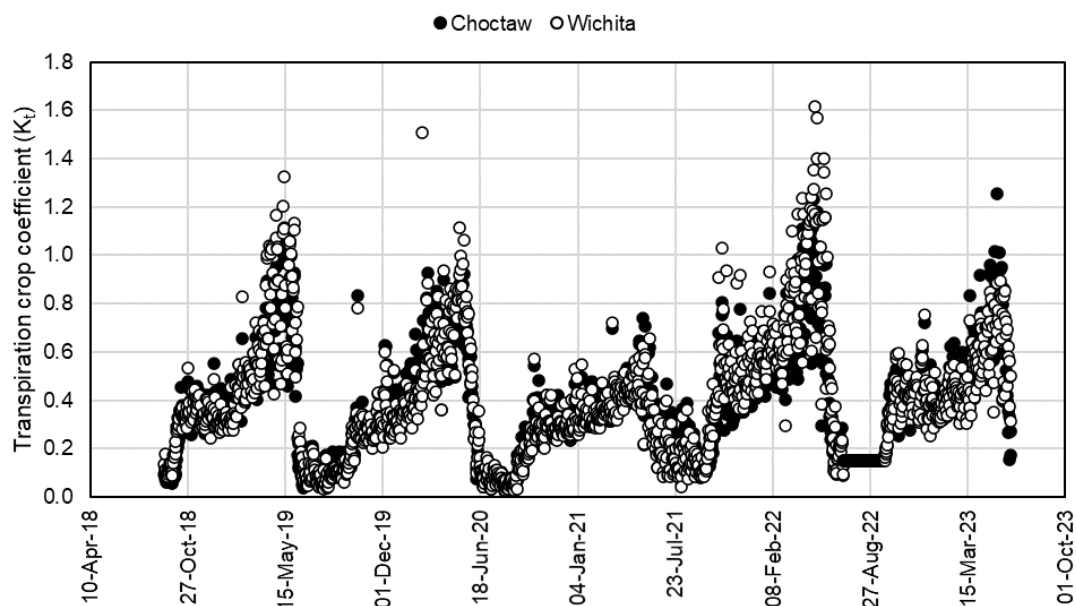


**Figure 4.12 Transpiration crop coefficients for the five seasons (2018-2023) for 'Wichita' and 'Choctaw' pecan trees at Vaalharts**

#### 4.1.3.2 Groblershoop

A similar trend in tree transpiration was observed in Groblershoop when compared to Vaalharts data, with a rapid increase in transpiration from the start of the season to a maximum between December and February (Figure 4.13). Once again, this change in transpiration occurred in concert with increases in canopy cover and changes in daily weather conditions. Transpiration started to decline rapidly towards the end May and into June as leaf senescence began. Transpiration rates throughout the season were related to the canopy cover % and  $ET_o$ , where maximum transpiration rates occurred during periods of highest canopy cover and hottest conditions. There were differences in the total volume of water transpired in a production season (September to May) between the two cultivars, with transpiration from the 'Wichita' trees being consistently higher than the 'Choctaw' trees. On average, across the four seasons, seasonal transpiration for 'Wichita' trees was 615 mm and 490 mm for 'Choctaw' trees. Maximum daily transpiration rate for the 'Wichita' trees was  $482 \text{ L tree}^{-1} \text{ day}^{-1}$  ( $4.82 \text{ mm day}^{-1}$ ), whilst for the 'Choctaw' trees the maximum transpiration rate was  $359 \text{ L tree}^{-1} \text{ day}^{-1}$  ( $3.59 \text{ mm day}^{-1}$ ) (Table 4.4). Average transpiration for the middle of the season (November to April) was  $300 \text{ L day}^{-1}$  ( $3.00 \text{ mm day}^{-1}$ ) for the 'Wichita' trees, whilst average transpiration for the 'Choctaw' trees for this period was  $250 \text{ L day}^{-1}$  ( $2.50 \text{ mm day}^{-1}$ ).

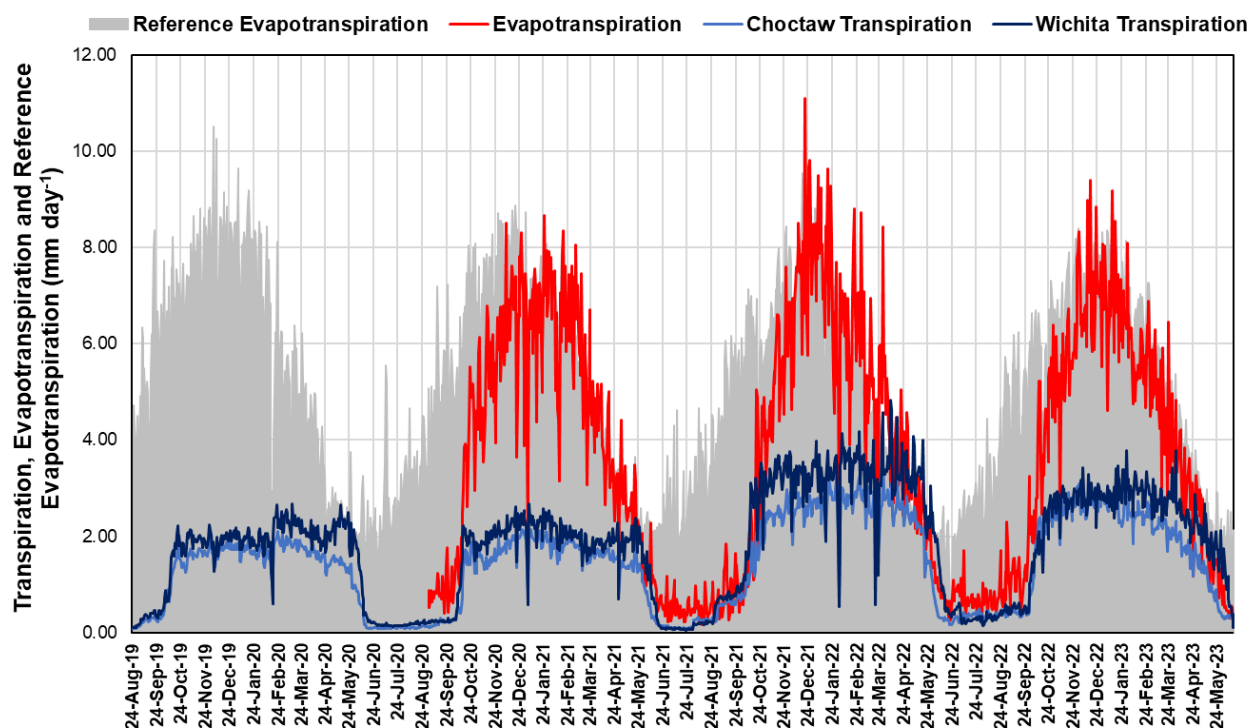


**Figure 4.13** Changes in transpiration (T) for ‘Choctaw’ and ‘Wichita’ trees in relation to evapotranspiration (ET) and reference evapotranspiration ( $ET_o$ ) over four seasons from 24 August 2019 to 14 June 2023 for Groblershoop.

Evapotranspiration measurements began in the middle of September 2020 and continued until June 2023. Over this period ET varied between 0.16 and 11.11  $\text{mm day}^{-1}$ , with an average of 3.75  $\text{mm day}^{-1}$  across the entire measurement period (Table 4.4). From October to February average ET was 5.78  $\text{mm day}^{-1}$ , whilst in the hottest time of the year (December to end of February) ET averaged 6.82  $\text{mm day}^{-1}$ . There was a significant difference between ET and T for most of the measurement period (except in spring and autumn for all three seasons) suggesting that evaporation (evaporation from the soil and some transpiration from the sparse understorey vegetation) is significant in this orchard, especially in the middle of the season. This is despite drip irrigation in the orchard, where the water is applied under the canopy and overnight.

**Table 4.4 Average, maximum and total seasonal transpiration, reference evapotranspiration and evapotranspiration for the 'Choctaw' and 'Wichita' trees in Groblershoop**

	<b>Choctaw</b>	<b>Wichita</b>
Spring (avg. T mm day <sup>-1</sup> )	1.29	1.59
Summer (avg. T mm day <sup>-1</sup> )	2.22	2.58
Autumn (avg. T mm day <sup>-1</sup> )	1.79	2.39
Max. transpiration (mm day <sup>-1</sup> / L day <sup>-1</sup> )	3.59 / 359	4.82 / 482
Avg. transpiration (Nov-Apr mm day <sup>-1</sup> / L day <sup>-1</sup> )	2.15 / 215	2.50 / 250
Seasonal transpiration 2019/20 (Sept-June, mm)	400	500
Seasonal transpiration 2020/21 (Sept-June, mm)	400	490
Seasonal transpiration 2021/22 (Sept-June, mm)	610	810
Seasonal transpiration 2022/23 (Sept-June, mm)	550	650
Seasonal reference evapotranspiration (Sept-June, mm) 2019/20	1670	
Seasonal reference evapotranspiration (Sept-June, mm) 2020/21	1560	
Seasonal reference evapotranspiration (Sept-June, mm) 2021/22	1460	
Seasonal reference evapotranspiration (Sept-June, mm) 2022/23	1540	
Season evapotranspiration (Sept-Aug, mm) 2020/21	1280	
Season evapotranspiration (Sept-Aug, mm) 2021/22	1320	
Season evapotranspiration (Sept-June*, mm) 2021/22	1220*	
	(1282 until 31 Aug using avg. K <sub>c</sub> )	

\*Only have data until 14 June

As in Vaalharts, Cullinan (Ibraimo et al., 2016) and New Mexico (Sammis et al., 2004c), transpiration crop coefficients (K<sub>t</sub>) followed a 6 stage crop coefficient curve in Groblershoop (Figure 4.14). A peak in K<sub>t</sub> values was found from March to May, which is associated with a flush of leaves and nut filling. Throughout the four seasons, K<sub>t</sub> values were slightly higher for the 'Wichita' trees than the 'Choctaw' trees, reflecting the higher transpiration rates and greater canopy cover of these trees. During the late spring and summer period (November to March) the average K<sub>t</sub> for the 'Wichita' trees was 0.49, whilst it was 0.41 for the same period for the 'Choctaw' trees. The fact that the same curve shape has occurred for four seasons in two cultivars and in two production regions (as mentioned above) suggests that this is not just an

artefact of the measurement technique. The strong increase in  $K_t$  values in the 2021/22 season reflects the greater canopy size of both cultivars during this season.

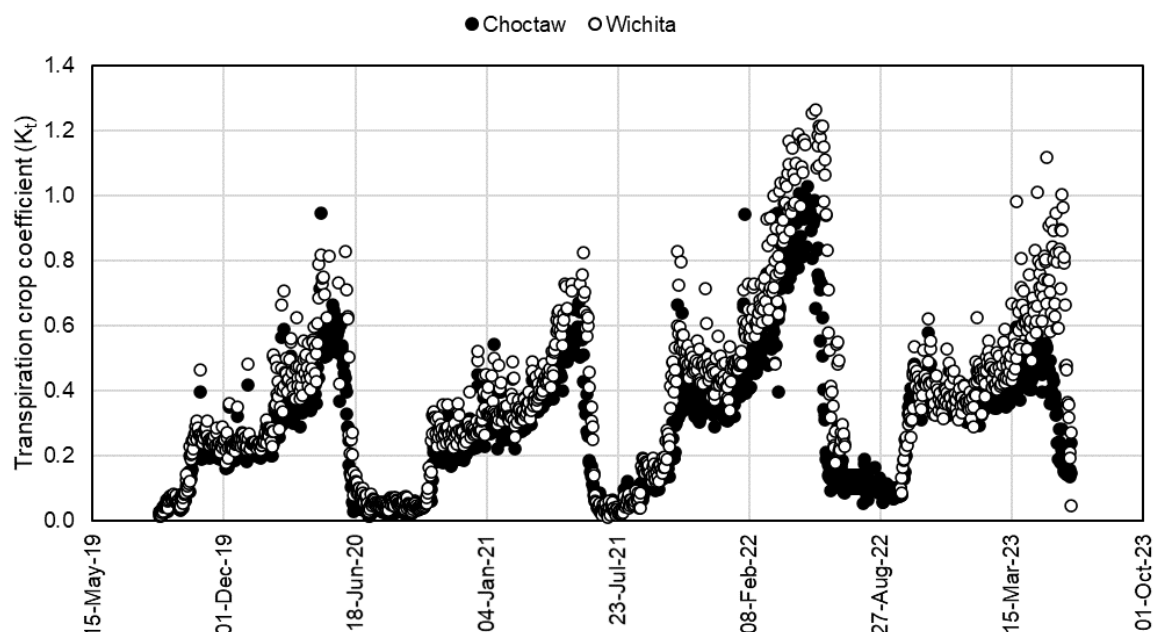


**Figure 4.14 Transpiration crop coefficients for the four seasons (2019-2023) seasons for 'Wichita' and 'Choctaw' pecan trees at Groblershoop**

#### 4.1.3.3 Transpiration crop coefficients and canopy size

In order to determine the impact of canopy size on  $K_t$  values, data from the Vaalharts and Groblershoop sites were combined and plotted against two estimates of canopy size, viz. fractional interception of PAR (FIPAR) and fractional canopy cover ( $fc_{\text{canopeo}}$ ) (Figure 4.15). It was evident that there was an increase in  $K_t$  as canopy size increased, however, as canopy cover increased over 0.7 there was a lot of scatter in the data and as a result  $R^2$  values for the relationships were fairly low. This scatter at high canopy cover can possibly be attributed to the increase in  $K_t$  values at the end of the season without a similar increase in canopy size. As a result, simple relationships between  $K_t$  values and canopy size can not be used to derive orchard specific  $K_t$  values, as has been found in peach (Ayars et al., 2003) and grapevine (Williams and Ayars, 2005a).

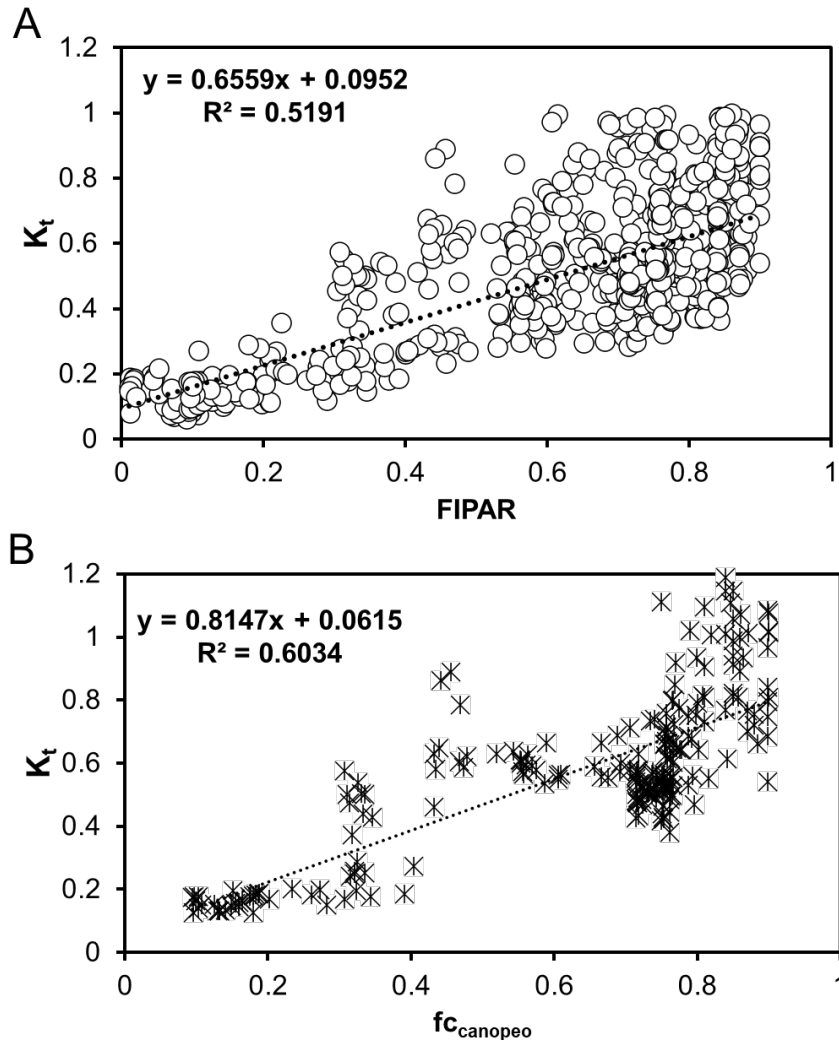


**Figure 4.15** The relationship between transpiration crop coefficients ( $K_t$ ) and canopy size determined by measuring A) fractional interception of PAR by the canopy (FIPAR) and B) canopy cover determined using the Canopeo app ( $fc_{\text{canopeo}}$ ) combined with aerial images of the orchard. The relationships were determined using data from both sites in the Northern Cape province.

#### 4.1.4 ECOPHYSIOLOGY

##### 4.1.4.1 Predawn leaf water potential and midday stem water potential

In order to assess possible water deficit stress at each trial site, predawn ( $\Psi_{pd}$ ) and stem water potential ( $\Psi_{smd}$ ) measurements were made throughout the study period during trips to each site. No results are available for the 2019/20 and 2020/21 seasons in both orchards, due to COVID-19 travel restrictions and rainfall occurring during many of the visits. In the 2021/22 season very few visits to Vaalharts did not coincide with rainfall which prevented measurements. Measurements indicated that water deficit stress was unlikely to have

occurred in the orchards, although it is impossible to determine if any stress occurred in between visits to each site. This was evident from the  $\Psi_{pd}$ , which ranged from -0.06 to -0.20 MPa for Groblershoop (Figure 4.16) and -0.12 to -0.23 for Vaalharts (Figure 4.17), with an average of -0.12 MPa for both sites. These values are well above the threshold of -0.45 MPa determined in the stress trial (see section 4.4).

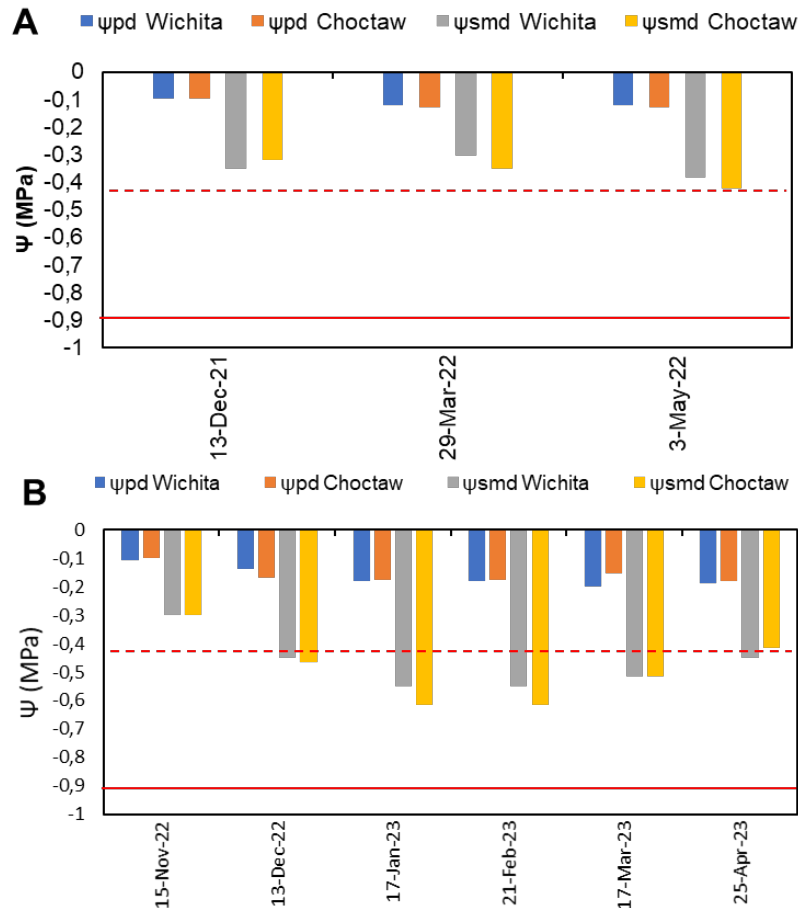


**Figure 4.16** Predawn leaf water potential ( $\Psi_{pd}$ ) and midday stem water potential ( $\Psi_{smd}$ ) for Groblershoop during the A) 2021/22 season. and B) 2022/23 seasons. The horizontal solid red line demonstrates the  $\Psi_{smd}$  threshold value (-0.90 MPa) for mild stress as outlined by Othman et al. (2014). The dotted red line indicates the threshold for  $\Psi_{pd}$  that corresponds to the  $\Psi_{smd}$  as determined in the stress trial during this study.

The  $\Psi_{smd}$  readings also indicated unstressed conditions in the orchards, with values not dropping below the -0.9 MPa threshold, s defined by Othman et al. (2014). Over the course of the measurements,  $\Psi_{smd}$  ranged from -0.30 MPa to -0.62 MPa in Groblershoop (Figure 4.16) and 0.31 to -0.75 MPa Vaalharts (Figure 4.17). However, the low values observed in January and February 2023 did indicate some mild stress conditions in Vaalharts (Figure 4.17C).



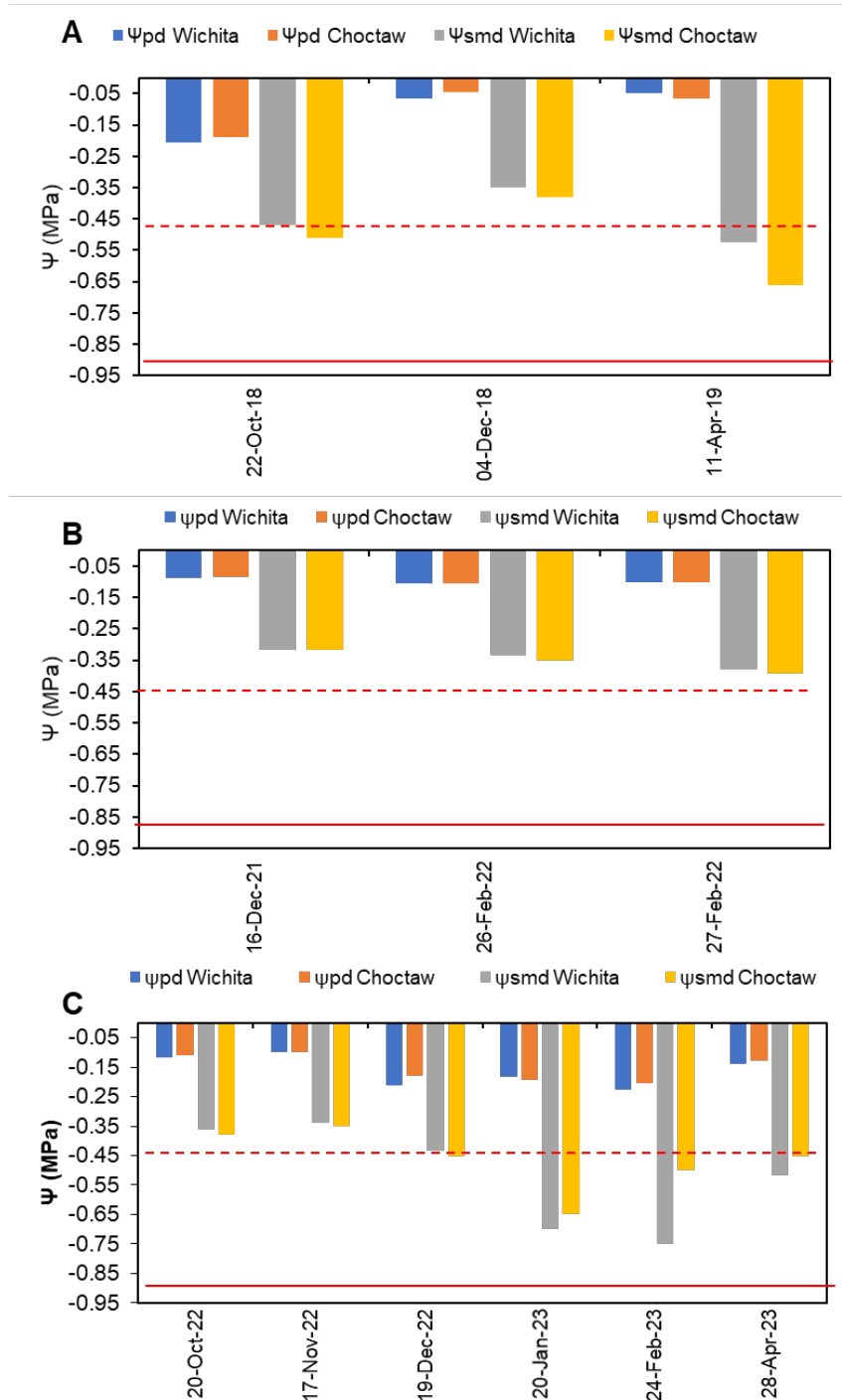


**Figure 4.17** Predawn leaf water potential ( $\psi_{pd}$ ) and midday stem water potential ( $\psi_{smd}$ ) for Vaalharts during the A) 2018/19, B) 2020/21 and C) 2022/23 season. The horizontal solid red line demonstrates the  $\psi_{smd}$  threshold value (-0.90 MPa) for mild stress as outlined by Othman et al. (2014). The dotted red line indicates the threshold for  $\psi_{pd}$  (-0.45 MPa) that corresponds to the  $\psi_{smd}$  as determined in the stress trial during this study.

#### 4.1.4.2 Transpiration response to environmental variables

The ability to choose appropriate modelling approaches for pecan water use relies on understanding the control of transpiration in pecan trees. By examining the response of transpiration ( $T$ ) to different environmental factors, it is possible to determine if pecan  $T$  is affected by differing environmental conditions. The response of hourly  $T$  to vapour pressure deficit (VPD), solar radiation ( $R_s$ ), air temperature ( $T_{air}$ ) and reference evapotranspiration ( $ET_o$ ) was determined for 'Wichita' and 'Choctaw' trees in Groblershoop (Figure 4.18) and Vaalharts (Figure 4.19). The response of  $T$  was typically a non-linear response to the four environmental variables, with an initial linear relationship at lower evaporative demands, but as evaporative demand increased,  $T$  reached an inflexion point and began to plateau. This trend was observed for the 'Choctaw' trees in Groblershoop, where  $T$  plateaued at an inflexion point between 0.1 and 0.15 mm h<sup>-1</sup>  $ET_o$ . This trend suggests that pecans have a limit to  $T$ , which may be due to the hydraulic limitations within the plants to match atmospheric evaporative demand (Maseda and Fernández, 2006). This is despite there being sufficient water in the soil as indicated by  $\Psi_{pd}$  and  $\Psi_{smd}$  measurements over the course of the study in both orchards (Figure 4.16 and Figure 4.17) and soil water measurements (see section 4.1.5). The inflexion point for VPD was reached between 0.9 and 1.5 kPa, whilst for  $R_s$  it was reached between 200 and 300 W m<sup>-2</sup> for both sites, which again suggests that pecans have a physiological control of transpiration in accordance with atmospheric evaporative demand, irrespective of location. This suggests that as it gets hotter and drier pecans do not transpire proportionally more water and any modelling approach needs to take this into account. The maximum transpiration ( $T_{max}$ ) rate differed between the cultivars, mainly as a result of differences in canopy size, but  $T_{max}$  was similar both the same cultivar in each region. For 'Choctaw' trees in Vaalharts and Groblershoop  $T_{max}$  was approximately 0.30 mm h<sup>-1</sup>. For 'Wichita' trees in Groblershoop and Vaalharts  $T_{max}$  was just over 0.35 mm h<sup>-1</sup>.

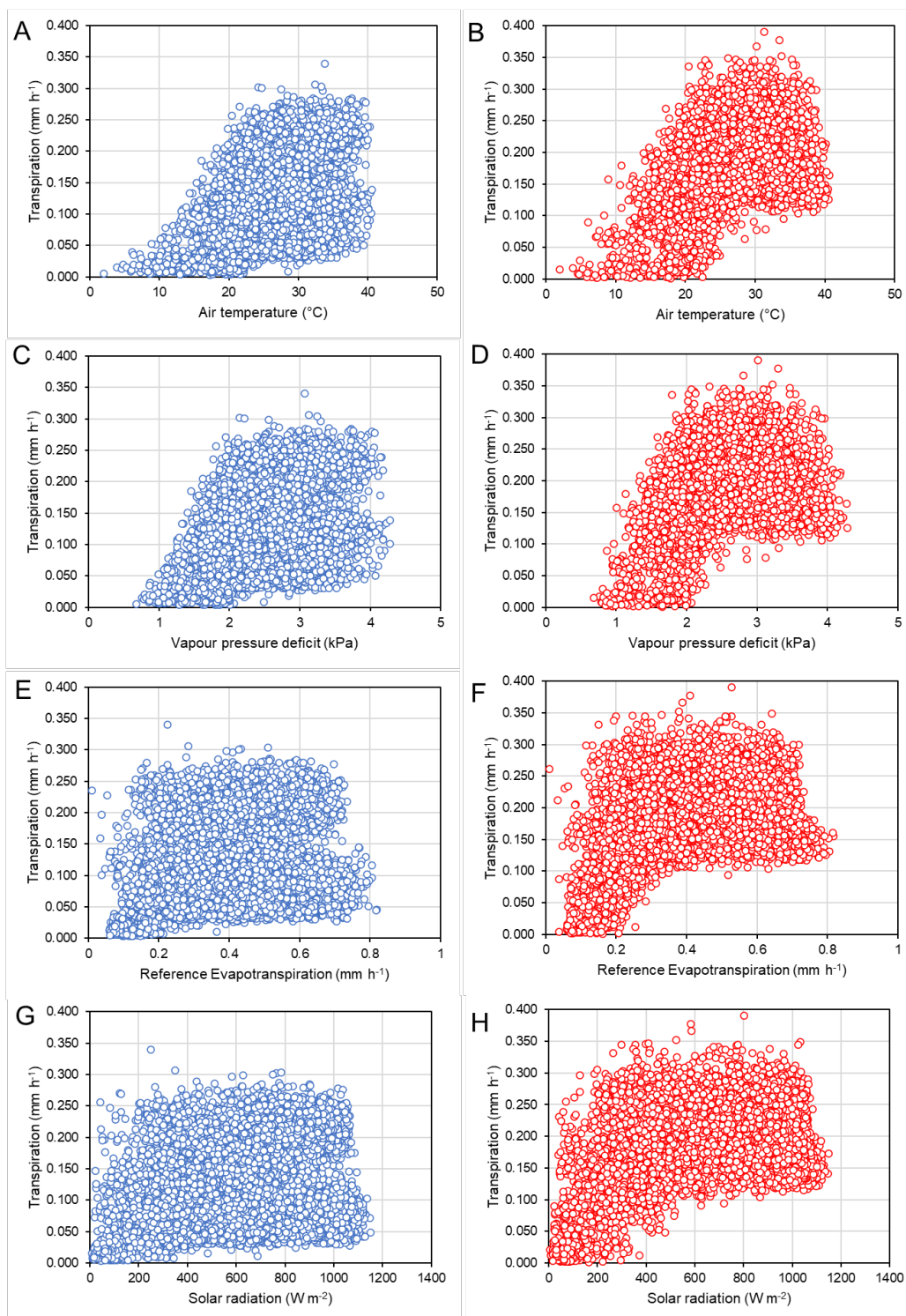


**Figure 4.18 Response of hourly transpiration of A, C, E, G) ‘Wichita’ and B, D, E, F) ‘Choctaw’ trees in Groblershoop to hourly A & B) air temperature, C & D) vapour pressure deficit, E & F) reference evapotranspiration and G & H) solar radiation. Data was for daylight hours (08:00 to 17:00) from November to April each season**

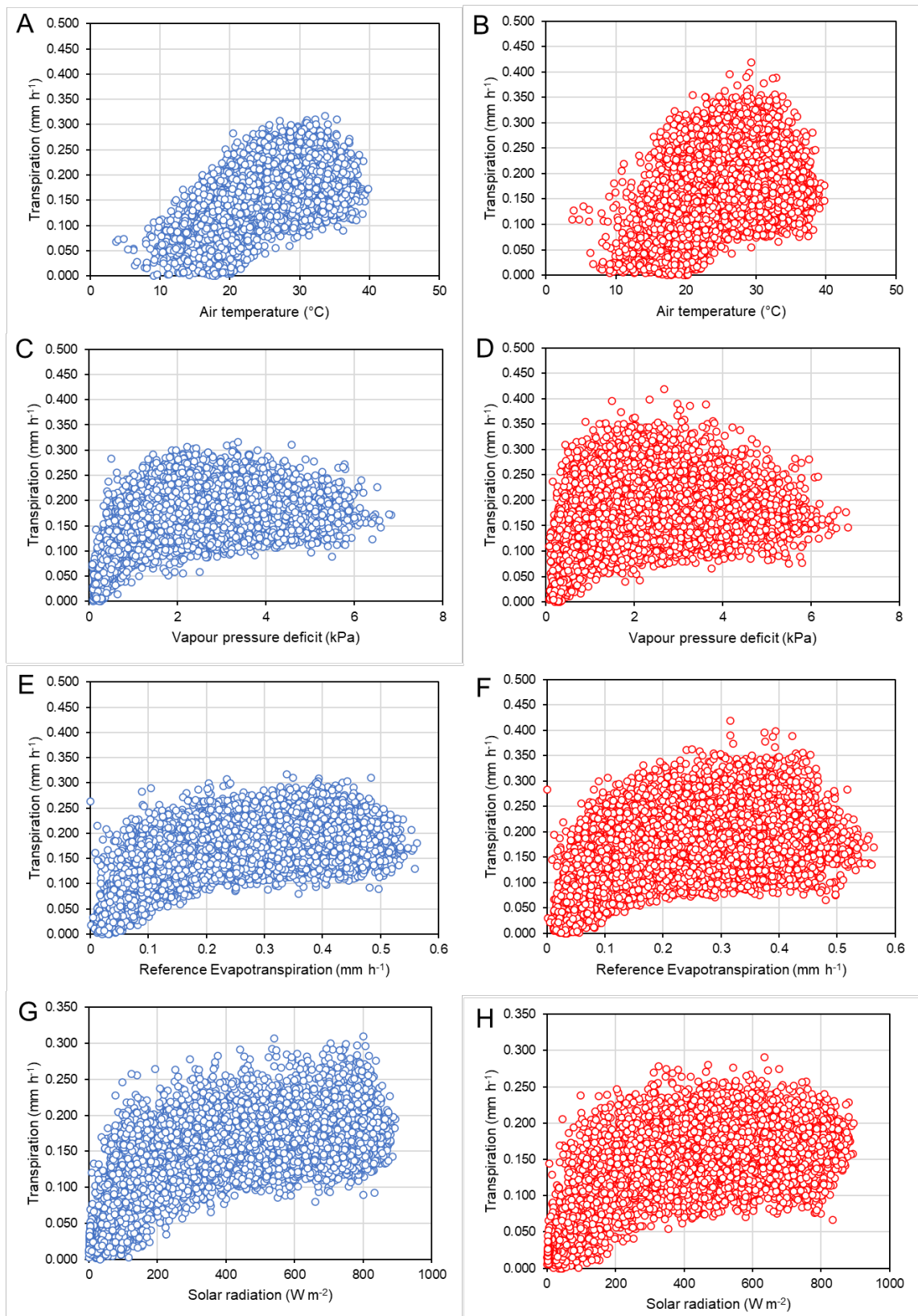


**Figure 4.19** Response of hourly transpiration of A, C, E, G) 'Wichita' and B, D, E, F) 'Choctaw' trees in Vaalharts to hourly A & B) air temperature, C & D) vapour pressure deficit, E & F) reference evapotranspiration and G & H) solar radiation. Data was for daylight hours (08:00 to 17:00) from November to April each season

With Figure 4.18 and Figure 4.19 showing that pecans have some form of physiological control of transpiration, the extent of this control needed to be determined. Most of the hydraulic control within the soil-plant-atmosphere continuum (SPAC) occurs through the closure of stomata, which is a crucial point in the system to limit water loss. The ability of the plant to control stomatal conductance is critical to defining the spectrum of hydraulic strategies. The hydraulic strategies of plants fall on a continuum from isohydric (strict control) to anisohydric (loose control), with very few plants occurring at each extreme (Martínez-Vilalta et al., 2014). Isohydric plants have strict control of stomatal closure to maintain plant water status and will commonly limit gaseous exchange to avoid drought stress, whilst anisohydric plants have loose control over stomatal conductance and do not maintain plant water status. Isohydric control is defined as the ability of the plant to maintain a minimum midday leaf water potential ( $\Psi_{md}$ ), whereas anisohydric control characteristically reaches more negative  $\Psi_{md}$  as they experience drier soils conditions and under high evaporative demand (Sperry and Hacke, 2002).

When comparing diurnal trends in leaf water potential ( $\Psi_L$ ) from 'Wichita' trees for seven days in Groblershoop, we can see that there is a considerable variation in minimum  $\Psi_L$ , whilst the trees experienced limited variation in the predawn water potential ( $\Psi_{pd}$ ) of the trees (Figure 4.20). The trees experienced days with the highest evaporative demand in December 2021 when  $\Psi_L$  at midday was -1.89 MPa, whilst experiencing the lowest evaporative demand in March 2022 and May 2022 when  $\Psi_L$  midday was -1.18 MPa and -0.89 MPa, respectively. A similar trend in changing  $\Psi_L$  was evident for each day. The  $\Psi_L$  was highest before dawn and decreased until midday when a minimum was reached. From midday, the  $\Psi_L$  began to increase as transpiration was stabilised by reduced  $g_s$  and evaporative demand decreased. Measurements of  $\Psi_L$  did not take place later than 16:00 due to the lack of sun leaves because the trees to the North within the orchard shaded the leaves within reach from the ground. Variation in daily trends could be attributed to the different phenological stages and different environmental conditions on the day. However, it is clear that midday  $\Psi_L$  varied considerably depending on prevailing conditions.

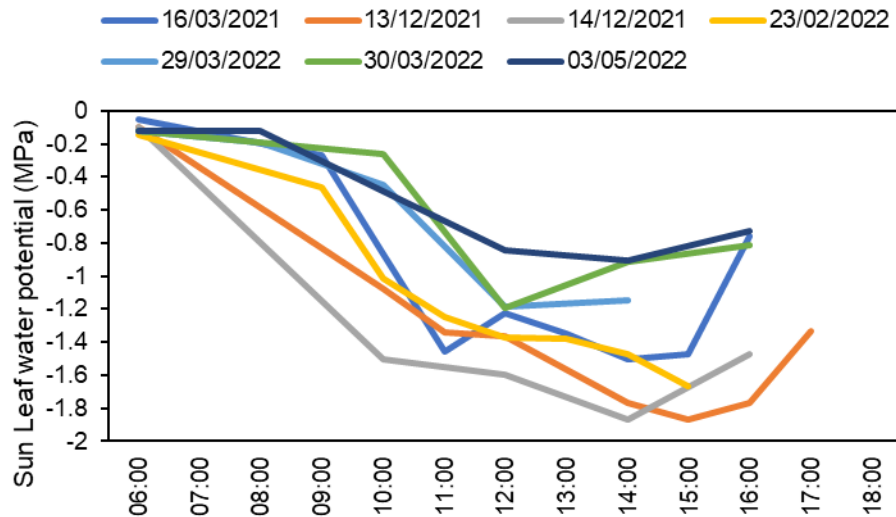


**Figure 4.20 Comparison of diurnal sun leaf water potential collected over the 2020/21 and 2021/22 growing seasons in Groblershoop.**

In order to try and determine the cause of the varying  $\Psi_L$  values at midday over the course of the season, the days with the most negative  $\Psi_L$  (14 December 2021) and the least negative  $\Psi_L$  values (3 May 2022) were chosen, and conditions on each day were compared, which included air temperature ( $T_{air}$ ),  $R_s$ , VPD,  $T$  and compared to stomatal conductance ( $g_s$ ) and  $\Psi_L$  (Figure 4.21).  $T_{air}$  and VPD for 14 December 2021 were higher (31.9°C and 3.10 kPa) than the values observed on 3 May 2022 (27.4°C and 2.56 kPa), which impacted evaporative demand (Figure 4.21B & C). Reference evapotranspiration was 7.33 mm on 14 December 2021 and 2.58 on 3 May 2022, which partly resulted from higher  $R_s$  in December than May. Maximum  $R_s$  on 14 December 2021 was 1081 W m<sup>-2</sup>, whilst on 3 May 2022 maximum  $R_s$  was 661 W m<sup>-2</sup> (Figure 4.21A). Although there was no difference in  $\Psi_{pd}$ , there was a considerable difference in  $\Psi_L$  at midday, with  $\Psi_L$  dropping to -1.9 MPa on 14 December 2021, but on 3 May 2022  $\Psi_L$  only decreased to -0.9 (Figure 4.21D). The difference  $\Psi_L$  is reflected in the difference in  $g_s$ , with higher  $g_s$  resulting in lower  $\Psi_L$  possibly due to higher water loss from the leaf. The difference in  $g_s$  could have been impacted by the lower  $R_s$  on 3 May as, as stomatal opening was affected by light intensity (Roelfsema and Hedrich, 2005).

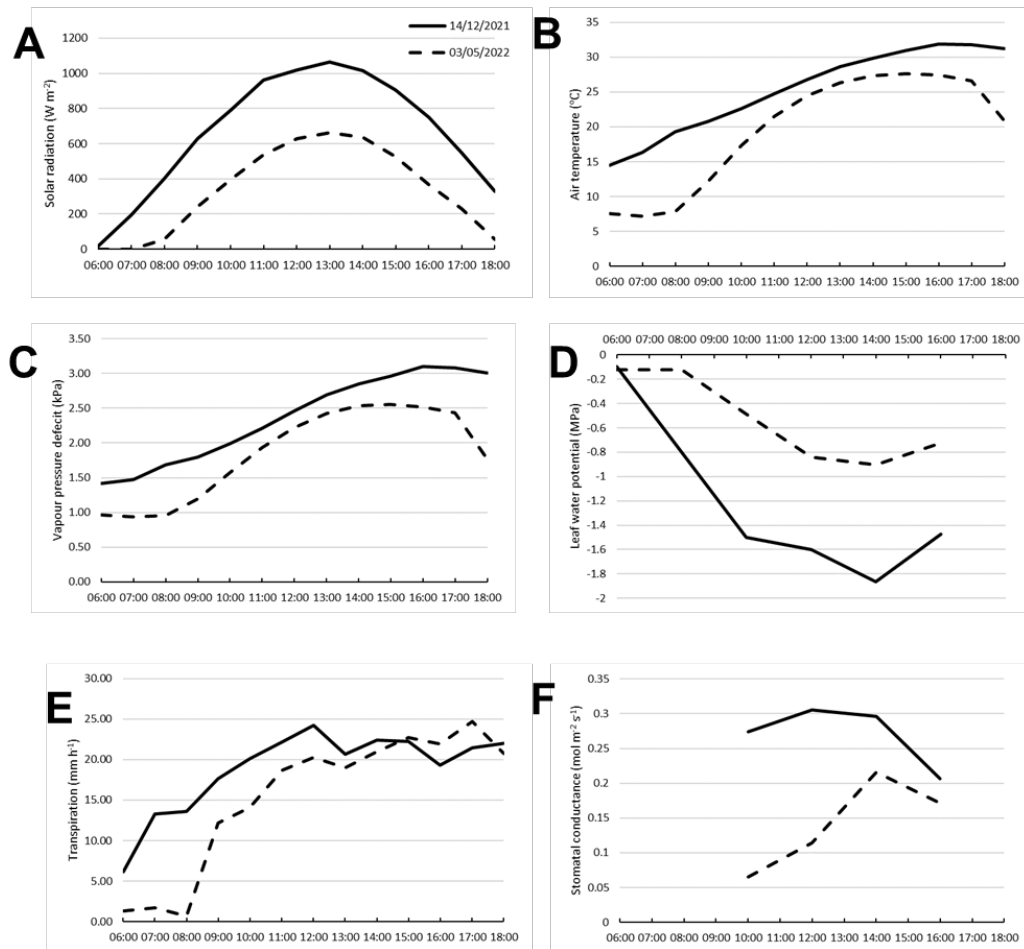


**Figure 4.21 Comparison of daily variation in A) solar radiation, B) air temperature, C) vapour pressure deficit, D) water potential, E) transpiration and F) stomatal conductance in ‘Wichita’ trees in Groblershoop from 06:00 to 18:00 on 14/12/2021 (black line) and 03/05/2022 (dotted line).**

The maximum  $g_s$  on 3 May was  $0.22 \text{ mol m}^{-2} \text{ s}^{-1}$ , as compared to  $0.31 \text{ mol m}^{-2} \text{ s}^{-1}$  on 14 December. Although  $\Psi_L$  differed between the two days, the trend for  $T$  is similar, and only slightly higher transpiration occurred on 14 December (2.99 mm) as compared to 5 May (2.79 mm). The timing of data collection could also have impacted the results as 5 May coincided with the start of shuck dehiscence and senescence, which may have caused the older leaves to behave differently from the mid-season leaves in December. These results suggest that pecans may tend to be slightly isohydric due to the variation in  $\Psi_L$  at midday, which depended on prevailing weather conditions. The small difference between  $T$  on two very contrasting days does suggest some form of control over transpiration.

One method used to quantify the hydraulic strategy of a plant is described by Martínez-Vilalta et al. (2014). The theoretical framework makes use of  $\Psi_{pd}$ , which is a measure of soil water



potential ( $\Psi_s$ ) and midday sun leaf water potentials ( $\Psi_{md}$ ). Martínez-Vilalta et al. (2014) described the response of  $\Psi_{md}$  and  $\Psi_{pd}$  as linear with the equation:

$$\Psi_{md} = \sigma\Psi_{pd} + \Lambda \quad (61)$$

Where  $\sigma$  is the slope of the line and  $\Lambda$  is the y-intercept (it is the maximum pulling capacity of the plant when the soil is saturated). In this framework,  $\sigma$  is used to determine the hydraulic strategy. If  $\sigma = 0$ , the plant is strictly isohydric, whilst if  $\sigma = 1$  the plant is strictly anisohydric. If  $0 < \sigma < 1$ , the plant is partially isohydric. To determine the hydraulic strategy,  $\Psi_{pd}$  values were compared to the corresponding  $\Psi_{md}$  for the stressed and non-stressed 'Wichita' trees at the Innovation Africa pecan orchard (Figure 4.22). This site was chosen due to the availability of lower  $\Psi_{pd}$  in the stress trial, and this was not the case over the past season, where excessive rain proved problematic and prevented stress from occurring. Stressed trees were seen to be more stressed than the control, but this stress was not significant ( $\Psi_{pd} < -0.42$  MPa).

A  $\sigma$  of 0.6153 puts pecan trees in the category of partial isohydry, with pecans having partial isohydry means that with increased drought conditions, the difference between  $\Psi_{md}$  and  $\Psi_{pd}$  decreases with decreasing  $\Psi_{pd}$ . The intercept ( $\Lambda$ ) was -1.5567 MPa, and the maximum transpiration rate per unit of water transport capacity at  $\Psi_s$  is 0. Further data is needed under more extreme water stress conditions to improve the graph's accuracy.  $\Psi_L$  values have a large variation due to several different factors influencing the value, which include the age of the leaf, the amount of time that the leaf has been exposed to the sun, the angle that the leaf is sitting at as well as the which side of the canopy the leaf is located on (Jones and Cumming, 1984).

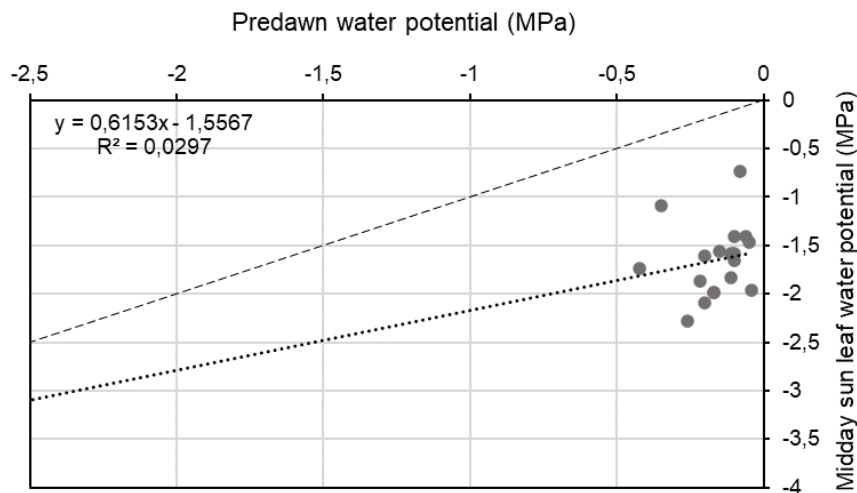


**Figure 4.22 Relationship between predawn water potentials and midday sun leaf water potentials. Data from both stressed and non-stressed 'Wichita' trees in Pretoria. The dotted line depicts the 1:1 line.**



When comparing  $\Psi_{pd}$  and midday stomatal conductance ( $g_{smd}$ ) from the stressed and non-stressed trees at the Innovation Africa@UP orchard, a non-significant trend was observed (Figure 4.23). An increased sample of  $\Psi_{pd}$  under more drought-stressed conditions is needed to observe how pecans regulate stomatal conductance in response to low soil water potentials. When the  $\Psi_L$  and corresponding  $g_{smd}$  values are compared, a non-significant trend was observed (Figure 4.24). Again, a wide variation in the data suggests that more data from stressed conditions is needed to draw an accurate conclusion on how pecan  $\Psi_L$  influences  $g_c$ . It is predicted that as  $\Psi_L$  decreases,  $g_s$  will decrease to reduce the loss of water through the stomata and thus increase or maintain  $\Psi_L$ .

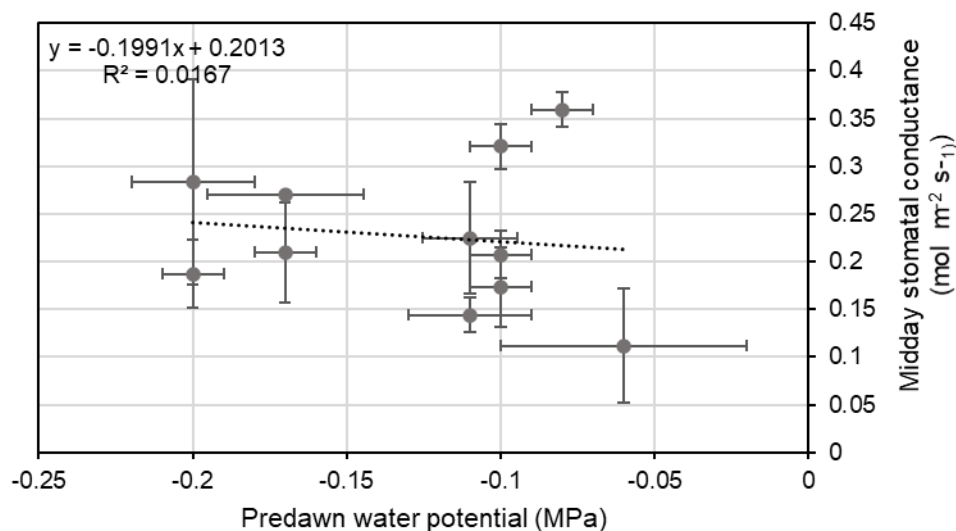


**Figure 4.23 Response of midday stomatal conductance to predawn water potential in 'Wichita' trees in Pretoria at Innovation Africa@UP**

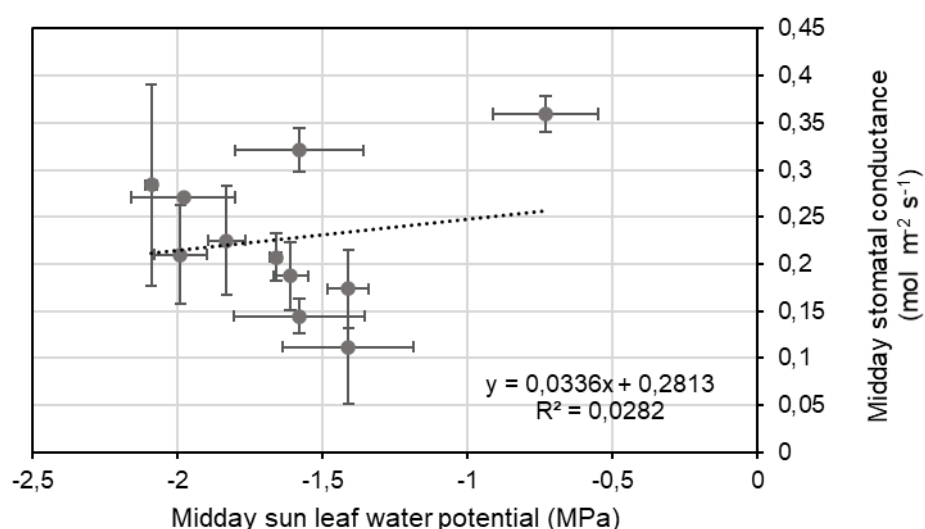


**Figure 4.24 Relationship between stomatal conductance and midday sun leaf water potential in 'Wichita' trees in Pretoria at Innovation Africa@UP**

Physiological control of transpiration by pecans, as with many other plants, is complicated, but it has been shown that trees do have control of transpiration. This control is seen to have partial isohydric characteristics, demonstrating that pecans limit the loss of water and as a result are able to control plant water status, by preventing  $\Psi_L$  from dropping to levels that could cause damage to the xylem. Further data under water-limited conditions are required to improve our understanding of how pecans control transpiration and leaf water potentials.

#### **4.1.5 IRRIGATION AND SOIL WATER CONTENT**

Irrigation, soil water content and the depth of the water table were monitored throughout the course of the study to aid in the assessment of possible soil water deficits or saturated conditions, which would have impacted tree water use. The aim was to measure unstressed water use or the maximum water use of orchards in order to accurately parameterise models and provide growers with the upper limit of water use. Cumulative transpiration, ET, ETo and rainfall + irrigation were determined for each season in the Vaalharts (Figure 4.25) and Groblersdal orchard (Figure 4.26). Unfortunately, irrigation was measured with manual water meters, resulting in readings only taken during visits to the site. As not all visits were at regular intervals, there are often sudden large increases in rainfall + irrigation at these points. However, it does allow for good comparison at the end of the season and when combined with soil water content data allows for an assessment of soil water conditions throughout the season. Evapotranspiration data is missing from the first season at each site (Figure 4.25A and Figure 4.26A) due to the unavailability of Eddy Covariance equipment until the second season at each site.

In all five seasons at Vaalharts irrigation + rainfall exceeded transpiration of both ‘Wichita’ and ‘Choctaw’ trees. In the 2019/20 season rainfall + irrigation closely matched ET, suggested well managed irrigation, but due to unusually high rainfall in 2020/21 (Figure 4.25C) and 2021/22 (Figure 4.25D) rainfall + irrigation exceeding ET quite considerably and even exceeded seasonal ETo. In the 2021/22 season yield may have been impacted by too much water during January and February, which was reflected in reduced yields in this season. In the final season (2022/23) rainfall + irrigation was closer to ET (Figure 4.25), due to rainfall being closer to the long term average.

A similar trend was observed in Groblershoop, but rainfall and irrigation were much closer to ET than in Vaalharts, especially in the 2020/21 (Figure 4.26B) and 2021/22 (Figure 4.26C)

seasons. Once again this suggests judicious irrigation scheduling in the orchard, with no obvious soil water deficits which could have impacted water use.

Profile water content was determined for the Vaalharts (Figure 4.27) and Groblershoop (Figure 4.28) orchards in order to assess plant available water in the root zone throughout each season for the pecan trees. The whole area allocated to a tree was considered. From root profile studies (data not shown) it was determined that the rooting depth was 75 cm and this is where the majority of water uptake by roots took place. In Vaalharts, soil water remained mostly above permanent wilting point, except in December 2018 and January 2019. In this region growers will often allow the soil to dry out in December and early January to allow room for rain, which typically only start in January. The trees could have experienced a degree of water stress during this time. Unfortunately, no water potential measurements were made over this time. However, for the vast majority of the study trees were unlikely to experience significant stress. In the 2019/20, 2020/21 and 2021/22 profile soil water content approached and at times exceeded the estimated field capacity. This was particularly noticeable in the 2020/21 season when over 300 mm of rain was recorded in December and January. At the end of each season there was a clear drying out of the profile as the trees senesced and irrigation is halted due to nuts lying on the ground.

In Groblershoop, profile water content did not fall below the permanent point at any time on the study, indicating the unlikeliness of stress in the orchard during the study (Figure 4.28). The sudden increases in profile soil water content in the 2019/20 and 2020/21 seasons were due to an increase in irrigation during the hottest times of the year when canopy cover was at a maximum (Figure 4.28A and B). The large increase in VWC in the 2021/22 season were largely caused by heavy rainfall events, with over 100 mm received in a single event in late January 2022. As with Vaalharts, the drying out of the profile late in the season was very noticeable.

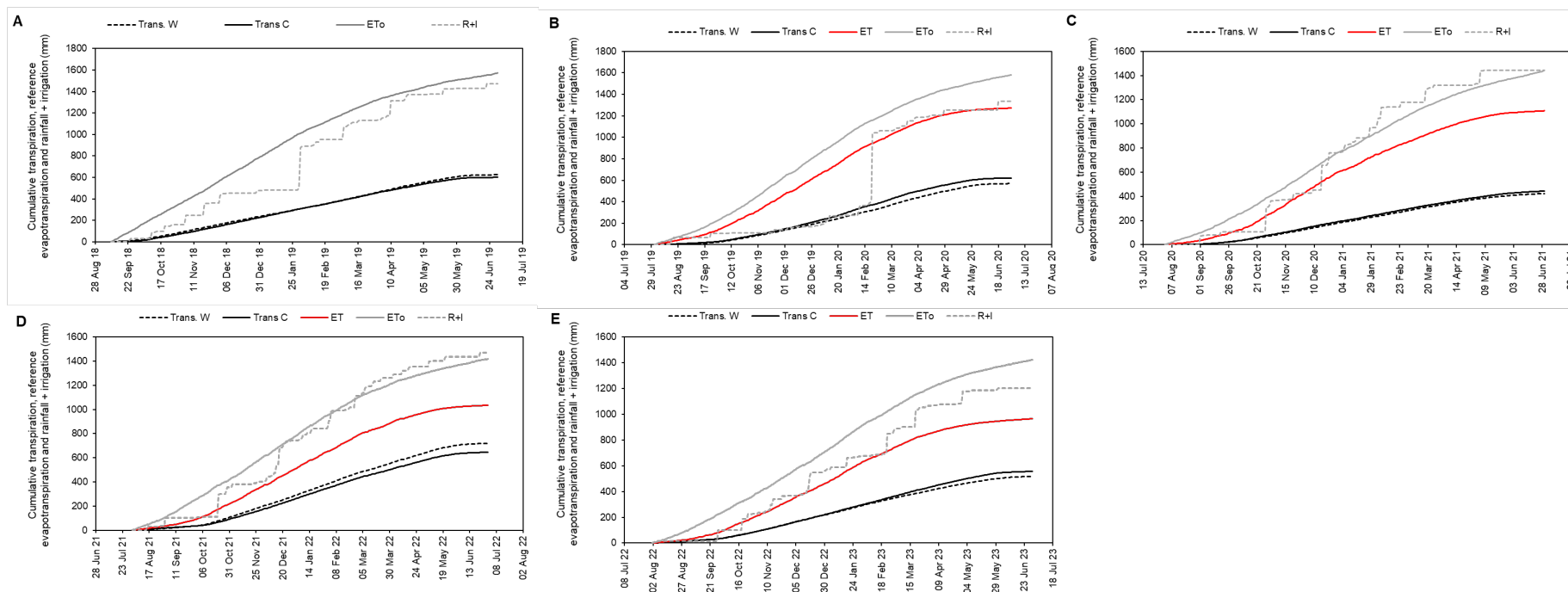


**Figure 4.25 Cumulative transpiration of 'Wichita' (Trans. W) and 'Choctaw' (Trans. C) trees, evapotranspiration (ET), reference evapotranspiration (ET<sub>0</sub>) and rainfall + irrigation (R+I) for the A) 2018/18, B) 2019/20, C) 2020/21, D) 2021/22 and E) 2022/23 seasons in Vaalharts.**

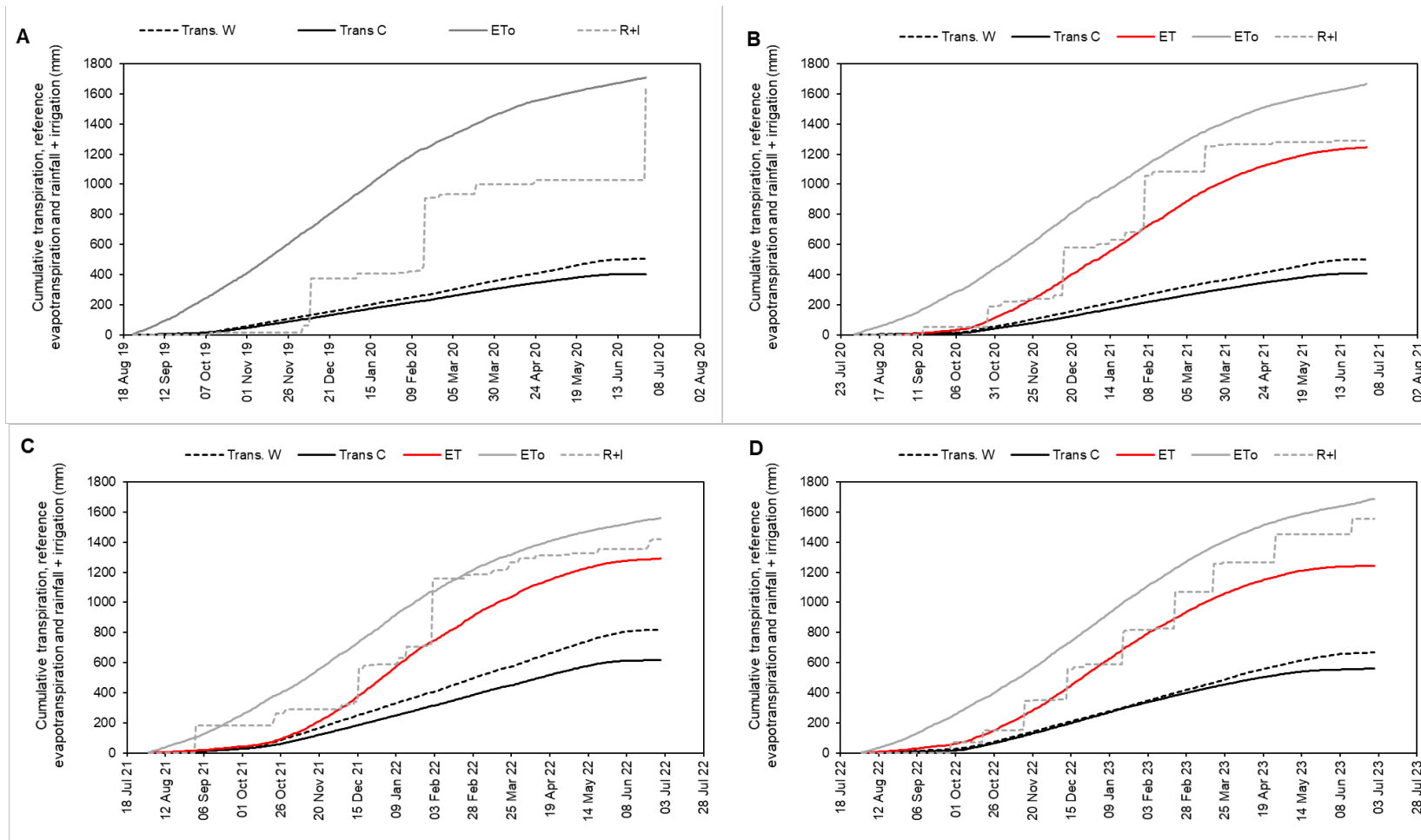


**Figure 4.26** Cumulative transpiration of 'Wichita' (Trans. W) and 'Choctaw' (Trans. C) trees, evapotranspiration (ET), reference evapotranspiration (ET<sub>o</sub>) and rainfall + irrigation (R+I) for the A) 2019/20, B) 2020/21, C) 2021/22 and D) 2022/23 seasons in Groblershoop

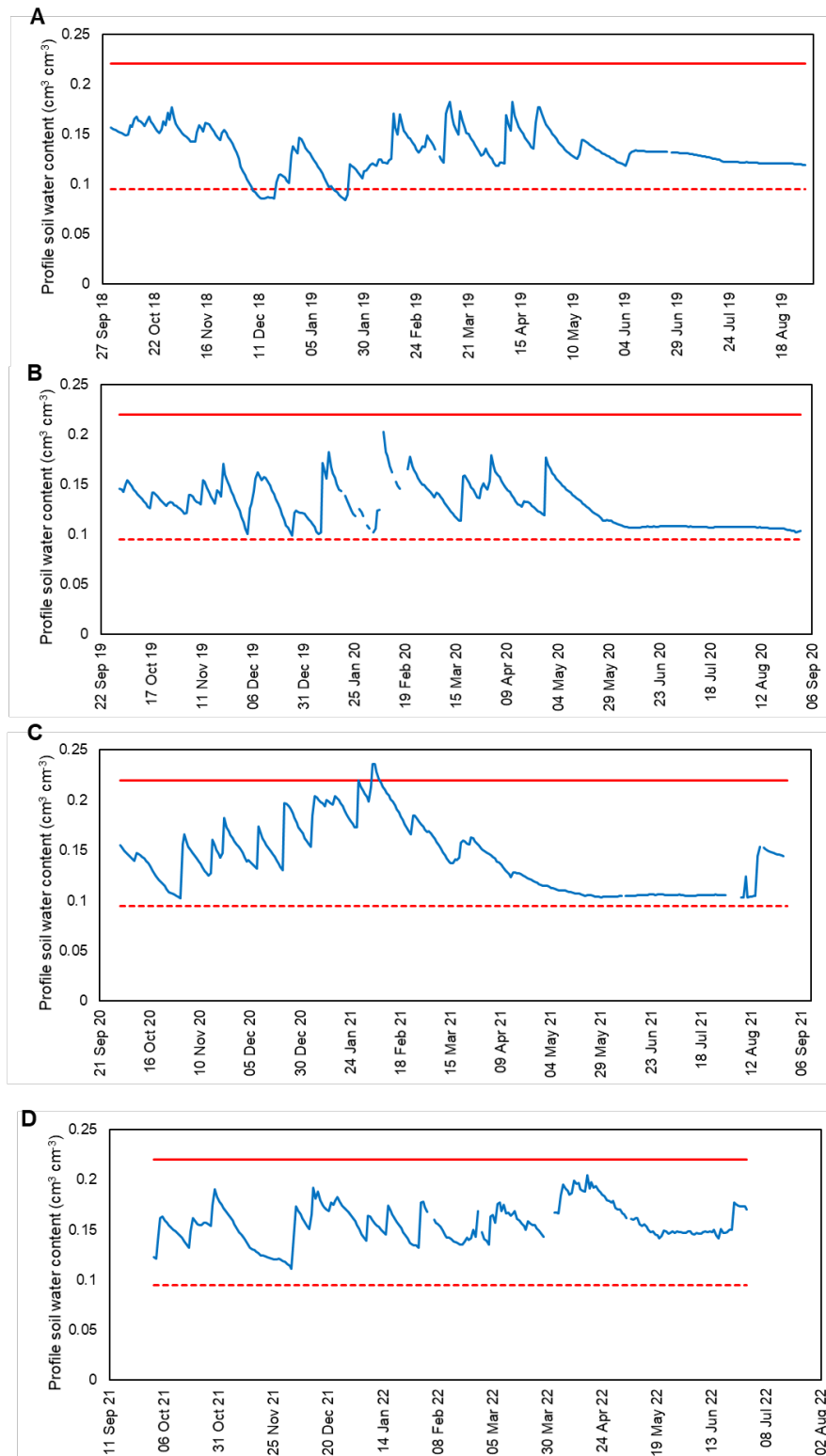


**Figure 4.27** Daily profile water content for the root zone (0-75 cm) for the Vaalharts site for the A) 2018/29, B) 2019/20, C) 2020/21 and D) 2021/22 seasons. The solid red line indicates field capacity and the dotted line permanent wilting point, as determined from soil texture and assessing drainage after large rainfall events. Plant available water lies between these two lines. Daily volumetric soil water content was taken at 5:00, when maximum water uptake for the day had taken place. Sensors were removed at the end of the 2021/22 season.

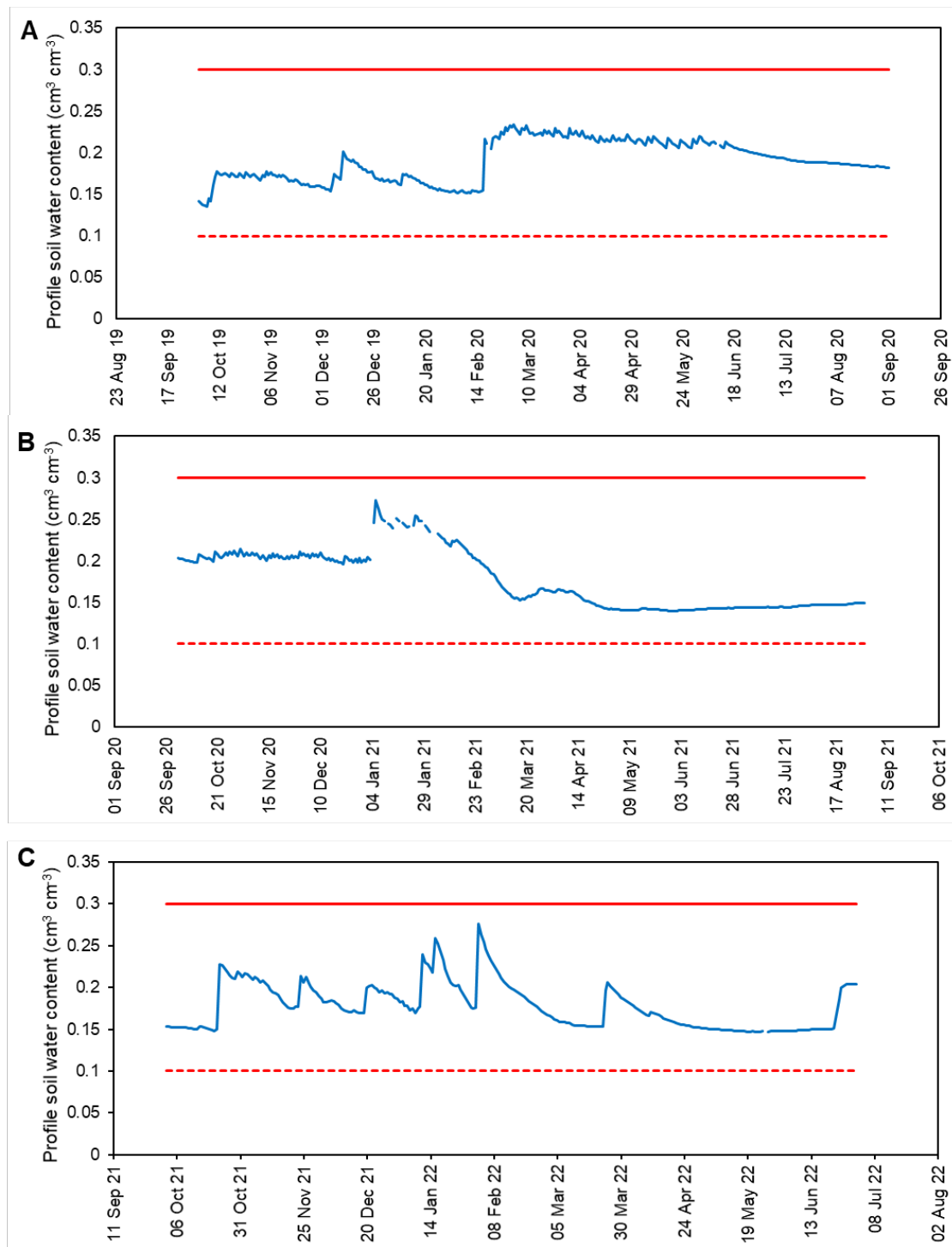


**Figure 4.28** Daily profile water content for the root zone (0-75 cm) for the Groblershoop site for the A) 2019/20, C) 2020/21 and D) 2021/22 seasons. The solid red line indicates field capacity and the dotted line permanent wilting point, as determined from soil texture and drainage following large rainfall events. Plant available water lies between these two lines. Daily volumetric soil water content was taken at 18:00, when maximum water uptake for the day had taken place and because the grower irrigated at night. Sensors were removed at the end of the 2021/22 season.

Piezometer readings to determine the depth of the water table below the soil surface were routinely taken throughout three of the five seasons. In the 2018/19 season in Vaalharts the water table remained close to 2 m from the soil surface (Figure 4.29A), with a similar trend assumed in the 2019/20 season due to very similar rainfall. However, in the 2020/21 season rainfall increased in Vaalharts and the water table was assumed to have risen. This was confirmed by measurements in the 2021/22 season when the water table varied between 1.2 and 1.6 m from the soil surface (Figure 4.29B) and high rainfall was received during the season. This could have impacted the trees by created anaerobic conditions in the soil where roots are found. In the 2022/23 season in Vaalharts the water table rose as the rains began to within 1.6 m of the soil surface (Figure 4.29C), but due to lower rainfall, the water table did not reach the levels of the 2021/22 season and was unlikely to impact plant physiological performance.

At the start of the trial in Groblershoop there was no signs of the water table within 3 m of the soil surface. This situation likely persisted throughout the 2019/20 and 2020.21 seasons due to low rainfall. However, in 2021/22 rainfall was extremely high for the season and by February 2022 the water table was within 1.3 m of the soil surface (Figure 4.29B). This was also attributed to flooding of the Orange River in late January. This high water table was maintained for the rest of the season and could have had an impact on plant physiological performance. However, rainfall was significantly lower in the 2022/23 season and the water table never came within 2 m of the soil surface (Figure 4.29C). There was a slight rise once again due to flooding of the Orange River in December.



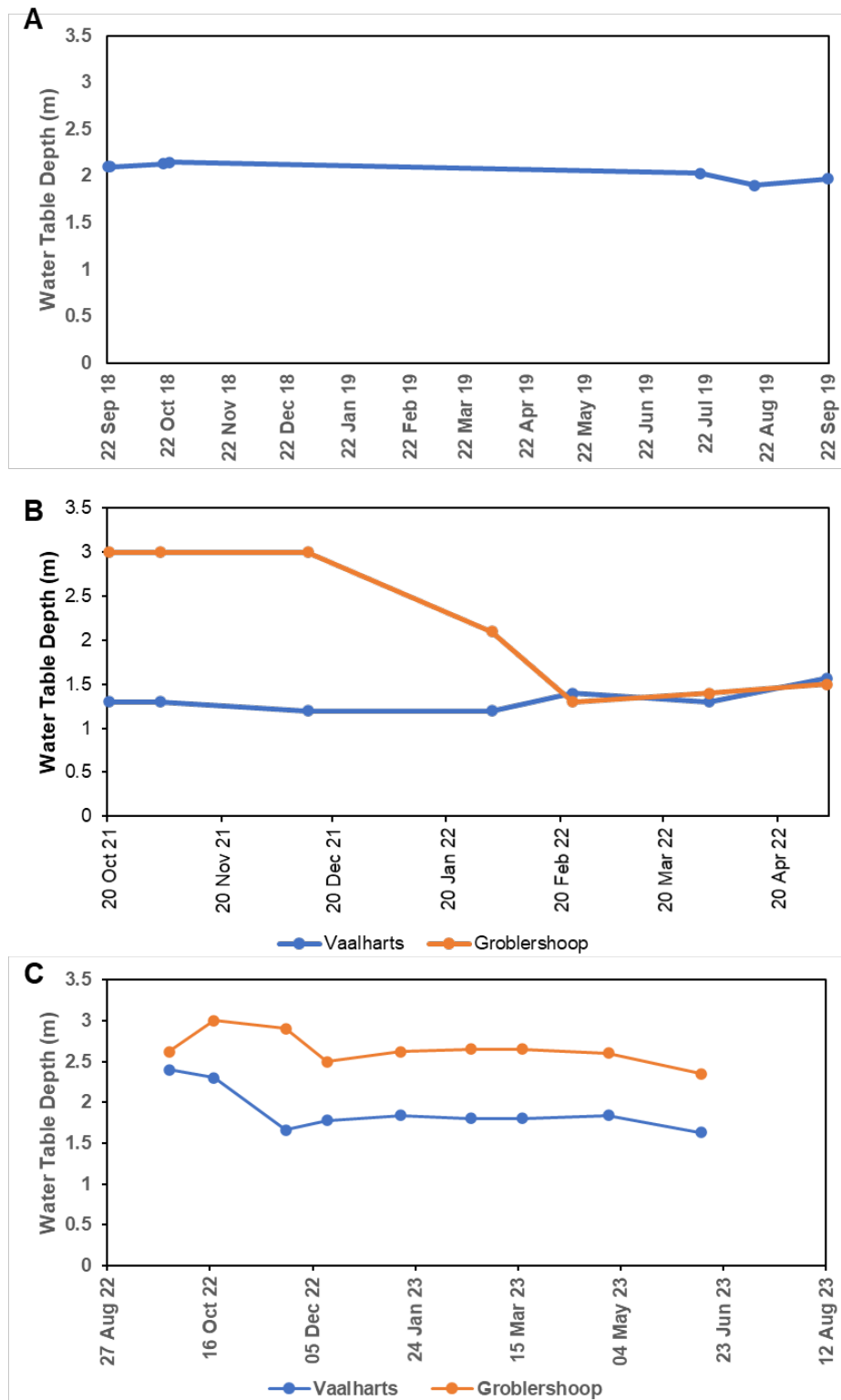


**Figure 4.29** Depth of the water table in the pecan orchards in A) Vaalharts in the 2018/19 season, B) Vaalharts and Groblershoop in the 2021/22 season and C) Vaalharts and Groblershoop in the 2022/23 season. Data from 2019-2021 is missing partly due to COVID lockdown restrictions.

Overall, there was very little evidence of possible water deficit stress in the two orchards throughout the course of the trial, although high water tables, resulting from high rainfall may have created saturated conditions in the Vaalharts orchard which could have impacted water use and yield in January 2021.

#### **4.1.6 SOIL EVAPORATION**

Accounting for the separate contribution of soil evaporation to evapotranspiration is critical when estimating water use in pecan orchards, from the sum of transpiration and evaporation. In order to determine the contribution of evaporation to orchard ET, measurements of soil evaporation were performed consistently over the 2021/22 and 2022/23 seasons. These measurements were used to parameterise evaporation models and data collected during the 2021/22 season was employed for the calibration of the various models. For the purpose of current report, data gathered during the 2022/23 season in Groblershoop and Vaalharts sites will be discussed.

##### *4.1.6.1 Groblershoop*

The measured seasonal change in evaporation ( $E_s$ ) for Groblershoop orchard is shown in Figure 4.30. The total  $E_s$  was relatively high at the beginning of the measurement period (October 2022), with a value of  $1.4 \text{ mm day}^{-1}$ , which then gradually decreased during the summer months as the canopy grew and a significant portion of the soil surfaces was shaded. A minimum value of  $0.2 \text{ mm day}^{-1}$  was measured in February. The spatial variation of  $E_s$  resembled the pattern of soil surface shading under the canopy throughout the season. The highest evaporation rates were recorded in the area that was wetted and exposed to radiation, followed by the wetted and shaded and dry and radiation exposed, and lastly the area that was dry and shaded. Micro-lysimeters which were positioned directly outside the dripline of the canopy, but located next to the dripper line (wetted and exposed to high radiation) recorded the highest  $E_s$  throughout the season. The weighted average  $E_s$  of wetted areas during summer at maximum canopy cover was  $0.37 \text{ mm day}^{-1}$ , whilst the dry areas recorded a value of  $0.18 \text{ mm day}^{-1}$ . Although only a part of the orchard floor was wet by the drip irrigation system, as compared to the full surface irrigation in Vaalharts, the contribution of the dry and shaded area was nearly equal to that of the wetted and shaded area in February, recording values of  $0.20 \text{ mm}$  and  $0.21 \text{ mm}$ , respectively. This highlights the significance of estimating the diurnal shaded patterns for the determination of orchard evaporation. Hence, monitoring

both hourly changes of canopy shade patterns and seasonal canopy variation is critical for water use modelling (Vélez et al., 2021).

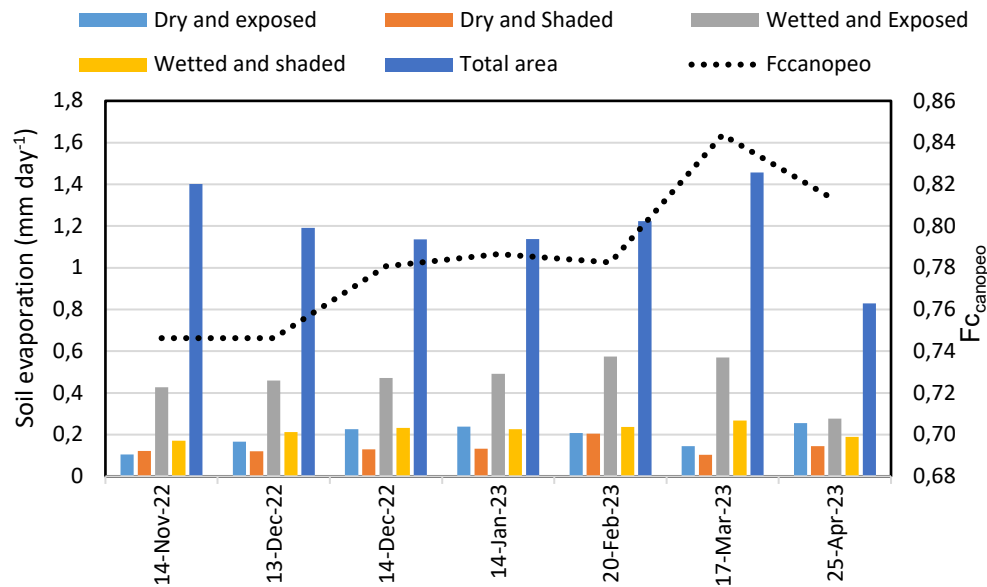


**Figure 4.30 Spatial and temporal variation of average daily soil evaporation ( $E_s$ ) (mm day<sup>-1</sup>) from micro-lysimeters throughout the 2022/23 season in the Groblershoop orchard. The fractional cover ( $fc_{canopeo}$ ) is plotted on the secondary y-axis.**

#### 4.1.6.2 Vaalharts

The change in  $E_s$  in Vaalharts during the 2022/2023 season is presented in Figure 4.31, along with the changes in canopy size. Similar to the pattern observed in Groblershoop, the highest  $E_s$  occurred at the beginning of the measurement period (November 2022), with a value of 1.5 mm day<sup>-1</sup>, which then gradual decreased during the summer months as the canopy grew and a significant portion of the soil surfaces was shaded. It reached a minimum value of 0.81 mm day<sup>-1</sup> in December 2022. As expected, the spatial variation of  $E_s$  resembled the pattern of soil surface shading under the canopy throughout the season. The highest evaporation rates were recorded in the area that was wetted and exposed to radiation, followed by the wetted and shaded and dry and radiation exposed, and lastly the area that was dry and shaded. The weighted average  $E_s$  of wetted areas during summer at maximum canopy cover was 2.1 mm day<sup>-1</sup>, whilst the dry areas 0.18 mm day<sup>-1</sup>. However, as expected  $E_s$  was higher in this macro-sprinkler irrigated orchard as compared to the drip irrigated orchard in Groblershoop.

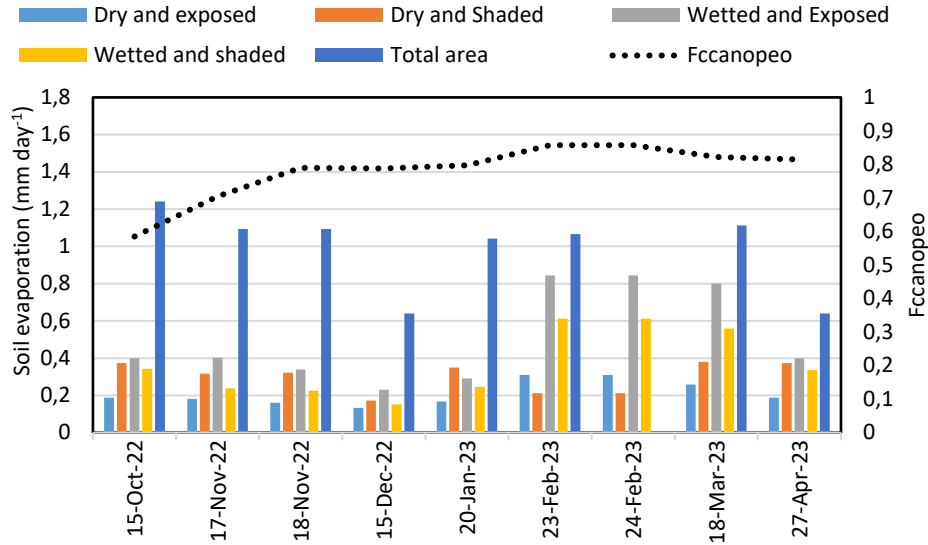


**Figure 4.31 Spatial and temporal variation of average daily soil evaporation ( $E_s$ ) (mm day<sup>-1</sup>) from micro-lysimeters in Vaalharts orchard during 2022/23 season. The fractional cover ( $f_{c_{canopeo}}$ ) is plotted on the secondary y-axis.**

#### 4.1.6.3 Modelling soil Evaporation: FAO-56 Approach

Evaporation was modelled for the pecan orchard in Groblershoop (Figure 4.32) using the FAO-56 approach. The modelled seasonal  $E_s$  trend followed the same pattern as the measured values. The highest daily  $E_s$  rates occurred in December with a maximum value of 8 mm day<sup>-1</sup>. This coincided with the high atmospheric evaporative demand during this period. The lowest values of  $E_s$  were observed in mid-January with values as low as 0.03 mm day<sup>-1</sup>, whilst the average value recorded during the season was 1.45 mm day<sup>-1</sup>. The total seasonal  $E_s$  values was 214.75 mm day<sup>-1</sup>. Although the model was able to estimate the seasonal change in  $E_s$  quite reasonably, the model was evaluated with low index statistics with MAPE =13.5%, D = 0.85, and RMSE < 0.22 mm day<sup>-1</sup>. This needs to be further evaluated and different models that can estimated the variation of  $E_s$  beneath the canopy on an hourly time stamp need to be tested. Such models include the model of Bonachela et al. (2001).

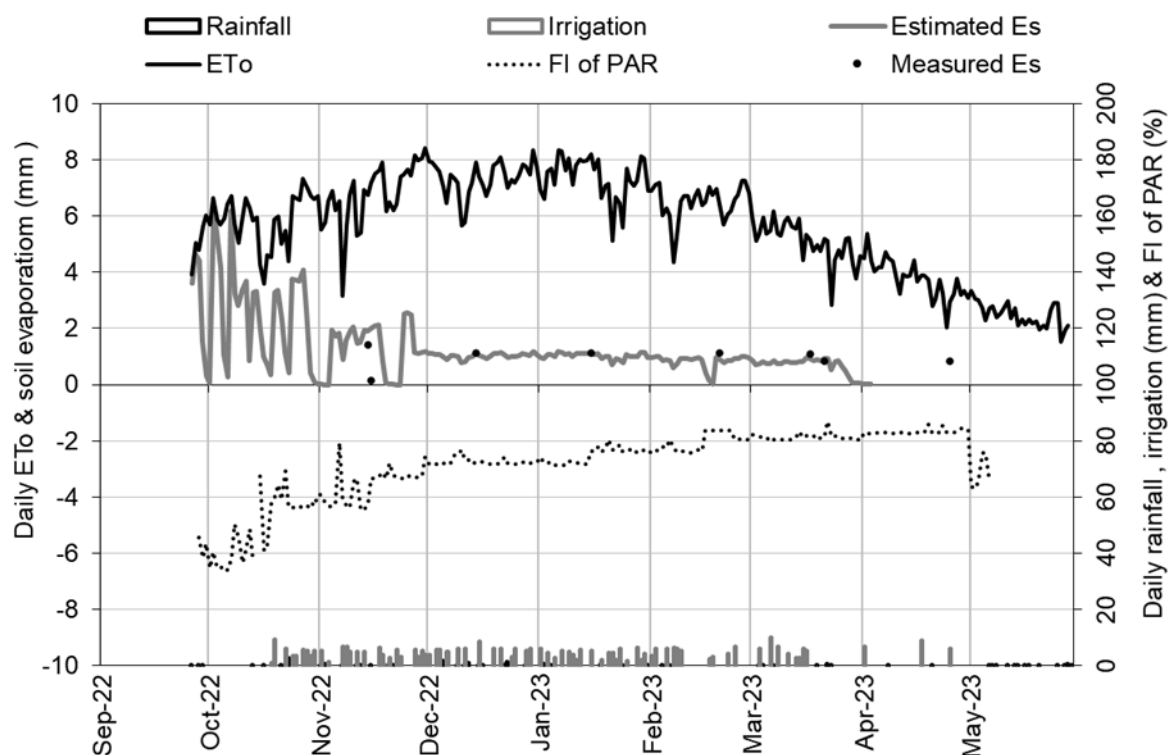


**Figure 4.32 Daily soil evaporation ( $E_s$ ) estimated using the FAO-56 dual  $K_c$  model for the (A) 2022/2023 growing seasons Groblershoop, as affected by changes in atmospheric evaporative demand ( $ET_0$ ), canopy size (estimated-FIPAR) and rainfall and irrigation events**

When evaluating the FAO-56 model for the pecan orchards in Vaalharts (Figure 4.33), the model estimated the seasonal trend reasonably well. As expected, high  $E_s$  values occurred at the beginning of the season, and similarly to the observed pattern in Groblershoop, the maximum values were  $E_s$  rates occurred in December with a maximum value of  $5.5 \text{ mm day}^{-1}$ . The lowest values of  $E_s$  were observed in mid-January with values as low as  $0.015 \text{ mm day}^{-1}$ , whilst the average value recorded during the season was  $1.6 \text{ mm day}^{-1}$ . The total seasonal  $E_s$  values was  $276.7 \text{ mm day}^{-1}$ . When evaluating the model's performance for Vaalharts orchards, low statistics indexes were observed with MAPE =13.5%, D = 0.79, and RMSE <  $0.27 \text{ mm day}^{-1}$ .

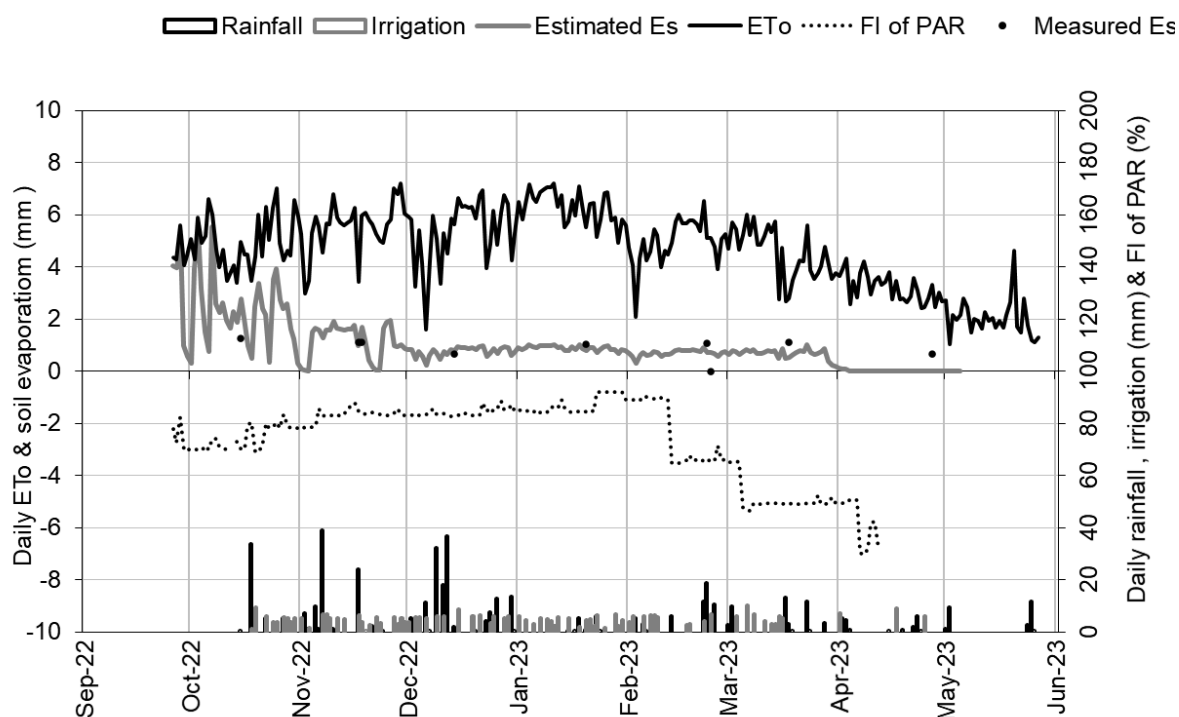


**Figure 4.33 Daily soil evaporation ( $E_s$ ) estimated using the FAO-56 dual  $K_c$  model for the (A) 2022/2023 growing seasons Groblershoop, as affected by changes in atmospheric evaporative demand ( $ET_o$ ), canopy size (estimated-FIPAR) and rainfall and irrigation events**

#### 4.1.7 CROP WATER PRODUCTIVITY

##### 4.1.7.1 Comparison of regions using transpiration and evapotranspiration

Crop water productivity, using transpiration volumes ( $WP_T$ ), varied from 0.11 to 0.93 kg m<sup>-3</sup> when considering values for both ‘Choctaw’ and ‘Wichita’ trees over five seasons in Vaalharts (Table 4.5). On average for both cultivars and over five seasons  $WP_T$  was  $0.52 \pm 0.25$  kg m<sup>-3</sup> (‘Wichita’ –  $0.55 \pm 0.19$  kg m<sup>-3</sup> and ‘Choctaw’ –  $0.48 \pm 0.32$  kg m<sup>-3</sup>). The variation over the seasons was largely as a result of differences in yield between seasons, which was particularly noticeable for ‘Choctaw’, which is known for its alternate bearing tendencies. The high values also largely reflect the high yields for the measurement trees, which on average exceeded the average for the area of 2.5 t ha<sup>-1</sup> (personal communication Hardus du Toit), except in the 2020/21 and 2022/23 seasons.

When considering Rands earned per m<sup>3</sup> of water transpired by the crop, or economic water productivity based on gross profit ( $EWP_T$ ), values varied from R8.26 to R53.04 per m<sup>3</sup> transpired. Over five years and for both cultivars  $EWP_T$  was R30.35 per m<sup>3</sup>. This value was

slightly higher for 'Wichita' ( $R32.13 \text{ m}^{-3}$ ) than 'Choctaw' trees ( $R28.58 \text{ m}^{-3}$ ) over the five years. A more in-depth analysis of crop water productivity and economic water productivity across both regions is presented in section 4.1.7.2. This analysis includes a comparison with other crops grown in each region.

Crop water productivity, using transpiration volumes ( $WP_T$ ), varied from 0.04 to  $1.41 \text{ kg m}^{-3}$  when considering values for both 'Choctaw' and 'Wichita' trees over four seasons in Groblershoop (Table 4.6). On average over both cultivars and two seasons  $WP_T$  was  $0.39 \pm 0.45 \text{ kg m}^{-3}$  ('Wichita' –  $0.61 \pm 0.57 \text{ kg m}^{-3}$  and 'Choctaw' –  $0.16 \pm 0.13 \text{ kg m}^{-3}$ ). These values suggest there was considerable variation in WUE between seasons for both 'Wichita' and 'Choctaw', which was largely a result of the large difference in yield between the four seasons. For 'Wichita' yield varied from  $71 \text{ kg tree}^{-1}$  in 2019/20 to  $6 \text{ kg tree}^{-1}$  in the 2020/21 season,  $50 \text{ kg tree}^{-1}$  in the 2021/22 season and  $19 \text{ kg tree}^{-1}$  in the 2022/23. The low yield in 2020/21 was associated with a large amount of flower drop in late October after a hail storm and late frost at the end of October. The very low  $WP_T$  values for 'Choctaw' in three of the four seasons reflect the low yields experienced in these seasons. In the third season higher yields were realised ( $4.8 \text{ t ha}^{-1}$ ), but quality was poor, with a large number of pops or poorly filled nuts, resulting in an economic yield of  $20 \text{ kg ha}^{-1}$ . In the fourth season yields for 'Choctaw' were once again very low with only  $2 \text{ kg tree}^{-1}$ . In the first season pruning contributed to lower yield, but in the second season a large amount of fruit drop occurred from late November to early January which contributed to low yield. Based on average yields for 'Choctaw' and 'Wichita' trees on the farm in Groblershoop over the past 10 years ( $1.84 \text{ t ha}^{-1}$  for 'Choctaw' and  $2.97 \text{ t ha}^{-1}$  for 'Wichita')  $WP_T$  would be on average  $0.38 \text{ kg m}^{-3}$  for 'Choctaw' and  $0.50 \text{ kg m}^{-3}$  for 'Wichita' for the three seasons of measurements.

Gross economic water productivity using transpiration volumes ( $EWP_T$ ) varied from  $R2.38 \text{ m}^{-3}$  to  $R18.74 \text{ m}^{-3}$  for the 'Choctaw' trees and  $R6.93 \text{ m}^{-3}$  to  $R103.24 \text{ m}^{-3}$  for 'Wichita' trees in Groblershoop. These changes are driven by changes in yield and quality. The average for both cultivars over the three years was  $R27.44 \pm 33.66 \text{ m}^{-3}$ . Average  $EWP_T$  was higher for 'Wichita' at  $R44.72 \pm 42.29 \text{ m}^{-3}$ , than for 'Choctaw' at  $R10.16 \pm 7.67 \text{ m}^{-3}$ .

**Table 4.5 Crop water productivity ( $WP_T$ ) and economic water productivity ( $EWP_T$ ) for the ‘Choctaw’ and ‘Wichita’ trees in an orchard in Vaalharts for the 2018/19, 2019/20, 2020/21, 2021/22 and 2022/23 seasons, based on transpiration values. Yield was adjusted to 4% moisture content.**

Season	2018/19		2019/20		2020/21		2021/22		2022/23	
Cultivar	Choctaw	Wichita	Choctaw	Wichita	Choctaw	Wichita	Choctaw	Wichita	Choctaw	Wichita
<b>Total Transpiration</b> ( $m^3\ ha^{-1}$ )	6 000	6 250	6 080	5 610	4 400	4 190	6 280	7 040	5 660	5 390
<b>Total Dry in Shell</b> <b>Nut Yield (<math>kg\ ha^{-1}</math>)</b>	2 784	4 584	5 674	3 610	1 166	2 493	4 075	3 925	645	1 294
<b>Total Gross Income</b> ( $R\ ha^{-1}$ )	213 850	296 000	322 325	193 300	73 194 <sup>#</sup>	134 949 <sup>#</sup>	184 150	202 100	46 785	96 310
<b><math>WP_T</math> (<math>kg\ m^{-3}</math>) - In</b> <b>Shell</b>	0.46	0.73	0.93	0.64	0.27	0.60	0.65	0.56	0.11	0.24
<b><math>EWP_T</math> (<math>R\ m^{-3}</math>) - In</b> <b>Shell</b>	35.60	47.37	53.04	34.45	16.65	32.24	29.34	28.73	8.26	17.86

<sup>#</sup>based on average quality for the orchard block



**Table 4.6 Crop water productivity ( $WP_T$ ) and economic water productivity ( $EWP_T$ ) for the ‘Choctaw’ and ‘Wichita’ trees in an orchard in Groblershoop for the 2019/20, 2020/21, 2021/22 and 2022/23 seasons, based on transpiration volumes. Yield was adjusted to 4% moisture content.**

Season	2019/20		2020/21		2021/22		2022/23	
Cultivar	Choctaw	Wichita <sup>#</sup>	Choctaw	Wichita	Choctaw	Wichita	Choctaw	Wichita
<b>Total Transpiration (<math>m^3</math>)</b>	4 020	5 030	4 040	4 947	6 091	8 124	5 537	6 572
<b>Total Dry in Shell Nut Yield (<math>kg\ ha^{-1}</math>)</b>	761	7 112	352	592	2 043	5 039	215	1 920
<b>Total Gross Income (<math>R\ ha^{-1}</math>)</b>	57 664	519 334	21 004	34 276	114 168	378 293	13 176	145 452
<b><math>WP_T</math> (<math>kg\ m^{-3}</math>) - In Shell</b>	0.19	1.41	0.09	0.12	0.34	0.62	0.04	0.29
<b><math>EWP_T</math> (<math>R\ m^{-3}</math>) - In Shell</b>	14.33	103.24	5.20	6.93	18.74	46.57	2.38	22.13

#### 4.1.7.2 Comparison of WP and EWP with other crops grown in the region

Data in Table 4.7 and Table 4.8 demonstrate that there was large seasonal variation in weather,  $ET_c$  and yield in both regions, and as a result  $WP_c$ ,  $WP_I$ ,  $EWP_c$  and  $EWP_I$  varied quite considerably across the four seasons in Vaalharts and three seasons in Groblershoop. Seasonal  $ET_c$  was related to seasonal  $ET_o$ , with higher  $ET_o$  and  $ET_c$  recorded in Groblershoop. Irrigation was related to rainfall, with irrigation volumes decreasing as seasonal rainfall increased. In general, there was a decline in  $ET_o$  over the measurement period due to higher rainfall experienced in the 2020/21 and 2021/22 seasons, resulting in cooler conditions. In 2022/23 in Groblershoop conditions were more typical of the region. Yield varied considerably at both sites and for all seasons from 1.4 to 3.4 t ha<sup>-1</sup> in Vaalharts and from 0.7 to 4.5 t ha<sup>-1</sup> in Groblershoop. Alternate bearing is well documented in pecan (Conner and Worley, 2000) and this could have been a contributing factor. However, in the 2021/21 season in Groblershoop late frost and hail resulted in significant nut drop in December resulting in very low yields for the season. As a result of the large variation in yield,  $WP_c$  varied between 0.05 and 0.37 kg m<sup>-3</sup>, whilst  $WP_I$  varied between 0.01 and 0.77 kg m<sup>-3</sup>. If average yields for both regions were considered (~2.5 t ha<sup>-1</sup>, based on long term yield data), together with average  $ET_c$  for the measurement seasons, then  $WP_c$  was 0.24 kg m<sup>-3</sup> for Vaalharts and 0.20 kg m<sup>-3</sup> for Groblershoop. These values are in line with published  $WP_c$  for pecans of between 0.15 and 0.31 kg m<sup>-3</sup> in USA and South Africa (Ibraimo et al., 2016, Miyamoto, 1990, Sammis et al., 2004c). If average irrigation was considered (in a normal rainfall year) together with average yields then  $WP_I$  was 0.30 kg m<sup>-3</sup> for Vaalharts and 0.18 kg m<sup>-3</sup> for Groblershoop. The higher values for Vaalharts were due to the higher summer rainfall volumes in this region as compared to Groblershoop. These results demonstrate that  $WP_c$  estimates for a single season can be very misleading, and depending on the season, under- or overestimates could result depending on whether it is an “on” or “off” year. Weather conditions also play a role and in hotter and drier regions,  $ET_c$  and irrigation is likely to be higher for the same crop resulting in lower  $WP_c$  and  $WP_I$ . Orchard conditions including canopy cover, pruning strategy, irrigation system and seasonal rainfall will also influence  $ET_c$  and therefore the  $WP_c$ , which needs to be considered if a single benchmark for  $WP_c$  is required (Katerji et al., 2008, Fereres et al., 2017). Fereres et al. (2017) suggested that when comparing production regions that differ in climate some procedure should be used for normalization by  $ET_o$ . If seasonal  $ET_c$  is divided by  $ET_o$  (a seasonal crop coefficient ( $K_c$ )) and the average 2.5 t ha<sup>-1</sup> is used as the numerator, then a value of 0.31 is obtained for Vaalharts and 0.33 for Groblershoop (the units are debatable).

As a result of the large variation in yield from year to year,  $EWP_c$  also showed considerable variation (Table 4.7 and Table 4.8). Values for the two orchards varied from no profit to

R21.99 m<sup>-3</sup>, with an overall average of R8.83 m<sup>-3</sup>. When considering the Rands earned per m<sup>3</sup> of irrigation water, higher values were realised and these values varied between no profit and R48.05 per m<sup>-3</sup>. The average for EWP<sub>I</sub> was R15.71 per m<sup>3</sup>.

**Table 4.7. Reference evaporation, evapotranspiration and water productivity indicators for the pecan orchard in Vaalharts (1 September to 30 June growing season).**

Season	2019/20	2020/21	2021/22	2022/23
Reference evapotranspiration (mm)	1480	1350	1310	1330
Total Evapotranspiration (m <sup>3</sup> )	12 127	10 742	10 010	9 370
Irrigation (m <sup>3</sup> )	9 191	8 008	6 388	7 396
Rainfall (m <sup>3</sup> )	4 730	6 780	8 050	4 490
Total In - Shell Nut Yield (kg ha <sup>-1</sup> )	2888	1829	3410	1 486
Total Gross Income (R ha <sup>-1</sup> )	179 100	104 071	242 110	114 405
Production cost (R)	47 995	47 687	63 411	59 282
WP <sub>c</sub> (kg m <sup>-3</sup> ) - In Shell	0.24	0.17	0.34	0.16
WP <sub>I</sub> (kg m <sup>-3</sup> ) - In Shell	0.31	0.23	0.53	0.20
EWP <sub>c</sub> (R m <sup>-3</sup> ) - In Shell	10.81	5.24	17.86	5.88
EWP <sub>I</sub> (R m <sup>-3</sup> ) - In Shell	19.49	7.04	27.97	7.45

WP<sub>c</sub> – crop water productivity, WP<sub>I</sub> – irrigation water productivity, EWP<sub>c</sub> – economic crop water productivity, EWP<sub>I</sub> – economic irrigation water productivity

**Table 4.8 Reference evaporation, evapotranspiration and water productivity indicators for the pecan orchard in Groblershoop (1 September to 30 June growing season)**

Season	2020/21	2021/22	2022/23
Reference evapotranspiration (mm)	1560	1460	1580
Total Evapotranspiration (m <sup>3</sup> )	12 459	12 838	12 214
Irrigation (m <sup>3</sup> )	12 043	5 843	14 567
Rainfall (m <sup>3</sup> )	1 770	6 580	980
Total In - Shell Nut Yield (kg ha <sup>-1</sup> )	752	4 510	668
Total Gross Income (R ha <sup>-1</sup> )	44 939	344 175	58 242
Production cost (R)	47 6875	63 411	59 282
WP <sub>c</sub> (kg m <sup>-3</sup> ) - In Shell	0.06	0.37	0.05
WP <sub>i</sub> (kg m <sup>-3</sup> ) - In Shell	0.06	0.77	0.01
EWP <sub>c</sub> (R m <sup>-3</sup> ) - In Shell	No profit	21.99	No profit
EWP <sub>i</sub> (R m <sup>-3</sup> ) - In Shell	No profit	48.05	No profit

WP<sub>c</sub> – crop water productivity, WP<sub>i</sub> – irrigation water productivity, EWP<sub>c</sub> – economic crop water productivity, EWP<sub>i</sub> – economic irrigation water productivity

Average ET and yield estimates for annual crops in Vaalharts and raisin grapes in Groblershoop used for WP<sub>c</sub> estimates are provided in Table 4.9.

**Table 4.9. Average evapotranspiration (ET<sub>c</sub>), average yields and average irrigation requirements for the predominant crops in Vaalharts and Groblershoop. Average yields for raisin grapes are from the 2020/21 and 2021/22 season based on estimates from Raisins South Africa. Data for 2023 is not currently available.**

Crop	Maize	Lucerne	Cotton	Wheat	Peanuts	Raisin grapes (micro*)	Raisin grapes (drip)
ET <sub>c</sub> (mm)	641	1442	759	492	855	885	885
Yield (t ha <sup>-1</sup> )	13.5	20	5.5	5.5	3.5	22.29/17.60	22.29/17.60
Irrigation (mm)	578	1501	688	561	932	869	764

\*microsprinkler

When comparing WP<sub>c</sub> and WP<sub>i</sub> between pecans and a number of annual crops in Vaalharts, it was evident that pecans had lower values than these crops, especially for maize, lucerne and wheat (Table 4.10).

**Table 4.10. Total gross income, production costs, water productivity and economic crop water productivity for the predominant crops in Vaalharts and Groblershoop, considering crop evapotranspiration and irrigation requirements. No 2022/23 production figures were available for raisin grapes.**

Crop	Season	Total Gross Income (R ha <sup>-1</sup> )	Production cost (R)	WP <sub>c</sub> (kg m <sup>-3</sup> )	WP <sub>i</sub> (kg m <sup>-3</sup> )	EWP <sub>c</sub> (R m <sup>-3</sup> )	EWP <sub>i</sub> (R m <sup>-3</sup> )
Maize	19/20	31 010	27 817	2.11	2.34	0.50	0.55
	20/21	40 163	30 860	2.11	2.34	1.45	1.61
	21/22	46 224	43 362	2.11	2.34	0.45	0.50
	22/23	54 959	44 213	2.11	2.34	1.68	1.86
Lucerne	19/20	52 750	30 031	1.39	1.33	1.58	1.51
	20/21	61 000	31 329	1.39	1.33	2.06	1.98
	21/22	58 000	41 512	1.39	1.33	1.14	1.10
	22/23	75 800	44 092	1.39	1.33	2.23	2.11
Cotton	19/20	51 865	37 779	0.72	0.80	1.86	2.05
	20/21	56 925	42 456	0.72	0.80	1.91	2.10
	21/22	79 420	53 612	0.72	0.80	3.40	3.75
	22/23	65 450	54 171	0.72	0.8	1.49	1.64
Wheat	19/20	33 968	24 117	1.63	1.43	2.00	1.76
	20/21	35 624	26 074	1.63	1.43	1.94	1.70
	21/22	43 992	37 154	1.63	1.43	1.39	1.22
	22/23	60 900	38 544	1.63	1.43	2.21	1.94
Peanuts	19/20	51 990	29 485	0.41	0.38	2.63	2.41
	20/21	52 780	36 534	0.41	0.38	1.90	1.74
	21/22	52 280	44 935	0.41	0.38	0.86	0.79
	22/23	60 900	45 387	0.41	0.38	1.81	1.66
Raisin grapes	20/21	110 046	83 087	2.52	2.57	3.05	3.10
(Micro)	21/22	73 357	83 095	1.99	2.03	net loss	net loss
Raisin grapes	20/21	110 046	83 087	2.52	2.92	3.05	3.55
(drip)	21/22	73 357	83 095	1.99	2.30	net loss	net loss

WP<sub>c</sub> – crop water productivity, WP<sub>i</sub> – irrigation water productivity, EWP<sub>c</sub> – economic crop water productivity, EWP<sub>i</sub> – economic irrigation water productivity

The same was true in Groblershoop, with raisin grapes under both microsprinkler and drip irrigation having higher  $WP_c$  values than pecans. The reason for pecans having such low  $WP_c$  is due to higher  $ET_c$  and lower yields, when compared to the other crops. The only other crop with comparable yields is peanuts, which is also an oil storing crop, but it has a slightly higher  $WP_c$  due to lower  $ET_c$ . The story, however, changes considerably when considering  $EWP_c$ , and  $EWP_i$  due to the high value of pecan nuts. Even during an “off” year in 2020/21 in Vaalharts,  $EWP_c$  was higher for pecans than all other crops. On average annual crops earned R1.72 per  $m^3$  evapotranspired and R1.70 per  $m^3$  of applied water. A net loss was realised for pecans in 2020/21 in Groblershoop and for raisin grapes in 2021/22, however, during a good season, the  $EWP_c$  for pecans was much higher than for raisin grapes.

The profitability of pecans per  $m^3$  of irrigation water applied explains why plantings are expanding so rapidly in the Northern Cape. In Vaalharts, more than half the scheme is now estimated to be planted to pecans. If only  $WP_c$  or  $WP_i$  was considered to determine the productive use of water in both regions and the sustainability of pecan production, pecans would likely be deemed to be unsustainable. This is important as this is the metric reported in popular literature for consumers. Whilst more water is required to produce a pecan crop than most other crops (except for lucerne) in Vaalharts, it can largely be attributed to a longer growing season than most other annual crops. However, if one considers summer-winter crop rotations, pecan annual water use is similar to these cropping systems. Concerns regarding the high water use of pecans relative to other crops are therefore not valid, and the total planted area on schemes relative to available water should rather be considered if plantings take place outside of existing allocations. If only the profitability of water evapotranspired or applied is considered, then pecans are the best use of water in both schemes when average or above average rainfall is received. However, in drought years when water allocations are restricted the flexibility allowed by annual crop production would be advantageous, in order to make the most of the given allocation.

What is very evident from the study is that data from a single season can be very misleading and averages over longer periods of time should be considered when deciding on benchmark values for these parameters. In pecans, the period after planting and before a crop is produced also needs to be considered, as the trees will use a considerable volume of water during this time without producing a yield. In addition, using one estimate for different climatic regions is unfair, due to differences in  $ET_o$  and rainfall which impact both  $ET_c$  and irrigation requirements. Whilst this was done for annual crops using SAPWAT 4 and long term averages, estimates for pecan using SAPWAT 4 were not accurate enough as a result of no water use data available for pecans at the time of release of SAPWAT 4. Improved modelling approaches for pecans could assist in running multiple year ET simulations for different irrigation systems.

Values for EWP are also season specific since both commodity price and production costs vary from year to year.

Importantly, none of the metrics used in this study are very useful when assessing the sustainability of water use, as suggested by Fereres et al. (2017). Evapotranspiration is largely dictated by atmospheric conditions, which the grower has no control over, and by only measuring irrigation it is impossible to assess how well irrigation is scheduled in an orchard. The assessment of the water balance in orchards and fields may provide a better understanding of the productive use of water in orchards, as deep drainage and surface run-off can be quantified. Deciding on the best use of irrigation water in a region should not be based on simple metrics alone, but needs to consider the whole soil-plant-atmosphere continuum and catchment under consideration holistically in order to provide meaningful data for the improvement of the productive use of water in agriculture.

## **4.2 MODELLING PECAN WATER USE**

### **4.2.1 PARAMETERISATION AND VALIDATION OF A CROP COEFFICIENT MODEL**

In order to try and account for stomatal control over transpiration in pecans, the approach of Allen and Pereira (2009) was followed for the pecan orchards in Vaalharts and Groblershoop, in a similar fashion to that outlined for citrus (Taylor et al., 2015). The model was parameterised using data from the 2021/22 season, where regular canopy size estimates in both regions were made throughout the season. In this approach, height and effective fractional cover ( $f_{c\text{ eff}}$ ) is used to adjust crop coefficients to derive orchard-specific transpiration crop coefficients ( $K_t$ ). In addition, a degree of stomatal control over transpiration relative to most agricultural crops can also be applied. As demonstrated in citrus (Taylor et al., 2015), this method could provide reasonable transpiration estimates, provided a dynamic estimate of mean leaf resistance ( $r_{\text{leaf}}$ ) can be obtained. This approach was therefore tested in the pecan orchards in the Northern Cape.

Changes in canopy size over the season were estimated from drone images taken of the orchard at 6 weekly intervals (Figure 4.34). Effective fractional cover ( $f_{c\text{ eff}}$ ) is the effective fraction of ground covered or shaded by the vegetation at solar noon and was determined according to Allen et al. (1998). The estimation of  $f_{c\text{ eff}}$  took into account the angle of the row from east-west and the height-to-width ratio of the trees over the season.

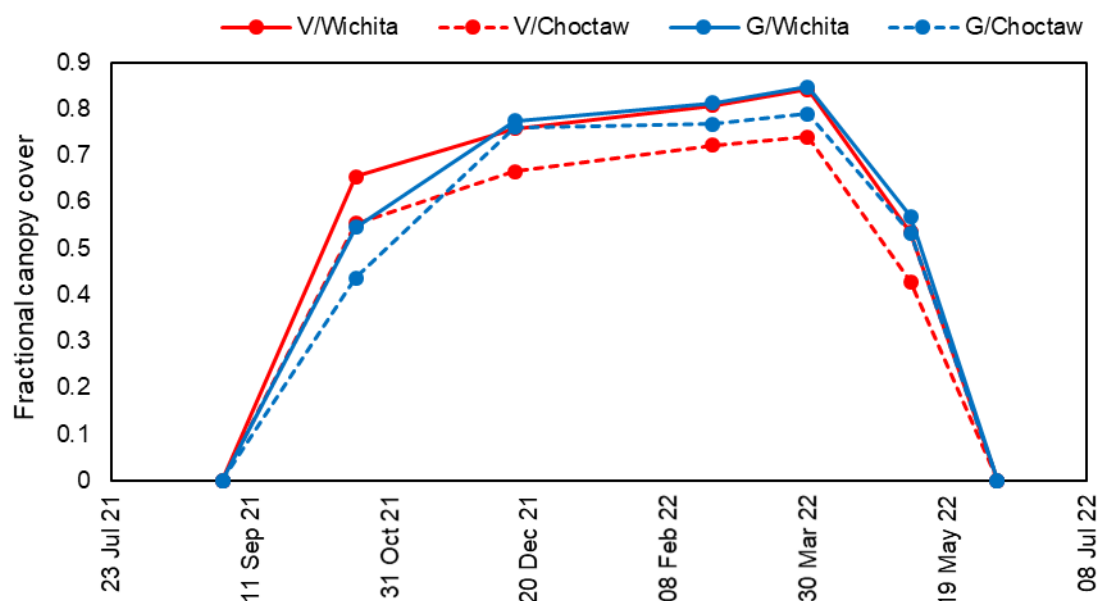


**Figure 4.34** Changes in fractional canopy cover in the orchards in Vaalharts (V) and Groblershoop (G) for the 2021/22 season. Fractional canopy cover was determined from drone images which were analysed with the Canopeo app. Values were an average of the four trees in each orchard.

As expected, daily estimates of  $r_{\text{leaf}}$  varied across the season, and although values were different for the different cultivars and regions, the trend in  $r_i$  across the season was fairly similar for both regions and cultivars (Figure 4.35). As the values for both cultivars in each region were fairly similar, an average fortnightly value of both cultivars was used to derive  $K_i$  values for each cultivar in each region. Fortnightly values were chosen to try and account for changes in canopy size over the season. It is envisaged that it would not be too time-consuming for growers to estimate canopy size every two weeks, especially at the start of the season.



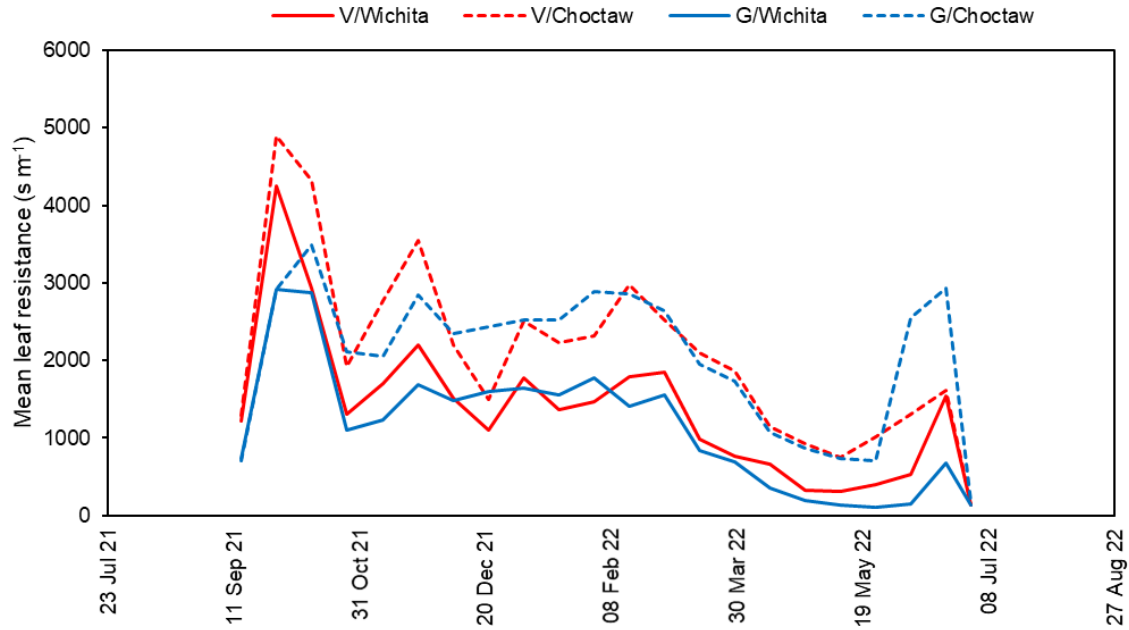


**Figure 4.35 Mean biweekly leaf resistance ( $r_{\text{leaf}}$ ) for the orchard in Vaalharts (V) and Groblershoop (G) determined using the approach of Allen and Pereira (2009). Data was from the 2021/22 season**

When comparing the measured and estimated fortnightly  $K_t$  values, there was a general trend to slightly underestimate  $K_t$  values using the average  $r_{\text{leaf}}$  values for each region, especially for ‘Wichita’ trees in both regions and ‘Choctaw’ trees in Vaalharts (Figure 4.36). This suggests that the average daily  $r_{\text{leaf}}$  values are overestimated, which causes a larger adjustment than necessary for stomatal control over transpiration, especially in trees that had the highest seasonal transpiration (the  $F_r$  term in the model). Transpiration crop coefficients were estimated the best for ‘Choctaw’ trees in Groblershoop and Vaalharts.

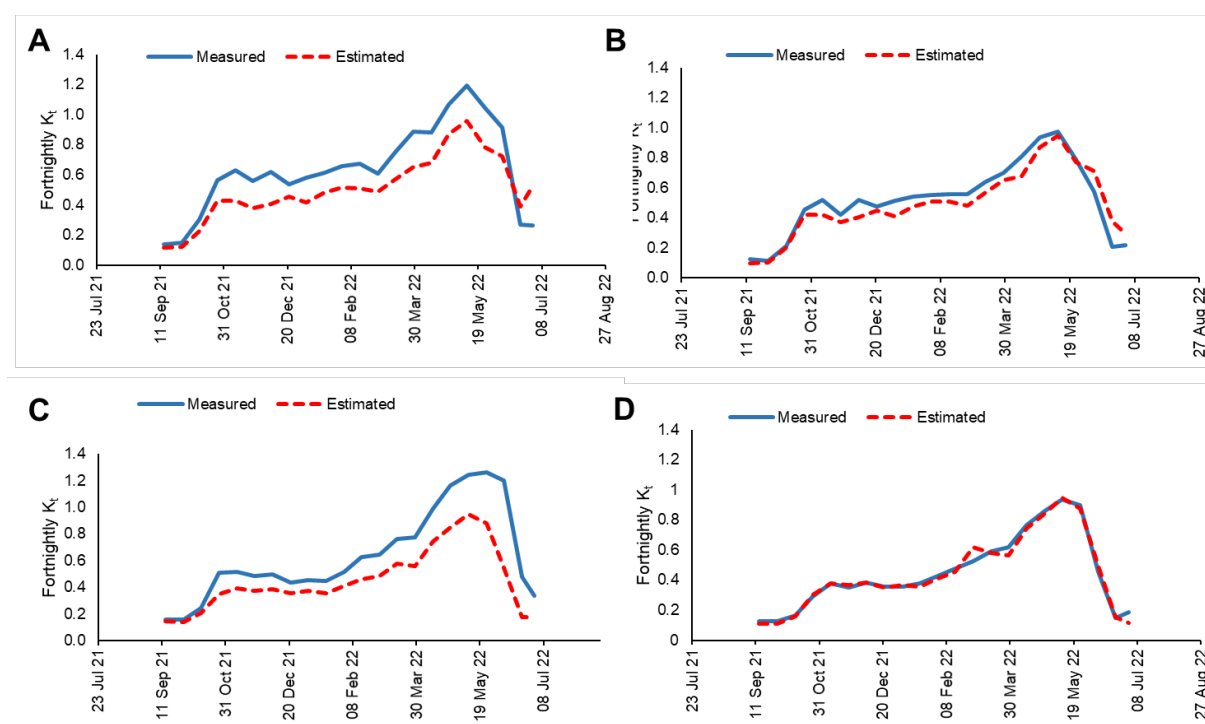


**Figure 4.36** Fortnightly measured and estimated transpiration crop coefficients ( $K_t$ ) for the A) 'Wichita' trees in Vaalharts, B) 'Choctaw' trees in Vaalharts, C) 'Wichita' trees in Groblershoop and D) 'Choctaw' trees in Groblershoop for the 2021/22 season.

The fortnightly  $K_t$  values were used together with daily  $ET_0$  to estimate daily water use (Figure 4.37), which was then compared on a monthly basis (Figure 4.38). As expected, the underestimation of  $K_t$  values for 'Wichita' trees resulted in an underestimation of daily transpiration for most of the season in both regions. However, daily transpiration was estimated in 'Choctaw' trees. There were periods when transpiration of 'Wichita' trees was well estimates, especially the start and end of the season in Vaalharts. On a seasonal basis, total measured transpiration in the 'Wichita' trees in Vaalharts was 751 mm, whilst estimation transpiration was 598 mm. In the 'Wichita' trees in Groblershoop, seasonal measured transpiration was 806 mm, and estimated transpiration was 605 mm. However, for the 'Choctaw' trees in Vaalharts, measured transpiration was 627 mm as compared to an estimated 585 mm. Finally, in Groblershoop, seasonal transpiration of 'Choctaw' trees was 609 mm and estimated 598 mm. The model's ability to estimate daily transpiration was evaluated using several statistical parameters (Table 4.11). Model performance was considered satisfactory when  $RMSE < \text{half the standard deviation of measured values}$ ,  $R^2 > 0.8$ ,  $MAE < 20\%$  and  $D > 0.8$  (de Jager, 1994). As expected, the model performed better on a monthly than daily basis. Whilst, some criteria were met for 'Wichita' trees in both regions, not

all criteria were met suggesting unsatisfactory model performance for 'Wichita' trees in both regions.

Monthly, the estimation of  $T$  was very good for 'Choctaw' trees in both regions, but estimation of monthly  $T$  for 'Wichita' trees was not as good, with a tendency to underestimate (Figure 4.38). This suggests that on both a daily and monthly basis, the model performed well for most scenarios tested. The model could take into account slightly different sized orchards, with slight differences in canopy growth over the season. However, the estimates relied heavily on the estimate of  $r_{\text{leaf}}$ , which varied across seasons and regions. This is perhaps not surprising given the findings that transpiration does tend to reach a plateau value at high atmospheric demand, which suggests some form of stomatal control. As the trend in  $r_{\text{leaf}}$  between cultivars and regions was very similar, it could be possible that differences in weather could explain the variation and also seems to be related to canopy size

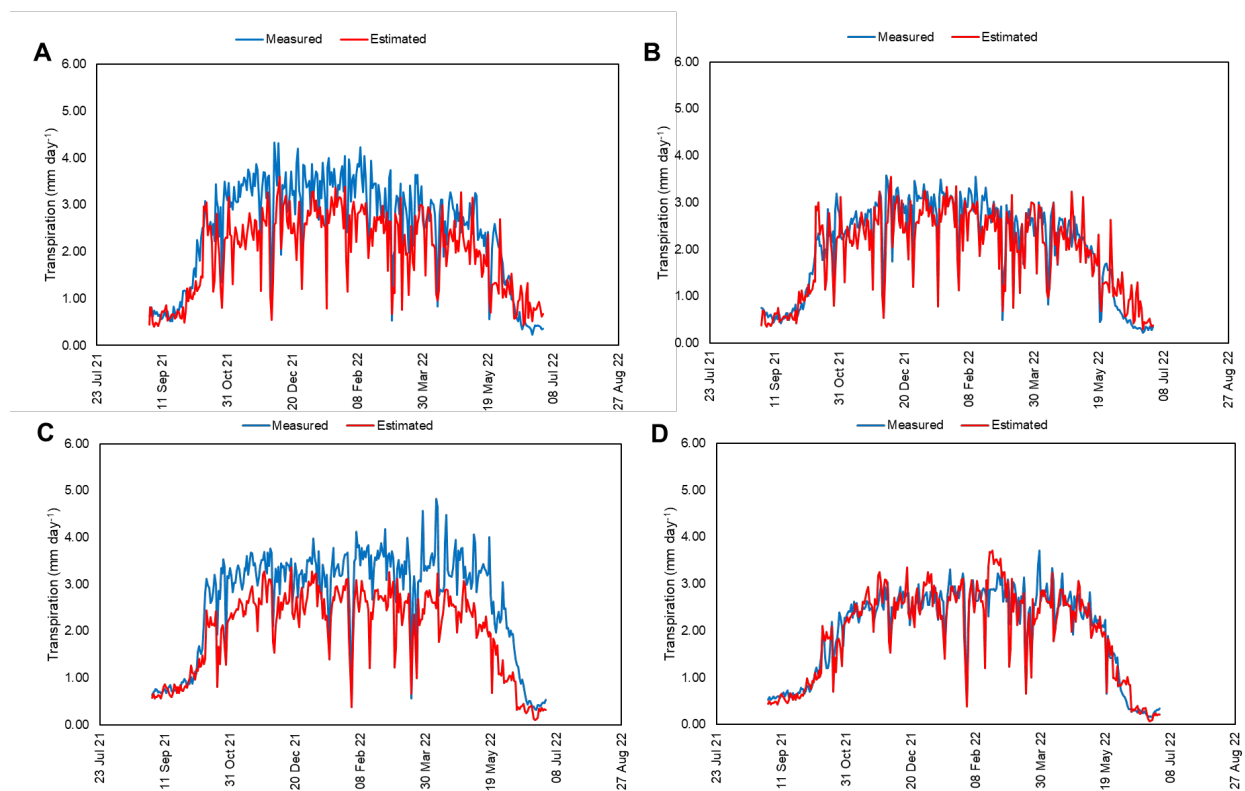


**Figure 4.37** Daily measured and estimated transpiration in A) 'Wichita' and B) 'Choctaw' trees in Vaalharts and C) 'Wichita' and D) 'Choctaw' trees in Groblershoop. Transpiration was estimated using fortnightly estimates  $K_t$  derived from average mean leaf resistance ( $r_{\text{leaf}}$ ) for each region.

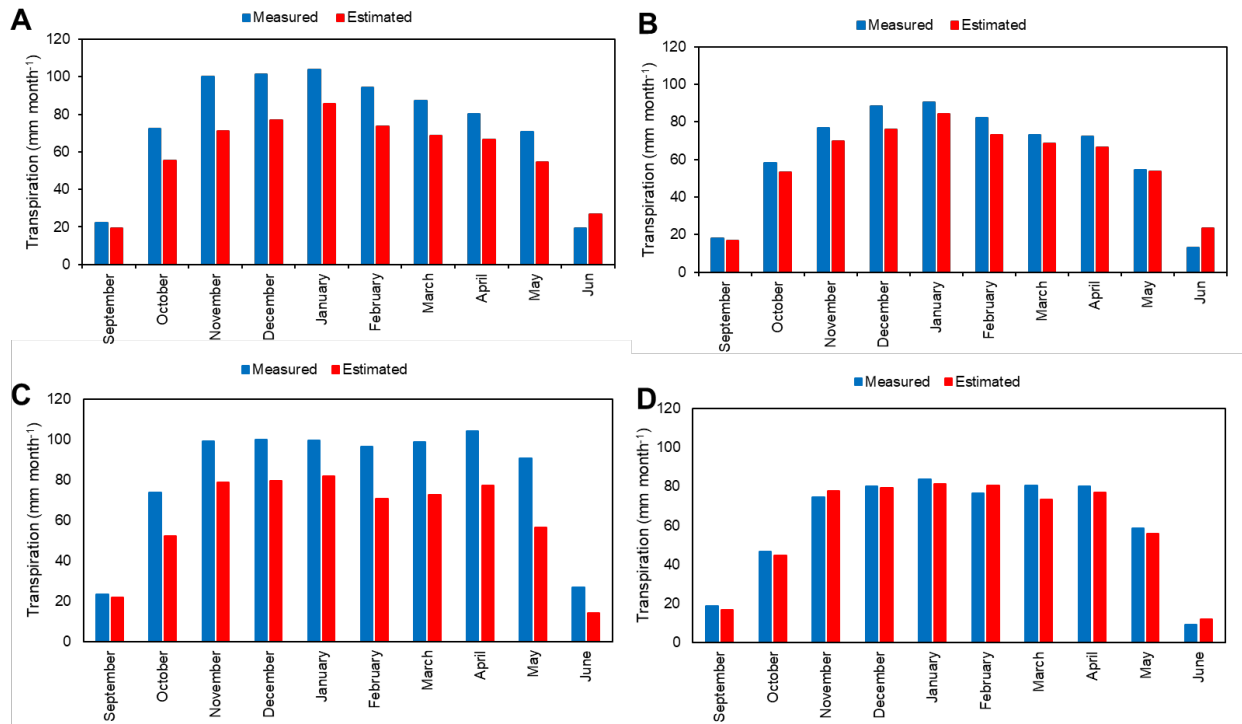


**Figure 4.38** Summed monthly measured and estimated transpiration in A) 'Wichita' and B) 'Choctaw' trees in Vaalharts and C) 'Wichita' and D) 'Choctaw' trees in Groblershoop for the 2021/22 season. Transpiration was estimated using fortnightly estimates  $K_t$  derived from average mean leaf resistance ( $r_{leaf}$ ) for each region. Monthly estimates were derived by summing transpiration for each month.

**Table 4.11** Modelling statistics for the estimation of transpiration in the orchards in Vaalharts and Groblershoop for the 2021/22 season

Region	Cultivar	Time step	R <sup>2</sup>	D	RMSE	MAE
Vaalharts	Wichita	Daily	0.77	0.86	0.75	24.64
		Monthly	0.96	0.87	19.32	22.43
	Choctaw	Daily	0.81	0.94	0.44	16.14
		Monthly	0.97	0.98	7.59	10.04
Groblershoop	Wichita	Daily	0.84	0.85	0.82	25.84
		Monthly	0.95	0.85	23.54	25.44
	Choctaw	Daily	0.86	0.96	0.36	12.64
		Monthly	0.98	0.99	3.57	4.91

As Taylor et al. (2015) found a good relationship between  $r_{leaf}$  and VPD, a similar relationship was tested in this study, together with  $ET_o$  (Figure 4.39). A reasonable relationship was found between  $r_{leaf}$  and VPD with an  $R^2$  value of 0.5738, but the relationship with  $ET_o$ , was not as

good with an  $R^2$  of 0.4847. This relationship was assessed to determine if it could provide reasonable estimates of  $K_t$  for the various orchards.

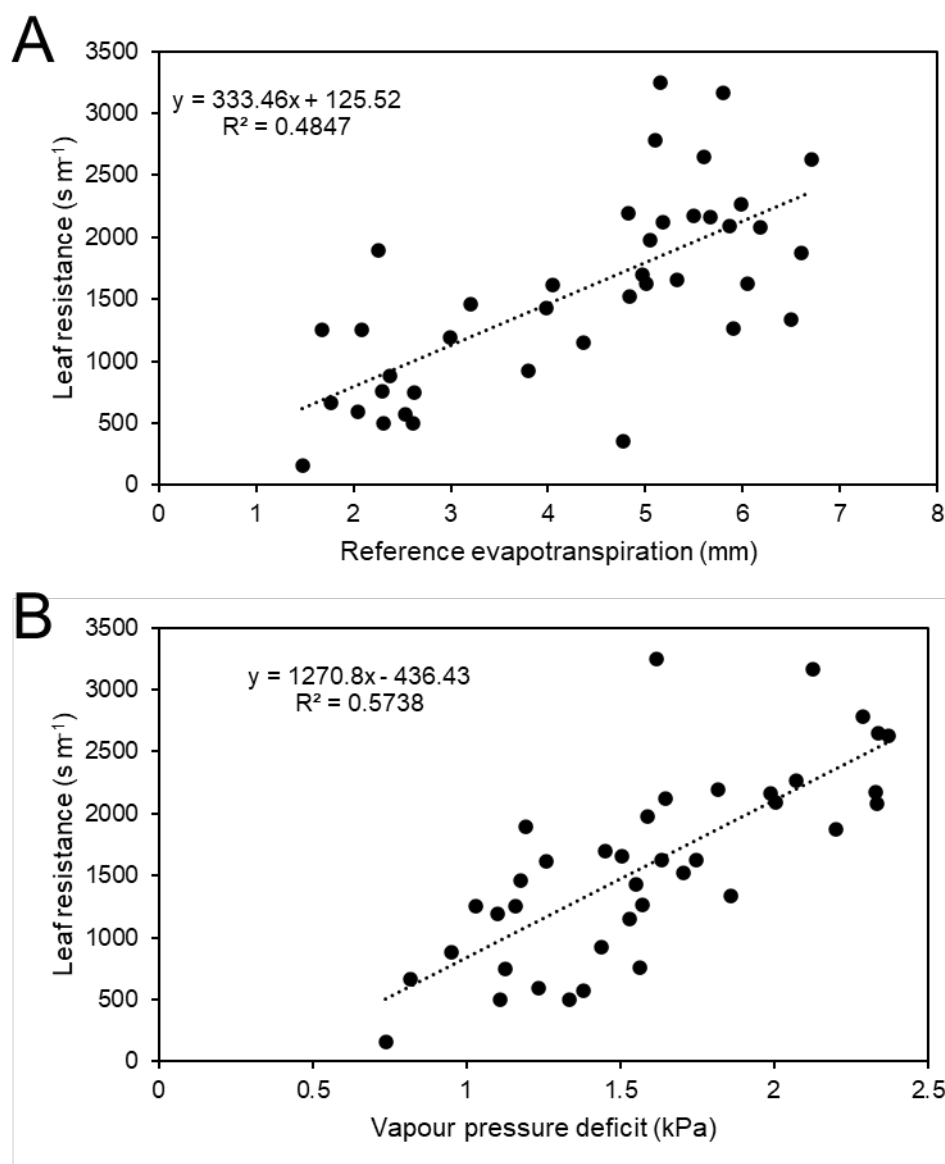


**Figure 4.39 Relationship between fortnightly mean leaf resistance and A) reference evapotranspiration and B) vapour pressure deficit using combined average leaf resistance data from Vaalharts and Groblershoop.**

In order to validate the ability of the relationship between VPD and  $r_{leaf}$  (Figure 4.39B) to determine orchard specific  $K_t$  values and transpiration, the relationship was tested on data from the 2022/23 season. The changes in canopy cover over the 2022/23 season for both cultivars and orchards are illustrated in Figure 4.40 and these values were used to determine  $f_{c\ eff}$ . There were slight differences in fractional canopy cover between the different regions and cultivars, with 'Choctaw' trees in both regions having a higher canopy cover at the start of the season as compared to 'Wichita', but there was very little difference in the cultivars and regions

close to the end of the season. These values, together with a derived  $r_{leaf}$  (Figure 4.41) were then used to calculate cultivar specific  $K_t$  values (Figure 4.42). The  $r_{leaf}$  values calculated using the relationship with VPD did not follow the same trend as those estimated from measured data, especially towards the end of the season. This is perhaps not surprising as the increase in measured  $K_t$  values at the end of the season is not related to weather but is most probably related to either a vegetative flush or a change in physiology associated with nut filling.

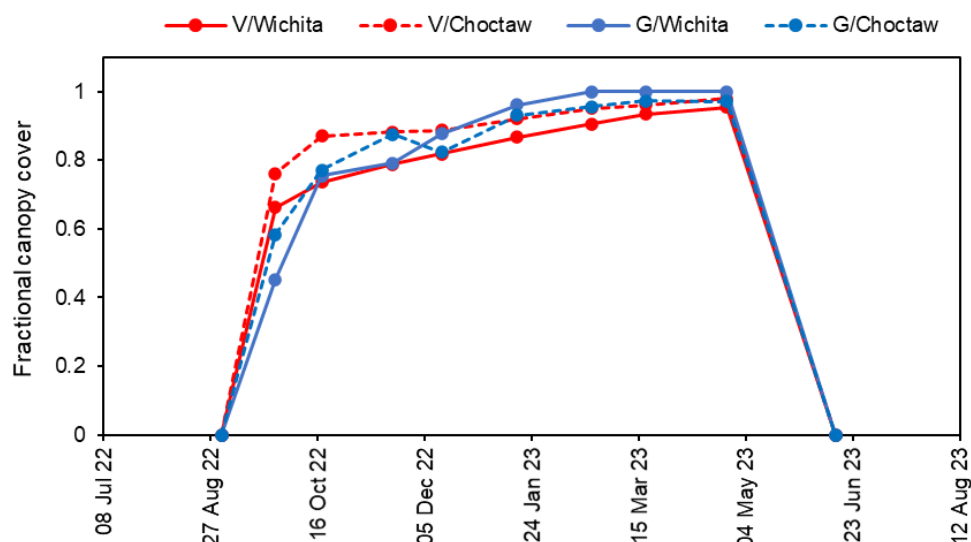


**Figure 4.40** Changes in fractional canopy cover in the orchards in Vaalharts (V) and Groblershoop (G) for the 2022/23 season. Fractional canopy cover was determined from drone images which were analysed with the Canopeo app. Values were an average of the four trees.

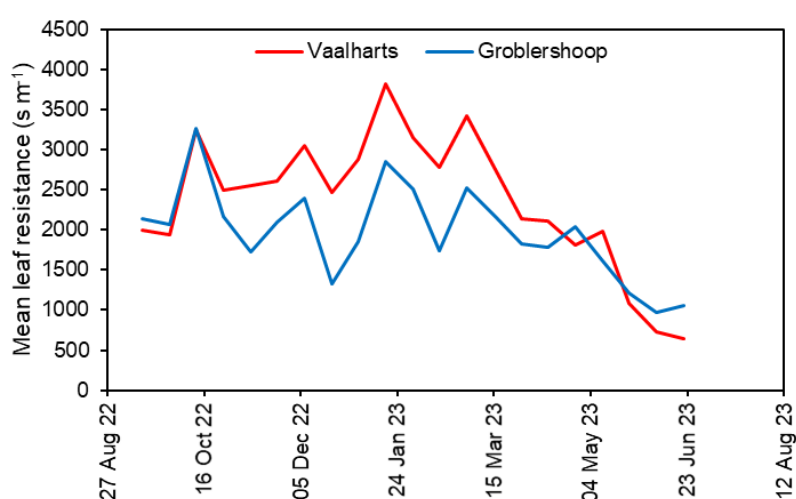


**Figure 4.41** Estimated mean biweekly leaf resistance ( $r_{leaf}$ ) for the orchard in Vaalharts and Groblershoop in the 2022/23 season determined using the relationship between VPD and  $r_{leaf}$  determined in the 2021/22 season.

Transpiration crop coefficients were typically well estimated at the start of the season in all four scenarios (Figure 60), but for three of the four situations, the  $K_t$  values were underestimated at the end of the season. This could be associated with the slightly different trend in  $r_{leaf}$  values between those determined from measured data and those determined using a relationship with VPD. Transpiration crop coefficient values were well estimated for the ‘Choctaw’ trees in Groblershoop, as was also observed in the 2021/22 season.

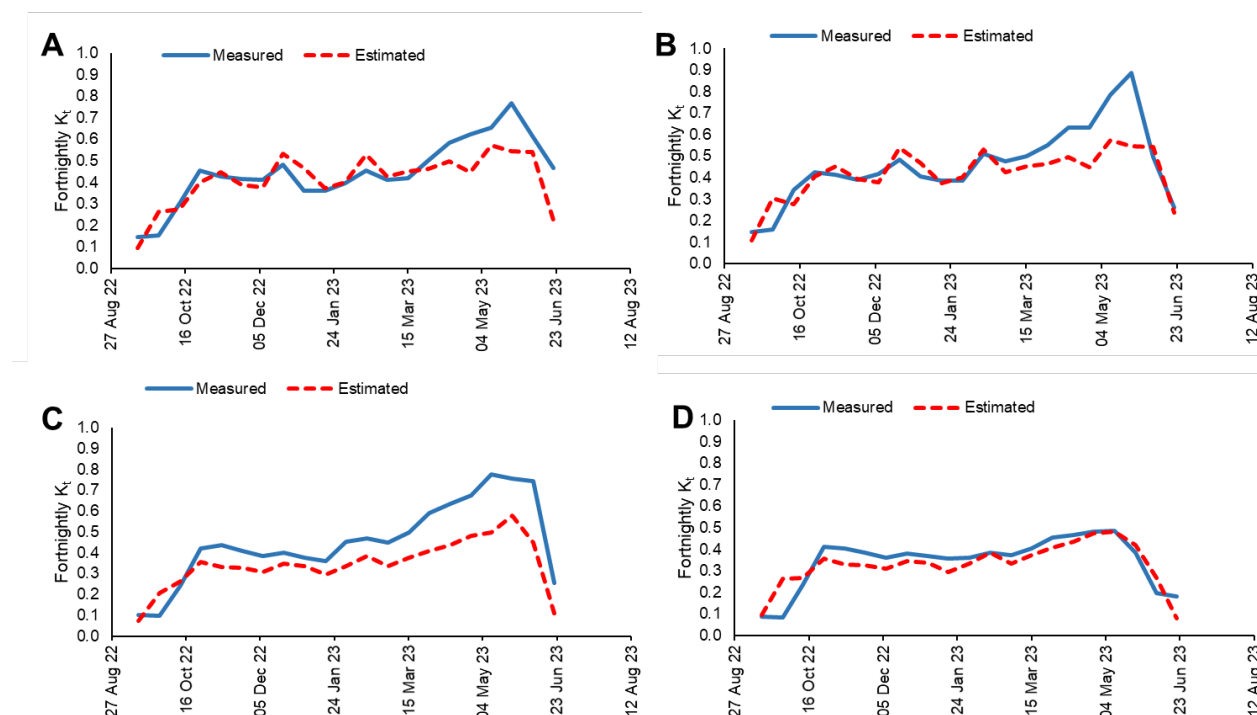


**Figure 4.42 Fortnightly measured and estimated transpiration crop coefficients ( $K_t$ ) for the A) ‘Wichita’ trees in Vaalharts, B) ‘Choctaw’ trees in Vaalharts, C) ‘Wichita’ trees in Groblershoop and D) ‘Choctaw’ trees in Groblershoop for the 2022/23 season.**

These  $K_t$  values were used combined with daily  $ET_o$  to provide a daily estimate of transpiration (Figure 4.43) for all four scenarios (2 regions and two cultivars). As expected from the  $K_t$  values, transpiration was generally well estimates at the start of the season, but not as well estimated towards the end of the season. Overall, model performance was fairly good for both regions and cultivars, except for ‘Wichita’ in Groblershoop where  $MAE > 20$  (Table 4.12). An  $R^2 > 0.8$  was only found for ‘Choctaw’ in Groblershoop which suggests variation between measured and estimated daily transpiration. Whilst, daily estimates are required for irrigation scheduling, monthly estimates of transpiration can be used for irrigation planning. The ability to estimate monthly water use of orchards with different canopy sizes and in different seasons could therefore be of use to pecan growers. Monthly estimates of transpiration using  $r_{leaf}$  values derived from VPD measurements compared very well to measured monthly transpiration

(Figure 4.44). All statistical criteria were met for monthly data suggested that the model performed very well on a monthly basis (Table 4.12). This approach for taking into account stomatal control over transpiration is therefore very promising for monthly estimates of transpiration of pecan orchards. The poorer performance in 'Wichita' trees, as opposed to 'Choctaw' should be investigated further.

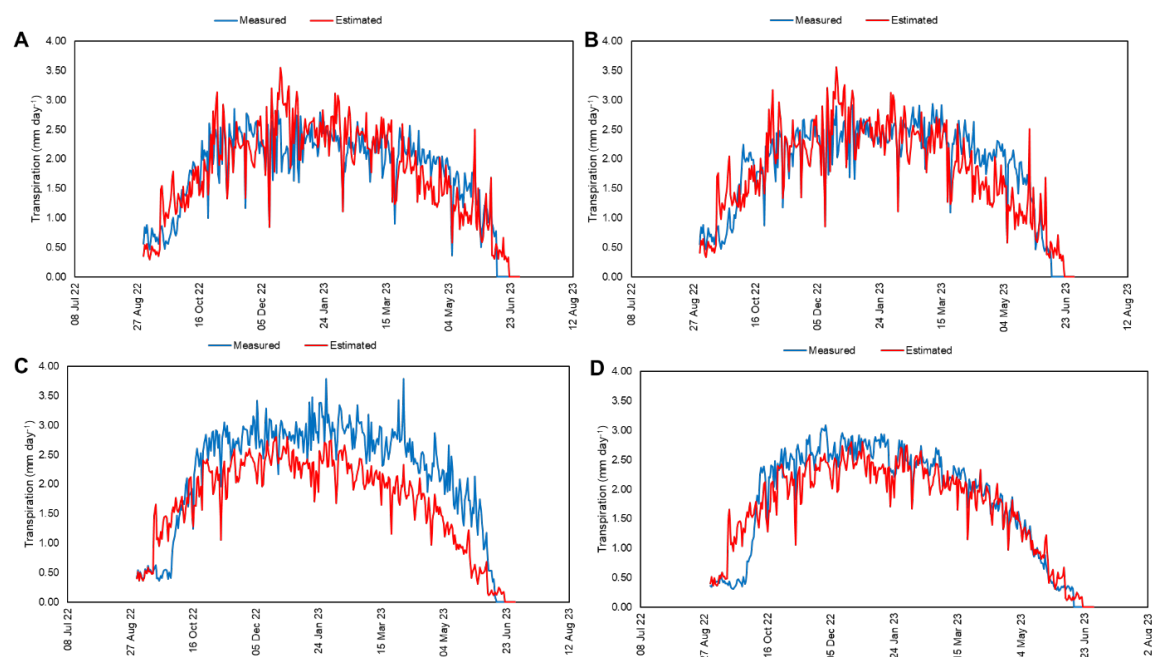


**Figure 4.43** Daily measured and estimated transpiration in A) 'Wichita' and B) 'Choctaw' trees in Vaalharts and C) 'Wichita' and D) 'Choctaw' trees in Groblershoop in the 2022/23 season. Transpiration was estimated using fortnightly estimates  $K_t$  derived from average mean leaf resistance determined from a relationship with VPD.

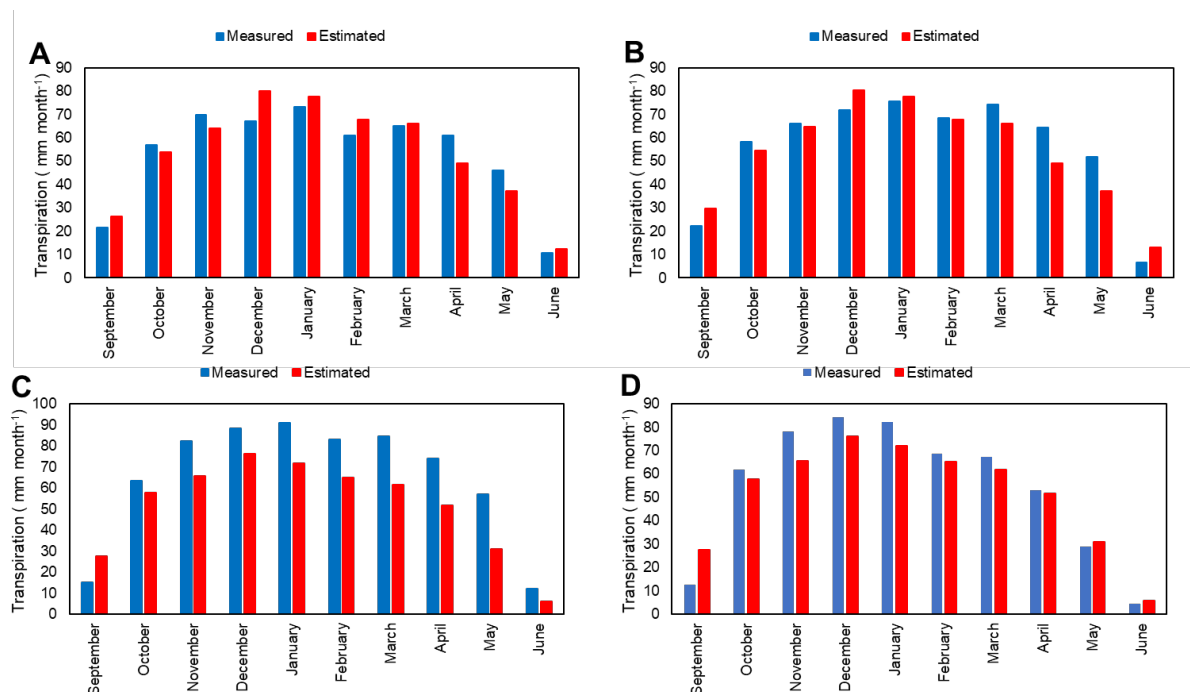




**Figure 4.44 Summed monthly measured and estimated transpiration in A) 'Wichita' and B) 'Choctaw' trees in Vaalharts and C) 'Wichita' and D) 'Choctaw' trees in Groblershoop in the 2022/23. Transpiration was estimated using fortnightly estimates  $K_t$  derived from mean leaf resistance ( $r_{leaf}$ ) determined using the relationship with VPD. Monthly estimates were derived by summing transpiration for each month.**

**Table 4.12 Modelling statistics for the estimation of transpiration in the orchards in Vaalharts and Groblershoop for the 2022/23 season**

Region	Cultivar	Time step	R <sup>2</sup>	D	RMSE	MAE
Vaalharts	Wichita	Daily	0.64	0.88	0.422	17.75
		Monthly	0.89	0.97	7.54	11.32
	Choctaw	Daily	0.62	0.88	0.44	17.50
		Monthly	0.86	0.96	8.43	12.22
Groblershoop	Wichita	Daily	0.68	0.82	0.66	24.49
		Monthly	0.87	0.88	18.32	24.70
	Choctaw	Daily	0.84	0.94	0.36	14.14
		Monthly	0.97	0.97	8.22	11.68

#### **4.2.2 PARAMETERISATION AND VALIDATION OF A RADIATION INTERCEPTION MODEL**

One of the ultimate goals in this research is to find an easy and hopefully mechanistic way, of estimating the canopy parameters needed for the radiation interception model, particularly the canopy porosity. This method could then be employed in pecan orchards and ultimately other orchard fruit trees. The use of a mobile phone application together with an external fish eye lens was tested to estimate the canopy porosity and further the radiation dynamics within pecan canopies. However, at times where such tools are not available, it is possible to provide a practical system where by this parameter could be estimated from easily measured canopy attributes such as fractional ground cover. Fractional ground cover is often estimated using visual estimates which can be subjective. However, the increased use of drones in orchards provides the possibility of estimating fractional ground cover with these tools which are often readily available to farmers. The possibility of using the relationship between the canopy porosity estimates (light sensors and VitiCanopy mobile application) and canopy cover estimated with the aerial images, was therefore tested to determine if fractional ground cover can be used as a proxy estimate for the canopy porosity and PAR interception in orchard trees. This relationship was further used to estimate hourly and daily PAR interception within the orchards.

The results of the relationship between fractional cover determined using the Canopeo application ( $fc_{\text{canopeo}}$ ) and canopy porosity ( $C_p$ ) indicated that  $C_p$  had a strong negative linear correlation with both measures of  $C_p$  (Viticanopy app and light sensors) (Figure 4.45C). The equations for the two methods were  $y = -0.7007x + 0.9696$  for Viticanopy and  $y = -0.7928x + 0.9537$  for PAR sensors). The  $fc_{\text{canopeo}}$  appeared to be better correlated with  $C_p$  measured with PAR sensors with a high correlation coefficient ( $R^2$ ) of 0.96 as compared to 0.78 for Viticanopy. When using the Viticanopy App,  $C_p$  varied from 0.97 at low fractional cover ( $fc_{\text{canopeo}}$  below 0.1) to 0.18 at maximum fractional cover ( $fc_{\text{canopeo}} \sim 0.8$ ), whilst with the PAR sensors,  $C_p$  varied from 0.99 at low  $fc_{\text{canopeo}}$  to 0.21 at maximum  $fc_{\text{canopeo}}$ . Importantly, the slope of the two regression lines very similar, which suggests that it may be possible to use either equation to estimate  $C_p$ , and ultimately PAR interception in tree canopies (Figure 4.45C), because of a fairly constant relationship between canopy cover and  $C_p$ . When testing the ability of this relationships to estimate daily and hourly light interception within the orchards, the results indicated that overall, the model provided good estimates of daily and hourly PAR interception (Figure 4.46). However, there was noticeable lack of agreement between the measured and estimated data at certain times (Figure 4.46). The lack of agreement in hourly estimates could be a result of the model's inability to account for the influence of neighbouring trees, which shade each other at low sun elevation angles thereby reducing incident radiation on the neighbouring tree. However, on a daily time step the model was able to estimate PAR interception well, which is sufficient for estimates of canopy size in pecan orchards for use in transpiration models (Figure 4.47).

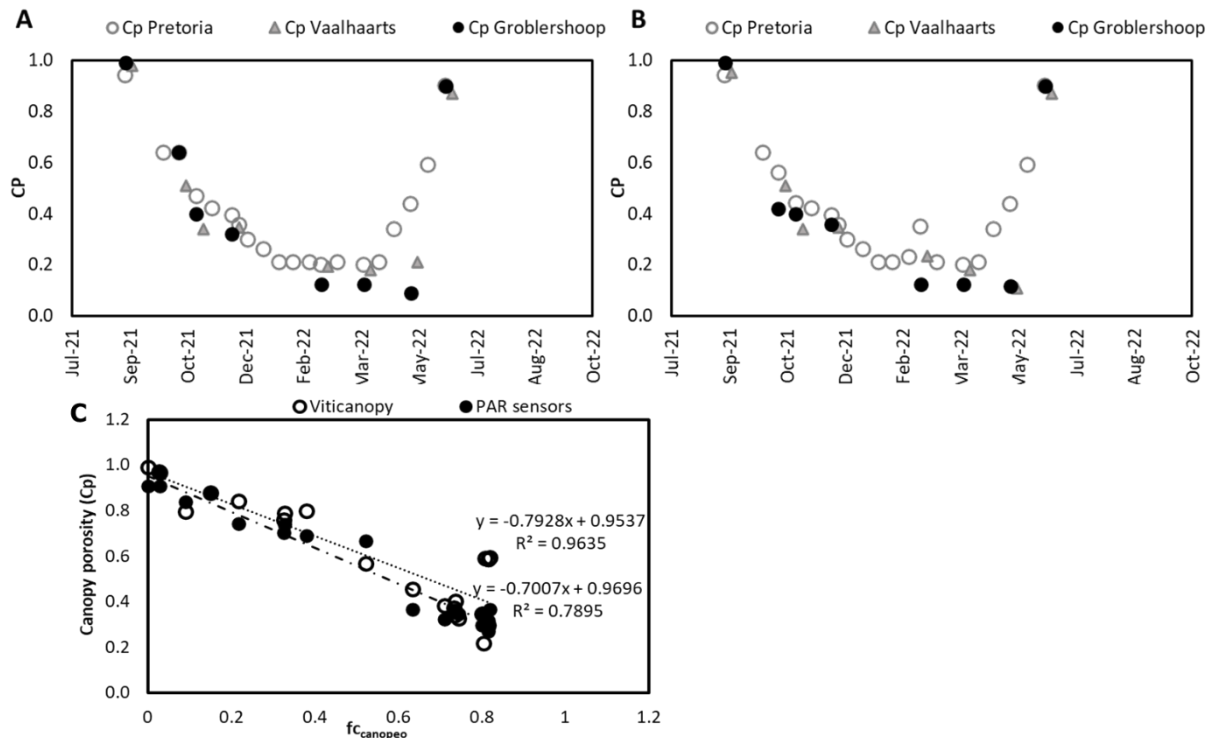


**Figure 4.45 Seasonal changes in maximum canopy porosity (Cp) for the three trial sites measured using A) the VitiCanopy mobile phone application, B) PAR interception sensors and C) the relationship between fractional ground cover measured using Canopeo app ( $f_{c_{canopeo}}$ ) and canopy porosity (Cp) measured using VitiCanopy application and PAR sensors (line quantum sensors and a Ceptometer).**

For comparable purposes, only 'Wichita' trees were considered for the estimation of hourly FIPAR (Figure 4.46). For this modelling the relationship between  $f_{c_{canopeo}}$  and Cp using measurements of PAR interception was used for Cp estimates. In general, the model estimated hourly FIPAR well at all three sites. However, there some errors were observed during the simulation period at all three sites (including trees at Innovation Africa@UP), especially when canopy cover was highest in summer (Figure 64 B, F and J). This could be attributed to the estimates of Cp from  $f_{c_{canopeo}}$ , as there was a high degree of scatter of data points at high fractional canopy cover (Figure 4.45). The prediction of Cp from  $f_{c_{canopeo}}$  was therefore likely to be less accurate during this period. The model slightly overestimated hourly FIPAR especially in the morning and in the afternoon. This was more pronounced when canopy size was at its maximum (i.e. during summer), which could be attributed to the interference of neighbouring trees, as the described above. Despite these discrepancies, the overall performance of the model for hourly FIPAR was acceptable for most of the growing period, as the index of agreement was greater than 0.8, MAPE values were below 20% and RMSE values were less than 1. However, the statistical indices indicated that the model could

be slightly unreliable in summer (Figure 4.46B, F and J) through to autumn (Figure 4.46C,G and K) when the trees are tall and have reached a height that is above 9.7 m.

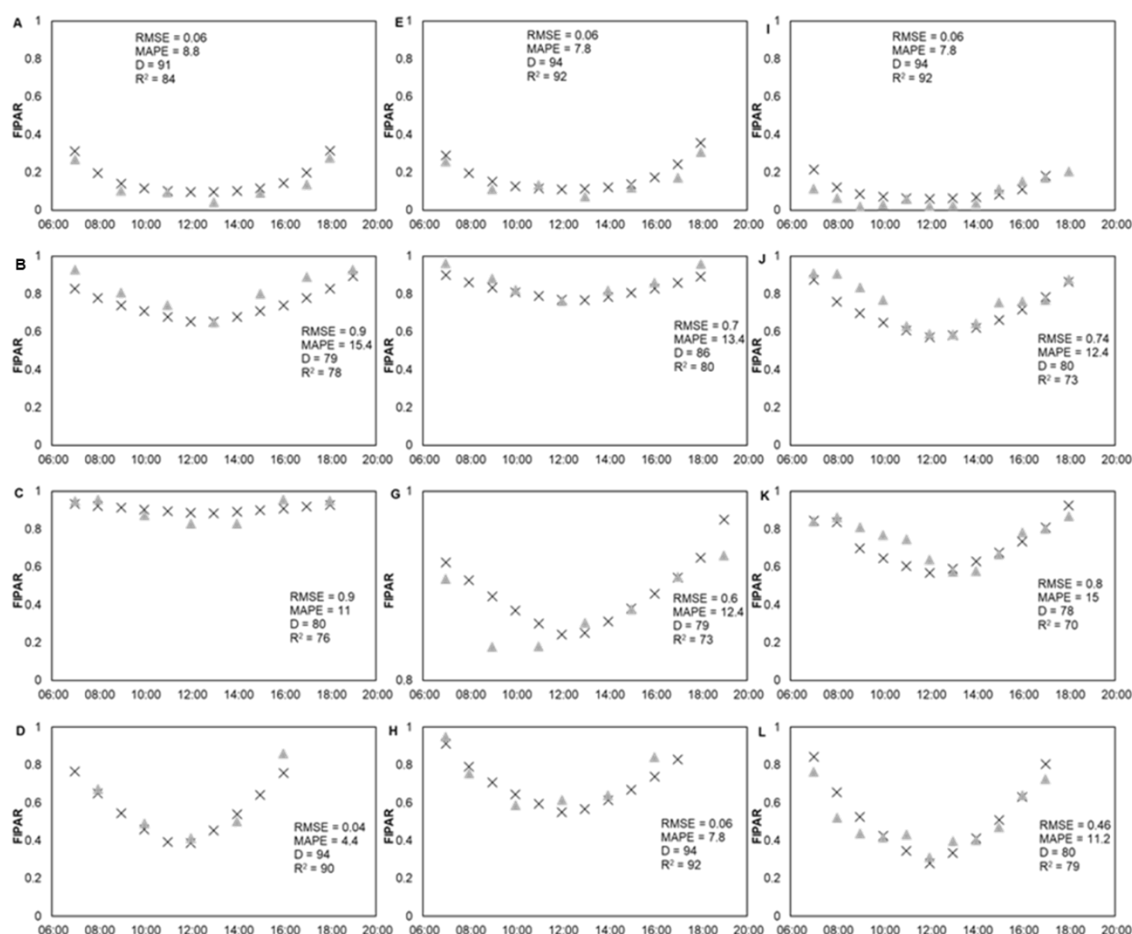


**Figure 4.46** Diurnal variation of hourly fractional interception of photosynthetically active radiation (FIPAR) for 'Wichita' trees grown in A, B, C and D) Vaalharts, E, F, G, and H) Groblershoop and I, J, K and L) Innovation Africa @ UP, Pretoria. Data was collected in A, E, and I) September 2021, B, F and J) February 2022, C, G and K) April 2023, and D, H, and L) May 2022. Triangles represent measured PAR interception, and crosses represent estimated PAR interception by the canopies. The Canopy porosity was estimated using equation  $y = -0.7928x + 0.9537$ .

The model performed better on a daily time step, as compared to hourly FIPAR values (Figure 4.47), with MAPE < 15.5%,  $D > 0.85$ , and RMSE < 0.15 for all cultivars across all three sites (Table 4.13). As observed for hourly estimates, there were observed errors in daily estimates which occurred occasionally during the rapid growth period (late October to November). This was more pronounced in both 'Choctaw' and the 'Wichita' trees in Groblershoop compared to the other two sites (Figure 65 C and D).

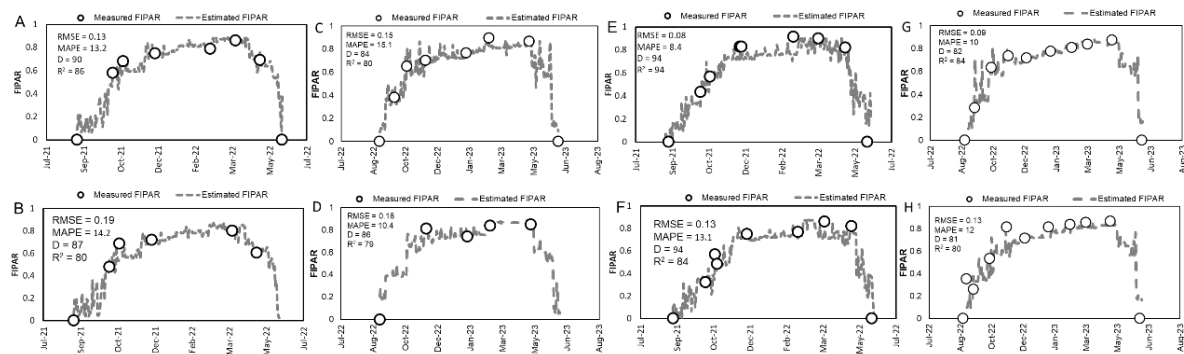


**Figure 4.47 Comparison between measured and estimated values of daily fractional interception of PAR for A) ‘Wichita’ trees in Vaalharts, B) ‘Choctaw’ trees in Vaalharts, C) ‘Wichita’ trees in Groblershoop, (D) ‘Choctaw’ trees in Groblershoop and (E) ‘Wichita’ trees in Pretoria**

**Table 4.13 Modelling statistics for the estimation of daily fractional interception of photosynthetically active radiation (FIPAR) in Vaalharts and Groblershoop orchards**

Region	Cultivar	Season	R <sup>2</sup>	D	RMSE	MAE
Vaalharts	Wichita	2021/22	0.8	0.81	0.16	18.3
		2022/23	0.80	0.80	0.15	15.1
	Choctaw	2021/22	0.81	0.94	0.44	16.14
		2022/23	0.79	0.86	0.18	10.4
Groblershoop	Wichita	2021/22	0.94	0.94	0.08	8.4
		2022/23	0.84	0.82	0.09	10.0
	Choctaw	2021/22	0.86	0.96	0.36	10.0
		2022/23	0.80	0.81	0.13	12

#### 4.2.3 PARAMETERISATION AND VALIDATION OF A CANOPY CONDUCTANCE MODEL

An approach by Villalobos et al. (2013) that accounts for the stomatal control of transpiration was used to estimate transpiration for the pecan orchards in Vaalharts and Groblershoop. The model estimates  $T$  as a function of total solar radiation and VPD together with derived parameters **a** and **b**, representing radiation use efficiency and the response of canopy conductance ( $G_c$ ) to VPD, as described in section 3.1.10.3. The model was calibrated with  $T$  datasets from 2020/2021 data set from Innovation Africa @UP (Figure 4.48) and validated using Vaalharts and Groblershoop. This was done to assess if the model is site-specific a single set of parameters can be used equally across the different sites and possibly different cultivars. The determination of **a** and **b** parameters resulted in a very good linear fit, with an

$R^2$  value of 0.9261 (Figure 4.48). This was then used to determine transpiration in Vaalharts and Groblershoop.

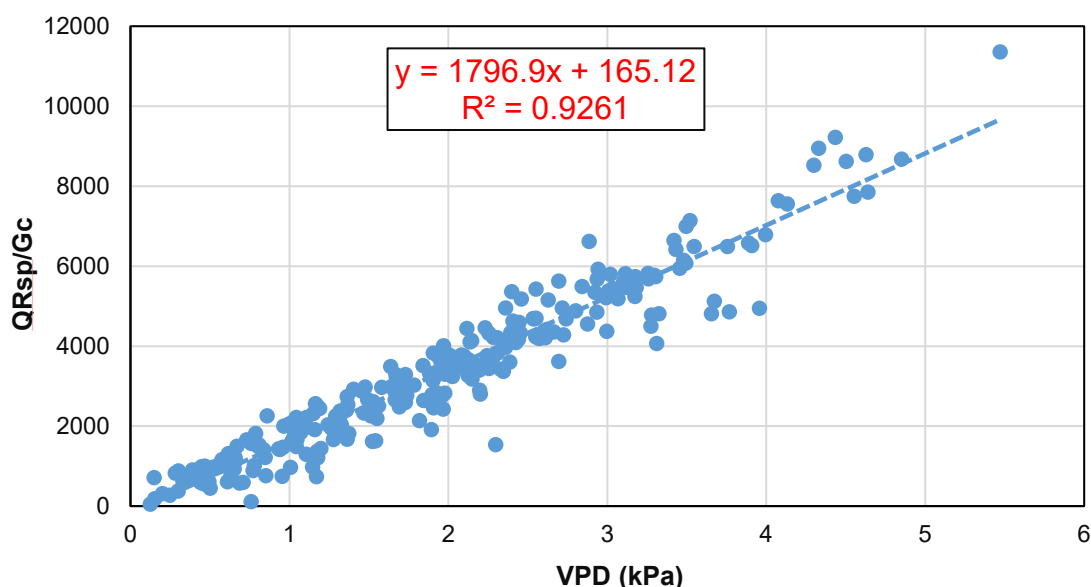


**Figure 4.48** The linear function relating fractional interception of solar radiation (QRsp) divided by canopy conductance (Gc) to vapour pressure deficit (D) to determine the slope and intercept of the curve for use in transpiration modelling. This relationship was determined in the pecan orchard at Innovation Africa@UP.

The performance of the calibrated model in the Groblershoop orchard is shown in Figure 4.49. The data shown excludes rainy days as the model is can not accurately estimate T under wet conditions.(Villalobos et al., 2013). Generally, the model estimated T fairly well. However, there was a noticeable lack of agreement between estimated and observed values of T towards the end of the 2021/2022 season (Figure 4.49 A and C). This could be partly be due to the estimates of FIPAR, especially in April where errors were observed ibn FIPAR estimates. However, this discrepancy in FIPAR estimates was observed in the 'Choctaw' cultivar. This in part, indicates that these errors could not only be attributed to the FIPAR estimates. It could be related to the observed increase in  $K_t$  values at the end of the season, which coincides with nut filling and a flush of leaves. The perceived increase in canopy conductance at this time might not be accounted for and as a result, T is poorly estimated in both model at this time. This seems to particularly be the case for 'Wichita' trees. Overall, the model indicated acceptable results for estimating daily T in the different cultivars across the different regions. As indicated by the model statistics, all the orchards were evaluated within the acceptable range (i.e. an  $RMSE < \text{half the standard deviation of measured values}$ ,  $R^2 > 0.8$ ,  $MAPE < 20\%$  and  $D > 0.8$  (de Jager, 1994).

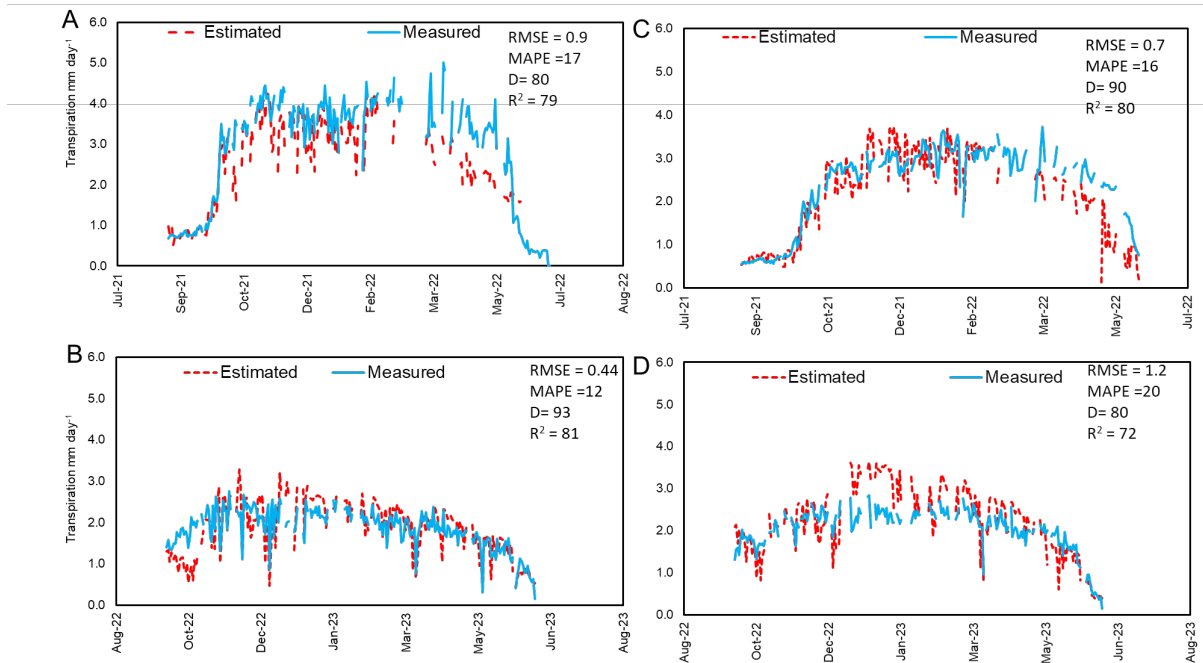


**Figure 4.49 Daily measured and estimated transpiration for Wichita' trees in A) 2021/22 and B) 2022/23 seasons and 'Choctaw' trees in the C) 2021/22 and (D) 2022/23 seasons in Groblershoop.**

When considering the seasonal dynamics of the modelled estimates versus measured transpiration in Vaalharts, better estimates for both cultivars were observed compared to Groblershoop during the 2021/2022 season (Figure 4.50 A and C). The model was evaluated with high statistic indices with a RMSE < half the standard deviation of measured values,  $R^2 > 0.8$ , MAPE < 20% and D > 08, except for 'Choctaw' the 2022/2023 season, where an  $R^2$  0.72 was observed. Again, when considering the FIPAR estimates during that period, it was evident that some of the part of the errors could be a result of poor estimates of the FIPAR

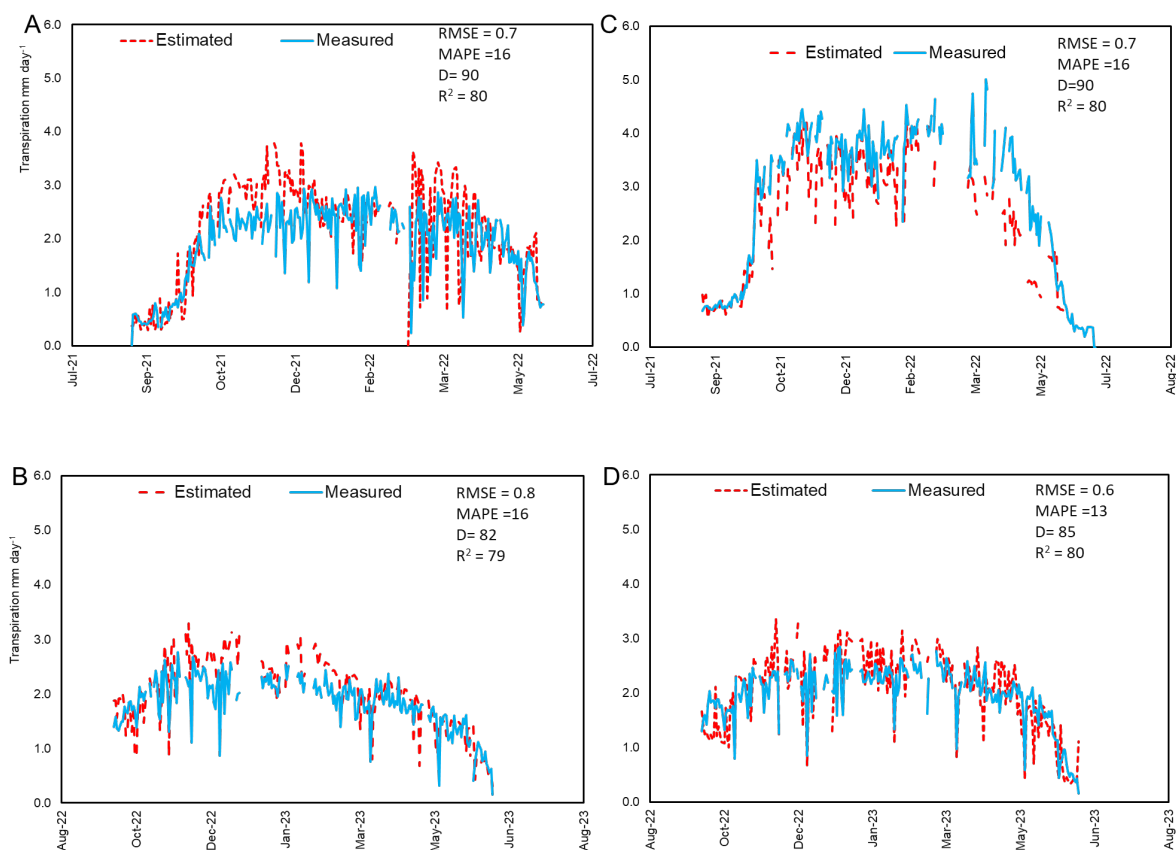


**Figure 4.50** Daily measured and estimated transpiration for 'Wichita' trees in **ABCD**

The model performed better for all the two trial sites when monthly estimates were considered in Groblershoop (Figure 4.51 and Figure 4.51). The model was evaluated with better statistical indices for most scenarios, except 'Wichita' in Groblershoop (Figure 4.51 B). These errors need to be further investigated as the inability of the model to accurately estimates T in this pecan orchards cannot be solely due to errors in the model inputs.



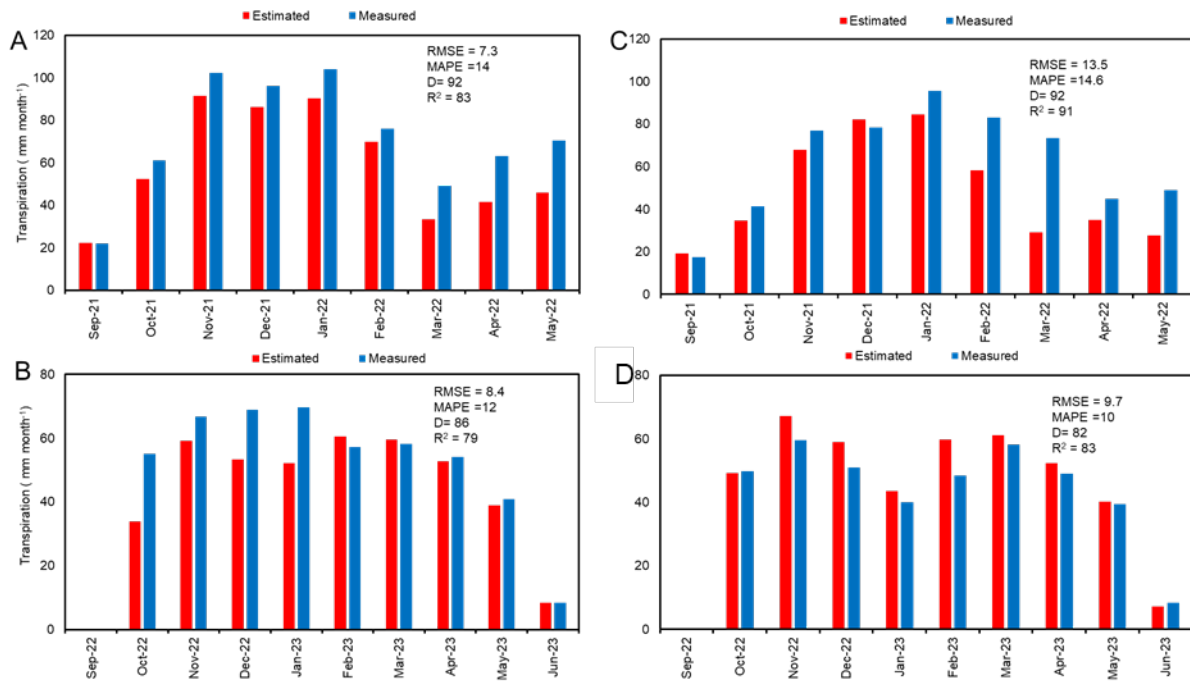


**Figure 4.51 Monthly measured and estimated transpiration for Wichita' trees in A) 2021/22 and B) 2022/23 seasons and 'Choctaw' trees in the C) 2021/22 and (D) 2022/23 seasons in Groblershoop.**

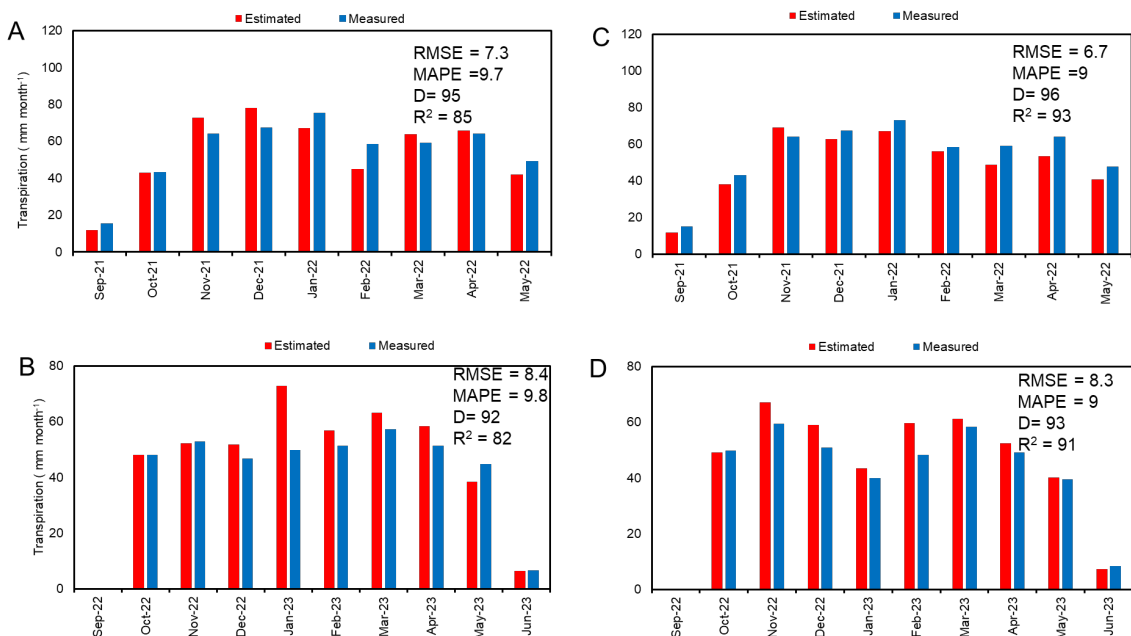


**Figure 4.52 Monthly measured and estimated transpiration for Wichita' trees in A) 2021/22 and B) 2022/23 seasons and 'Choctaw' trees in the C) 2021/22 and (D) 2022/23 seasons in Vaalharts**

### 4.3 CONCLUSIONS

Water use of two pecan orchards in two production regions was successfully quantified over a number of years in each location. This included transpiration, evapotranspiration and evaporation measurements. Values reported in this study fell in the range of those reported in literature, although ET in Groblershoop exceeded reported values in the hottest seasons. Tree transpiration was clearly impacted by both canopy size and the prevailing weather conditions, with transpiration tending to increase with both canopy size and atmospheric evaporative demand. However, the relationship with both of these was not linear. It was evident that transpiration did not increase at the same rate throughout the full range of  $ET_o$  values, with a plateau in transpiration reached as it became too hot and dry. Whilst there was a good relationship between transpiration and canopy size at the start of a season, when maximum canopy cover was reached canopy size could not explain all the variation in transpiration. This is the period associated with an increase in  $K_t$  values despite a similar increase in canopy size not occurring. This trend was observed across both cultivars and regions. This suggests that stomata play a role in regulating water use in pecans.

As a result of the stomatal control over transpiration two approaches were tested to model transpiration, a crop coefficient approach taking into consideration stomatal control over transpiration and a canopy conductance approach based on intercepted radiation by the canopy. Both models estimated transpiration well on a monthly basis, but not as well on a daily basis. As a result, either model could be used for irrigation planning and irrigation system design. Both models were parameterised in one season and validated in another using generic values for pecans. The good performance of the model was therefore particularly satisfying as it performed well across regions and cultivars, suggesting the parameters are transferable across regions.

As expected, evaporation rates were dependent on soil water availability in the top soil layer and energy reaching the soil surface, which was impacted by the canopy cover in the orchard. The FAO-56 approach performed reasonably well in both orchards, but a number of parameters are required in order to model  $E_s$  successfully which limits the ability to employ this model readily in orchards to estimate ET using a dual modelling approach.

The profitability of pecans per  $m^3$  of irrigation water applied explains why plantings are expanding so rapidly in the Northern Cape. In Vaalharts, more than half the scheme is now estimated to be planted to pecans. If only  $WP_c$  or  $WP_l$  was considered to determine the productive use of water in both regions and the sustainability of pecan production, pecans

would likely be deemed to be unsustainable. This is important as this is the metric reported in popular literature for consumers. Whilst more water is required to produce a pecan crop than most other crops (except for lucerne) in Vaalharts, it can largely be attributed to a longer growing season than most other annual crops. However, if one considers summer-winter crop rotations, pecan annual water use is similar to these cropping systems. Concerns regarding the high water use of pecans relative to other crops are therefore not valid, and the total planted area on schemes relative to available water should rather be considered if plantings take place outside of existing allocations. If only the profitability of water evapotranspired or applied is considered, then pecans are the best use of water in both schemes when average or above average rainfall is received. However, in drought years when water allocations are restricted the flexibility allowed by annual crop production would be advantageous, in order to make the most of the given allocation.

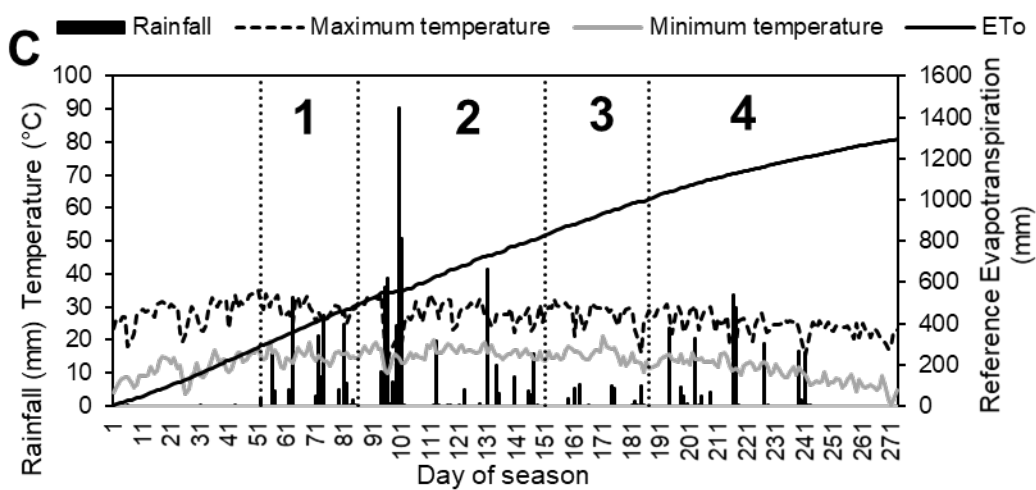
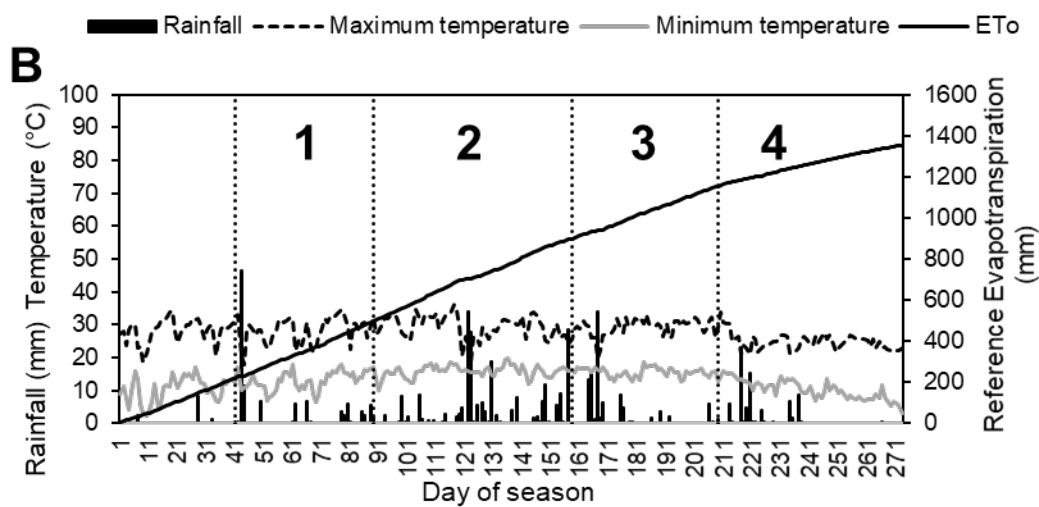
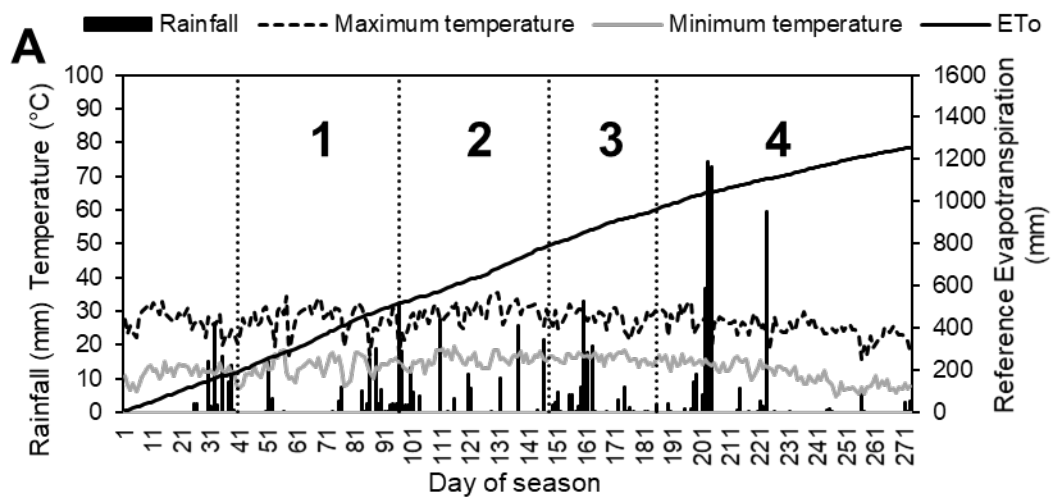
What is very evident from the study is that data from a single season can be very misleading and averages over longer periods of time should be considered when deciding on benchmark values for these parameters. In addition, using one estimate for different climatic regions is unfair, due to differences in  $ET_o$  and rainfall which impact both  $ET_o$  and irrigation requirements. Whilst this was done for annual crops using SAPWAT 4 and long term averages, estimates for pecan using SAPWAT 4 were not accurate enough as a result of no water use data available for pecans at the time of release of SAPWAT 4. Improved modelling approaches for pecans could assist in running multiple year ET simulations for different irrigation systems. Values for EWP are also season specific since both commodity price and production costs vary from year to year.

Importantly, none of the metrics used in this study are very useful when assessing the sustainability of water use, as suggested by Fereres et al. (2017). Evapotranspiration is largely dictated by atmospheric conditions, which the grower has no control over, and by only measuring irrigation it is impossible to assess how well irrigation is scheduled in an orchard. The assessment of the water balance in orchards and fields may provide a better understanding of the productive use of water in orchards, as deep drainage and surface run-off can be quantified. Deciding on the best use of irrigation water in a region should not be based on simple metrics alone, but needs to consider the whole soil-plant-atmosphere continuum and catchment under consideration holistically in order to provide meaningful data for the improvement of the productive use of water in agriculture. Further research should be done to determine if  $ET_o$  could be used to normalise ET of the crops in different regions to allow for fair comparisons between regions.

## **4.4 IMPACT OF WATER STRESS AT DIFFERENT PHENOLOGICAL STAGES ON YIELD AND QUALITY OF PECANS**

### **4.4.1 WEATHER VARIABLES**

Daily weather data for each season and each phenological stage is presented in Figure 4.53. The maximum temperatures for the season were recorded during flowering and nut set for 2019/20, 2020/21 and 2021/22 seasons, whilst for the 2017/18, 2018/19 and 2022/23 seasons the maximum temperature was recorded in mid-summer during nut sizing. In the first three seasons the maximum temperature was 1-2°C higher than the last three seasons. In terms of average temperatures, the fourth and fifth seasons were 1°C cooler than the other seasons. This is largely explained by the differences in rainfall and is also reflected in differences in seasonal  $ET_o$ . In terms of total  $ET_o$  from 1 September to 31 May of each season, the seasons were fairly similar with total  $ET_o$  for the growing season being 1255 mm, 1353 mm, 1298 mm, 1199 mm, 1154 mm and 1214 mm in the first, second, third, fourth, fifth and sixth season respectively. Rainfall, however, differed quite considerably for the five seasons, with the lowest rainfall (500 mm) recorded in the second season, compared to the first (790 mm), third season (750 mm) and fourth season (715 mm), fifth (990 mm) and sixth seasons (790 mm). In the first, third and sixth seasons there were rainfall events which exceeded 50 mm in a single day (Figure 4.53). These values made a big contribution to total seasonal rainfall, but due to the intensity of the events very little would have been available to the trees. Rainfall was generally very low before flowering and at shuck dehiscence with the most rain received during nut sizing and nut filling. Minimum temperatures in winter have been very similar, with the winter of 2020 recording the lowest temperature of the five seasons. However, chill unit accumulation has differed quite significantly over the five seasons (Figure 4.54). In the 2017, 2018 and 2019 season chill unit accumulation was less than 300 positive chill units (PCU), but in the 2020, 2021 and 2022 seasons more than 500 PCUs were accumulated. This together with heat in spring impacts canopy development of pecan orchard (Sparks, 1993)



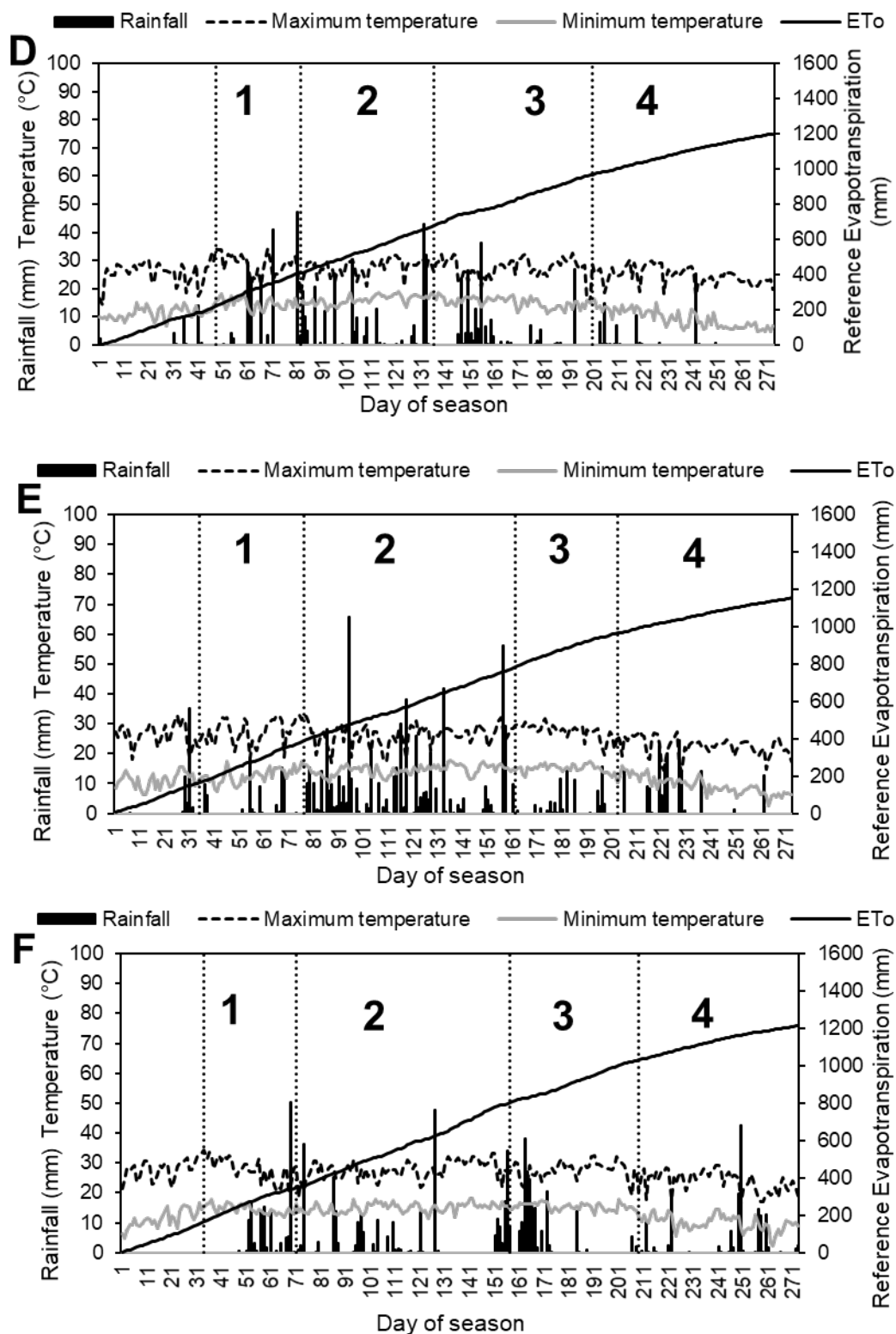


**Figure 4.53 Daily weather variables (1 September to 31 May) on the Hatfield Experimental Farm (Innovation Africa@UP) for the A) 2017/18, B) 2018/19, C) 2019/20, D) 2020/21, E) 2021/22 and F) 2022/23 seasons, indicating each phenological stage. 1 – flowering, 2 – nut sizing, 3 – nut filling, 4 – shuck dehiscence.  $ET_o$  – reference evapotranspiration**

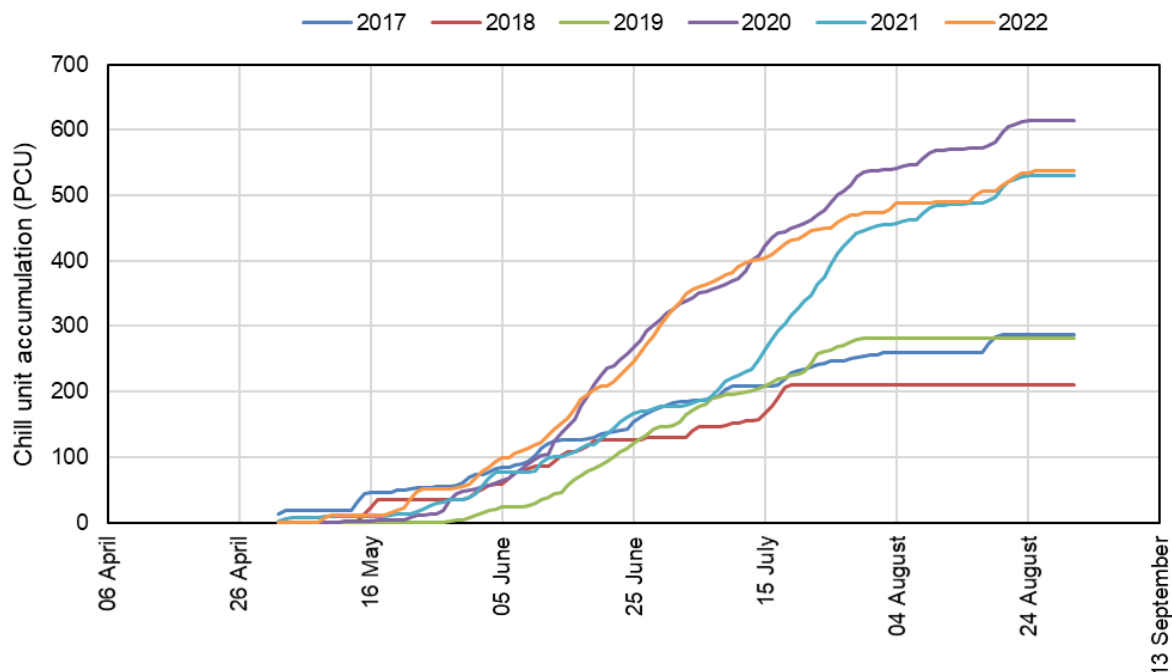


**Figure 4.54 Chill unit accumulation in winter from 2017 to 2022. Chill units were calculated using the positive daily chill unit model of Linsley-Noakes et al. (1995)**

#### 4.4.2 IRRIGATION MANAGEMENT

The volume of water, as rainfall and irrigation, received by the orchard, for the six seasons is presented in Table 4.14. The total irrigation applied for the well-watered control for season one (2017/18), two (2018/19), three (2019/20), five (2021/2022), and six was 144 mm, 215 mm, 220 mm, 76 mm and 263 mm respectively and the total amount of water per season, including rainfall was 937 mm for season one, 715 mm for season two, 973 mm for season three, 1065 mm for season five and 1056 mm for season six. During the fourth season (2020/2021), water meter readings were not recorded and total irrigation for each treatment was therefore not determined. The variation in the volume of irrigation water applied in each season was due to the differences in the amount of rainfall received. For instance, more irrigation (215 mm) was applied in the second season compared to the first season due to lower rainfall in the second season (500 mm). Although 753 mm was received in the third season, irrigation volumes were still fairly high (220 mm) as 260 mm of rainfall fell within 8 days in December 2019 and therefore rainfall for the rest of the season was comparable to the 2018/2019 season. Although irrigation was not recorded in the 2020/21 season, rainfall was quite high and well distributed throughout the season, resulting in fewer irrigation events than the previous seasons. The 2021/2022 season was the wettest season recorded in this study, with a total rainfall of 989 mm throughout the season (Figure 4.55). A large proportion

of this rainfall fell during the nut sizing stage (610 mm), which resulted in only a 7% reduction in irrigation as compared to the well-watered treatment. As expected, the well-watered treatment (control) received the highest irrigation across all treatments in all five seasons as it was irrigated optimally. As water stress was implemented at each phenological stage, a reduction in irrigation water at flowering and nut set, nut sizing, nut filling and shuck dehiscence resulted in water savings of 13%, 14%, 15% and 41% in the first season, 5%, 3%, 16% and 30% in the second season, 35%, 28%, 33% and 49% in the third season, 47%, 7%, 21 and 12% in the fifth season, and 27%, 47%, 41 and 52% in the sixth respectively, when compared to the well-watered control (Table 4.14).

The distribution of the higher rainfall in the 2020/21 to 2022/23 seasons is shown in Figure 4.55. In all three of these seasons, rainfall was well distributed throughout the season, with regular rainfall events. This was particularly noticeable in the 2021/22 season (Figure 4.55B).

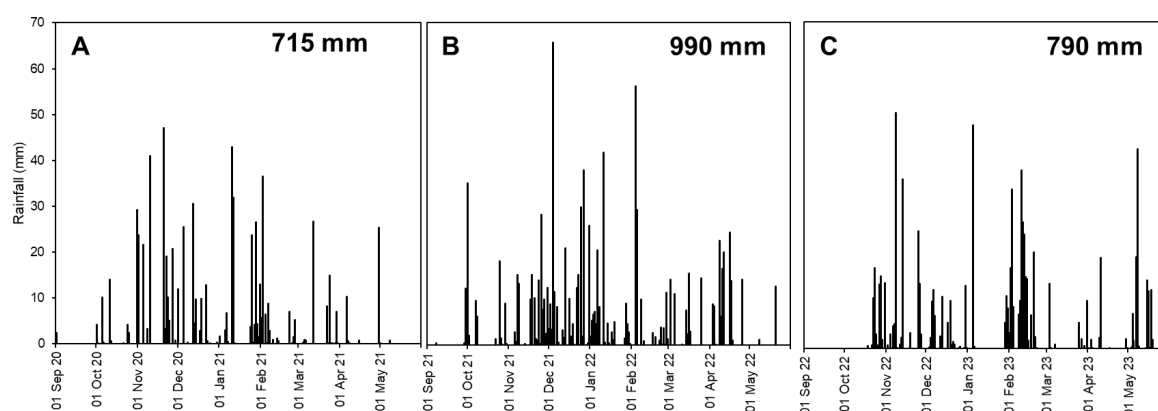


**Figure 4.55 Seasonal rainfall at Innovation Africa@UP for the A) 2020-2021, B) 2021-2022 and C) 2022-2023 growing seasons**



**Table 4.14 Seasonal water application; Irrigation and rainfall water applied at the different phenological stages as water stress was implemented for five seasons. Season one (2017/2018), season two (2018/2019), season three (2019/2020), season four (2020/2021), season five (2021/2022), and season six (2022/23). ND-not determined**

	Treatment	Rainfall (mm)	Irrigation (mm)	% irrigation water saved	Total (mm)
<b>Season 1</b>	Well-watered	793	144		937
<b>2017/2018</b>	Flowering and nut set	700	125	13	825
	Nut sizing	604	124	14	728
	Nut filling	675	123	15	798
	Shuck dehiscence	491	84	42	575
<b>Season 2</b>	Well-watered	500	215		715
<b>2018/2019</b>	Flowering and nut set	400	163	24	563
	Nut sizing	283	144	33	427
	Nut filling	401	137	36	538
	Shuck dehiscence	428	168	22	596
<b>Season 3</b>	Well-watered	753	220		973
<b>2019/2020</b>	Flowering and nut set	591	147	33	738
	Nut sizing	377	168	24	545
	Nut filling	718	149	32	867
	Shuck dehiscence	574	171	22	745
<b>Season 4</b>	Well-watered	713	90		ND
<b>2020/2021</b>	Flowering and nut set	537	ND	ND	ND
	Nut sizing	460	ND	ND	ND
	Nut filling	529	ND	ND	ND
	Shuck dehiscence	644	ND	ND	ND
<b>Season 5</b>	Well-watered	989	76		1065
<b>2021/2022</b>	Flowering and nut set	910	40	47	950
	Nut sizing	380	71	7	451
	Nut filling	908	60	21	968
	Shuck dehiscence	823	67	12	890
<b>Season 6</b>	Well-watered	793	263		1056
<b>2022/2023</b>	Flowering and nut set	571	192	27	763
	Nut sizing	586	138	47	724
	Nut filling	583	154	41	737
	Shuck dehiscence	650	126	52	776

#### **4.4.3 CANOPY DEVELOPMENT AND SENESCENCE**

Canopy development at the beginning of the season and senescence at the end of each season was assessed to determine the effect of water stress on the canopy. Early canopy growth and development were impacted by water stress implemented during the flowering and nut set stage, with clear differences between the stressed and well-watered treatments. Canopy growth was slightly delayed by water stress from October to November in both seasons, reaching the maximum canopy growth a week after the well-water treatment (Figure 4.56). Since the water stress at the nut sizing and nut filling stages were implemented when the canopy had achieved its final size, there were no differences in canopy cover between these treatments and the well-watered control. However, the impact of water stress at the end of the season (final stage, shuck dehiscence) hastened leaf fall/senescence, resulting in a faster decline in canopy size. This is evident by the clear differences observed from April to June in both seasons, with the stressed treatment reaching 0% canopy cover a week before the well-water treatments (Figure 4.56). This could have an impact on stored reserves in these trees and alternate bearing patterns, as Wood (1995b) found that the post-fruiting period is very important for building reserves for the following season. According to Wells (2018), as the crop approaches maturity, the tree's physiology changes from sending energy to the developing kernels to storage in storage tissues (stem, roots, trunk). The early leaf senescence when stress is imposed during shuck dehiscence may impact long terms storage of carbohydrates and canopy development and lowering in the following season. Despite this hastening of leaf senescence in the shuck dehiscence treatment, it did not appear to impact yield the following season. Although in the last two seasons very little stress was achieved in this final phenological stage.

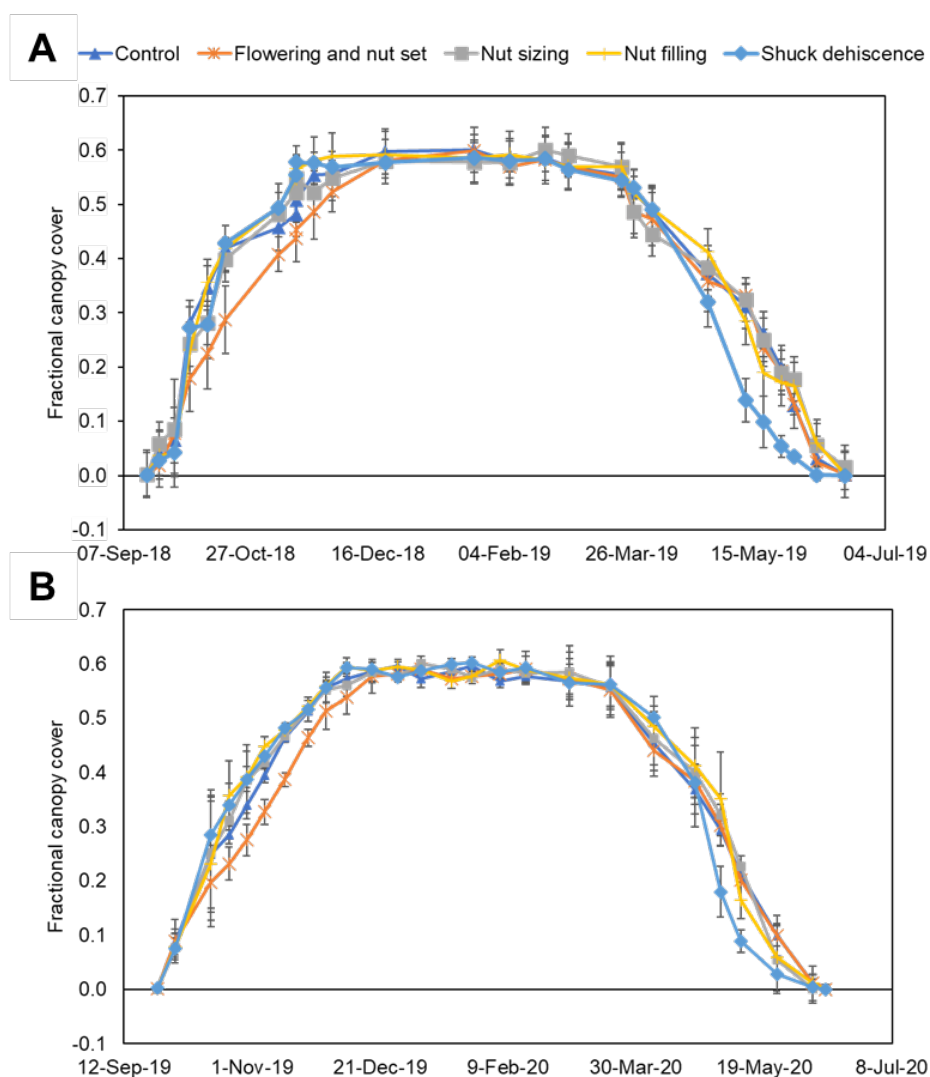


**Figure 4.56** Changes in fractional canopy cover for the various treatments for the A) 2018/2019 season and B) 2019/2020 season

#### 4.4.4 MIDDAY AND PREDAWN STEM WATER POTENTIAL

Measurements of leaf water potentials (predawn and midday) were taken throughout six growing seasons from 2017 to 2023 to monitor plant water stress, with stress at each phenological stages being compared to the well-water control. Jones (2007) indicates that this is a good integrator of the soil, water and climatic parameters. Increasing soil water deficits at each phenological stage led to decreasing midday stem water potential ( $\psi_{smd}$ ) values (Figure 4.57). Water stress was evident at all phenological stages in the second and third season as  $\psi_{smd}$  values fell below the threshold value of -0.90 MPa, as outlined by Othman et al. (2014). However, for the first season (Figure 4.57A), the trees did not experience significant water stress at the final phenological stage (shuck dehiscence), with minimum  $\psi_{smd}$  values of -0.82

MPa and this was due to high rains received at this stage (280 mm from mid-March to mid-April). Nevertheless, during the flowering and nut set stage, the  $\psi_{\text{smd}}$  decreased to -1.10 MPa, -1.11 MPa at nut sizing and fell to -1.18 MPa during nut filling, as irrigation was withdrawn. In the second season, the lowest average  $\psi_{\text{smd}}$  value obtained at flowering and nut stage was -1.01 MPa, -1.35 MPa at nut sizing, -1.23 MPa at nut filling and -1.38 MPa at shuck dehiscence (Figure 4.57B). Importantly, during this season there was a decrease in  $\psi_{\text{smd}}$  in the control treatment during the flowering and nut set stage, which was caused by a temporary breakdown in the irrigation system to this treatment, which then had to be irrigated by hand. Water stress was also achieved in the third season, with lowest  $\psi_{\text{smd}}$  values of -1.12 MPa, -1.15 MPa, -1.17 MPa and -1.32 MPa at flowering and nut set, nut sizing, nut filling and shuck dehiscence respectively during stress at each of these phenological stages (Figure 4.57). During this season, a sudden increase of  $\psi_{\text{smd}}$  was observed in all treatments during the nut sizing stage due to the very high rainfall during December 2019 (260 mm in 8 days). In the fourth season, stress was only implemented in the nut filling stage, with a minimum value of -1.16 MPa (Figure 4.57 D). The minimum  $\psi_{\text{smd}}$  of the flowering and nut set, nut sizing and shuck dehiscence were -0.49 MPa, -0.89 MPa and -0.89 MPa respectively. From the middle of the fourth season,  $\psi_{\text{smd}}$  was only measured in the control and stressed treatment. In the fifth season, a mild stress could not be implemented throughout the season, although the relevant treatment trees were had lower  $\psi_{\text{smd}}$  than the other treatments (Figure 4.57). This was largely due to the regular rainfall that was received throughout the season which prevented the soil from drying. In addition, despite plastic covering the area allocated to the stressed trees, water seemed to move laterally in the soil and the plastic was therefore insufficient to eliminate rainfall when rainfall events were too high. The lowest  $\psi_{\text{smd}}$  in the fifth season for flowering and nut set, nut sizing, nut filling and shuck dehiscence was -0.74 MPa, -0.54 MPa, -0.89 and -0.77 MPa respectively.

In the sixth season, mild stress could not be implemented, with only a slight stress occurrence during the shuck dehiscence stage with an average  $\psi_{\text{smd}}$  value of -0.81 MPa (Figure 4.57 F). The lack of successful stress induction during this season was primarily attributed to the high rainfall, with a total of 797 mm recorded. This marked the second highest amount of rainfall received during the six seasons of stress implementation.

In all six seasons, after the completion of each phenological stage, the trees were re-watered and as a result the water potentials increased, reaching the well-watered control midday stem water potential values soon after the completion of the stress cycle.

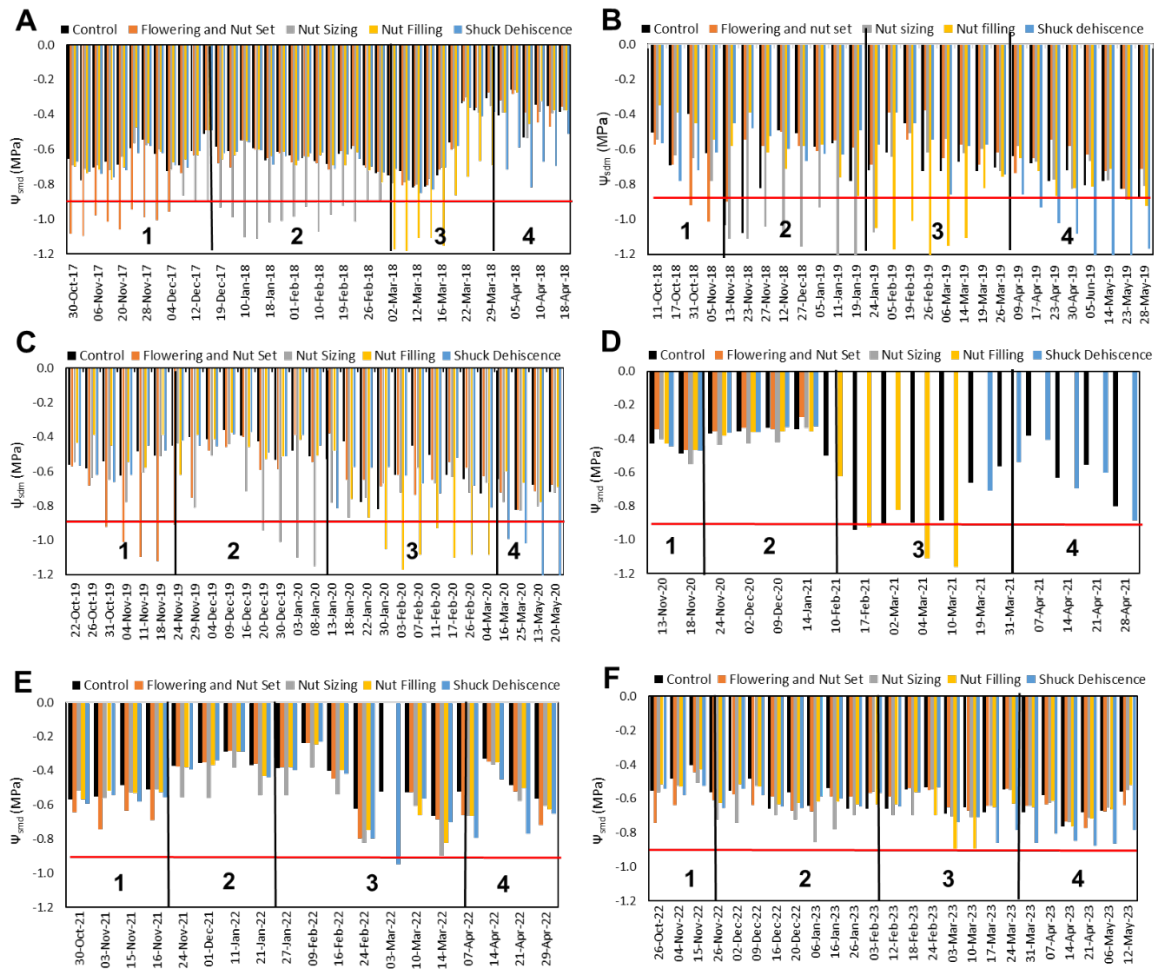


**Figure 4.57** Midday stem water potential ( $\psi_{smd}$ ) for the six seasons. A) season one (2017/18), B) season two (2018/19), C) season three (2019/20), D) season four (2020/21) E) season five (2021/22) and season six (2022/23). The vertical lines on each figure indicates the different phenological stages (1 – flowering and nut set, 2 – nut sizing, 3 – nut filling and 4 – shuck dehiscence). The horizontal red line demonstrates the stem water potential threshold value (-0.90 MPa) for mild stress as outlined by Othman et al. (2014)

Predawn leaf water potentials ( $\psi_{pd}$ ) measurements were also determined for the five different seasons (Figure 4.58), which exhibited the same pattern as the midday stem water potential values. In this study, it was found that a threshold  $\psi_{smd}$  of 0.9 MPa corresponded to a  $\psi_{pd}$  of 0.42 MPa. For the first season, minimum  $\psi_{pd}$  values of -0.38 MPa, -0.41 MPa, -0.48 MPa and -0.20 MPa were recorded during stress at flowering and nut set, nut sizing, nut filling and shuck dehiscence, respectively (Figure 4.58A). Figure 4.58B, presents  $\psi_{pd}$  values for the second season and recorded minimum values of -0.54 MPa at flowering and nut set stage, -0.71 MPa at nut sizing, -0.57 MPa at nut filling and -0.63 MPa at the final stage of nut development (shuck dehiscence). Likewise, a similar response to water stress imposed at different

phenological stages was observed during the third season, with minimum  $\psi_{pd}$  values of -0.66 MPa, -0.76 MPa, -0.58 MPa and -0.68 MPa were obtained during stress at flowering and nut set, nut sizing, nut filling and shuck dehiscence stages, respectively (Figure 4.58C).

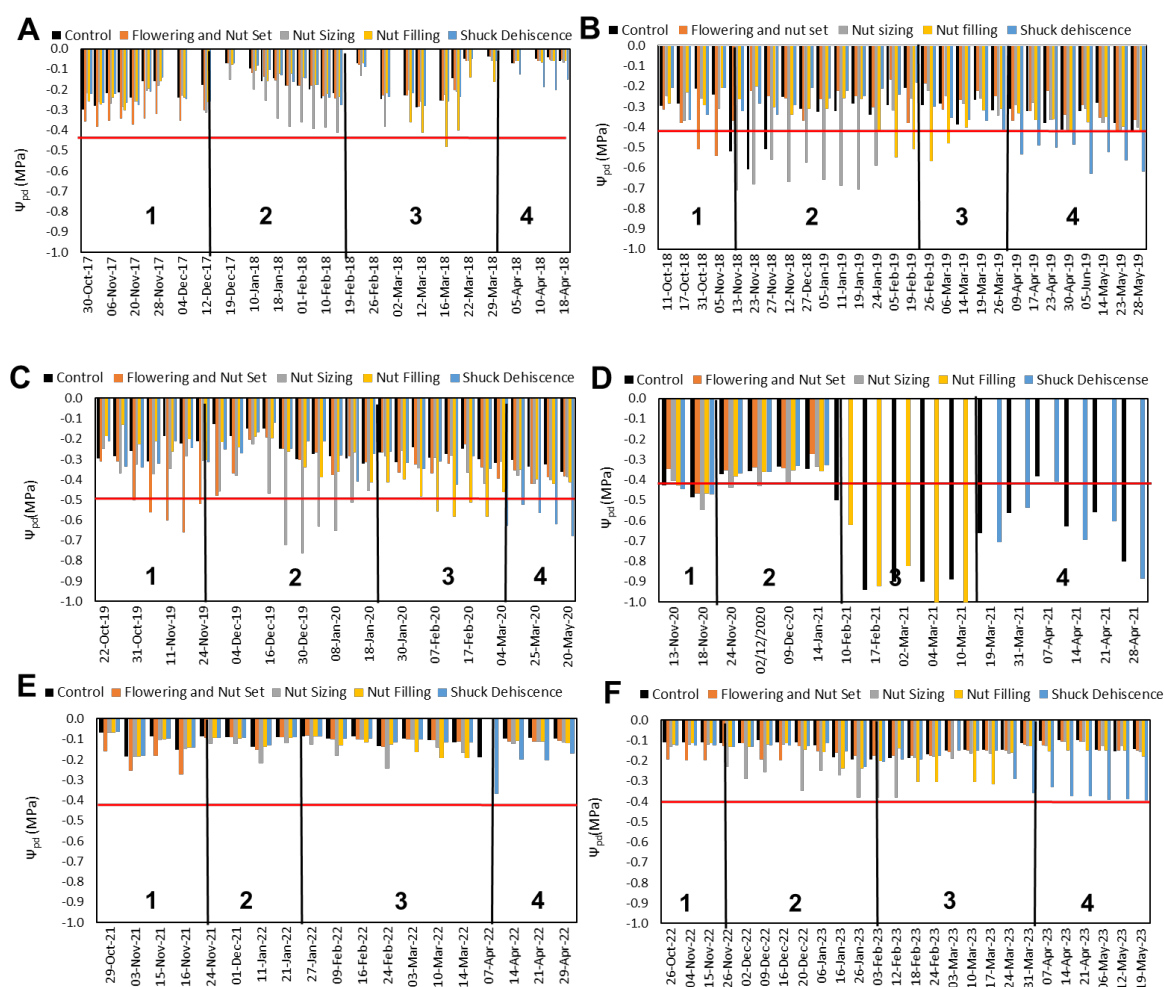


**Figure 4.58** Predawn leaf water potential ( $\psi_{pd}$ ) for the five seasons. A) season one (2017/18), B) season two (2018/19), C) season three (2019/20), D) season four (2020/21), E) season five (2021/22) and F) season six (2022/23). The vertical lines on each figure indicate the different phenological stages (1 – flowering and nut set, 2 – nut sizing, 3 – nut filling and 4 – shuck dehiscence). The horizontal red line demonstrates the predawn water potential threshold value (-0.45 MPa) for mild stress as determined in this study from the relationship between  $\psi_{pd}$  and  $\psi_{smd}$ .

In the fourth season the trend of  $\psi_{pd}$  measurements showing the same trend as  $\psi_{smd}$  continued but measurements suggest that some stress was experienced at the end of the nut sizing stage (Figure 4.58D). Minimum  $\psi_{pd}$  values of -0.40 MPa, -0.44 MPa, -0.47 MPa and -0.33 MPa were recorded when stress was applied during flowering and nut set, nut sizing, nut filling and shuck dehiscence stages, respectively. In the fifth season of the trial, no stress was recorded for all the treatments, which reflected what was found with  $\psi_{smd}$  measurements for the same

period. The lowest  $\psi_{pd}$  for flowering and nut set, nut sizing, nut filling and shuck dehiscence stages were -0.27 MPa, -0.25 MPa, -0.20 MPa and -0.35 MPa respectively (Figure 4.58 E). In the sixth season,  $\psi_{pd}$  in the stressed trees was lower than in the control trees for most phenological stages, but these values did not exceed the stress threshold. The lowest  $\psi_{pd}$  for flowering and nut set, nut sizing, nut filling and shuck dehiscence stages were -0.20 MPa, -0.40 MPa, -0.30 MPa and -0.40 MPa respectively (Figure 4.58 F).

It is evident that for the vast majority of the first three seasons, mild stress was achieved during each of the stress periods, apart from shuck dehiscence in the first season. Valid conclusions regarding the impact of a mild water stress at different phenological stages on the yield and quality of pecan trees can therefore be made from these seasons. Unfortunately, due to high rainfall experience in the 2020/21, 2021/22 and 2022/23 seasons, data from these seasons have not contributed to our understanding of how water stress at different phenological stages impacts yield and quality.

Since similarities in  $\psi_{smd}$  and  $\psi_{pd}$  were observed throughout the trial, the data was correlated to establish the relationship between the two parameters (Figure 4.59). A close linear relationship existed between  $\psi_{smd}$  and  $\psi_{pd}$ , with both values decreasing as available soil water was depleted.  $R^2$  values of 0.71, 0.73 and 0.74 were obtained for season one, two and three respectively (Figure 4.59). In the final three seasons, stress was not successfully implemented and thus a poor correlation was observed, with  $R^2$  values of 0.03, 0.23 and 0.52 for season four, season five and season six respectively. The poor correlation in season four can also be attributed to two different individuals measuring  $\psi_{pd}$  and  $\psi_{smd}$  in the orchard. There was an increased discrepancy between measurements when two people manually measure the water potentials and this may have increased the variability of the measurements, thus lowering the correlation. Bias as a result of user error is well known for measurements of leaf water potential (Prof E Fereres, personal communication). Better correlation in between  $\psi_{smd}$  and  $\psi_{pd}$  was observed in season 2022/23 (Figure 4.59 F) when compared to season 2020/21 and 2021/22 (Figure 4.59 D and E). However, there was a considerable amount of scatter between the two variables, resulting in a correlation coefficient ( $R^2$ ) of 0.53.

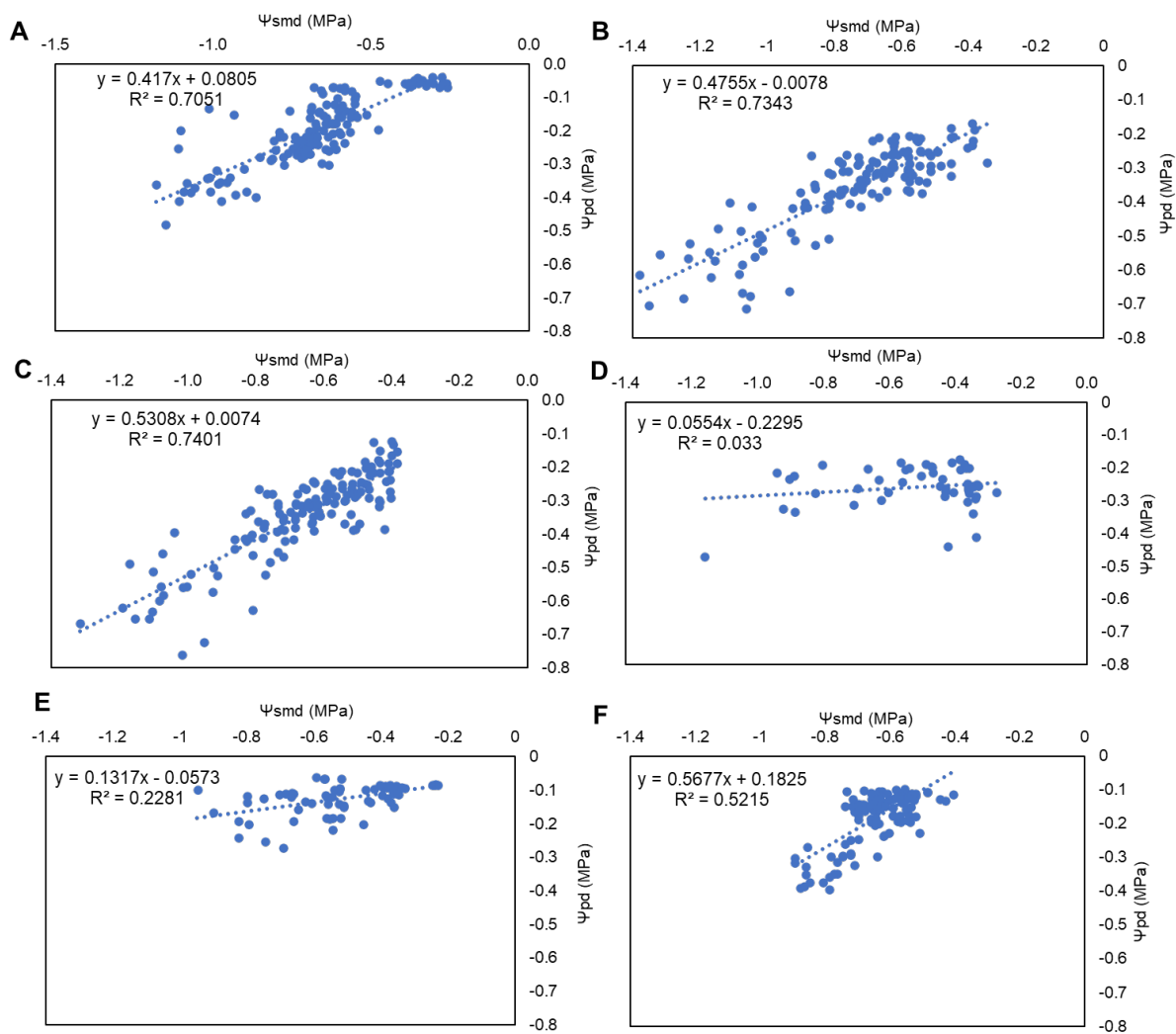


**Figure 4.59 Relationship between midday stem water ( $\Psi_{smd}$ ) and predawn leaf water potential ( $\Psi_{pd}$ ) for the six seasons. A) season one (2017/18), B) season two (2018/19), C) season three (2019/20), D) season four (2020/21), E) season five (2021/22) and F) season six (2022/23)**

When the data from all six seasons was combined, a linear relationship existed between  $\Psi_{smd}$  and  $\Psi_{pd}$ , with both values decreasing as available soil water was depleted. However, the observed  $R^2$  value was 0.54 which indicated a high scatter between two variables. This was largely influenced by the high scatter that was observed in the data from the past three seasons. When considering data from the 2018/19 and 2019/20 seasons, which gave the most consistent relationship, the  $\Psi_{pd}$  corresponding to a  $\Psi_{smd}$  of -0.90 MPa was -0.45 MPa.



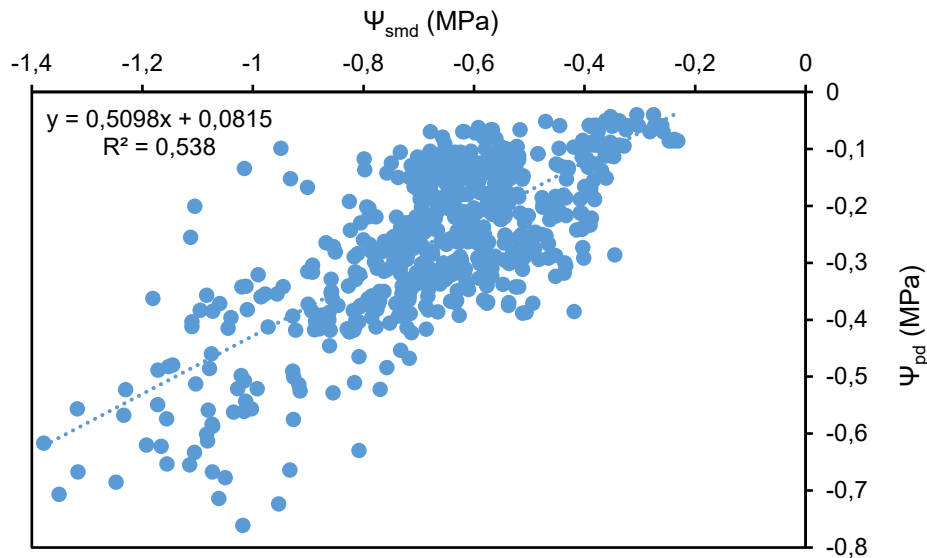


**Figure 4.60 Relationship between midday stem water ( $\Psi_{smd}$ ) and predawn leaf water potential ( $\Psi_{pd}$ ) for the six seasons combined**

#### 4.4.5 PHOTOSYNTHESIS AND STOMATAL CONDUCTANCE

The impact of water stress on gas exchange and photosynthesis at the different phenological stages was evaluated, since stomatal closure is amongst the first plant responses to rising soil water deficits (Cifre et al., 2005). Diurnal measurements of photosynthesis and stomatal conductance were taken before and during the implementation of water stress at each phenological stage (flowering and nut set, nut sizing, nut filling and shuck dehiscence) and compared with the well-watered control. Measurements were made during the second season, 2018/19.

##### 4.4.5.1 Flowering and nut set

During the flowering and nut set stage in season two (2018/19), a mild water stress ( $< -0.9$  MPa) was only successfully implemented towards the end of this phenological stage. Before stress implementation, there were no differences in stomatal conductance and photosynthesis between the well-watered control and stress treatment (Figure 4.61 A,C). In the morning, both stomatal conductance and photosynthesis were low and started to increase as the day progressed, with the highest values obtained close to midday, following which values began to decline. During the water stress period, highest stomatal conductance and photosynthesis values of the water stressed treatment were not significantly different from the control, but

there were clear differences between the control and stressed treatment as both stomatal conductance and photosynthesis declined during the afternoon (Figure 4.61 B,D). The highest stomatal conductance values were  $g_s = 0.314 \text{ mol m}^{-2} \text{ s}^{-1}$  and  $0.215 \text{ mol m}^{-2} \text{ s}^{-1}$  (Figure 4.61 B) and for photosynthesis were  $A_n = 15.03 \text{ } \mu\text{mol m}^{-2} \text{ s}^{-1}$  and  $11.98 \text{ } \mu\text{mol m}^{-2} \text{ s}^{-1}$  (Figure 4.61 D) for the well-watered and water stressed treatments respectively at midday.

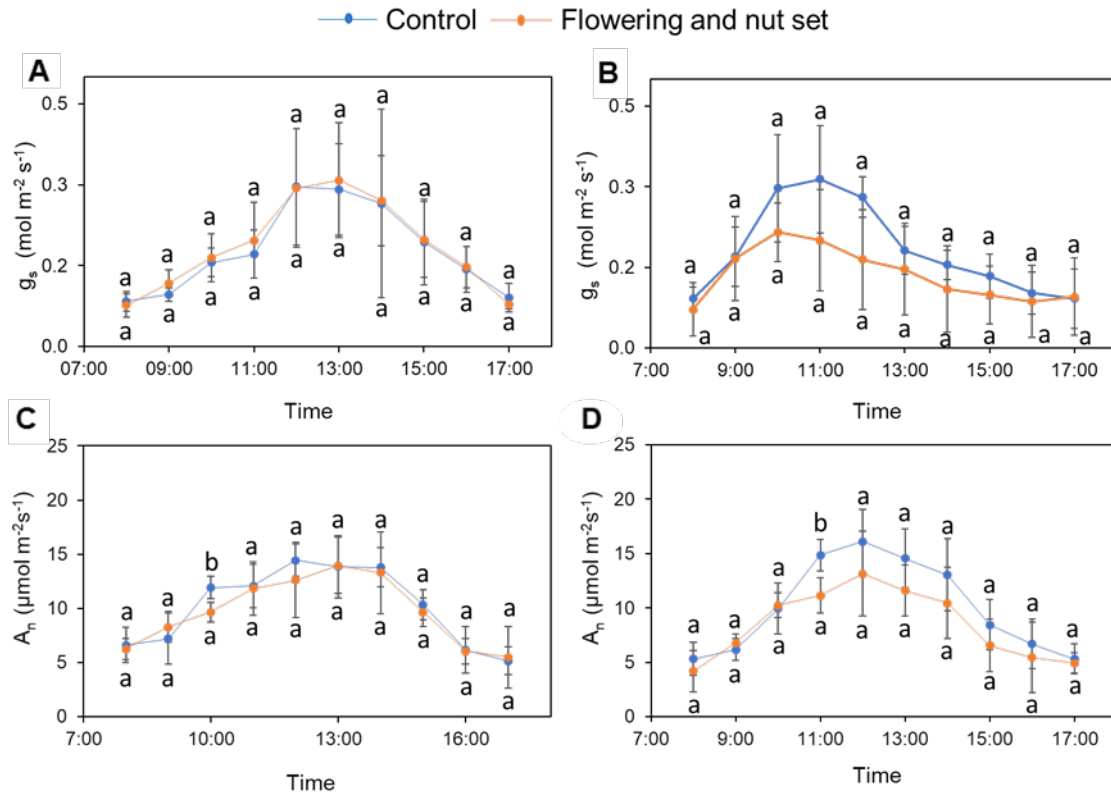


**Figure 4.61** Diurnal stomatal conductance ( $g_s$ ) A) before and B) during the water stress and photosynthesis ( $A_n$ ) C) before and D) during the water stress at the flowering and nut set stage. Each value was an average of 4-6 leaves from 4 trees. Mean values with the same letters are not significantly different from each other ( $p > 0.05$ )

#### 4.4.5.2 Nut sizing

The effects of water stress during this stage were noticeable by a decline in stomatal conductance and photosynthesis at midday (Figure 4.62 B,D). However, before the trees were exposed to water stress, there were no differences between stomatal conductance and photosynthesis for trees from the well-watered control and those trees to be stressed during the nut sizing stage (Figure 4.62 A,C). Although there were no significant differences at this stage between the well-watered control and the stressed treatment, some differences in values were evident (Figure 4.62 B,D). During the stress period there was a decline in both stomatal conductance and photosynthesis in the stressed trees. Midday stomatal conductance

values of  $g_s = 0.280 \text{ mol m}^{-2} \text{ s}^{-1}$  and  $0.201 \text{ mol m}^{-2} \text{ s}^{-1}$  (Figure 4.62 B) and photosynthesis of  $A_n = 15.03 \text{ } \mu\text{mol m}^{-2} \text{ s}^{-1}$  and  $11.98 \text{ } \mu\text{mol m}^{-2} \text{ s}^{-1}$  (Figure 4.62 D) were recorded for the control and the water stressed treatment, respectively.

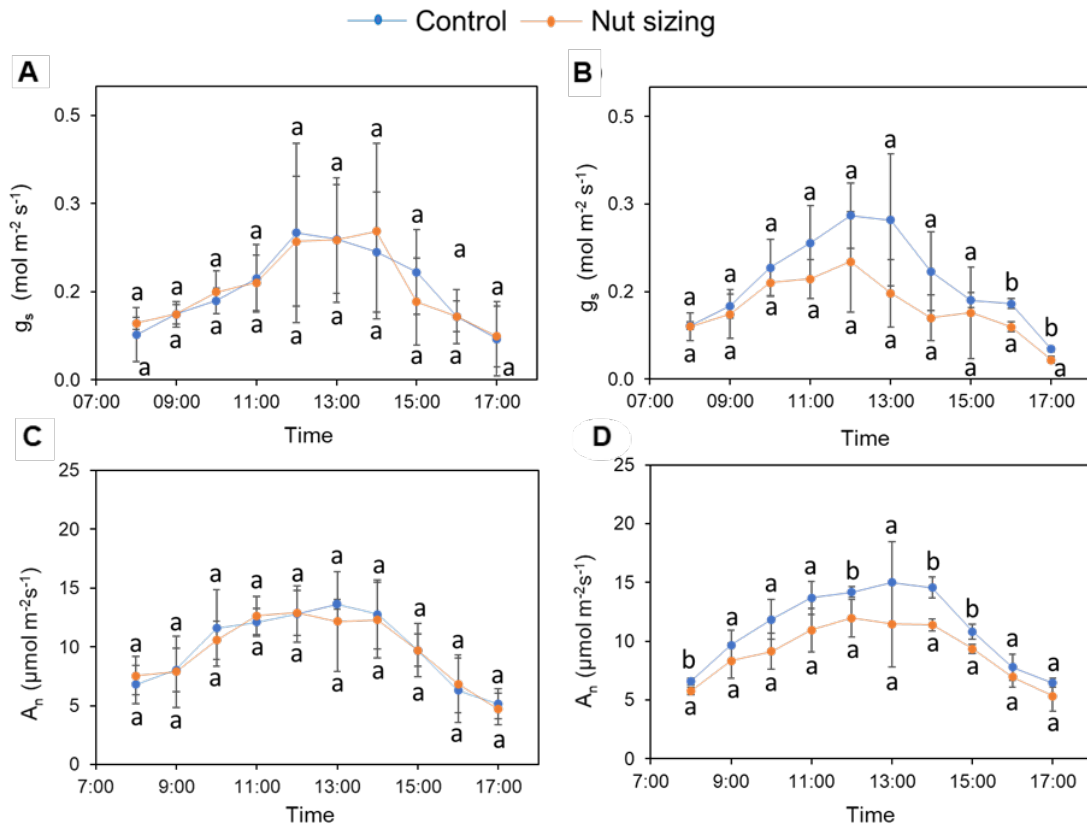


**Figure 4.62** Diurnal stomatal conductance ( $g_s$ ) (a) before and (b) during the water stress and photosynthesis ( $A_n$ ) (c) before and (d) during the water stress at the nut sizing stage. Each value was an average of 4-6 leaves from 4 trees. Mean values with the same letters are not significantly different from each other ( $p > 0.05$ )

#### 4.4.5.3 Nut filling

Before stress implementation at the nut filling stage, there were no differences between the two treatments recording highest stomatal conductance values of  $g_s = 0.236 \text{ mol m}^{-2} \text{ s}^{-1}$  and  $g_s = 0.253 \text{ mol m}^{-2} \text{ s}^{-1}$  for the control and the water stressed treatment respectively (Figure 4.63 A). The highest values for photosynthesis were  $A_n = 17.12 \text{ } \mu\text{mol m}^{-2} \text{ s}^{-1}$  and  $17.45 \text{ } \mu\text{mol m}^{-2} \text{ s}^{-1}$  for the well-watered and stress treatment respectively (Figure 4.63 C). During water stress in the nut filling there were no significant differences between the well-watered control and water stressed treatment, but stomatal conductance and photosynthesis tended to be lower in the water stressed treatment (Figure 4.63 B,D). The well-watered control recorded a maximum stomatal conductance of  $g_s = 0.280 \text{ mol m}^{-2} \text{ s}^{-1}$  which was higher than water stressed treatment where  $g_s = 0.201 \text{ mol m}^{-2} \text{ s}^{-1}$  (Figure 4.63 B). The highest average value for

photosynthesis was  $A_n=14.56 \mu\text{mol m}^{-2}\text{s}^{-1}$  and  $11.90 \mu\text{mol m}^{-2}\text{s}^{-1}$  (Figure 4.63 D) for the control and stressed treatment, respectively.

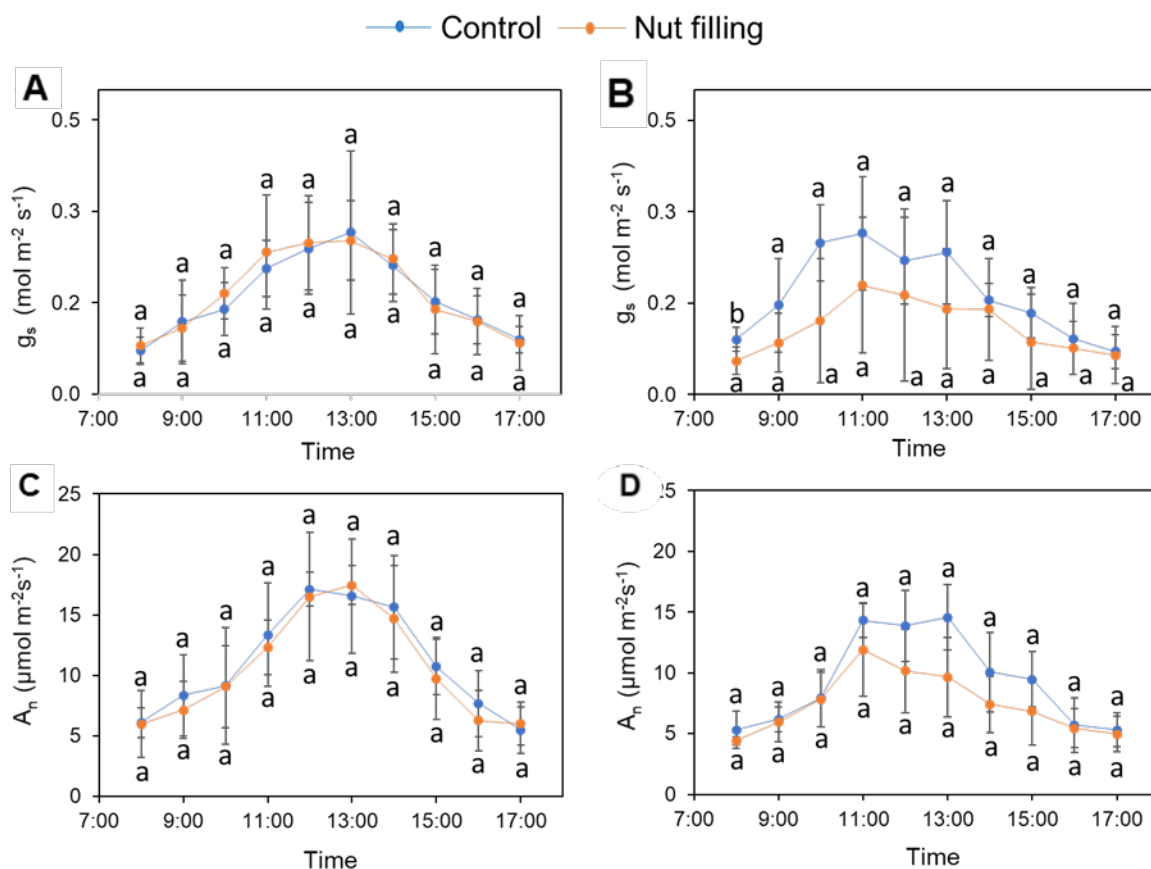


**Figure 4.63** Diurnal stomatal conductance ( $g_s$ ) A) before and B) during the water stress and photosynthesis ( $A_n$ ) C) before and D) during the water stress at the nut filling stage. Each value was an average of 4-6 leaves from 4 trees. Mean values with the same letters are not significantly different from each other ( $p > 0.05$ )

#### 4.4.5.4 Shuck dehiscence

The shuck dehiscence stage is the maturation stage of nut development. During this stage, an overall decrease in stomatal conductance and photosynthesis was observed due to the start of leaf senescence before entering the dormant stage. Before the onset of water stress there were no significant differences in stomatal conductance or photosynthesis between trees in the well-watered control and trees in the stress treatment (Figure 4.64 A,C). The highest stomatal conductance values before stress implementation were  $g_s = 0.207 \text{ mol m}^{-2} \text{s}^{-1}$  and  $g_s = 0.214 \text{ mol m}^{-2} \text{s}^{-1}$  for the well-watered and water stressed treatment respectively (Figure 4.64 A). Maximum photosynthesis values before stress implementation were  $A_n=11.31 \mu\text{mol m}^{-2}\text{s}^{-1}$  and  $10.22 \mu\text{mol m}^{-2}\text{s}^{-1}$  for the well-watered and water stressed treatment respectively (Figure 4.64c). During the stress period, lower stomatal conductance values were recorded

for the water stressed treatment when compared to the well-watered control (Figure 4.64 B). The values were  $g_s = 0.241 \text{ mol m}^{-2} \text{ s}^{-1}$  and  $g_s = 0.128 \text{ mol m}^{-2} \text{ s}^{-1}$  for the well-watered and water stressed treatment, respectively. Similar differences were observed for  $A_n$  during the stress period, with the water stressed treatment recording lower values than the well-watered control (Figure 4.64 B). The values were  $A_n = 9.95 \mu\text{mol m}^{-2} \text{ s}^{-1}$  and  $5.70 \mu\text{mol m}^{-2} \text{ s}^{-1}$  for the well-watered and water stressed treatment, respectively.

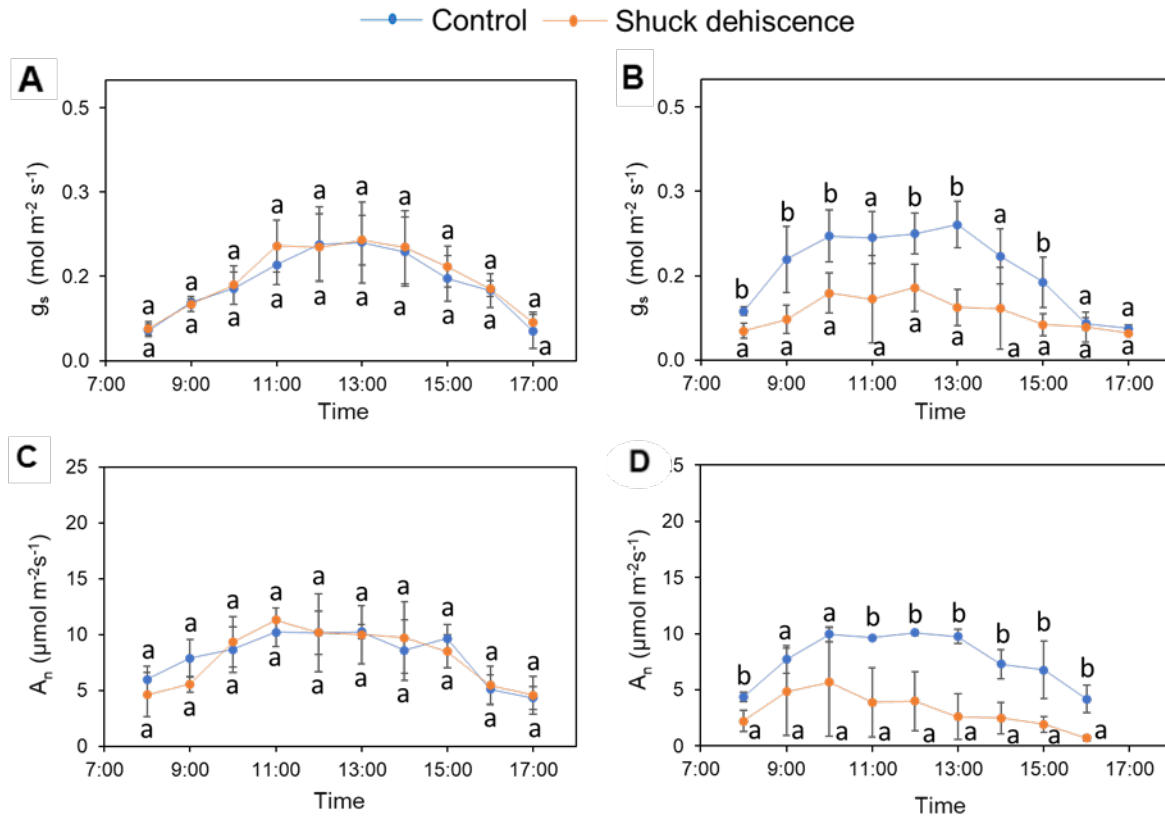


**Figure 4.64** Diurnal stomatal conductance ( $g_s$ ) A) before and B) during the water stress and photosynthesis ( $A_n$ ) C) before and D) during the water stress at the shuck dehiscence stage. Each value was an average of 4-6 leaves from 4 trees. Mean values with the same letters are not significantly different from each other ( $p > 0.05$ )

#### 4.4.5.5 Relationship between stem water potential and photosynthesis and stomatal conductance

A clear response of  $g_s$  and  $A_n$  to increasing water stress was evident throughout the trial, with both  $g_s$  and  $A_n$  declining as  $\Psi_{smd}$  decreased (Figure 4.65). A decline in leaf water potential led to a decline in  $g_s$ , which in turn resulted in a reduction in gas exchange and therefore  $A_n$ . Under water stress conditions stomata start to close to prevent leaf water potential from dropping to a point where cavitation occurs.

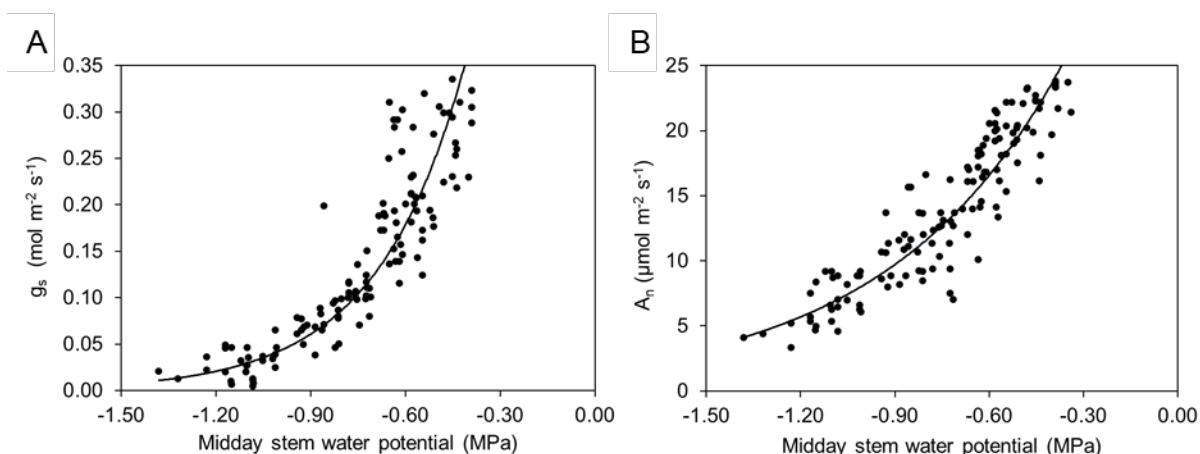


**Figure 4.65 The response of A) stomatal conductance and B) photosynthesis to increasing water stress as indicated by midday stem water potential in pecan trees**

#### 4.4.6 FLOWERING AND NUT SET

Flowering and nut set were recorded for the different treatments in the second and third season. The appearance of female flower was recorded from 5 October 2018 to 6 November 2018 in the second season (Figure 4.66A) and from 3 October 2019 to 13 November 2019 in the third season (Figure 4.66B). The duration of flowering and nut set was approximately five weeks in both seasons. During the first week of data collection, the average number of female flowers per cluster was approximately eight across all the treatments, with no statistical differences between treatments (Figure 4.66). However, differences between treatments started to become apparent from week two in both seasons, with a reduction in flower number in the treatment where water stress was applied during flowering and fruit set. This difference became significant in week four and five, when the total number of female flowers or nuts set per cluster in the water stressed treatment dropped significantly compared to the other treatments in both seasons. The final average nut set in the last week (week five) for the stressed treatment was approximately three nuts per cluster and approximately five nuts set per cluster in the other treatments, which received sufficient water during this stage for both seasons (Figure 4.66). This indicates that water stress at this stage (flowering and nut set) resulted in the increased abortion of flowers and nut drop, and thus a reduction in the final number of nuts set compared to the well-watered treatments. Importantly, the impact of earlier canopy senescence when stress is imposed during the shuck dehiscence stage does not seem to have an impact on flowering in the second and third season.

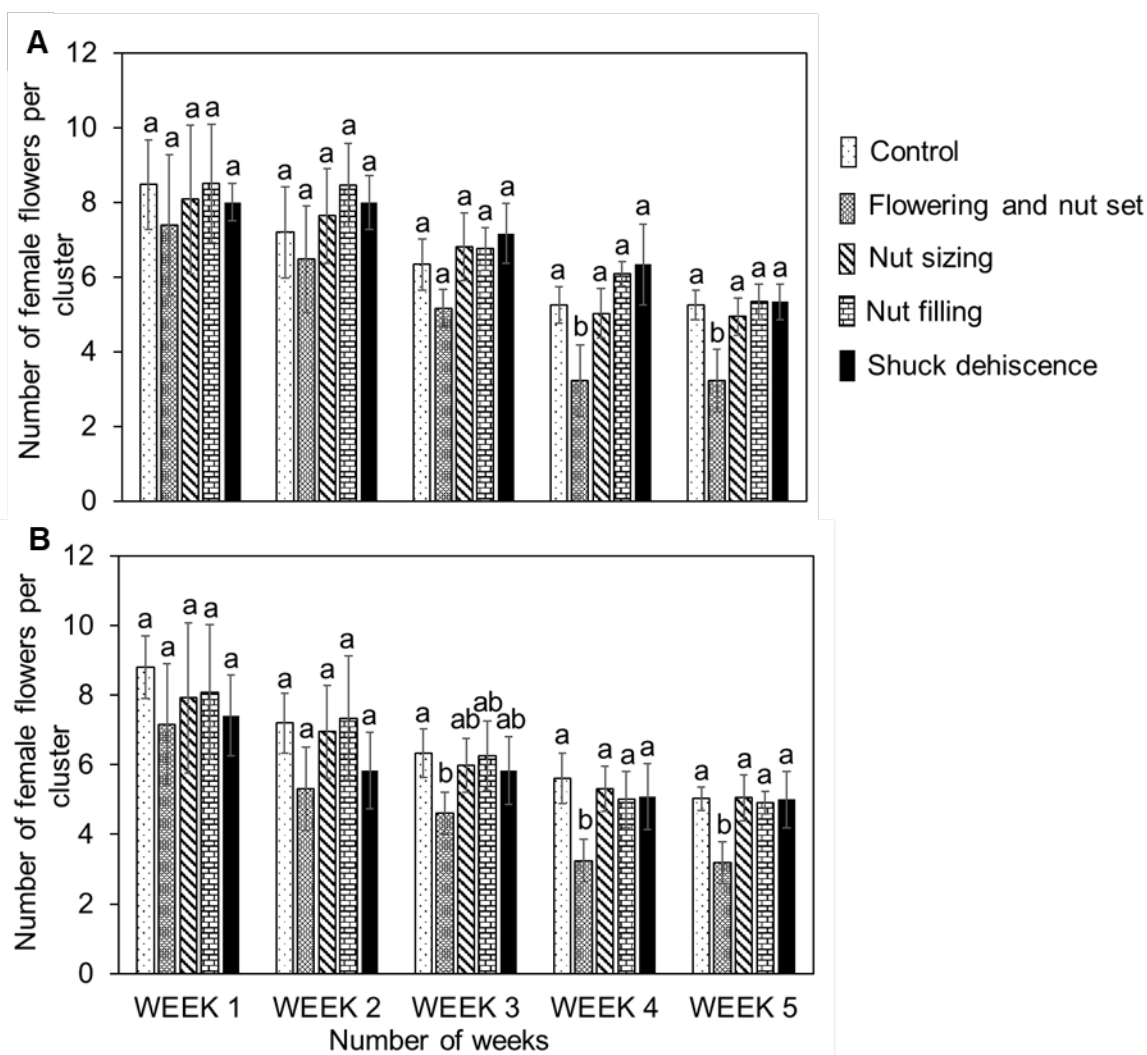


**Figure 4.66** The impact of water stress during flowering and nut set stage on number of female flowers per cluster for the A) 2018/2019 season and B) 2019/2020 season. Treatments with the same letter are not significantly different from each other ( $p < 0.05$ )

#### 4.4.7 NUT GROWTH

Nut growth was evaluated on a weekly basis after nuts were successfully set until they reached their final size as indicated by a plateau in growth (Figure 4.67). Both nut length and diameter were determined for both seasons. As observed in Figure 4.67, nut growth was measured for 18 weeks from the 1 November 2018 to 19 February 2019 in the second season and 10 November 2019 to 22 February 2020 in the third season. An increment in nut size from 0.83 cm to 5.01 cm and 0.79 cm to 4.80 cm (length) for the control and water stressed treatment (at nut sizing) respectively, whilst diameter increased from 0.41 cm to 2.72 cm and 0.41 cm to 2.72 cm for the control and water stressed treatment respectively (Figure 4.67 A,C) for the second season. Likewise, in the third season, a similar increase in nut length from 0.79 cm to

5.08 cm and 0.80 cm to 4.79 cm for the control and water stressed treatment respectively and diameter from 0.49 cm to 3.01 cm and 0.46 cm to 2.85 cm for the control and water stressed treatment respectively (Figure 4.67 B,D) was noted. The nuts reached their final size, both in length and diameter, 15 weeks after the start of measurements in both seasons. There were, however, no statistically significant differences in both length and diameter during nut growth for the control and water stressed treatment in both seasons. However, what is worth noting are the differences from week seven (second season) and week nine (third season) in terms of nut elongation rate, which was slightly decreased in the water stressed treatment. This resulted in final nut size being slightly reduced by 0.21 cm and 0.29 cm compared to the control in the second and third season respectively (Figure 4.67 A,B). Differences in nut expansion (diameter) were also observed from week 13 (second season) and week 12 (third season), with the nut expansion rate decreased slightly in the water stressed treatment. Final nut diameter of the water stressed trees was reduced by 0.07 cm and 0.16 cm in the second and third season respectively from the nuts of the well-watered control (Figure 4.67 C,D).

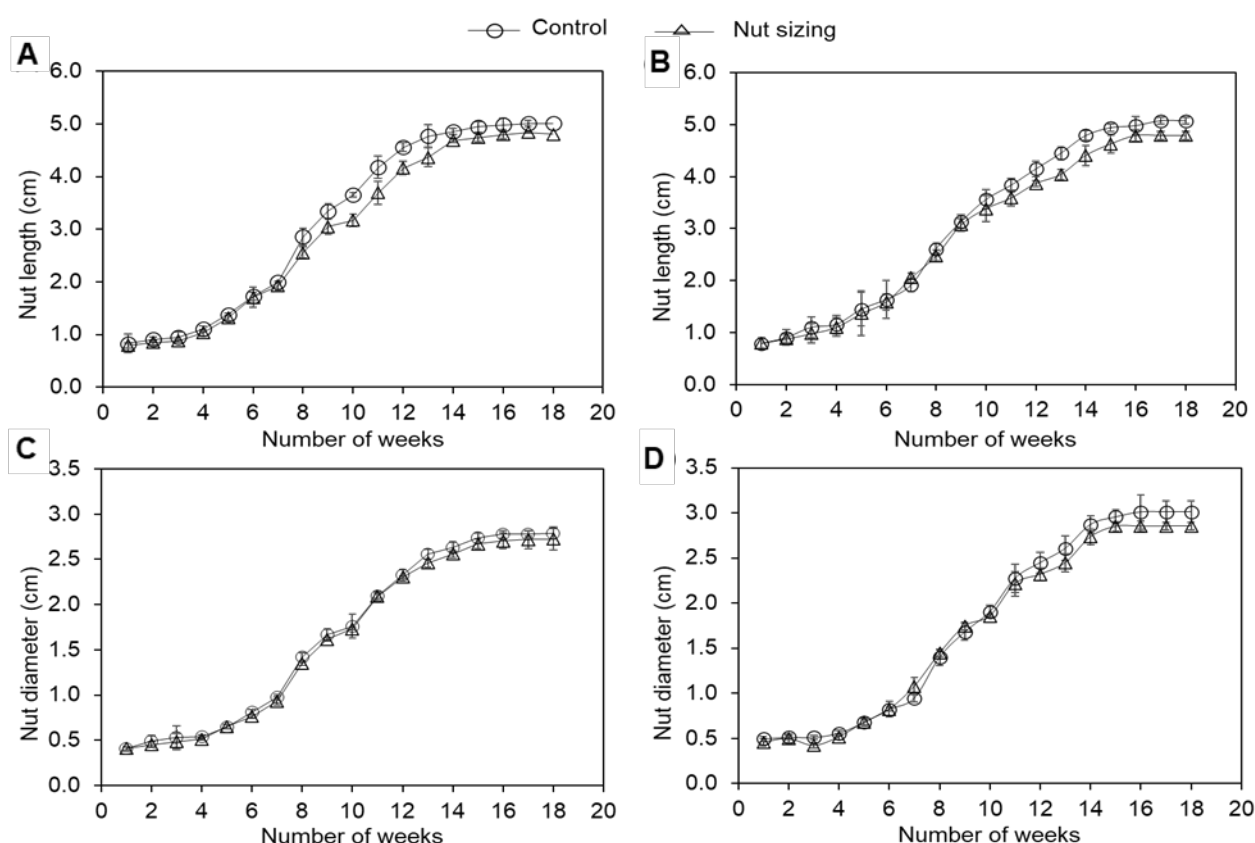


**Figure 4.67 Nut elongation (length) during the A) 2018/19 season and B) 2019/20 season and nut expansion (diameter) during the C) 2018/19 season, D) 2019/20 season as influenced by water stress during the nut sizing stage**



#### 4.4.8 NUT DROP

The assessment of nut drop was performed for six seasons after pollination, when nut set had been completed, until the end of the trial to evaluate the effects of water stress at different phenological stages on nut retention for the three seasons. A significantly greater percentage of nut drop was evident when stress was implemented during flowering and nut set across the first three seasons, recording 20% in the first season, 22% in the second season and 19% nut drop in the third season (Figure 4.68 A, B and C). A significant amount of nut drop was also noted at nut sizing during the first and third seasons with values of 18% in the first season and 13% in the third season (Figure 4.68 A and C). However, this was only significantly different to the control during the first season. In the fourth and fifth seasons, water stage fruit split was experienced due to high rainfall during the period of transition from nut sizing to nut filling, which resulted in a very large percentage of nut drop in all treatments and as a result, yields were greatly reduced in these two seasons (Figure 4.69 and Figure 4.70). The water stage fruit split resulted in all treatments dropping a significant number of nuts, with a minimum of 34% of nut drop at this stage (Figure 4.68 D and E). In the fourth and fifth seasons, the nut sizing treatments dropped significantly less nuts than the other treatments, this is due to the plastic covering the soil preventing water from entering the soil in these treatments, which prevented the rapid increase in turgor causing fruit split in the other treatments. In treatments where the soil was not covered in plastic, rainfall caused a sudden and substantial increase in soil water content resulting in a sudden increase in turgor and water stage fruit split. Water stress at nut filling and shuck dehiscence did not result in any nut drop that was significantly different to the well-watered control in all seasons. Less nut drop was observed during the sixth season (2022/23) season as compared the two previous seasons (2020/21 and 2021/2022) (Figure 4.68 F). Lower nut drop was recorded in the control, nut sizing and shuck dehiscence stages, at 14.8%, 9.2% and 15.3% respectively. These values were not statistically significant from each other ( $p < 0.05$ ). The highest nut drop in season 2022/2023 was observed during flowering and nut set and nut filling stage, 19% and 16.2% respectively, which were significantly different to the low nut drop recorded in the nut sizing treatment. The higher nut drop observed during the nut filling stage could be a result of light hail that fell in the orchard during this stage.

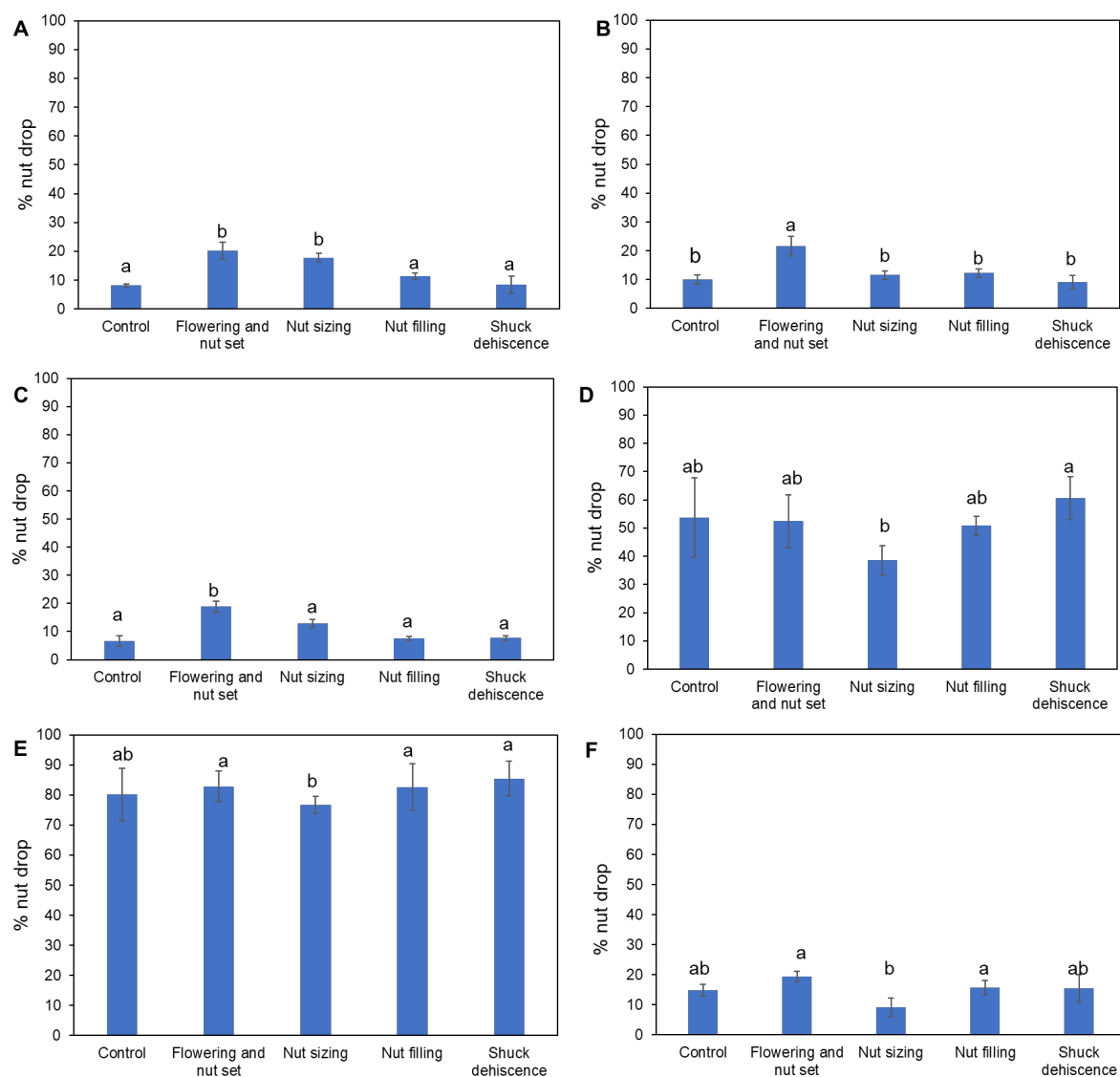


**Figure 4.68 Percentage nut drop in the A) first season (2017/18), B) second season (2018/19), C) third season (2019/20), D) fourth season (2020/21), E) fifth season (2021/22) and F) sixth season (2022/23). Treatments with the same letter are not significantly different from each other ( $p < 0.05$ )**



**Figure 4.69** Water stage fruit split in the experimental orchard during the 2020/2021 season. A) Split nuts in the tree, B) split nuts on the tree which have senesced, C and D) nut drop because of water stage fruit split and E) longitudinal section of split nuts

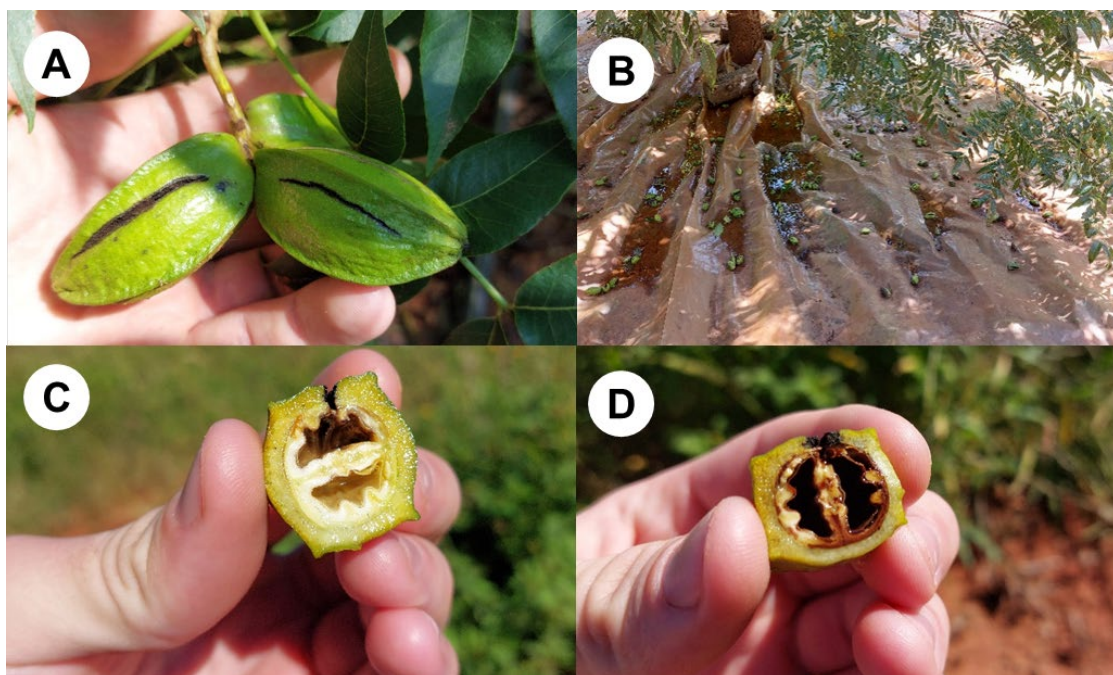


**Figure 4.70** Water stage fruit split in the experimental orchard during the 2021/2022 season. A) Split nuts on the tree, B) split nuts that have fallen off the tree, C) and D) longitudinal section of split nuts

#### 4.4.9 YIELD

Yield per tree was determined immediately after completion of the harvest and the results are shown in Table 4.15. For the first two seasons (2017/18 and 2018/19), water stress during flowering and nut set and nut filling significantly reduced yield relative to the well-watered control (Table 4.15). The yield during flowering and nut set is largely attributed to a reduced number of nuts, as % nut drop was higher when water stress was implemented during flowering and nut set. However, reduced yield at nut filling stage was most likely a result of poorly filled nuts which resulted in the reduced mass of individual nuts, relative to the well-watered control. Water stress during nut sizing and shuck dehiscence did not result in any differences between yields from these treatments and the control, except for the fifth season when yield was significantly higher in the nut sizing treatment when compared to the control. This is due to the lower nut drop experienced during this stage, due to the soil being covered with plastic, as explained above. The lack of a significant effect of water stress on yield during shuck dehiscence during the first season could be attributed to a lack of stress, as indicated by the  $\Psi_{smd}$  for this treatment which were similar to the control. However, in the second and third season significant stress was achieved during this stage and there was still no impact on yield. The lack of an impact of water stress at shuck dehiscence on yield is probably due to the fact that nuts are fully developed at this stage. The lack of a significant effect on yield during the third season during the flowering and nut set stage and nut filling could be due to the breakdown of the irrigation system for the control during the flowering and nut set period in this season, which resulted in stress in the control treatment (Figure 4.57 C). Despite this breakdown, the highest yields were achieved during this season. In the fourth (2020/21) and fifth (2021/22) seasons (reduced yield was noted for all the treatments, which was largely as a result of nut drop due to water stage nut split (Figure 4.69 and Figure 4.70). In the 2020/21 season there were no differences in yield between treatments due to the impact of water stage fruit split. There was also no significant stress at any of the phenological stages due to high rainfall throughout the season. In the 2021/22 season yield from the treatment stressed during the nut sizing stage was significantly higher than all the other treatments, which was probably due to the plastic covering these trees preventing too much water entering the soil. In the other treatments the high rainfall at this time resulted in more nut drop due to water stage fruit split. In addition, based on  $\Psi_{smd}$  and  $\Psi_{pd}$  measurements, mild stress was not achieved in this season, which would have impacted yield. In the sixth season there were no significant differences in yield between any of the treatments, which reflects the lack of significant stress imposition during any of the phenological stages. Once again this is because of the high and regular rainfall received throughout the season. Although yields were low, very little water stage fruit split was noted during this season. Other factors, such as nutrition could be limiting

yield in the orchard. There was also a lot of cloudy weather during nut filling which seemed to impact yields across the region.

**Table 4.15 Average in shell yield for the different stress treatments in the 2017/18 season, 2018/19 season, 2019/20 season, 2020/21 season, 2021/22 and 2022/23 season. Yield was adjusted to 4% moisture content. Treatments with the same letter are not significantly different from each other ( $p < 0.05$ )**

	Yield t ha <sup>-1</sup>					
Treatment	2017/18	2018/19	2019/20	2020/21	2021/22	2022/23
Control	1.73a	1.54a	2.70a	0.67a	1.27a	0.76a
Flowering and nut set	0.91b	1.03b	2.80ab	0.43a	1.49ab	0.79a
Nut sizing	1.39ab	1.44a	3.22a	0.83a	1.97b	0.64a
Nut filling	1.07b	1.16ab	2.24b	0.71a	1.43ab	0.66a
Shuck dehiscence	1.69a	1.47a	3.09a	0.51a	1.46ab	0.59a

#### 4.4.10 QUALITY

The quality parameters for the 2017/18, 2018/19, 2019/20, 2020/21, 2021/22 and 2022/23 seasons are presented in Table 4.16, Table 4.17, Table 4.18, Table 4.19, Table 4.20 and Table 4.21 respectively. For the first season (2017/18), stress during the nut filling stage resulted in a significantly great percentage of wafer/air pockets and higher number of nuts per kg (Table 4.16). Water stress had no significant effect on kernel percentage for any of the phenological stages. The number of nuts per kg did not differ from the control when trees were stressed during flowering and nut set and shuck dehiscence (2017/18). For the second season 2018/19, there were no significant differences between treatments for average diameter of nuts and kernel % (Table 4.17). There was a slight reduction in nut diameter at the nut sizing stage which could be an indication of reduced nut size, which resulted in a significantly higher average number of nuts per kg when compared to the well-watered control. Water stress at nut filling resulted in reduced individual nut mass and a higher number of nuts per kg due to poorly filled nuts (great wafer/pops %) when compared to the control. Water stress during nut filling had a significantly higher percentage of unsound kernel (pops) of 7.9%, and wafer/air pockets (22.3%) when compared to the control. Stress during the shuck dehiscence stage resulted in an increased percentage of stick tights (14.4%), which was significantly higher than any of the other treatment.

**Table 4.16 Quality parameters including number of nuts kg<sup>-1</sup>, percent kernel, m and wafers/air pockets percentage of pecan trees for the fully irrigated control and water stressed treatments in the 2017/18 season**

Treatment	No. of nuts kg <sup>-1</sup>	Kernel %	Wafer/air pockets %
Control	163 ± 8.40 a	55.2 ± 1.27 a	15.8 ± 0.65
Flowering and nut set	166 ± 10.88 a	54.3 ± 1.58 a	15.4 ± 0.75 a
Nut sizing	161 ± 11.70 a	55.5 ± 1.20 a	15.4 ± 0.95 a
Nut filling	177 ± 3.77 b	55.6 ± 2.35 a	124.1 ± 0.85 b
Shuck dehiscence	164 ± 9.22 a	54.4 ± 2.30 a	15.5 ± 1.22 a

Treatments with the same letter are not significantly different from each other (p < 0.05)

**Table 4.17 Quality parameters including average nut diameter, number of nuts kg<sup>-1</sup>, percent kernel, unsound kernel (percentage pops), wafers/air pockets percentage and percent stick tights of pecan trees for the fully irrigated control and water stressed treatment in the 2018/19 season**

Treatment	Diameter (mm)	No. of nuts kg <sup>-1</sup>	Kernel %	Unsound Kernel (% pops)	Wafers/air pockets %	Stick tights %
Control	21 ± 0.19a	153 ± 1.07a	58.4 ± 0.57a	2.5 ± 0.47a	13.9 ± 0.34a	6.2 ± 0.76a
Flowering and nut set	21 ± 0.64a	152 ± 0.89a	62.0 ± 1.09a	2.0 ± 0.43a	14.1 ± 0.44a	6.8 ± 0.73a
Nut sizing	19 ± 1.13a	174 ± 1.88b	57.0 ± 0.64a	1.6 ± 0.32a	14.7 ± 0.46a	7.2 ± 0.58a
Nut filling	21 ± 0.41a	172 ± 2.23b	58.0 ± 0.46a	7.9 ± 0.68b	22.3 ± 0.67b	7.1 ± 0.67a
Shuck dehiscence	21 ± 0.68a	159 ± 1.61a	57.0 ± 0.55a	2.9 ± 0.67a	14.3 ± 0.43a	14.4 ± 1.25b

Treatments with the same letter are not significantly different from each other (p < 0.05)

There were no significant differences in the average diameter of nuts between treatments in the third season (2019/20) (Table 4.18). Although not significant, the reduced nut diameter in the nut sizing treatment resulted in a significantly greater number of nuts per kg when compared to the well-watered control. Water stress at nut filling also resulted in reduced individual nut mass because of poorly filled nuts (great wafer/pops %). Although the number of nuts per kg in this treatment was higher than the control, it was not significantly different to the control. Water stress at any of the other phenological stage had no significant effect on kernel percentage. Stressing at nut filling resulted in a significantly higher percentage of

unsound kernel or pops (9.0%), and wafer/air pockets (18.3%) as compared to the control. Water stress during the shuck dehiscence stage resulted in an increased percentage of stick tights (10.1%), which was significantly higher than any other treatment.

**Table 4.18 Quality parameters including average nut diameter, number of nuts kg<sup>-1</sup>, percent kernel, unsound kernel (percentage pops), wafers/air pockets percentage and percent stick tights of pecan trees for the fully irrigated control and water stressed treatments in the 2019/20 season**

Treatment	Diameter (mm)	No. of nuts kg <sup>-1</sup>	Kernel %	Wafers/air pockets %	Unsound Kernels or pops %	Stick tights %
Control	20.0 ± 0.59a	165 ± 4.43a	59.8 ± 1.13a	6.6 ± 0.94a	2.5 ± 0.90a	5.1 ± 1.78a
Flowering and nut set	20.1 ± 0.84a	160 ± 5.19a	60.0 ± 1.17a	6.1 ± 1.76a	2.0 ± 0.73a	5.0 ± 2.14a
Nut sizing	19.1 ± 1.06a	216 ± 6.34b	59.3 ± 1.96a	7.6 ± 2.20a	1.6 ± 0.40a	3.9 ± 1.07a
Nut filling	20.6 ± 0.16a	171 ± 1.77a	58.3 ± 2.12a	18.3 ± 3.57b	9.0 ± 0.54b	4.5 ± 2.85a
Shuck dehiscence	20.4 ± 0.51a	167 ± 1.41a	59.0 ± 2.66a	7.1 ± 2.31a	5.3 ± 1.02a	10.1 ± 1.03b

Treatments with the same letter are not significantly different from each other (p < 0.05)

In the fourth season (2020/2021) due to the low yields there were no significant differences between all the treatments for number of nuts per kg and kernel % (Table 4.19). This can be attributed to the water stage fruit split, as well an overall inability to induce mild water stress throughout the season due to good rains received throughout the season (Figure 4.57). Unfortunately, sticktights were not determined in this season, although they were expected to be low due to the very low yield. In this season there was a significantly higher % wafers/ air pockets and unsound kernel in the nut filling treatment as compared to the control. However, this treatment was not significantly different to the nut sizing treatment in terms of % wafers/air pockets.



**Table 4.19 Quality parameters including number of nuts kg<sup>-1</sup>, percent kernel, percent unsound kernel or pops and wafers/air pockets percentage of pecan trees for the fully irrigated control and water stressed treatments in the 2020/21 season**

Treatment	No. of nuts per kg	Kernel %	Unsound kernel or pops %	wafers/air pockets %
Control	160 ± 4.08a	52.3 ± 2.40a	0.7 ± 0.30a	11.9 ± 0.44a
Flowering and nut set	157 ± 6.60a	53.0 ± 2.52a	0.7 ± 0.20a	12.2 ± 0.74a
Nut sizing	165 ± 2.36a	54.5 ± 6.10a	0.4 ± 0.2a	12.6 ± 0.85ab
Nut filling	160 ± 6.24a	53.8 ± 4.88a	2.2 ± 0.6b	13.9 ± 1.04b
Shuck dehiscence	157 ± 7.26a	52.6 ± 6.36a	0.9 ± 0.6a	12.3 ± 0.59a

Treatments with the same letter are not significantly different from each other (p < 0.05)

Yield and quality in the fifth season (2021/2022) were also influenced by water stage fruit split, which contributed to few differences between the treatments (Table 4.20). The lack of any clear differences between treatments is also attributed to the high rainfall during this season, which resulted in very little imposed stress at any phenological stage. Although yields were higher in this season than in 2020/21, the high yield resulted in smaller nuts throughout treatments. There was an increase in the number of nuts per kg from the fourth season to the fifth season for the control. For the first four seasons the number of nuts per kg for the control was between 150 and 160, but in the fifth season this was 180. The nut filling treatment, however, had the lowest number of nuts per kg which was significantly lower than the control, suggesting larger nuts and when combined with the low % of wafers and high kernel %, also better filled nuts. Due to the large reduction in nut number prior to nut filling in the fourth season, it could be possible that a higher number of nuts set in the fifth season, which results in smaller nuts at the end of nut sizing, which then filled quite well during the nut filling stage, after the reduction in nut number as a result of water stage fruit split and nut drop. Kernel percentage was generally quite high indicating well filled nuts. Although there were differences in % air pockets between treatments, the variation between replicates in each treatment was high resulting in no significant differences. There was a high percentage of stick tights in this season, especially for the control, with the lowest during nut sizing. These were the only two treatments that were significantly different from each other. This could reflect the high amount of rainfall received during this season, resulting in fairly waterlogged conditions at times, which did not occur in the nut sizing treatment because of the plastic over the soil surface. Unfortunately, unsound kernel (pops) was not determined in this season.



**Table 4.20 Quality parameters including number of nuts kg<sup>-1</sup>, percent kernel, moisture percentage and wafers/air pockets percentage of pecan trees for the fully irrigated control and water stressed treatments in the 2021/22 season**

Treatment	No of nuts per kg	Kernel %	wafers/air pockets %	Stick tights %
Control	182 ± 3.27a	58.9 ± 26.07a	17.2 ± 18.2a	17.6 ± 6.3a
Flowering and nut set	179 ± 5.74ab	51.6 ± 18.23a	12.7 ± 15.5a	10.1 ± 5.4ab
Nut sizing	189 ± 7.18a	63.5 ± 4.43a	4.6 ± 6.4a	6.4 ± 2.9b
Nut filling	168 ± 7.62b	66.3 ± 0.72a	2.1 ± 2.4a	9.3 ± 1.1ab
Shuck dehiscence	181 ± 7.04a	66.3 ± 1.42a	17.1 ± 18.3a	12.7 ± 5.2ab

Treatments with the same letter are not significantly different from each other (p < 0.05)

In the sixth season (2022/23), there were very few differences in quality parameters between the treatments (Table 4.20). The yields were low and very similar to the 2020/21 season and once again significant water stress (below the threshold values) was not achieved during any of the phenological stages. As in the 2021/22 season, there was an increase in the number of nuts per kilogram, with the well-watered treatment yielding 178 nuts kg<sup>-1</sup>, which was higher than the first four seasons. There were significantly more nuts per kg in the shuck dehiscence treatment than the well-watered control. Stress during this phenological stage resulted in a big impact on quality, as kernel % was reduced during this stage, whilst the number of sticktights increased relative to the control. Overall, the 2022/23 season showed poor nut quality compared to the first three seasons. This is indicated by the relatively high percentage of unsound kernels during the different stages (Figure 4.71). This percentage was higher than the other five seasons.



**Figure 4.71 A) Sound and B) unsound kernel during the 2022/23 season. A high percentage of unsound kernel was found during this season in a number of treatments**

**Table 4.21 Quality parameters including number of nuts kg<sup>-1</sup>, percent kernel, and wafers/air pockets percentage of pecan trees for the fully irrigated control and water stressed treatments in the 2022/23 season**

Treatment	No of nuts per kg	Kernel %	Unsound Kernel %	wafers/air pockets %	Stick tights %
Control	178 ± 6.61a	45± 6.46ab	10.9 ± 3.62ab	5.2 ± 3.22a	0.8 ± 0.94a
Flowering and nut set	182 ± 7.66a	44.8 ± 5.7ab	10.6 ± 4.36ab	5.3 ± 1.54a	2.8 ± 3.28ab
Nut sizing	183 ± 8.23ab	50.2 ± 2.5a	6.8 ± 2.40a	3.7 ± 2.52a	2.5 ± 3.41ab
Nut filling	183 ± 5.00a	50± 3.4a	5.9 ± 1.96a	4.5 ± 1.614a	0.8 ± 0.47a
Shuck dehiscence	192 ± 1.63b	41± 5.1b	13.2 ± 4.26b	6.9 ± 1.01a	4.9 ± 3.32b

Treatments with the same letter are not significantly different from each other (p < 0.05)

#### 4.4.11 TOTAL INCOME AS A RESULT OF IMPOSING WATER AT KEY PHENOLOGICAL STAGES

Gross income per season per treatment was determined after the nuts were graded (Table 4.22). Whilst clear differences were noted between the control and the various stress treatments in the first three seasons, the impact of water stage fruit split on income was clearly demonstrated in the fourth and fifth seasons, when income was greatly reduced due to the low yields. In the first two seasons the negative impact of water stress during flowering and nut set and nut filling was very evident. However, in the third season, due to stress in the control treatment at the start of the season, only the nut filling stage yielded a lower income than the control. The reduction in income when a stress was imposed during flowering and nut set was largely a result of a decrease in yield, whilst during nut filling it reflects reduced quality. The lowest income was recorded in the fourth season due to the very low yields. In this season the lowest income was found when a water stress was imposed during flowering and nut set and shuck dehiscence, which reflected the lower yield in these treatments. Income for the control treatment in the fifth season was also reduced compared to the first three seasons. The control had the lowest income, with the nut sizing treatment having the highest income, which again reflects differences in yield. In the sixth season yields were once again very low, which when combined with the reduced nut size, resulted in reduced income, across treatments. Especially for the shuck dehiscence stage, where quality was very poor. When considering total income over six seasons, income for the flowering and nut set and nut filling treatments had lowest total income.

**Table 4.22 Total income received as a result of imposing water stress at different phenological stages.**

Season	2017/18	2018/19	2019/20	2020/21	2021/22	2022/23	Cumulative income
Control	R102 150	R91 609	R136 680	R35 683	R75 619	R49 455	R491 196
Flowering and nut set	R53 700	R60 396	R141 780	R23 075	R88 912	R51 025	R418 888
Nut sizing	R82 350	R76 410	R130 790	R44 127	R117 019	R41 399	R492 095
Nut filling	R54 340	R59 386	R112 710	R37 525	R97 338	R42 910	R404 209
Shuck dehiscence	R99 900	R86 247	R143 820	R27 318	R86 884	R37 986	R482 155

#### 4.4.12 CONCLUSIONS

Six seasons of stress implementation and measurements were completed in the pecan orchard on the University of Pretoria's Experimental Farm (Innovation Africa@UP). During these six seasons, a mild stress was successfully implemented in only three of the six seasons. The failure to implement stress was largely attributed to high rainfall, and at these times the plastic covering the soil surface was insufficient to prevent a change in soil water content, either due to lateral flow in the soil or entry of water at the edges of the plastic. In the first and second season this only occurred during one phenological stage in each season, but in the fourth, fifth and sixth seasons most stages were impacted due to the very regular occurrence of rainfall events. In the 2020/21 season some stress was achieved during nut filling and in the 2022/23 season stress just below the threshold value was achieved during nut filling and shuck dehiscence. However, in the 2022/23 season very little stress was achieved throughout the season. As a result, very little information regarding the impact of a mild water stress on yield on quality can be obtained from the last three seasons of measurements. However, the deleterious effect of too much water, as a result of high rainfall, at the end of nut sizing and beginning of nut filling on water stage fruit split was clearly evident in two seasons. Nut quality in the last season also seemed to be affected by cloudy weather in February and March which resulted in poor nut quality in the trees stressed during shuck dehiscence.

In terms of maintaining a well-watered control, the breakdown of the irrigation system to this treatment resulted in some significant stress in the second season towards the end of flowering and fruit set (December 2018) and during nut filling in the third season in early January. A number of measurements were also missed from mid-March to the end of April 2020 due to lockdown level 5 and the students not having access to the experimental farm. In the fourth season a mild stress was achieved towards the end of nut filling and shuck dehiscence, but not in any of the other phenological stages. In the fifth season very little irrigation was needed in the orchard due to the high rainfall and as a result  $\Psi_{\text{smd}}$  seldom approached the threshold value of -0.90 MPa. Once again in the sixth season the threshold for  $\Psi_{\text{smd}}$  was not exceeded, with only measurements during shuck dehiscence approaching these values. Importantly due to the length of the study, a number of different students have been responsible for measurements and this has resulted in differences in water potential measurements which is evident in the regression of  $\Psi_{\text{pd}}$  and  $\Psi_{\text{smd}}$ .

During season two the impact of water stress on gas exchange was investigated to confirm the successful implementation of water stress and to determine the impact of water stress on

the physiology of the trees. A reduction in stomatal conductance and as a result a reduction in photosynthesis was observed during the implementation of stress during each phenological stage. From additional analyses it would also appear that there are both stomatal and non-stomatal limitations to photosynthesis as a result of the implementation of the water stress. The reduction in photosynthesis, especially during nut filling could explain the negative effect of a water deficit stress on yield.

During the first three seasons it is evident that stress during nut filling consistently resulted in a reduction in yield, which was because of poorly filled nuts (reduced mass), as evidenced by an increase in the % of wafer or air pockets. As a result, income received for nuts from trees stressed during this phenological stage was always reduced in the first three seasons. It is therefore recommended that stress during this period is avoided, as it will result in a yield and quality penalty and thus reduced income.

Flowering and nut set also seemed to be a particularly sensitive stage for water stress, as stress during this stage significantly reduced yield during two of the first three seasons. This reduction in yield was linked to increased nut drop, which resulted in a lower total number of nuts per tree which were similar in size to the control or slightly larger. Canopy development was also slowed during this stage, which could have impacted the time of the sink-source transition of the canopy as a whole, thereby impacted initial whole tree photosynthesis.

The implementation of stress during the shuck dehiscence stage resulted in an increased percentage of stick tights in three of the first six seasons, however, stick tights were not measured in 2017/18 and 2020/21. Although yield was not impacted, stick tights impact harvesting and can increase harvesting costs as the husk needs to be removed from these nuts, provided they have filled properly. Canopy senescence was also more rapid when stress was implemented during this stage and this could impact the period for accumulating stored reserves following nut maturation. Although the early senescence in this treatment could have had an impact on stored reserves for flowering the following season, no yield penalty was noted in this treatment throughout the trial. However, this could have been masked in the fourth and fifth season by the high percentage nut drop in all treatments as a result of water stage fruit split and the low yields in the sixth season. Importantly, overall nut quality was very reduced in the shuck dehiscence treatment in the sixth season when a slight degree of stress was achieved.

The phenological stage for which yield seemed to be the least affected by water stress was the nut sizing stage. However, nut size was impacted in season two and three, as seen by the

significantly greater number of nuts per kg when stress was implemented during this phenological stage. As a result, income was reduced for this treatment relative to the control in the first three seasons. In season four to six an impact on nut size was not noted, probably due to the low yields and water stage fruit split.

The impact of stress at different phenological stages on yield and quality could not be determined in the last three seasons because of the high rainfall experienced, which caused a high percentage nut drop in late January and early February of each season in the fourth and fifth seasons, as the nuts stopped growing and nut filling began. There is therefore a danger for pecan producers to experience a significant yield loss if high rainfall is received at the time and the soil becomes very wet. In both seasons, the yield penalty was less in the nut sizing treatment where some rainfall was excluded by the plastic, indicating that it was the impact of too much water that resulted in significant water stage fruit split and nut drop. The low yield in the control also suggests that too much water can have a negative impact on yield and thus overirrigation should be avoided.

When considering the three seasons where a mild stress was successfully achieved it is evident that all four phenological stages assessed in this study were sensitive to water stress when considering both yield, quality and gross income. Ideally, pecans should not be subjected to mild water stress (as defined by Othman et al. (2014)) if yield and quality are to be maintained at optimal levels. However, in seasons where water allocations are reduced, it may be possible to make some water savings during nut sizing and shuck dehiscence without compromising yield. However, some reduction in quality may result if the trees are stressed during these stages.

## **4.5 REMOTE SENSING**

### **4.5.1 WATER STRESS DETECTION BY VEGETATION INDICES**

The results of the attempts to detect water stress using common VIs showed no clear trend between VIs and measures of water stress, including. No meaningful correlation was found between any of the VIs and the plant-measured water stress indicators,  $\psi_{\text{smd}}$  and  $g_s$ . This was observed during both seasons of data collection, as can be seen in Table 4.23.

**Table 4.23 Relationships between vegetation indices (VIs) and midday stem water potential ( $\psi_{smd}$ ) collected during the 2020/21 and 2021/22 seasons, stomatal conductance ( $g_s$ ) collected during the 2020/2021 season and  $\psi_{smd}$  collected on 24 February 2022**

Vegetation indices	$R^2$ values			
	$\psi_{smd}$		$g_s$	$\psi_{smd}$
	2020/2021	2021/2022	2020/2021	24/02/ 2022
<b>GNDVI</b>	0.0002	0.1827	0.2482	0.0024
<b>NDVI</b>	0.122	ND	0.0035	0.0079
<b>MCARI</b>	0.0086	0.0001	0.0009	0.0728
<b>MCARI-1</b>	0.052	0.055	0.003	0.0062
<b>OSAVI</b>	0.0006	0.0019	0.0027	0.0872
<b>RDVI</b>	0.0015	0.0056	0.006	0.0851
<b>TCARI</b>	0.0459	0.0698	0.0008	0.0018
<b>ResRI</b>	0.0033	0.0101	0.1323	0.0081
<b>RNDVI</b>	0.0289	0.034	0.002	0.0026
<b>SRI</b>	0.0998	0.0948	0.0196	0.000001

If taken in isolation, data collected between February and April 2021 (Table 4.23), suggests that there may be some correlation between the VIs; GNDVI and ReSR, and  $\psi_{smd}$  and  $g_s$ . However, when considering a larger dataset collected during the 2021/2022 season, it was evident that no real relationship existing between VIs and ground measurements of plant stress, as the  $R^2$  for these relationships were very low. This agrees with what has been found in other crops, where some correlation was observed between specific VIs and water stress, with most other VIs showing very little correlation with stress. In cotton, a slight relationship was found between water stress and NDVI (Bian et al., 2019). In grapevine, promising VIs included GNDVI, SRI, MCARI, NDVI and TCARI (Baluja et al., 2012), while another study found only NDVI to have a moderate relationship with water stress, and the other VIs to be ineffective (Zarco-Tejada et al., 2013). NDVI was also found to be a good predictor of water stress in almond (Zhao et al., 2017), but only for individual flights. In this study, the absolute NDVI value was found to have a weaker relationship with water stress when compared with data collected at different times (Zhao et al., 2017). The relatively poor performance in pecan of many of the VIs that were found to be effective in other crops may be explained by the morphological response to water stress of pecan trees. It was observed early on that mature pecan leaves do not wilt under water stress, nor do they drop their leaves unless water stress is very severe (Sparks, 1989). Thus, water stress generally causes no structural change to

pecan canopies. Therefore, as expected, VIs which indicate structural changes in canopies did not correlate well with water stress in pecan, while they may have been found to be effective in crops which do wilt such as grapevine (Baluja et al., 2012). While not causing any changes to the structure of the canopy, water stress has been found to reduce the chlorophyll content of pecan leaves (Wells, 2017). It would, therefore, be expected that VIs which are sensitive to leaf chlorophyll content, such as TCARI and MCARI, and those that quantify photosynthetic activity, like NDVI, would be sensitive to water stress. However, this was found not to be the case. It may be that only leaves that developed under water stressed conditions exhibit reduced chlorophyll, while there is no change in the chlorophyll content of leaves that are stressed after full expansion. It has also been found in several species that there may actually be an increase in chlorophyll content under a low level of water stress, while chlorophyll only decreases significantly under severe water stress (Pirzad et al., 2011). Indices that respond to chlorophyll, would, therefore, not show a linear relationship with the level of water stress. Some indication of this can be observed in Table 15, for the OSAVI, TCARI, RDVI and RNDVI VIs. Importantly, due to unusually high rainfall in both seasons, a high level of water stress ( $\psi_{\text{smd}} < 0.9$  MPa) was not achieved, which could have created sufficient contrast between well-watered and stressed trees to find a reasonable correlation between VIs and measurements of plant stress. Despite this, it seems unlikely that VIs could detect mild stress in pecan orchards that would ordinarily trigger irrigation events.

Vegetation indices are affected directly by environmental factors external to the target vegetation, which include solar radiation intensity, aerosols in the air, longwave or diffuse radiation and illumination angle, that is, the angle of the sun incident on the canopy (Suomalainen et al., 2021, Jackson and Huete, 1991). Some of these sources of error, such as incoming solar radiation intensity, can be corrected for during pre-processing (Kingra et al., 2016). If not adequately corrected, the only way to reliably use multispectral remote sensing data would be to only compare data collected at a single point in time, to ensure that all environmental variables are the same. To test whether inadequate atmospheric correction was responsible for the large scatter and lack of correlation observed in some of the VI plots in Table 15, data from a single flight was plotted independently against  $\psi_{\text{smd}}$  (Table 4.23). The day chosen was 24 February 2021 as there was a large variation in the water stress values observed, including both heavily stressed and unstressed trees. Poor correlations were found between the VIs tested and water stress, indicated by  $\psi_{\text{smd}}$ , even though all atmospheric variables were constant. A significant challenge with this approach is the collection of sufficient data to be able to test the assumptions. All water stress data must be collected within a short space of time, as it is known that both canopy reflectance and plant water stress parameters can change within a period of time as short as an hour (Ishihara et al., 2015). It is possible



that the small number of data points may be responsible for the lack of correlation observed, if more data points were to be collected at the same time, relationships between VIs may become apparent.

A major weakness of this study is the variability in the times of remote sensing data collection. Differences in flight times results in differences in solar zenith angle during the flight. This means that during each of the flights during the season, the tree canopies were illuminated from a slightly different angle. This results in changes in the reflectance of light from the canopy detected by the camera, and ultimately the value of any VIs calculated (Jackson and Huete, 1991, Ishihara et al., 2015). The effect of illumination angle on the VI value is further complicated by diffuse radiation incident on the leaves (Ishihara et al., 2015). Due to the high rainfall during the 2021/22 season, some flights were conducted on overcast days, data from which were not used, or when there was partial cloud cover. Data from canopies that were visibly shaded were not used, however, it is likely that longwave radiation interception varied greatly between flights and even between canopies at the same time, due to intermittent cloud cover during the flight. It has also been found that the effect of illumination angle on VI values is affected by the amount of diffuse radiation present, and that the effect is not the same for all VIs (Ishihara et al., 2015, Emmel et al., 2020).

Canopy properties, including architecture and Leaf Area Index (LAI), also have an impact on the average canopy reflectance, and therefore VI values calculated from the reflectance (Emmel et al., 2020). There are two factors that affect light reflectance from a canopy. The first is light scattering within a canopy (Emmel et al., 2020), and the second is the amount of soil reflectance transmitted through the canopy to the sensor above (Zhao et al., 2017). The more heterogenous a canopy is, the greater the scattering of incident radiation within the canopy before being reflected back to the sensor. This allows for greater absorption of photosynthetically active radiation (Emmel et al., 2020), changing the ratio of red to NIR light reaching the sensor (Jackson and Huete, 1991), which will affect VIs that use these bands. A more vertically oriented canopy will also scatter more of the incoming radiation horizontally, and less directly towards the sensor directly above, changing the average reflectance of the canopy in most bands (Jackson and Huete, 1991). Many VIs have also been found to be exceptionally sensitive to LAI, indeed, VIs like those derived from the Soil Adjusted VI and the RDVI are used primarily to detect canopy density and biomass, often quantified by the LAI (Broge and Leblanc, 2001). Since the canopies making up a pecan orchard are usually not completely homogenous, especially in a canopy that has not closed into a hedgerow, they can be expected to vary greatly in both architecture and density. Such canopies cannot, therefore,

be realistically expected to show correlations between VIs and an external factor such as water stress.

#### 4.5.2 WATER STRESS DETECTION BY THERMAL REMOTE SENSING

Under water stress, amongst the first responses of plants is stomatal closure to reduce transpirational water loss. This results in an increase in leaf temperature, due to the absence of transpirational cooling. The temperature of a leaf can, therefore, be used to quantify water stress. However, leaf temperature is also heavily influenced by atmospheric variables, the most important of these being the  $T_a$  and VPD. The importance of taking these factors into account is illustrated by Figure 4.72. Beside the low correlation between water stress, as quantified by  $\psi_{smd}$ , and canopy temperature, it can also be observed that leaf temperatures are found as distinct groups. This suggests that there are factors apart from water stress alone that influences the temperature of the individual leaves and the canopy as a whole.

The canopy temperature is corrected for air temperature using the stress degree day, which is the difference canopy and air temperature ( $T_c - T_a$ ). This parameter can be effective at detecting water stress in areas where there is very little variation in VPD throughout the season. This is not the situation in Pretoria, as shown by Figure 4.73.

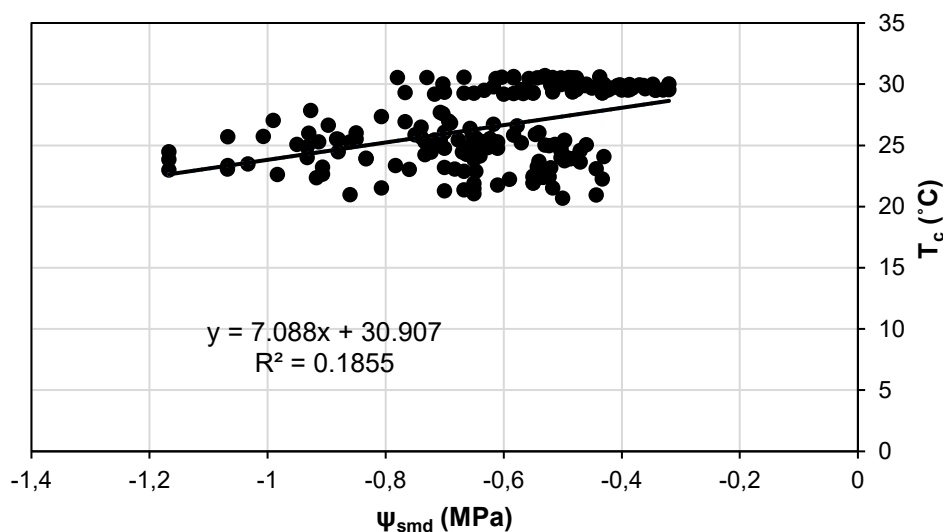


**Figure 4.72 The relationship between canopy temperature ( $T_c$ ) and midday stem water potential ( $\psi_{midday}$ ), showing the problems with using leaf temperature alone to detect water stress**

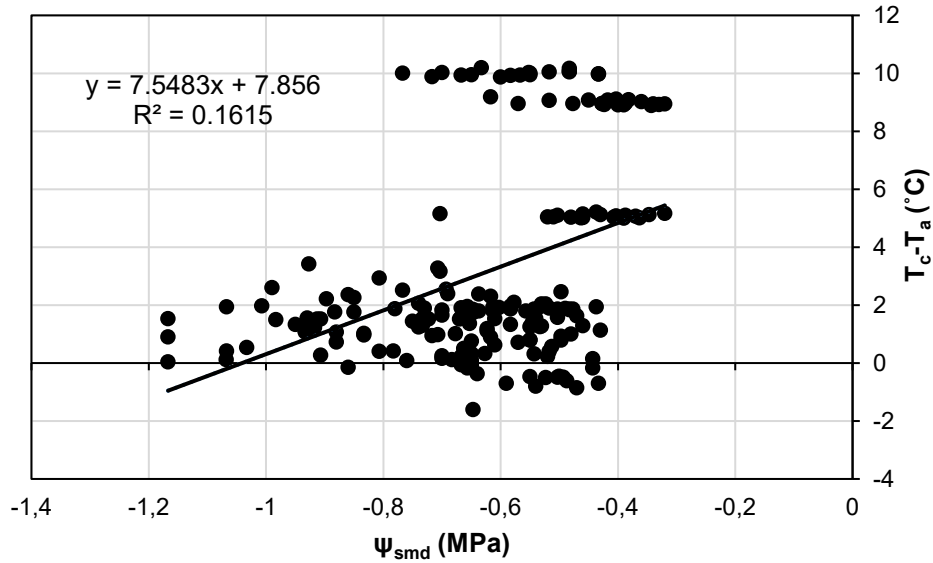


**Figure 4.73 Relationship between the difference between canopy and air temperature ( $T_c - T_a$ ) and midday stem water potential ( $\Psi_{smd}$ ), showing that correcting for  $T_a$  alone is not sufficient for detecting water stress**

In Figure 4.73 it is evident that there are several groups of points where the canopy temperature is far higher than the air temperature at the same  $\Psi_{smd}$ . These may correspond to days with unusual VPD, or even solar radiation or windspeed, conditions. Figure 4.73 also shows a number of implausibly high  $T_c - T_a$  values. This is likely a result of the thermal sensor overestimating canopy temperatures, an issue that was encountered throughout both seasons of measurement.

Under non-stressed conditions, the  $T_c - T_a$  is almost always negative, that is, the canopy temperature is lower than the air temperature. Figure 4.73 shows most such data points where they would be expected to be, at unstressed  $\Psi_{smd}$  values. However, there are several points that fall within the stressed range. These points may have been collected on a day with a very high VPD. Under high VPD, atmospheric demand is so high that enough transpiration takes place even with a degree of stomata closure for there to be a leaf cooling effect. It may also be linked to a quirk of the pecan stomatal control regime. It is still, however, necessary to take the VPD at the time of measurement into account.

#### 4.5.3 THE NON-WATER-STRESSED-BASELINE

The oldest method used to correct the canopy temperature for both the air temperature and the VPD is the NWSB. The individual NWSB plots from each season are presented in Figure 4.74 and Figure 4.75.

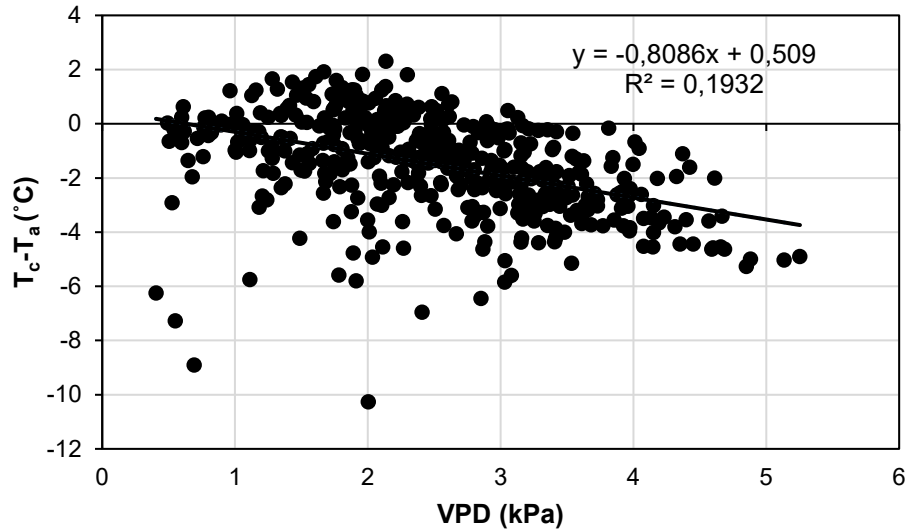


**Figure 4.74 Non-water stressed baseline (NWSB) plotted from data collected during the 2020/21 season at the Vaalharts site**

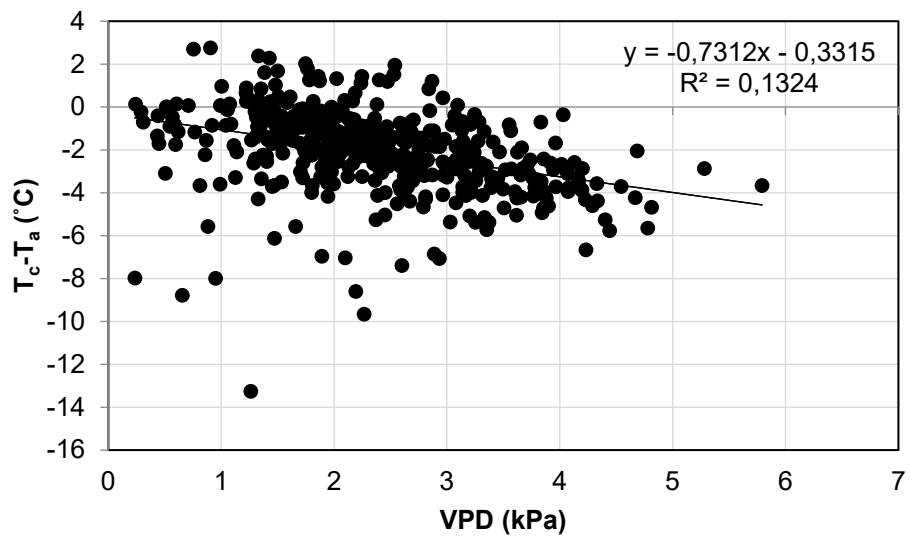


**Figure 4.75 Non-water stressed baseline (NWSB) plotted from data collected during the 2021/22 season at the Vaalharts site**

The data in both Figure 4.74 and Figure 4.75 was from only between 11:00 and 14:00 during the part of the season when the canopy was in full leaf. This was to ensure that only leaf temperatures were measured, and not the soil or bare bark, and to ensure that there were no extreme changes in solar angle or intensity in the measurement period. It can, therefore, be assumed that the NWSBs represent the canopy transpiring at the maximum rate for the conditions. The intercept of the 2020/21 NWSB was slightly positive, while the 2021/22 NWSB was slightly negative. This may be explained by the prevailing conditions during the season. The intercept of the NWSB is the  $T_c - T_a$  at a VPD value of zero, or a completely

saturated atmosphere, at which very little gaseous exchange takes place between the interior of the leaf and the atmosphere. A negative intercept means that, under a saturated atmosphere, the air temperature is higher than the canopy temperature, so there is still a slight cooling effect. If the intercept is positive, it means that, in a saturated atmosphere, gaseous exchange is so low that canopy temperature rises above air temperature, even without any water stress. This may be due to the effects of solar radiation and wind. With a higher wind speed, boundary layer resistance is lower, and there may still be a significant amount of transpiration, even in a saturated atmosphere. The higher the solar radiation, the more transpiration is required to lower the canopy temperature below the air temperature, an effect which is magnified in a saturated atmosphere, where VPD is no longer a consideration. Figure 4.76 is a combined NWSB using data from both seasons, where the intercept is almost zero. This supports the assumption that the differences in slope and intercept are due to the effects of seasonal conditions and are not characteristic of the crop.

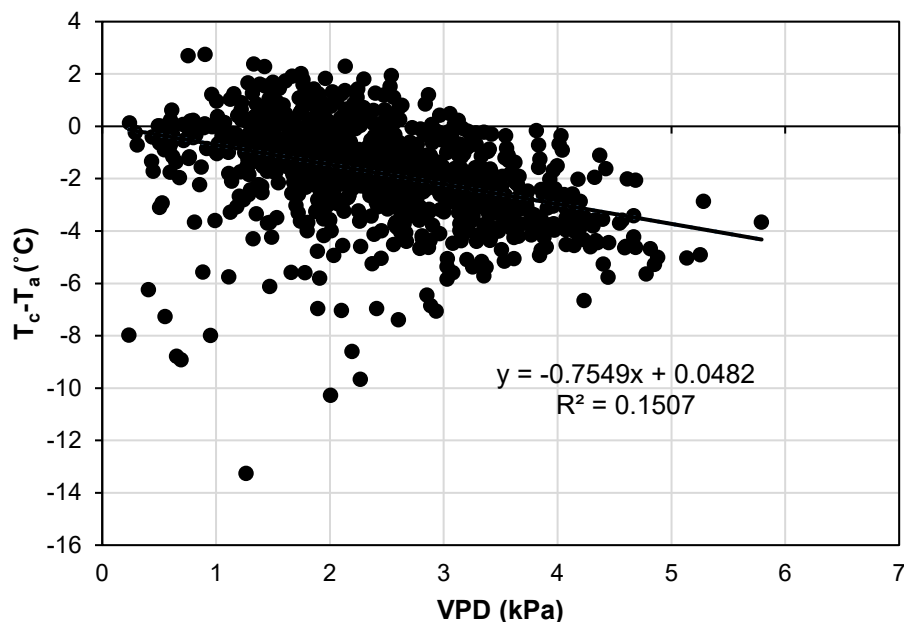


**Figure 4.76 Combined non-water stressed baseline (NWSB) from both measurement season**

To give a better understanding of the effects of insufficient attention to detail when creating the NWSB, Figure 4.77 and Figure 4.78 are presented. In Figure 4.77, only data from the morning and evening is used, when the solar zenith angle is large and the stomata have not yet opened.

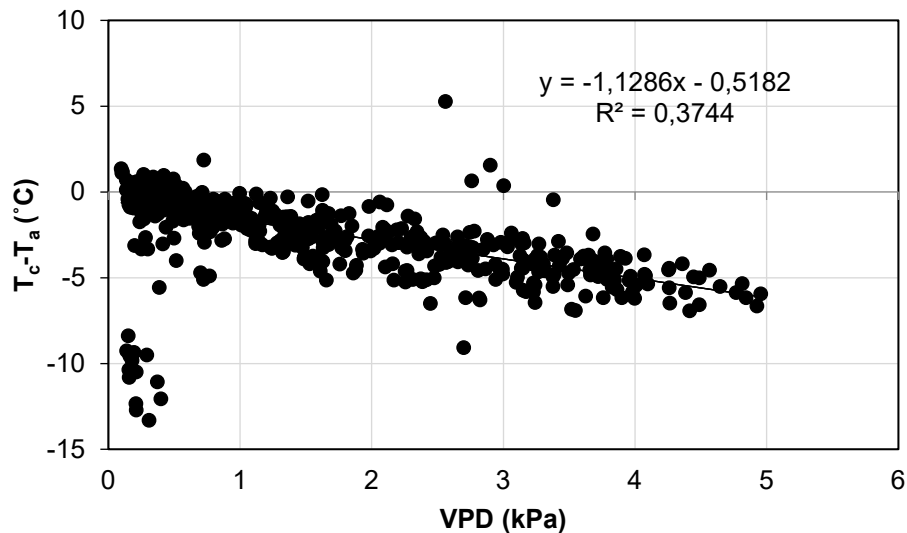


**Figure 4.77 Non-water stressed baseline (NWSB) from the 2020/21 season using only data from the two hours after sunrise and two hours before sunset**

The most obvious difference between Figure 4.77, and the correctly created NWSB in Figure 4.76 is the greater slope. This means that for every VPD value, the canopy temperature is much lower than the air temperature. However, this is not as a result of more efficient cooling by transpiration, but rather, a decreased solar heating effect. It therefore, does not reflect the conditions of the majority of the day, and such data should not be included in a NWSB used to quantify water stress.

The impact of inaccurate estimates of canopy temperature on the NWSB due to the measurement of background temperatures (bark or soil) is presented in Figure 4.78. Data from two IR radiometers are plotted together, with one of them measuring the temperature of a bare branch that was within the target canopy area. If this NWSB were to be used in the CWSI, the lower limit would have been above the actual canopy temperature.

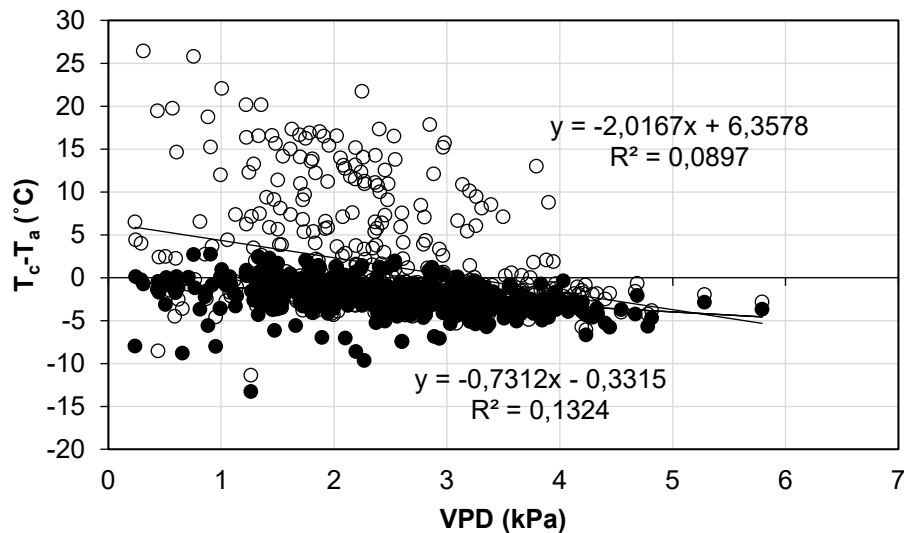


**Figure 4.78 Non-water stressed baseline (NWSB) from the 2021/22 season including data from the infrared radiometer detecting the temperature of a bare branch within the canopy (indicated by open circles)**

#### 4.5.4 THE CROP WATER STRESS INDEX

All canopy temperatures used to calculate the CWSI were collected by the UAV based thermal sensor, with orthomosaicing in Pix4D Fields and extraction of canopy temperatures in QGIS. The  $(T_c - T_a)_{LL}$ , or the  $T_c - T_a$  of a canopy transpiring at the potential rate was calculated using the NWSB and the thermal image histogram. The  $(T_c - T_a)_{UL}$  was found using the image histogram, a static Upper Limit of  $T_c - T_a = +6^\circ\text{C}$  was also tested. The negative VPD method of finding the Upper Limit yielded an Upper Limit of approximately  $+0.1^\circ\text{C}$  between canopy and air temperature on all the days it was tested. It was found that the thermal sensor consistently provided data that was above the plausible surface temperature for the conditions. Hence, all canopy temperatures, and the CWSI limits from the thermal image histograms are overestimated. Due to this, the histogram Upper Limit could not be used with the NWSB, and the Histogram Lower Limit could not be used with the static limit to calculate the CWSI. Therefore, the CWSI was calculated using data from the 2020/21, 2021/22 seasons and the two seasons' combined NWSB and  $T_c - T_a = 6^\circ\text{C}$  as the upper limit. The CWSI was also calculated using both limits from the thermal image histogram. The CWSI was calculated for each measurement tree, using the data from each day. All the data collected throughout the 2021/22 season was used to calculate the CWSI, all CWSIs from the entire season were plotted together against the corresponding  $\psi_{smd}$  (Figure 4.79).

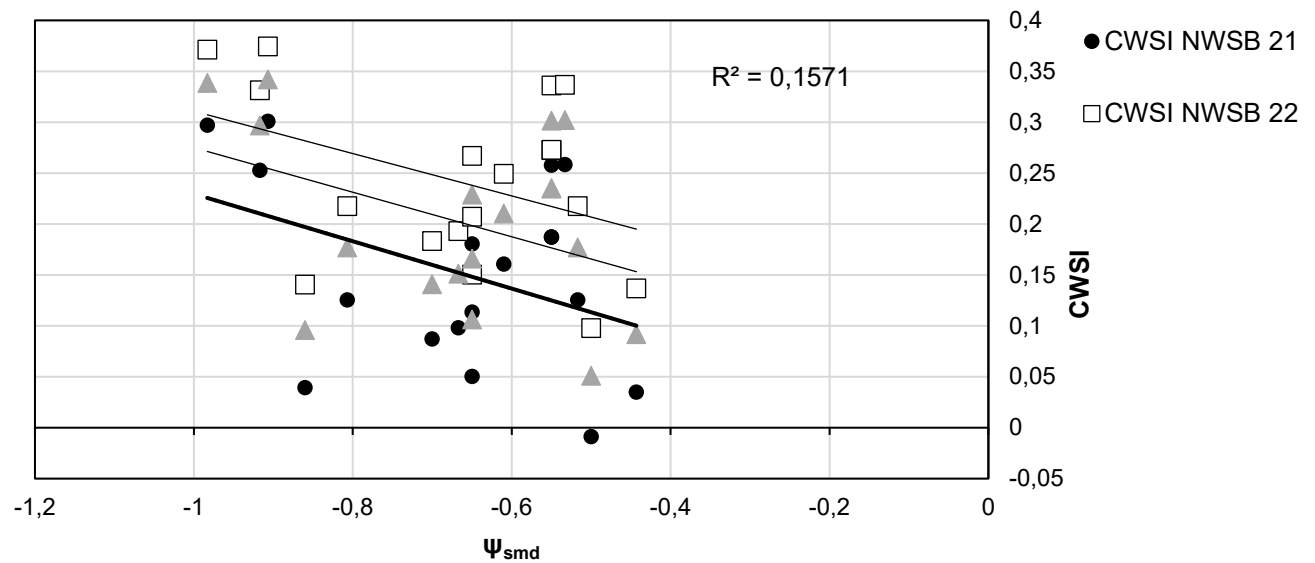


**Figure 4.79 Relationship between the crop water stress index (CWSI) calculated using the non-water stressed baseline (NWSB) and the static Upper Limit for each season, and the midday stem water potential ( $\psi_{smd}$ )**

The NWSB created from data from each season were similar enough that they caused little difference in the ability of the CWSI to detect water stress, even though the actual value of the CWSI differed (Figure 4.79). In this case, the CWSI using the NWSB was found to be mostly unable to detect water stress. This may be due to an inherent inaccuracy in the thermal sensor. It may also be as a result of the variability in both time-of-day and environmental conditions during data collection. These include cloud cover and solar angle, which affect the temperature of the leaf without taking air temperature and VPD into account.

The CWSI calculated using the reference surfaces and the image histogram limits would be expected to perform better, if the problem with the NWSB method is the effect of factors besides  $T_a$  and VPD which are specific to the day. This was, however, not found to be the case when the entire season was plotted together, as Figure 4.80 and Figure 4.82 show.



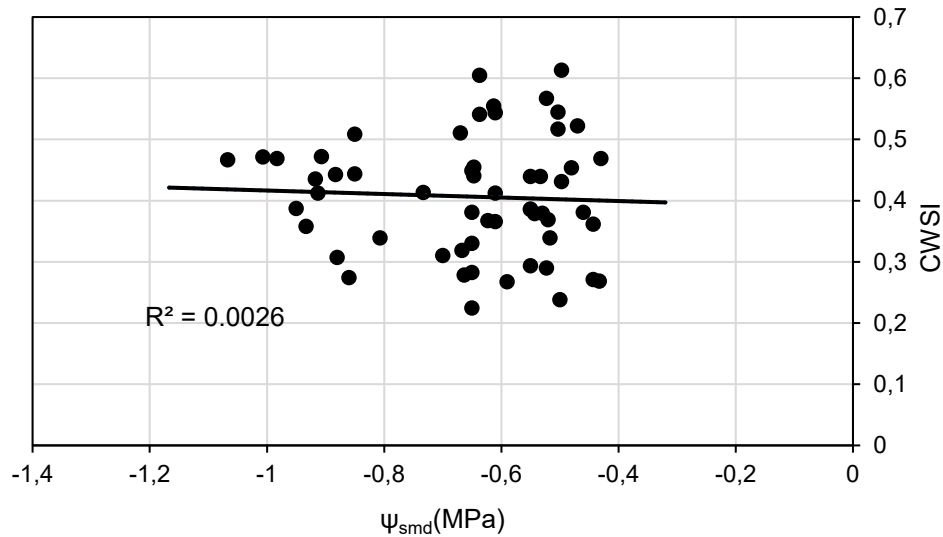


**Figure 4.80 Relationship between the crop water stress index (CWSI) with a lower limit found from a wet reference surface and an upper limit of 6°C, and midday stem water potential ( $\psi_{smd}$ )**

A possible explanation of the low correlation between the reference surface CWSI and  $\psi_{smd}$  is the difference in the illumination of the reference panel on different days, that the sensor system could not correct for. This is supported by data in Figure 4.82, which shows a slightly better correlation between the reference surface CWSI when a single day's data is plotted compared to several days in Figure 4.82.

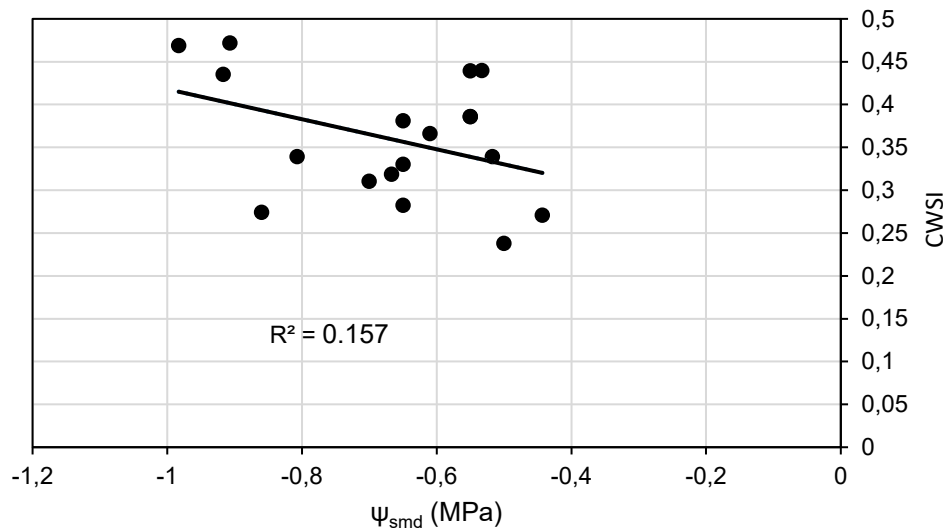


**Figure 4.81 Relationship between the CWSI with a lower limit found from a wet reference surface and an upper limit of 6°C on 13 April 2022, and midday stem water potential ( $\psi_{smd}$ )**

A very similar pattern was observed when the CWSI calculated using the thermal image histogram was tested for the data days (Figure 4.82).

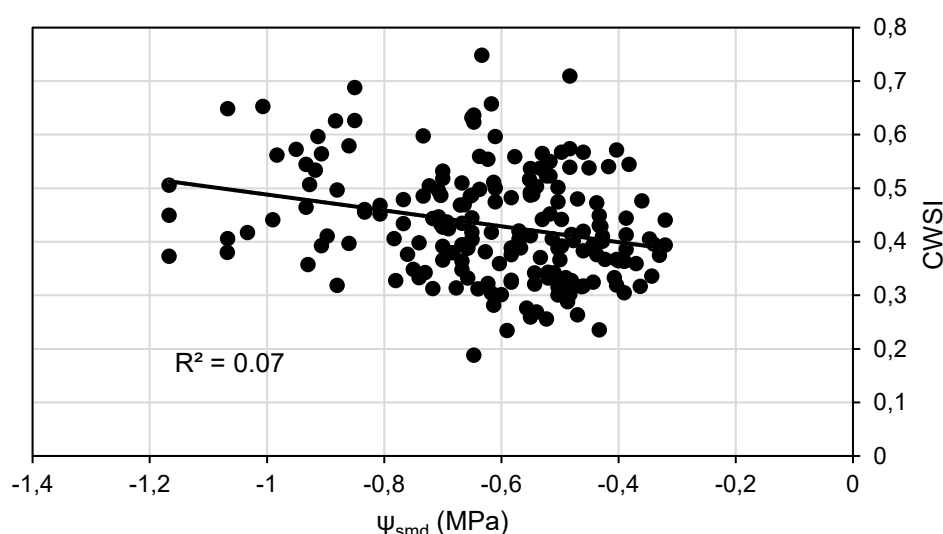


**Figure 4.82 Relationship between the crop water stress index (CWSI) calculated using the thermal image histogram, and midday stem water potential ( $\Psi_{smd}$ )**

Since the image histogram does not use an external device or method to correct for the atmospheric differences at the time of data collection, there are only two possible sources of variability in the thermal data, and the CWSI. The first is a high variability amongst the trees that were tested, so that they responded differently to water stress in terms of the regulation of water loss and leaf temperature. The other is inaccuracy in the sensor or the pre-processing software or methodology, so that environmental differences are able to influence the surface temperature recorded. It is possible that, on a single day, not enough data was collected for any relationship to become apparent when all external conditions are the same. The fact, however, remains that no CWSI method could be found which was able to provide an indication of water stress under all atmospheric conditions, which is the purpose of the CWSI, particularly the more empirical methods which do not rely on the NWSB.

#### 4.5.5 CONCLUSIONS

Research on detecting water stress in pecan trees using remote sensing tools has proved largely inconclusive. Firstly, the measurements only began in February 2021, due to the late procurement of a drone, and took place during seasons where very little stress was recorded in the orchard, due to a season with very high rainfall. As a result, very little contrast between stressed and unstressed trees was achieved to test correlations between ground

measurements and vegetation indices. However, the nature of the water stress response in pecans might not lend itself to detection of stress via VIs. Vegetation indices quantify changes in canopy structure (e.g. wilting) or changes in chlorophyll content, which are linked to water stress in some crops. As pecan leaves do not wilt, it does not seem possible to use VIs which detect structural changes, as with other crops. This, however, needs to be confirmed in a season when a greater level of stress is achieved. Parametrising the CWSI for pecans has also not been successful in the trial. Whilst a lot of progress was made, the parameters required for the accurate estimation of the CWSI could not be accurately estimated. This is a notoriously difficult thing to do and now that we have a much more accurate thermal camera, we are hoping that it will be possible in future, as this may be the most reliable way to detect water stress in pecan canopies. This work will be ongoing in future projects, as the experimental orchard at Innovation Africa @UP is ideally set up to allow for trees to be stressed at various growth stages, allowing the careful quantification of stress versus a well-watered control.

## 5. GENERAL DISCUSSION AND CONCLUSIONS

The first aim of the project was to measure water use in two orchards located within the Northern Cape Province to capture maximum water use from these orchards (transpiration evaporation and evapotranspiration) in order parameterise water use models for pecans that would be applicable across growing regions in South Africa. Despite numerous challenges during the course of the project water use measurements were successfully conducted for 5 years in Vaalharts and 4 years in Groblershoop. Measurements also included canopy size, water potentials, soil water content and the depth of the water table. For the majority of the study unstressed water use was measured, but there were occasions when there were slight water deficits in the orchard in Vaalharts and in the 2020/21 season a very high water table could have resulted in waterlogged conditions. As expected, water use varied from year to year and from site to site according to the prevailing weather conditions and changes in canopy size. As Groblershoop was hotter and drier than Vaalharts, evapotranspiration was higher in this orchard throughout the study, but tree transpiration was very much dependent on canopy size (Table 5.1). Importantly transpiration did not always increase at the same rate as atmospheric evaporative demand, as represented by vapour pressure deficit (VPD) and reference evapotranspiration ( $ET_o$ ) and when VPD increased above 1.5 kPa and  $ET_o$  above  $0.15 \text{ mm h}^{-1}$  transpiration started to plateau, suggesting some form of physiological control over transpiration.

The dependence of transpiration on tree size highlighted the need for accurate quantification of canopy size when modelling transpiration and a radiation interception model (Oyarzun et al., 2007) was therefore successfully parameterised for pecans. Estimates of radiation interception for pecan orchards were then used in a canopy conductance approach of Villalobos et al. (2013). This approach was parameterised in the pecan orchard in Pretoria and validated in the Northern Cape orchards and provided accurate estimate transpiration of these orchards over two seasons on a daily and monthly basis. This model therefore shows great promise for irrigation scheduling. A transpiration crop coefficient of Allen and Pereira (2009) was also parameterised for pecan in the Northern Cape orchards, which included methodology to take into account stomatal control over transpiration. Through a simple relationship between vapour pressure deficit and leaf resistance ( $r_{\text{leaf}}$ ), estimated according to Allen and Pereira (2009), good estimates of weekly and monthly transpiration were obtained. This model would be more appropriate for planning purposes, allowing good seasonal estimates of transpiration based on long term weather data. While soil evaporation was well estimated with two models, the inputs to the model are quite detailed, which hinders the ease with which the models can

be used. Future research needs to focus on making the transpiration and evaporation models easily implemented by growers to aid in water management.

**Table 5.1 Summary of tree water use of the orchards in the Northern Cape. T – transpiration, ET – evapotranspiration,  $WP_c$  – crop water productivity, EWP – economic water productivity**

	Vaalharts		Groblershoop	
	‘Choctaw’	‘Wichita’	‘Choctaw’	‘Wichita’
Avg. annual T (mm)	560	560	490	620
Max. T per day (mm (L))	3.60 (360)	4.20 (420)	3.60 (360)	4.80 (480)
Avg. T per day <sup>a</sup> (mm (L))	2.40 (240)	2.30 (230)	2.20 (220)	2.50 (250)
Avg max canopy cover	0.68	0.73	0.72	0.78
Avg. seasonal <sup>b</sup> $ET_o$ (mm)	1 410		1 570	
Avg. seasonal ET (mm)	1 060		1 250	
$WP_c \pm SE$ ( $kg\ m^{-3}$ ) <sup>c</sup>	$0.23 \pm 0.08$		$0.16 \pm 0.18$	
$EWP_c \pm SE$ ( $R\ m^{-3}$ )	$15.49 \pm 10.13$		$16.02 \pm 27.74$	

<sup>a</sup>in the period November to February

<sup>b</sup>seasonal is for when the trees are in leaf from 1 September to 30 June

<sup>c</sup>estimated from evapotranspiration and yield of the whole orchard

The second aim was to assess the crop water productivity ( $WP_c$ ) and economic water productivity ( $EWP_c$ ) of pecan orchards in the Northern Cape. When comparing water productivity ( $WP_c$ ) of pecans with other annual and perennial crops cultivated in each region, pecan performs poorly, due to relatively low yields and high water use. For both sites over the course of the study pecan  $WP_c$  varied from 0.05 to 0.37  $kg\ m^{-3}$ , whilst for annual crops it varied between 0.41 and 2.11  $kg\ m^{-3}$  and 1.99 to 2.52  $kg\ m^{-3}$  for raisin grapes. It was evident that  $WP_c$  varied considerable from year to year, especially in Groblershoop, and this was attributed to the alternate bearing nature of pecans (especially ‘Choctaw’) and weather conditions in Groblershoop which caused excessive nut drop at times. One value for crops such as pecan can be very misleading and long term ranges in values would better represent the situation on

the ground. Despite the poor  $WP_c$  for pecans when compared to the other crops, when comparing economic water productivity ( $EWP_c$ ) with other crops grown in each region it is clearly evident why pecan production has expanded so much in this region. Pecan had much higher values than other crops due to the high value of the harvested nut. Values for pecans ranged from no profit in years when yields were very low to  $R21.99\text{ m}^{-3}$ , whilst for annual crops it ranged between  $R0.45$  and  $R3.40\text{ m}^{-3}$ . From two years of data raisin grapes varied between no profit and  $R3.05\text{ m}^{-3}$ . Additional research should be conducted to determine  $WP_c$  and  $EWP_c$  over the life time of an orchard to make fair comparisons with other crops.

The third aim was to determine the impact of a water deficit stress at different phenological stages on the yield and quality of pecan orchards. This trial was conducted for six seasons, with stress being reliably induced in only three of these seasons. Rainfall was exceptionally high for the final three seasons which resulted in sufficient plant available water in the soil for the majority of the season. When stress was successfully imposed it was evident that flowering and nut set and nut filling were the most sensitive stages in terms of yield and quality. Stress during these stages can have a very negative impact on yield through a reduction in nut number during flowering and nut set and very poor nut filling during the nut filling stage. In some seasons nut size was also reduced when trees were stressed during nut sizing, which resulted in a reduction in income due to a lower price for smaller nuts. There was also an increase in stick tights in some seasons when trees were stressed during shuck dehiscence. Stick tights can either have well filled nuts or are pops which are poorly filled. If they are well filled there is an extra cost with processing to remove the shuck from the nuts. From a simple economic analysis of gross profit it was evident that over the course of the trial there was a penalty for implementing a stress at each phenological stage, suggesting that when water is not limiting, care should be taken to avoid a water deficit stress throughout the season through judicious irrigation management. However, in seasons when water allocations are reduced below the full ET requirements of the crop some savings may be possible during nut sizing and shuck dehiscence without a major impact on yield and quality. Guidelines for inducing slight water deficits in pecan orchards should be developed in future.

## 6. RECOMMENDATIONS

Water use was quantified over a number of seasons in two orchard with varying weather conditions and differences in canopy size. Using this data two transpiration and two evaporation models were parameterised for pecan orchards. Whilst both parameterisation and validation of these models were performed in this study, it will be important to test these models in other orchards relative to applied irrigation to assess the ability of the models to be used practically for irrigation management.

Whilst attempts were made to investigate the environmental and physiological control over transpiration in pecans, the seasons targeted for these measurements were much wetter than the norm and sufficient measurements to gain a thorough understanding of this control were not possible. These measurements should be continued, especially under the hot and dry conditions in the Northern Cape.

The project highlighted that canopy size was major determinant of seasonal water use volumes and not yield. Water use in “off years” (low yields) will therefore be the same as “on years” (good yields), if canopy size is similar, resulting in a wide variation in water productivity. In order to improve water productivity across seasons it may be feasible to prune trees to maintain a smaller canopy with similar yield. This needs to be tested to determine how much water can be saved and if more consistent yields can be achieved.

With the increased accessibility of remote sensing tools it will be important to test these tools in pecan for the assessment of plant stress across an orchard. Instead of doing laborious water potential measurements to assess stress, remote sensing tools could be used to assess stress across an entire orchard. It is very important that these tools are tested against ground measurements in more than one location. This could increase yield per hectare, as well as optimising irrigation scheduling. The testing of various methods to detect stress in pecans needs to be continued, as very little success was achieved in the current study. Using remote sensing to determine spatial and season ET of orchards could also aid in improved water use management within and across orchards in a region. These models need to be tested in pecan orchards against ground-based methods. Data from the current study could be used to do this.

Water productivity and economic water productivity calculations should be performed over the life time of an orchard, as is done for water footprinting analyses to take into account water required before they come into production. This will allow fairer comparisons between crops and allow growers to make more informed decisions on the water cost of growing pecans

compared to other crops and the impact pecan production has on water resources on a catchment level. This will allow the assessment of what area can sustainably be planted to pecans in an area.



## REFERENCES

- ABRAHA, M. G. & SAVAGE, M. J. 2010. Validation of a three-dimensional solar radiation interception model for tree crops. *Agriculture Ecosystems & Environment*, 139, 636-652.
- ABUDU, S., SHENG, Z., MICHELSEN, A., RODRIGUEZ, O. & KING, J. Evapotranspiration and Crop Coefficient for Pecan Trees in El Paso, Texas. Proc. Irrigation Show and Education Conference, December, 2016. 4-7.
- ACKERLY, D. D., DUDLEY, S. A., SULTAN, S. E., SCHMITT, J., COLEMAN, J. S., LINDER, C. R., SANDQUIST, D. R., GEBER, M. A., EVANS, A. S. & DAWSON, T. E. 2000. The Evolution of Plant Ecophysiological Traits: Recent Advances and Future Directions: New research addresses natural selection, genetic constraints, and the adaptive evolution of plant ecophysiological traits. *AIBS Bulletin*, 50, 979-995.
- AL-JAMAL, M., SAMMIS, T. & BALL, S. 2001. A case study for adopting the chloride technique for evaluating irrigation efficiency and nitrate-nitrogen to groundwater in farmers' fields. *Appl. Eng. Agric*, 17, 601-610.
- ALARCÓN, J., DOMINGO, R., GREEN, S., NICOLÁS, E. & TORRECILLAS, A. 2003. Estimation of hydraulic conductance within field-grown apricot using sap flow measurements. *Plant and soil*, 251, 125-135.
- ALBEN, A. 1955. Studies on relation of drought injury of pecan trees to soil textures and profiles. *Proc. Tex. Pecan Growers Assoc*, 34, 32-38.
- ALLEN, R. G. 2008. Quality assessment of weather data and micrometeorological flux – impacts on evapotranspiration calculation. *Journal of Agricultural Meteorology*, 64, 191-204.
- ALLEN, R. G. & PEREIRA, L. S. 2009. Estimating crop coefficients from fraction of ground cover and height. *Irrigation Science*, 28, 17-34.
- ALLEN, R. G., PEREIRA, L. S., RAES, D. & SMITH, M. 1998. *Crop evapotranspiration: guidelines for computing crop water requirements*, Irrigation and Drainage Paper 56, Rome <http://www.fao.org/docrep/X0490E/X0490E00.htm>, United Nations FAO.
- ALLEN, R. G., PEREIRA, L. S., SMITH, M., RAES, D. & WRIGHT, J. L. 2005. FAO-56 dual crop coefficient method for estimating evaporation from soil and application extensions. *Journal of irrigation and drainage engineering*, 131, 2-13.
- ANDALES, A., WANG, J., SAMMIS, T. W., MEXAL, J. G., SIMMONS, L. J., MILLER, D. R. & GUTSCHICK, V. P. 2006. A model of pecan tree growth for the management of pruning and irrigation. *Agricultural Water Management*, 84, 77-88.
- ANDERSEN, P. & BRODBECK, B. 1988a. Net CO<sub>2</sub> assimilation and plant water relations characteristics of pecan growth flushes. *Journal of the American Society for Horticultural Science*, 113, 444-450.

- ANDERSEN, P. & CROCKER, T. 2004. The pecan tree.: Florida Cooperative Extension Service, Institute of Food and Agricultural Sciences, University of Florida, .
- ANDERSEN, P. C. & BRODBECK, B. V. 1988b. Net CO<sub>2</sub> assimilation and plant water relations characteristics of pecan growth flushes. *Journal of the American Society for Horticultural Science*, 113, 444-450.
- ANDÚJAR, D., MORENO, H., BENGOCHEA-GUEVARA, J. M., DE CASTRO, A. & RIBEIRO, A. 2019. Aerial imagery or on-ground detection? An economic analysis for vineyard crops. *Computers and electronics in agriculture*, 157, 351-358.
- ANGELOCCI, L. R., MARIN, F. R., OLIVEIRA, R. F. & RIGHI, E. Z. 2004. Transpiration, leaf diffusive conductance, and atmospheric water demand relationship in an irrigated acid lime orchard. *Brazilian Journal of Plant Physiology*, 16, 53-64.
- ANNANDALE, J., JOVANOVIĆ, N., CAMPBELL, G., DU SAUTOY, N. & LOBIT, P. 2004. Two-dimensional solar radiation interception model for hedgerow fruit trees. *Agricultural and Forest Meteorology*, 121, 207-225.
- ANNANDALE, J. G., BENADE, N., JOVANOVIĆ, N. Z., STEYN, J. M. & DU SAUTOY, N. 1999. *Facilitating irrigation scheduling by means of the Soil Water Balance model*. , Pretoria, South Africa, Water Research Commission.
- ANTHONY, B. M. & MINAS, I. S. 2021. Optimizing peach tree canopy architecture for efficient light use, increased productivity and improved fruit quality. *Agronomy*, 11, 1961.
- ATTIA, Z., DOMEK, J.-C., OREN, R., WAY, D. A. & MOSHELION, M. 2015. Growth and physiological responses of isohydric and anisohydric poplars to drought. *Journal of experimental botany*, 66, 4373-4381.
- AYARS, J. E., JOHNSON, R. S., PHENE, C. J., TROUT, T. J., CLARK, D. A. & MEAD, R. M. 2003. Water use by drip-irrigated late-season peaches. *Irrigation Science*, 22, 187-194.
- BALUJA, J., DIAGO, M. P., BALDA, P., ZORER, R., MEGGIO, F., MORALES, F. & TARDAGUILA, J. 2012. Assessment of vineyard water status variability by thermal and multispectral imagery using an unmanned aerial vehicle (UAV). *Irrigation Science*, 30, 511-522.
- BAWAZIR, A. & KING, J. 2004. Crop Evapotranspiration (ET) Study for Doña Ana County, New Mexico. *Las Cruces, NM: New Mexico Water Resources Research Institute. Technical Completion Report*.
- BELLOCCHI, G., RIVINGTON, M., DONATELLI, M. & MATTHEWS, K. 2011. Validation of biophysical models: issues and methodologies. *Sustainable Agriculture Volume 2*. Springer.
- BIAN, J., ZHANG, Z., CHEN, J., CHEN, H., CUI, C., LI, X., CHEN, S. & FU, Q. 2019. Simplified evaluation of cotton water stress using high resolution unmanned aerial vehicle thermal imagery. *Remote Sensing*, 11, 267.

- BLACKMAN, C. J., CREEK, D., MAIER, C., ASPINWALL, M. J., DRAKE, J. E., PFAUTSCH, S., O'GRADY, A., DELZON, S., MEDLYN, B. E. & TISSUE, D. T. 2019. Drought response strategies and hydraulic traits contribute to mechanistic understanding of plant dry-down to hydraulic failure. *Tree Physiology*, 39, 910-924.
- BONACHELA, S., ORGAZ, F., VILLALOBOS, F. J. & FERERES, E. 1999. Measurement and simulation of evaporation from soil in olive orchards. *Irrigation Science*, 18, 205-211.
- BONACHELA, S., ORGAZ, F., VILLALOBOS, F. J. & FERERES, E. 2001. Soil evaporation from drip-irrigated olive orchards. *Irrigation Science*, 20, 65-71.
- BROGE, N. H. & LEBLANC, E. 2001. Comparing prediction power and stability of broadband and hyperspectral vegetation indices for estimation of green leaf area index and canopy chlorophyll density. *Remote sensing of environment*, 76, 156-172.
- BURGESS, S. S. O., ADAMS, M. A., TURNER, N. C., BEVERLY, C. R., ONG, C. K., KHAN, A. A. H. & BLEBY, T. M. 2001. An improved heat pulse method to measure low and reverse rates of sap flow in woody plants. *Tree Physiology*, 21, 589-598.
- CAMPBELL, G. S. & NORMAN, J. 2012. *An introduction to environmental biophysics*, Springer Science & Business Media.
- CAMPBELL, G. S. & NORMAN, J. M. 1998. Radiation fluxes in natural environments. *An introduction to environmental biophysics*. Springer.
- CAMPOS, I., NEALE, C. M. U. & CALERA, A. 2017. Is row orientation a determinant factor for radiation interception in row vineyards? *Australian Journal of Grape and Wine Research*, 23, 77-86.
- CASTEL, J. R. 2000. Water use of developing citrus canopies in Valencia, Spain. Proc IX International Citrus Congress, Orlando, Florida, December 2000. Orlando, Florida, 3-7.
- CHARLES-EDWARDS, D. & THORNLEY, J. 1973. Light interception by an isolated plant a simple model. *Annals of Botany*, 37, 919-928.
- CHAVES, M. M., PEREIRA, J. S., MAROCO, J., RODRIGUES, M. L., RICARDO, C. P. P., OSÓRIO, M. L., CARVALHO, I., FARIA, T. & PINHEIRO, C. 2002. How plants cope with water stress in the field? Photosynthesis and growth. *Annals of botany*, 89, 907-916.
- CHORTYK, O., YATES, I. & REILLY, C. 1995. Changes in cuticular compounds of developing pecan leaves. *Journal of the American Society for Horticultural Science*, 120, 329-335.
- CIFRE, J., BOTA, J., ESCALONA, J., MEDRANO, H. & FLEXAS, J. 2005. Physiological tools for irrigation scheduling in grapevine (*Vitis vinifera* L.): An open gate to improve water-use efficiency? *Agriculture, Ecosystems & Environment*, 106, 159-170.
- COHEN, S., FUCHS, M., MORESHET, S. & COHEN, Y. 1987. The distribution of leaf area, radiation, photosynthesis and transpiration in a Shamouti orange hedgerow orchard. Part II. Photosynthesis, transpiration, and the effect of row shape and direction. *Agricultural and Forest Meteorology*, 40, 145-162.

- COHEN, S., RAO, R. S. & COHEN, Y. 1997. Canopy transmittance inversion using a line quantum probe for a row crop. *Agricultural and Forest Meteorology*, 86, 225-234.
- COHEN, Y., FUCHS, M. & COHEN, S. 1983. Resistance to water uptake in a mature citrus tree. *Journal of Experimental Botany*, 34, 451-460.
- CONNER, P. J. & WORLEY, R. E. 2000. Alternate bearing intensity of pecan cultivars. *HortScience*, 35, 1067-1069.
- CONSOLI, S., O'CONNELL, N. & SNYDER, R. 2006. Estimation of evapotranspiration of different-sized navel-orange tree orchards using energy balance. *Journal of Irrigation and Drainage Engineering*, 132, 2-8.
- DAAMEN, C. C., SIMMONDS, L., WALLACE, J., LARYEA, K. & SIVAKUMAR, M. 1993. Use of microlysimeters to measure evaporation from sandy soils. *Agricultural and Forest Meteorology*, 65, 159-173.
- DAFF 2006. Fruit and nut production in Kwazulu-Natal. In: DEPARTMENT OF AGRICULTURE & FORESTRY AND FISHERIES, S. A. (eds.).
- DE BEI, R., FUENTES, S., GILLIHAM, M., TYERMAN, S., EDWARDS, E., BIANCHINI, N., SMITH, J. & COLLINS, C. 2016. VitiCanopy: A free computer App to estimate canopy vigor and porosity for grapevine. *Sensors*, 16, 585.
- DE JAGER, J. M. 1994. Accuracy of vegetation evaporation ratio formulae for estimating final wheat yield. *WATER SA-PRETORIA*, 20, 307-314.
- DE VRIES, F. P. 1975. The cost of maintenance processes in plant cells. *Annals of Botany*, 39, 77-92.
- DEB, S. K., SHUKLA, M. K. & MEXAL, J. G. 2012. Estimating midday leaf and stem water potentials of mature pecan trees from soil water content and climatic parameters. *HortScience*, 47, 907-916.
- DONG, X., ZHANG, Z., YU, R., TIAN, Q. & ZHU, X. 2020. Extraction of information about individual trees from high-spatial-resolution UAV-acquired images of an orchard. *Remote Sensing*, 12, 133.
- EMMEL, C., D'ODORICO, P., REVILL, A., HÖRTNAGL, L., AMMANN, C., BUCHMANN, N. & EUGSTER, W. 2020. Canopy photosynthesis of six major arable crops is enhanced under diffuse light due to canopy architecture. *Global change biology*, 26, 5164-5177.
- ESPADAFOR, M., ORGAZ, F., TESTI, L., LORITE, I. J. & VILLALOBOS, F. J. 2015. Transpiration of young almond trees in relation to intercepted radiation. *Irrigation science*, 33, 265-275.
- FERERES, E., GOLDHAMER, D. & SADRAS, V. 2012. Yield response to water of fruit trees and vines: guidelines. *FAO Irrigation and Drainage Paper*, 246-497.

- FERERES, E., VILLALOBOS, F., ORGAZ, F., MINGUEZ, M., VAN HALSEMA, G. & PERRY, C. 2017. Commentary: On the water footprint as an indicator of water use in food production. Springer.
- FERNÁNDEZ, J., ALCON, F., DIAZ-ESPEJO, A., HERNANDEZ-SANTANA, V. & CUEVAS, M. 2020. Water use indicators and economic analysis for on-farm irrigation decision: A case study of a super high density olive tree orchard. *Agricultural Water Management*, 237, 106074.
- FINCH, A. H. & VAN HORN, C. W. 1936. *The physiology and control of pecan nut filling and maturity*, College of Agriculture, University of Arizona (Tucson, AZ).
- FLUMIGNAN, D. L., FARIA, R. T. D. & LENA, B. P. 2012. Test of a microlysimeter for measurement of soil evaporation. *Engenharia Agrícola*, 32, 80-90.
- GAGO, J., DOUTHE, C., COOPMAN, R., GALLEGOS, P., RIBAS-CARBO, M., FLEXAS, J., ESCALONA, J. & MEDRANO, H. 2015. UAVs challenge to assess water stress for sustainable agriculture. *Agricultural water management*, 153, 9-19.
- GARROT, D. J., KILBY, M. W., FANGMEIER, D. D., HUSMAN, S. H. & RALOWICZ, A. E. 1993. Production, growth, and nut quality in pecans under water stress based on the crop water stress index. *Journal of the American Society for Horticultural Science*, 118, 694-698.
- GAUTAM, D., OSTENDORF, B. & PAGAY, V. 2021. Estimation of grapevine crop coefficient using a multispectral camera on an unmanned aerial vehicle. *Remote Sensing*, 13, 2639.
- GIULIANI, R., MAGNANINI, E., FRAGASSA, C. & NEROZZI, F. 2000. Ground monitoring the light-shadow windows of a tree canopy to yield canopy light interception and morphological traits. *Plant, Cell & Environment*, 23, 783-796.
- GOODWIN, I., WHITFIELD, D. M. & CONNOR, D. J. 2006. Effects of tree size on water use of peach (*Prunus persica* L. Batsch). *Irrigation Science*, 24, 59-68.
- GRAUKE, L., STOREY, J. & EMINO, E. 1987. Influence of leaf age on the upper and lower leaf surface features of juvenile and adult pecan leaves. *J. Amer. Soc. Hort. Sci.*, 112, 835-41.
- GREEN, S., MCNAUGHTON, K., WÜNSCHE, J. & CLOTHIER, B. 2003. Modeling light interception and transpiration of apple tree canopies. *Agronomy Journal*, 95, 1380-1387.
- GUTSCHICK, V. P. & SHENG, Z. 2013. Control of atmospheric fluxes from a pecan orchard by physiology, meteorology, and canopy structure: Modeling and measurement. *Agricultural water management*, 129, 200-211.
- HARGREAVES, G. H. & SAMANI, Z. A. 1985. Reference crop evapotranspiration from temperature. *Applied engineering in agriculture*, 1, 96-99.
- HERRERA, E. A. 1990. Fruit Growth and Development of Ideal and Western Pecans. *Journal of the American Society for Horticultural Science*, 115, 915-923.

- HOWELL, T. 1994. Irrigation engineering, evapotranspiration. *Encyclopedia of agricultural science/edited by Charles J. Arntzen, Ellen M. Ritter*.
- HUBBARD, R., RYAN, M., STILLER, V. & SPERRY, J. 2001. Stomatal conductance and photosynthesis vary linearly with plant hydraulic conductance in ponderosa pine. *Plant, Cell & Environment*, 24, 113-121.
- IBRAIMO, N. A. 2018. *Water use of deciduous and evergreen tree nut crops: a case study using pecans and macadamias*. PhD University of Pretoria.
- IBRAIMO, N. A., TAYLOR, N. J., STEYN, J. M., GUSH, M. B. & ANNANDALE, J. G. 2016. Estimating water use of mature pecan orchards: A six stage crop growth curve approach. *Agricultural Water Management*, 177, 359-368.
- IDSO, S. B. 1982. Non-water-stressed baselines: A key to measuring and interpreting plant water stress. *Agricultural Meteorology*, 27, 59-70.
- ISBELL, C. L. 1928. Growth studies of the pecan.
- ISHIHARA, M., INOUE, Y., ONO, K., SHIMIZU, M. & MATSUURA, S. 2015. The impact of sunlight conditions on the consistency of vegetation indices in croplands—Effective usage of vegetation indices from continuous ground-based spectral measurements. *Remote Sensing*, 7, 14079-14098.
- JACKSON, J. & PALMER, J. 1979. A simple model of light transmission and interception by discontinuous canopies. *Annals of Botany*, 44, 381-383.
- JACKSON, R. D. & HUETE, A. R. 1991. Interpreting vegetation indices. *Preventive veterinary medicine*, 11, 185-200.
- JACKSON, R. D., IDSO, S., REGINATO, R. & PINTER JR, P. 1981. Canopy temperature as a crop water stress indicator. *Water resources research*, 17, 1133-1138.
- JARVIS, A. J. & DAVIES, W. J. 1998. The coupled response of stomatal conductance to photosynthesis and transpiration. *Journal of Experimental Botany*, 399-406.
- JENNINGS, S. B., BROWN, N. D. & SHEIL, D. 1999. Assessing forest canopies and understorey illumination: canopy closure, canopy cover and other measures. *Forestry: An International Journal of Forest Research*, 72, 59-74.
- JIMÉNEZ-BRENES, F. M., LÓPEZ-GRANADOS, F., DE CASTRO, A., TORRES-SÁNCHEZ, J., SERRANO, N. & PEÑA, J. 2017. Quantifying pruning impacts on olive tree architecture and annual canopy growth by using UAV-based 3D modelling. *Plant Methods*, 13, 1-15.
- JOHNSON, M.-V. V., KINIRY, J. R. & BURSON, B. L. 2010. Ceptometer deployment method affects measurement of fraction of intercepted photosynthetically active radiation. *Agronomy journal*, 102, 1132-1137.
- JOHNSON, R. S., AYARS, J. & HSIAO, T. 2002. Modeling young peach tree evapotranspiration. *Acta horticulturae*, 584, 107-113.

- JOHNSON, R. S., AYARS, J., TROUT, T., MEAD, R. & PHENE, C. 2000. Crop coefficients for mature peach trees are well correlated with midday canopy light interception. *III International Symposium on Irrigation of Horticultural Crops* 537, 537, 455-460.
- JONES, H. & CUMMING, I. 1984. Variation of leaf conductance and leaf water potential in apple orchards. *Journal of horticultural science*, 59, 329-336.
- JONES, H. G. 2007. Monitoring plant and soil water status: established and novel methods revisited and their relevance to studies of drought tolerance. *Journal of Experimental Botany*, 58, 119-130.
- JOVANOVIĆ, N., PEREIRA, L., PAREDES, P., PÔÇAS, I., CANTORE, V. & TODOROVIC, M. 2020. A review of strategies, methods and technologies to reduce non-beneficial consumptive water use on farms considering the FAO56 methods. *Agricultural water management*, 239, 106267.
- KASPAR, T. & BLAND, W. L. 1992. Soil temperature and root growth. *Soil Science*, 154, 290-299.
- KATERJI, N., MASTRORILLI, M. & RANA, G. 2008. Water use efficiency of crops cultivated in the Mediterranean region: Review and analysis. *European Journal of Agronomy*, 28, 493-507.
- KILBY, M. 1980. Fall irrigation of pecans. *Pecan South*.
- KINGRA, P., MAJUMDER, D. & SINGH, S. P. 2016. Application of remote sensing and GIS in agriculture and natural resource management under changing climatic conditions. *Agric Res J*, 53, 295-302.
- KLEINHENZ, M. D., BAMBERG, J. B. & PALTA, J. P. 1995. Use of stomatal index as a marker to screen backcross populations of two wild potato species segregating for freezing tolerance. *American potato journal*, 72, 243-250.
- KOOL, D., AGAM, N., LAZAROVITCH, N., HEITMAN, J., SAUER, T. & BEN-GAL, A. 2014. A review of approaches for evapotranspiration partitioning. *Agricultural and forest meteorology*, 184, 56-70.
- KOZŁOWSKI, T. 1992. Carbohydrate sources and sinks in woody plants. *The Botanical Review*, 58, 107-222.
- KRUSE, E. G. 1978. Describing irrigation efficiency and uniformity. *Journal of the Irrigation and Drainage Division*, 104, 35-41.
- KUDEN, A. B., BAYAZIT, S., YILDIRIM, B. & IMRAK, B. 2013. Studies on the chilling requirements of pecan nut (*Carya illionensis* Koch) cultivars. *African Journal of Agricultural Research*, 8, 3159-3165.
- LACOINTE, A. 2000. Carbon allocation among tree organs: a review of basic processes and representation in functional-structural tree models. *Annals of Forest Science*, 57, 521-533.

- LAMBERS, H., CHAPIN, F. S. & PONS, T. L. 2008a. Photosynthesis. *Plant physiological ecology*. Springer.
- LAMBERS, H., CHAPIN, F. S. & PONS, T. L. 2008b. *Plant physiological ecology*, Springer.
- LIANG, L., SCHWARTZ, M. D. & FEI, S. 2012. Photographic assessment of temperate forest understory phenology in relation to springtime meteorological drivers. *International journal of biometeorology*, 56, 343-355.
- LINSLEY-NOAKES, G., LOUW, M. & ALLAN, P. 1995. Estimating daily positive Utah chill units using daily minimum and maximum temperatures. *Journal of Southern African Society for Horticultural Sciences (South Africa)*.
- LOESCHER, W. H., MCCAMANT, T. & KELLER, J. D. 1990. Carbohydrate reserves, translocation, and storage in woody plant roots. *HortScience*, 25, 274-281.
- LOMBARDINI, L. 2006. One-time pruning of pecan trees induced limited and short-term benefits in canopy light penetration, yield, and nut quality. *HortScience*, 41, 1469-1473.
- LYR, H. & HOFFMANN, G. 1967. Growth Rates and Growth Periodicity of Tree Roots. In: ROMBERGER, J. A. & MIKOLA, P. (eds.) *International Review of Forestry Research*. Elsevier.
- MAES, W. H., BAERT, A., HUETE, A. R., MINCHIN, P. E., SNELGAR, W. P. & STEPPE, K. 2016. A new wet reference target method for continuous infrared thermography of vegetations. *Agricultural and Forest Meteorology*, 226, 119-131.
- MAHHOU, A., DEJONG, T. M., CAO, T. & SHACKEL, K. S. 2005. Water stress and crop load effects on vegetative and fruit growth of 'Elegant Lady' peach [*Prunus persica* (L.) Batch] trees. *Fruits*, 60, 55-68.
- MANNING, W. E. 1938. The morphology of the flowers of the Juglandaceae. I. The inflorescence. *American Journal of Botany*, 407-419.
- MANNING, W. E. 1940. The morphology of the flowers of the Juglandaceae. II. The pistillate flowers and fruit. *American Journal of Botany*, 839-852.
- MARISCAL, M., ORGAZ, F. & VILLALOBOS, F. 2000. Modelling and measurement of radiation interception by olive canopies. *Agricultural and Forest Meteorology*, 100, 183-197.
- MARSAL, J., GIRONA, J., CASADESUS, J., LOPEZ, G. & STÖCKLE, C. O. 2013. Crop coefficient (K<sub>c</sub>) for apple: comparison between measurements by a weighing lysimeter and prediction by CropSyst. *Irrigation Science*, 31, 455-463.
- MARSAL, J., JOHNSON, S., CASADESUS, J., LOPEZ, G., GIRONA, J. & STÖCKLE, C. 2014. Fraction of canopy intercepted radiation relates differently with crop coefficient depending on the season and the fruit tree species. *Agricultural and Forest Meteorology*, 184, 1-11.



- MARTÍNEZ-VILALTA, J., POYATOS, R., AGUADÉ, D., RETANA, J. & MENCUCCINI, M. 2014. A new look at water transport regulation in plants. *New phytologist*, 204, 105-115.
- MASEDA, P. H. & FERNÁNDEZ, R. J. 2006. Stay wet or else: three ways in which plants can adjust hydraulically to their environment. *Journal of Experimental Botany*, 57, 3963-3977.
- MEINZER, F. C. 2002. Co-ordination of vapour and liquid phase water transport properties in plants. *Plant, Cell & Environment*, 25, 265-274.
- MIRFENDERESGI, G., BOHRER, G., MATHENY, A. M., FATICHI, S., MORAES FRASSON, R. P. & SCHÄFER, K. V. R. 2016. Tree level hydrodynamic approach for resolving aboveground water storage and stomatal conductance and modeling the effects of tree hydraulic strategy. *Journal of Geophysical Research: Biogeosciences*, 121, 1792-1813.
- MIYAMOTO, S. 1983. Consumptive water use of irrigated pecans. *Journal of the American Society of Horticultural Science*, 108, 676-681.
- MIYAMOTO, S. 1990. Scheduling irrigation for pecans. *Acta Horticulturae*, 275, 513-522.
- MONSI, M. & SAEKI, T. 1953. The light factor in plant communities and its significance for dry matter production. *Japanese Journal of Botany*, 14, 22-52.
- MONTEITH, J. L. 1977. Climate and the efficiency of crop production in Britain. *Phil. Trans. R. Soc. Lond. B*, 281, 277-294.
- MORESHET, S. & GREEN, G. C. 1984. Seasonal trends in hydraulic conductance of field-grown 'Valencia' orange trees. *Scientia horticulturae*, 23, 169-180.
- NARDINI, A. & TYREE, M. T. 1999. Root and shoot hydraulic conductance of seven *Quercus* species. *Annals of Forest Science*, 56, 371-377.
- NEMATİ, A. 1968. Comparative leaf anatomy of six pecan cultivars *Carya illinoensis* Koch.
- NHAMO, L., EBRAHIM, G. Y., MABHAUDHI, T., MPANDELI, S., MAGOMBEYI, M., CHITAKIRA, M., MAGIDI, J. & SIBANDA, M. 2020. An assessment of groundwater use in irrigated agriculture using multi-spectral remote sensing. *Physics and Chemistry of the Earth, Parts A/B/C*, 115, 102810.
- NTSHIDI, Z., DZIKITI, S., MAZVIMAVI, D. & MOBE, N. 2021. Contribution of understorey vegetation to evapotranspiration partitioning in apple orchards under Mediterranean climatic conditions in South Africa. *Agricultural Water Management*, 245, 106627.
- ORGAZ, F., TESTI, L., VILLALOBOS, F. & FERERES, E. 2006. Water requirements of olive orchards – II: determination of crop coefficients for irrigation scheduling. *Irrigation Science*, 24, 77-84.
- OSTER, J., MEYER, J., HERMSMEIER, L. & KADDAH, M. 1986. Field studies of irrigation efficiency in the Imperial Valley. *Hilgardia*, 54, 1-15.

- OTHMAN, Y., VANLEEUEWEN, D., HEEREMA, R. & HILAIRE, R. S. 2014. Midday stem water potential values needed to maintain photosynthesis and leaf gas exchange established for pecan. *Journal of the American Society for Horticultural Science*, 139, 537-546.
- OUYANG, J., DE BEI, R., FUENTES, S. & COLLINS, C. 2020. UAV and ground-based imagery analysis detects canopy structure changes after canopy management applications. *OENO One*, 54, 1093-1103.
- OYARZUN, R. A., STÖCKLE, C. O. & WHITING, M. D. 2007. A simple approach to modeling radiation interception by fruit-tree orchards. *Agricultural and Forest Meteorology*, 142, 12-24.
- PAÇO, T., FERREIRA, M., ROSA, R., PAREDES, P., RODRIGUES, G., CONCEIÇÃO, N., PACHECO, C. & PEREIRA, L. 2012. The dual crop coefficient approach using a density factor to simulate the evapotranspiration of a peach orchard: SIMDualKc model versus eddy covariance measurements. *Irrigation Science*, 30, 115-126.
- PALMER, J. 1977. Diurnal light interception and a computer model of light interception by hedgerow apple orchards. *J. Appl. Ecol.*, 601-614.
- PARKER, T. A., PALKOVIC, A. & GEPTS, P. 2020. Determining the genetic control of common bean early-growth rate using unmanned aerial vehicles. *Remote Sensing*, 12, 1748.
- PATRIGNANI, A. & OCHSNER, T. E. 2015. Canopeo: A powerful new tool for measuring fractional green canopy cover. *Agronomy journal*, 107, 2312-2320.
- PHILLIPS, N. & OREN, R. A comparison of daily representations of canopy conductance based on two conditional time-averaging methods and the dependence of daily conductance on environmental factors. *Annales des Sciences Forestieres*, 1998. EDP Sciences, 217-235.
- PIRZAD, A., SHAKIBA, M. R., ZEHTAB-SALMASI, S., MOHAMMADI, S. A., DARVISHZADEH, R. & SAMADI, A. 2011. Effect of water stress on leaf relative water content, chlorophyll, proline and soluble carbohydrates in *Matricaria chamomilla* L. *Journal of Medicinal Plants Research*, 5, 2483-2488.
- PREGITZER, K. S., KING, J. S., BURTON, A. J. & BROWN, S. E. 2000. Responses of tree fine roots to temperature. *The New Phytologist*, 147, 105-115.
- PUPPO, L., GARCÍA, C., BAUTISTA, E., HUNSAKER, D. J., BERETTA, A. & GIRONA, J. 2019. Seasonal basal crop coefficient pattern of young non-bearing olive trees grown in drainage lysimeters in a temperate sub-humid climate. *Agricultural Water Management*, 226, 105732.
- RITCHIE, J. T. 1972. Model for predicting evaporation from a row crop with incomplete cover. *Water resources research*, 8, 1204-1213.

- ROBINSON, D. 1994. The responses of plants to non-uniform supplies of nutrients. *New Phytologist*, 127, 635-674.
- RODRÍGUEZ-GAMIR, J., INTRIGLIOLO, D. S., PRIMO-MILLO, E. & FORNER-GINER, M. A. 2010. Relationships between xylem anatomy, root hydraulic conductivity, leaf/root ratio and transpiration in citrus trees on different rootstocks. *Physiologia plantarum*, 139, 159-169.
- ROELFSEMA, M. R. G. & HEDRICH, R. 2005. In the light of stomatal opening: new insights into 'the Watergate'. *New Phytologist*, 167, 665-691.
- ROJO, F., DHILLON, R., UPADHYAYA, S., JENKINS, B., LAMPINEN, B., ROACH, J. & METCALF, S. Modeling canopy light interception for estimating potential yield in almond and walnut trees. 2014 Montreal, Quebec Canada July 13-July 16, 2014, 2014. American Society of Agricultural and Biological Engineers, 1.
- ROSELL, J. & SANZ, R. 2012. A review of methods and applications of the geometric characterization of tree crops in agricultural activities. *Computers and Electronics in Agriculture*, 81, 124-141.
- RUBKE, F. E. R. 2015. *Modeling canopy PAR interception for estimating potential yield in almond and walnut trees*, University of California, Davis.
- SADE, N. & MOSHELION, M. 2014. The dynamic isohydric-anisohydric behavior of plants upon fruit development: taking a risk for the next generation. *Tree physiology*, 34, 1199-1202.
- SAGARAM, M., LOMBARDINI, L. & GRAUKE, L. 2007. Variation in leaf anatomy of pecan cultivars from three ecogeographic locations. *Journal of the American Society for Horticultural Science*, 132, 592-596.
- SAMANI, A. & BAWAZIR, S. 2015. Improving evapotranspiration estimation using remote sensing technology. *Technical Completion Report, Account Number (Index#)*, 125548.
- SAMANI, Z., BAWAZIR, A. S., BLEIWEISS, M., SKAGGS, R., LONGWORTH, J., TRAN, V. D. & PINON, A. 2009. Using remote sensing to evaluate the spatial variability of evapotranspiration and crop coefficient in the lower Rio Grande Valley, New Mexico. *Irrigation Science*, 28, 93-100.
- SAMANI, Z., BAWAZIR, S., SKAGGS, R., LONGWORTH, J., PIÑON, A. & TRAN, V. 2011. A simple irrigation scheduling approach for pecans. *Agricultural Water Management*, 98, 661-664.
- SAMMIS, T., ANDALES, A., SIMMONS, L. & GUTSCHICK, V. Adjustment of closed canopy crop coefficients of pecans for open canopy orchards. Thirty-eighth Western Pecan Conference Proceedings, Las Cruces Hilton, Las Cruces, New Mexico, 2004a. 28-32.

- SAMMIS, T., GUTSCHICK, V., WANG, J. & MILLER, D. R. 2013. Model of water and nitrogen management in pecan trees under normal and resource-limited conditions. *Agricultural Water Management*, 124, 28-36.
- SAMMIS, T., MEXAL, J. & MILLER, D. 2004b. Evapotranspiration of flood-irrigated pecans. *Agricultural water management*, 69, 179-190.
- SAMMIS, T., RILEY, W. & LUGG, D. 1988. Crop water stress index of pecans. *Applied Engineering in Agriculture*, 4, 39-45.
- SAMMIS, T. W. 1980. Comparison of Sprinkler, Trickle, Subsurface, and Furrow Irrigation Methods for Row Crops 1. *Agronomy Journal*, 72, 701-704.
- SAMMIS, T. W., MEXAL, J. G. & MILLER, D. 2004c. Evapotranspiration of flood-irrigated pecans. *Agricultural Water Management*, 69, 179-190.
- SARGENT, R. G. 2013. Verification and validation of simulation models. *Journal of simulation*, 7, 12-24.
- SAXTON, K., RAWLS, W. J., ROMBERGER, J. & PAPENDICK, R. 1986. Estimating generalized soil-water characteristics from texture 1. *Soil science society of America Journal*, 50, 1031-1036.
- SCHOLANDER, P. F., BRADSTREET, E. D., HEMMINGSEN, E. & HAMMEL, H. 1965. Sap pressure in vascular plants: negative hydrostatic pressure can be measured in plants. *Science*, 148, 339-346.
- SCHULTZ, H. R. 2003. Differences in hydraulic architecture account for near-isohydric and anisohydric behaviour of two field-grown *Vitis vinifera* L. cultivars during drought. *Plant, Cell & Environment*, 26, 1393-1405.
- SHAO, H.-B., CHU, L.-Y., JALEEL, C. A. & ZHAO, C.-X. 2008. Water-deficit stress-induced anatomical changes in higher plants. *Comptes Rendus Biologies*, 331, 215-225.
- SHUHART, D. V. 1927. *The morphological differentiation of the pistillate flowers of the pecan*, US Government Printing Office.
- SIMARD, S. W. & DURALL, D. M. 2004. Mycorrhizal networks: a review of their extent, function, and importance. *Canadian Journal of Botany*, 82, 1140-1165.
- SINOQUET, H., LE ROUX, X., ADAM, B., AMEGLIO, T. & DAUDET, F.-A. 2001. RATP: a model for simulating the spatial distribution of radiation absorption, transpiration and photosynthesis within canopies: application to an isolated tree crown. *Plant, Cell & Environment*, 24, 395-406.
- SMIT, T. G., TAYLOR, N. J. & MIDGLEY, S. J. 2020. The seasonal regulation of gas exchange and water relations of field grown macadamia. *Scientia Horticulturae*, 267, 109346.
- SMITH, M. W., CARROLL, B. L. & CHEARY, B. S. 1992. Chilling requirement of pecan. *Journal of the American Society for Horticultural Science*, 117, 745-748.
- SPARKS, D. 1989. Drought stress induces fruit abortion in pecan. *HortScience*, 24, 78-79.

- SPARKS, D. 1992. Stress factors affecting the Georgia pecan crop in 1991 and fruit set in 1992. *Annual report (USA)*.
- SPARKS, D. 1993. Chilling and heating model for pecan budbreak. *Journal of the American Society for Horticultural Science*, 118, 29-35.
- SPARKS, D. 2001. Managing pecan nut growth. *Proc. SE Pecan Growers Assn*, 94, 129-147.
- SPARKS, D. 2002. Effect of topography, crop load, and irrigation on pecan nut volume and percentage kernel. *Annu. Rpt. N. Nut Growers Assn*, 93, 87-92.
- SPARKS, D. 2005. Adaptability of pecan as a species. *HortScience*, 40, 1175-1189.
- SPARKS, D. 2006. Drought reduces Georgia's 2006 Pecan Production.
- SPARKS, D. & HEATH, J. 1972. Pistillate flower and fruit drop of pecan as a function of time and shoot length. *HortScience*.
- SPARKS, D., REID, W., YATES, I., SMITH, M. W. & STEVENSON, T. G. 1995. Fruiting stress induces shuck decline and premature germination in pecan. *Journal of the American Society for Horticultural Science*, 120, 43-53.
- SPERRY, J. S. & HACKE, U. G. 2002. Desert shrub water relations with respect to soil characteristics and plant functional type. *Functional Ecology*, 16, 367-378.
- SPERRY, J. S., MEINZER, F. C. & MCCULLOH, K. A. 2008. Safety and efficiency conflicts in hydraulic architecture: scaling from tissues to trees. *Plant, Cell & Environment*, 31, 632-645.
- STEINBERG, S. L., MCFARLAND, M. J. & WORTHINGTON, J. W. 1990. Comparison of trunk and branch sap flow with canopy transpiration in pecan. *Journal of experimental botany*, 41, 653-659.
- STEPPE, K. 2004. *Diurnal dynamics of water flow through trees: design and validation of a mathematical flow and storage model*. Ghent University.
- STEPPE, K., DE PAUW, D. J. & LEMEURE, R. 2008. A step towards new irrigation scheduling strategies using plant-based measurements and mathematical modelling. *Irrigation Science*, 26, 505.
- SUOMALAINEN, J., OLIVEIRA, R. A., HAKALA, T., KOIVUMÄKI, N., MARKELIN, L., NÄSI, R. & HONKAVAARA, E. 2021. Direct reflectance transformation methodology for drone-based hyperspectral imaging. *Remote Sensing of Environment*, 266, 112691.
- TAYLOR, N. J., MAHOHOMA, W., VAHRMEIJER, J. T., GUSH, M. B., ALLEN, R. G. & ANNANDALE, J. G. 2015. Crop coefficient approaches based on fixed estimates of leaf resistance are not appropriate for estimating water use of citrus. *Irrigation Science*, 33, 153-166.
- TEH, C. 2006. *Introduction to mathematical modeling of crop growth: How the equations are derived and assembled into a computer model*, Brown Walker Press.

- TERASHIMA, I. & HIKOSAKA, K. 1995. Comparative ecophysiology of leaf and canopy photosynthesis. *Plant, Cell & Environment*, 18, 1111-1128.
- TESTI, L., GOLDHAMER, D., INIESTA, F. & SALINAS, M. 2008. Crop water stress index is a sensitive water stress indicator in pistachio trees. *Irrigation science*, 26, 395-405.
- TESTI, L., VILLALOBOS, F., ORGAZ, F. & FERERES, E. 2006. Water requirements of olive orchards: I simulation of daily evapotranspiration for scenario analysis. *Irrigation Science*, 24, 69-76.
- TEZZA, L., HÄUSLER, M., CONCEIÇÃO, N. & FERREIRA, M. I. 2019. Measuring and Modelling Soil Evaporation in an Irrigated Olive Orchard to Improve Water Management. *Water*, 11, 2529.
- TICHÝ, L. 2016. Field test of canopy cover estimation by hemispherical photographs taken with a smartphone. *Journal of Vegetation Science*, 27, 427-435.
- TORRES-SÁNCHEZ, J., LÓPEZ-GRANADOS, F., BORRA-SERRANO, I. & PEÑA, J. M. 2018. Assessing UAV-collected image overlap influence on computation time and digital surface model accuracy in olive orchards. *Precision Agriculture*, 19, 115-133.
- TU, Y.-H., JOHANSEN, K., PHINN, S. & ROBSON, A. 2019. Measuring canopy structure and condition using multi-spectral UAS imagery in a horticultural environment. *Remote Sensing*, 11, 269.
- TYREE, M. T., VELEZ, V. & DALLING, J. 1998. Growth dynamics of root and shoot hydraulic conductance in seedlings of five neotropical tree species: scaling to show possible adaptation to differing light regimes. *Oecologia*, 114, 293-298.
- VAN HEERDEN, P. & WALKER, S. 2016. Tool to estimate the irrigation water use of crops: revised edition-SAPWAT 4. *WRC Report*.
- VÉLEZ, S., POBLETE-ECHEVERRÍA, C., RUBIO, J. A. & BARAJAS, E. 2021. Estimation of Leaf Area Index in vineyards by analysing projected shadows using UAV imagery. *OENO One*, 55, 159-180.
- VILLALOBOS, F., ORGAZ, F., TESTI, L. & FERERES, E. 2000. Measurement and modeling of evapotranspiration of olive (*Olea europaea* L.) orchards. *European Journal of Agronomy*, 13, 155-163.
- VILLALOBOS, F., TESTI, L., HIDALGO, J., PASTOR, M. & ORGAZ, F. 2006. Modelling potential growth and yield of olive (*Olea europaea* L.) canopies. *European Journal of Agronomy*, 24, 296-303.
- VILLALOBOS, F. J., TESTI, L., ORGAZ, F., GARCÍA-TEJERA, O., LOPEZ-BERNAL, A., GONZÁLEZ-DUGO, M. V., BALLESTER-LURBE, C., CASTEL, J. R., ALARCÓN-CABAÑERO, J. J. & NICOLÁS-NICOLÁS, E. 2013. Modelling canopy conductance and transpiration of fruit trees in Mediterranean areas: a simplified approach. *Agricultural and forest meteorology*, 171, 93-103.

- WANG, D. & WANG, L. 2017. Dynamics of evapotranspiration partitioning for apple trees of different ages in a semiarid region of northwest China. *Agricultural Water Management*, 191, 1-15.
- WANG, J., MILLER, D. R., SAMMIS, T. W., GUTSCHICK, V. P., SIMMONS, L. J. & ANDALES, A. A. 2007a. Energy balance measurements and a simple model for estimating pecan water use efficiency. *Agricultural Water Management*, 91, 92-101.
- WANG, J., SAMMIS, T. W., ANDALES, A. A., SIMMONS, L. J., GUTSCHICK, V. P. & MILLER, D. R. 2007b. Crop coefficients of open-canopy pecan orchards. *Agricultural water management*, 88, 253-262.
- WANG, J., SAMMIS, T. W., ANDALES, A. A., SIMMONS, L. J., GUTSCHICK, V. P. & MILLER, D. R. 2007c. Crop coefficients of open-canopy pecan orchards. *Agricultural Water Management*, 88, 253-262.
- WANG, Y. & JARVIS, P. 1990. Description and validation of an array model—MAESTRO. *Agricultural and Forest Meteorology*, 51, 257-280.
- WARD, F. A. & MICHELSEN, A. 2002. The economic value of water in agriculture: concepts and policy applications. *Water policy*, 4, 423-446.
- WEINBERGER, J. H. Chilling requirements of peach varieties. Proceedings of the American Society for Horticultural Science, 1950. 122-28.
- WELLS, L. 2016. *Pecan Water Requirements and Irrigation Scheduling* [Online]. <http://extension.uga.edu/publications/detail.html?number=C1106&title=Pecan%20Water%20Requirements%20and%20Irrigation%20Scheduling>. [Accessed].
- WELLS, L. 2017. Response of young pecan trees to irrigation in a humid climate. *HortScience*, 52, 457-462.
- WELLS, L. 2018. Crop Maturity and Leaf Senescence. *UGA Pecan Extension*.
- WELLS, L. & CONNER, P. 2007. *Southeastern pecan growers' handbook*, Georgia, USA, Cooperative Extension Service, University of Georgia College of Agricultural & Environmental Sciences.
- WELLS, M. L. & HARRISON, K. A. 2010. Cultural management of commercial pecan orchards.
- WHITE JR, A. & EDWARDS, J. Soil profile distribution and seasonal growth of pecans roots. Proceedings of the Annual Convention Southeast Pecan Growers Association, 1978.
- WILLIAMS, L. & AYARS, J. 2005a. Grapevine water use and the crop coefficient are linear functions of the shaded area measured beneath the canopy. *Agricultural and Forest Meteorology*, 132, 201-211.
- WILLIAMS, L., PHENE, C., GRIMES, D. & TROUT, T. 2003. Water use of mature Thompson Seedless grapevines in California. *Irrigation Science*, 22, 11-18.

- WILLIAMS, L. E. & AYARS, J. E. 2005b. Grapevine water use and the crop coefficient are linear functions of the shaded area measured beneath the canopy. *Agricultural and Forest Meteorology*, 132, 201-211.
- WILLIAMS, M., BOND, B. & RYAN, M. 2001. Evaluating different soil and plant hydraulic constraints on tree function using a model and sap flow data from ponderosa pine. *Plant, Cell & Environment*, 24, 679-690.
- WILLMOTT, C. J. 1981. On the validation of models. *Physical geography*, 2, 184-194.
- WOOD, B. 1995a. Relationship of reproductive and vegetative characteristics of pecan to previous-season fruit development and postripening foliation period. *Journal of the American Society for Horticultural Science*, 120, 635-642.
- WOOD, B. W. 1995b. Relationship of reproductive and vegetative characteristics of pecan to previous-season fruit development and postripening foliation period. *Journal of the American Society for Horticultural Science*, 120, 635-642.
- WOOD, B. W. 1996. Canopy morphology of pecan cultivars. *HortScience*, 31, 139-142.
- WOOD, B. W. 2000. Pollination characteristics of pecan trees and orchards. *HortTechnology*, 10, 120-126.
- WOOD, B. W., CONNER, P. J. & WORLEY, R. E. Insight into alternate bearing of pecan. XXVI International Horticultural Congress: Key Processes in the Growth and Cropping of Deciduous Fruit and Nut Trees 636, 2002. 617-629.
- WOOD, B. W., CONNER, P. J. & WORLEY, R. E. 2003. Relationship of alternate bearing intensity in pecan to fruit and canopy characteristics. *HortScience*, 38, 361-366.
- WOOD, B. W., SMITH, M. W., WORLEY, R. E., ANDERSON, P. C., THOMPSON, T. T. & GRAUKE, L. 1997. Reproductive and vegetative characteristics of pecan cultivars. *HortScience*, 32, 1028-1033.
- WOODROOF, J. 1926. FRUIT-BUD DIFFERENTIATION AND SUBSEQUENT DEVELOPMENT OF THE FLOWERS IN THE HICORIA PECAN<sup>1</sup>. *Journal of Agricultural Research*, 33.
- WOODROOF, J. & WOODROOF, N. 1926. Fruit-bud differentiation and subsequent development of the flowers in the Hicoria Pecan. *Journal of Agricultural Research*, 33, 677-685.
- WOODROOF, J. & WOODROOF, N. 1927. The development of the pecan nut (Hicoria pecan) from flower to maturity. *Journal of Agricultural Research*, 34, 1049-1063.
- WOODROOF, J. & WOODROOF, N. C. 1934. Pecan root growth and development. *J. agric. Res*, 49, 511-530.
- WOODROOF, J. G., WOODROOF, N. C. & BAILEY, J. 1928. Unfruitfulness of the pecan.



- WÜNSCHE, J. N., LAKSO, A. N. & ROBINSON, T. L. 1995. Comparison of four methods for estimating total light interception by apple trees of varying forms. *HortScience*, 30, 272-276.
- YATES, I. & SPARKS, D. 1992. External morphological characteristics for histogenesis in pecan anthers. *Journal of the American Society for Horticultural Science*, 117, 181-189.
- YATES, I. & SPARKS, D. 1994. Anatomy differs for aborting and nonaborting pistillate flowers in pecan. *Journal of the American Society for Horticultural Science*, 119, 949-955.
- ZARATE-VALDEZ, J. L., METCALF, S., STEWART, W., USTIN, S. L. & LAMPINEN, B. 2015. Estimating light interception in tree crops with digital images of canopy shadow. *Precision agriculture*, 16, 425-440.
- ZARCO-TEJADA, P. J., GONZÁLEZ-DUGO, V., WILLIAMS, L., SUÁREZ, L., BERNI, J. A., GOLDHAMER, D. & FERERES, E. 2013. A PRI-based water stress index combining structural and chlorophyll effects: Assessment using diurnal narrow-band airborne imagery and the CWSI thermal index. *Remote sensing of environment*, 138, 38-50.
- ZERTUCHE, M. I. 1982. *The effect of various irrigation treatments and levels of nitrogen and potassium upon vivipary of pecans (Carya illinoensis (Wang), K.Koch)*. Texas A&M University.
- ZHAO, L., XIA, J., XU, C.-Y., WANG, Z., SOBKOWIAK, L. & LONG, C. 2013. Evapotranspiration estimation methods in hydrological models. *Journal of Geographical Sciences*, 23, 359-369.
- ZHAO, T., STARK, B., CHEN, Y., RAY, A. L. & DOLL, D. 2017. Challenges in water stress quantification using small unmanned aerial system (suas): Lessons from a growing season of almond. *Journal of Intelligent & Robotic Systems*, 88, 721-735.

## APPENDIX A – CAPACITY BUILDING

### DEGREE PURPOSES

**Mr Werner Rossouw (M.Sc. (Agric) Horticulture):** “Water use of mature pecan orchards under semi-arid conditions”

Mr Rossouw registered in 2018 at the University of Pretoria and started his measurements in September 2018. Mr Rossouw focussed on the measurement and modelling of pecan water use for mature orchards in the Vaalharts region. In order for this to be done accurately, an understanding of water relations of this tree nut crop was obtained. Mr Rossouw submitted his dissertation in March 2023 and in August 2023 he was awarded a distinction (cum Laude) by his examiners.

“Judicious and sensible water supply is vital for optimal fruit production, and as a result most orchard crops depend on supplemental irrigation, especially in areas in South Africa, where rainfall patterns are unpredictable and sparsely distributed. Through accurate quantification or estimation of crop water use or evapotranspiration (ET), the need for supplemental irrigation can be quantified. In addition, by partitioning ET into its components, a better understanding of the factors that govern water loss from an orchard can be obtained, which is critical for determining where water savings can be made. This study aimed to measure ET and its components (canopy transpiration ( $T_c$ ) and soil evaporation ( $E_s$ )) of a 14-year-old mixed cultivar pecan orchard in the semi-arid Northern Cape Province of South Africa. This is one of the hotter and drier pecan production regions in South Africa and was expected to differ from where most of the pecan water use research was conducted in the United States of America (U.S.A), due mainly to a longer growing season in the Northern Cape. The current data used for water management of pecan orchards are primarily based on research done in other countries or by using an empirical model to estimate water use. As different regions are characterized by its own unique climate and management practices, modelling approaches were developed that adjust pecan crop coefficient curves ( $K_c$ ) to specific climatic conditions and managements practices through weather variables, thermal time, fractional canopy cover and crop height (Allen and Pereira, 2009; Miyamoto, 1983; Samani et al., 2011; Sammis et al., 2004; Taylor et al., 2015). These empirical models may not be applicable to South African growing conditions as they contain artefacts of the regions from where they were developed, potentially leading to inaccurate ET predictions (Ibraimo, 2018). In the study by Ibraimo (2018), it was highlighted that modelling pecan ET according to a four stage  $K_c$  approach (Allen et al., 1998b) yielded accurate results on a seasonal basis, but not at a monthly time step, mainly

because pecan exhibit a six stage  $K_c$  curve. A second approach was tested by Ibraimo (2018), whereby a set of reference  $K_c$  were adjusted according for canopy size and growing degree days (GDD) to derive orchard specific  $K_c$  (Samani et al., 2011; Sammis, 2004). The ET estimates correlated well with actual measurements at the study site in Cullinan, South Africa, but it was further hypothesized that the method of adjusting  $K_c$  values for climate would not be transferable to hotter production areas where GDD exceeds 1500. Ibraimo (2018) [proposed that a better method could be to adjust  $K_c$  curve according to observed phenological stages and that the approach would work better in orchards whereby  $E_s$  is a minor component ( $\leq 20\%$ ) of ET. By measuring the two ET components separately it is possible that this approach could be applied to a wider range of orchards, which would allow for improved estimation, as well as the contribution of  $E_s$  towards total ET.

Field trials were conducted over the 2018/2019 production season on a farm in the Vaalharts irrigation scheme to measure  $T_c$  and model  $E_s$  separately, which was then used to obtain seasonal ET values. From the results it was observed that the application of the empirical equation of Sammis et al. (2004b) for adjusting  $K_c$  values according to thermal time does not hold true in Vaalharts that has a GDD accumulation exceeding 1500 (1861 for the 2018/19 season) during the growing season. The approach proposed by Ibraimo (2018), whereby the  $K_c$  curve was adjusted according to phenological stages allowed for more accurate estimations of  $K_c$ . The method was shown to successfully estimate monthly ET of mature pecan trees in this study, when the adjusted  $K_{c-ref}$  values were further adjusted for canopy size as described by Samani et al. (2011). There was a slight overestimation by the model between November 2018 and January 2019, ultimately accounting for a 6% overestimation of estimated ET as compared to ET estimated as the sum of  $T_c$  and modelled  $E_s$ . The performance of the model was determined by comparing the accuracy of monthly ET modelling against determined monthly ET. From this comparison the coefficient of determination ( $R^2$ ) value was 0.86, which is considerable to be acceptable. The Willmott index of agreement (D) value was 0.91, root mean square error (RMSE) 23.22, mean absolute error (MAE) of 13.60 and coefficient of residual mass (CRM) of 1.01. The MAE is below the threshold of 20% which indicates that the slight deviation is still within acceptable limits. Based on the positive CRM value the deviation is attributed to an overestimation of the model. This data suggests that by allowing for the adjustment of the  $K_{c-ref}$  curve according to local growing conditions and canopy cover, good estimates of monthly ET can be obtained. Through this method it was possible to determine the main contributing factors that drive water loss, through both  $T_c$  or  $E_s$ , as well as some of the factors driving the water loss.”

**Mr Mhlonishwa Zwane (M.Sc. (Agric) Horticulture):** “Relating canopy size of pecan (*Carya illinoensis* (Wagenh.) K.Koch) trees to transpiration”

Mr Zwane registered in 2018 at the University of Pretoria and started measurements in February 2018. Mr Zwane focussed on the comparison of techniques for estimating canopy size of pecan trees. He also examined the relationship between canopy size and transpiration, in order to improve our water use modelling approaches for pecan. Mr Zwane is funded by the Mastercard Foundation Scholarship programme. Mr Zwane submitted his dissertation for examination in November 2022 and was awarded his degree in April 2023.

“The South African pecan (*Carya illinoensis* (Wagenh.) K.Koch) sector is not exempt from water scarcity difficulties, so effective irrigation management techniques are required in pecan orchards to help growers maximize production with a limited water supply. One of the first steps in irrigation management is to have a means of estimating orchard water use ( $ET_c$ ), which usually involves a modelling approach. Canopy size is a key determinant of water use when soil water is not limiting and is used together with prevailing weather conditions in many water use models. The FAO-56 approach, in which  $ET_c$  is calculated as a product of reference evapotranspiration and a crop coefficient ( $K_c$ ), is the most widely used method of estimating  $ET_c$ . Previous research in several fruit trees demonstrated a linear relationship between  $K_c$  or transpiration crop coefficients ( $K_t$ ) and canopy size, indicating that  $K_c$  and/or  $K_t$  values, and ultimately  $ET_c$  or  $T$ , can be estimated from a measure of canopy size. It is therefore critical to capture canopy size accurately for future modelling exercises and irrigation scheduling in order to optimise yield, growth, and quality of pecan nuts. This study was therefore initiated to quantify the canopy size and water use of a mature pecan orchard at Innovation Africa@UP in Pretoria. Aerial photography was assessed as a means of providing accurate estimates of canopy cover in pecan orchards. Canopy cover estimates of trees in the orchard were compared using red green blue (RGB) images from above the canopy and the Canopeo app, which selects green pixels, with estimates of fractional interception of photosynthetically active radiation (FI-PAR), leaf area index and canopy cover calculated using the shaded area under the canopy. A sap flow technique was used to monitor transpiration rates in the orchards. Results suggest that canopy size can be accurately estimated with aerial photography as it is digitalized and can capture canopy size for large orchards faster. There was a good relationship between canopy cover determined using the Canopeo app and FI-PAR estimated using the ceptometer, with an  $R^2$  value of 0.85. There was a poor relationship between canopy cover determined using the Canopeo App and LAI, with the lowest  $R^2$  value of 0.56. The results support the hypothesis that the use of photographs captured from above the canopy and image analysis (Canopeo App which selects green pixels) can provide reliable estimates

of canopy size, as compared to measurements of FI-PAR by the canopy and canopy cover calculated using the shaded area. Canopy development is influenced by thermal time, thereby the results from this study demonstrated dependency between growing degree days and leaf senescence. The regression between  $K_t$  and the different canopy size measures indicated a positive linear correlation, however, this relationship was not good enough to be used in deriving orchard specific values using canopy cover in pecans. The  $R^2$  value for the relationship between canopy cover determined using the Canopeo App and  $K_t$  values was 0.66, whilst it was 0.7 for midday FI-PAR and  $K_t$ , and 0.54 for canopy cover determined as the area on the ground shaded by the tree and  $K_t$ . There was a poor correlation between  $K_t$  values and LAI measurements, as indicated by an  $R^2$  value of 0.41. Despite the fact that this study revealed a poor correlation between  $K_t$  and the canopy size measured with Canopeo App, an attempt was made to use the relationship derived in one season to derive weekly  $K_t$  values for the 2020/21 season, but a poor relationship was found between measured and estimated  $T$ , yielding an  $R^2$  value of 0.58. This underestimation was due to a peak in  $K_t$  values near the end of the season, which corresponds to the nut filling stage and a minor vegetative flush. Despite some shortcomings, the findings of this study can potentially benefit the pecan industry as the Canopeo App method provided good canopy cover estimates, when compared to widely accepted methods using very expensive equipment.”

**Mr Muhammad Pandor (MSc):** Potential of unmanned aerial vehicle-based remote sensing to detect water stress and estimate yield in pecan

Mr Pandor registered in 2020 at the University of Pretoria and started his measurements in September 2020 in Upington, Vaalharts and the University of Pretoria’s experimental farm. Mr Pandor managed the pecan water stress trial for the 2020/2021 and 2021/22 seasons. Mr Pandor submitted his dissertation in April 2023 and his degree was awarded in July 2023.

“Three potential uses for UAV remote sensing in pecan were tested in this study over two seasons, the 2020/21 and 2021/22 seasons. The use of vegetation indices (VIs) to detect water stress, the use of remotely sensed canopy temperature to detect water stress, and the use of remote sensing to estimate yield were all tested. Vegetation indices were of absolute importance in the processing of raw images by allowing the separation of pecan canopy from background soil and vegetation. The Simple Ratio Index (SRI) was found to be the best suited of all the VIs tested for this purpose, due to ease of calculation and the large range of values. Vegetation indices were found to have a weak relationship with water stress. The best relationship found between a VI and midday stem water potential ( $\psi_{\text{midday}}$ ) during the 2020/21 season was an  $R^2$  of 0.122 with normalised difference vegetation index (NDVI). Most other

VIs tested had an  $R^2$  an order of magnitude smaller. During the 2021/22 season, the Green NDVI (GNDVI) had the best relationship of all the VIs with  $\psi_{\text{midday}}$  ( $R^2 = 0.183$ ). GNDVI also had the best relationship ( $R^2 = 0.248$ ) of all the VIs tested with stomatal conductance ( $g_s$ ). However, these relationships were far too weak to conclude that VIs can be used to detect or quantify water stress. It is suspected that variability in the conditions during different remote data collection flights contributed to the poor relationships between VIs and water stress, due to variability in both intercepted and reflected radiation from the canopy. When data from a single flight was tested against  $\psi_{\text{midday}}$ , to eliminate variability in conditions, the relationship did not improve ( $R^2 < 0.1$ ), this suggests that VIs are inherently poor at detecting water stress.

The stress degree day ( $T_c - T_a$ ) and the crop water stress index (CWSI) were the thermal indices tested to allow water stress detection using remotely sensed canopy temperature ( $T_c$ ), while adjusting for the effects of air temperature ( $T_a$ ) and vapour pressure deficit (VPD). A weak relationship was found between  $T_c$  and  $\psi_{\text{midday}}$  ( $R^2 = 0.186$ ), adjusting for  $T_a$  using the stress degree day did not improve the relationship ( $R^2 = 0.16$ ). This proved the necessity of adjusting for VPD as well, through the CWSI. The baselines of the CWSI were calculated using the non-water-stressed baseline (NWSB), reference surfaces and the warmest and coldest pixels of the orchard canopy-only thermal image. Destructive measurement of the non-transpiring baseline was attempted, but the resulting data was never used due to extreme variability observed in leaf-scale measurements. The equation of the NWSB was  $(T_c - T_a) = -0.8086\text{VPD} + 0.509$  for the 2020/21 season, and  $(T_c - T_a) = -0.7312\text{VPD} - 0.3315$  for the 2021/22 season. The differences in intercept are the result of the prevailing conditions during each season, with regards to factors other than  $T_a$  and VPD, and include radiation and windspeed. The combined NWSB using data from both seasons was  $(T_c - T_a) = -0.7549\text{VPD} + 0.0482$ . Water stress data was regressed against the CWSI from each season's own NWSB and the combined NWSB. The importance of using  $T_c$  data from a full canopy only during the hours either side of midday was also shown. Data collected during the early morning and late evening, and from a porous canopy yielded a NWSB that differed greatly in both slope and intercept from one collected using the accepted methodology. these also differed greatly from any published NWSB for pecan.

All the methods of obtaining the CWSI baselines yielded a CWSI that did not correlate well with  $\psi_{\text{midday}}$  (NWSB and  $6^\circ\text{C}$  constant upper limit:  $R^2 = 0.157$ , wet reference surface and  $6^\circ\text{C}$  constant upper limit:  $R^2 = 0.0026$ , warmest and coolest pixels:  $R^2 = 0.07$ ). Unexpectedly the NWSB method performed the best, while the methods that relied on the extraction of the CWSI limits from the thermal image performed exceptionally poorly. This is evidence that the fault lies not in the method, but in some aspect of the thermal data itself, or the extraction of the reference data from the thermal data. The poor performance of the NWSB method relative to

examples in the literature may have been as a result of inaccurate  $T_c$  from the thermal camera used. More work will need to be done, with accurate equipment, before the CWSI can be used to quantify water stress in pecans.

Yield estimation was performed by finding the relationship between yield and canopy fractional cover, change in canopy size over the season and % change in canopy size over the season. Canopy fractional cover gave a relationship strong enough to estimate yield, but only in an “on”, or heavy bearing, year of an alternate bearing cycle, and performed better in a high yielding cultivar in the area (‘Western Schley’  $R^2 = 0.603$ ) than a low yielding one (‘Wichita’  $R^2 = 0.497$ ). Both of these relationships were observed at the beginning of March of the season when each cultivar had an “on” year. A good relationship between yield and canopy fractional cover was also observed early in the second measurement season (November) when ‘Wichita’ trees were in an “on” year ( $R^2 = 0.535$ ), no data was available for the first half of the first measurement season. Both the absolute change in fractional canopy cover and the % change in canopy cover performed poorly ( $R^2 < 0.3$ ) relative to fractional canopy cover on its own for both cultivars during the second season, when data was available for both the start and the end of the season, enabling the calculation of change in canopy cover.

Reasonable relationships between VIs and yield were primarily observed in the last two months of the season (March and April) during the 2021/22 season, while only data from these months was available for the 2020/21 season. The VIs that performed best were RDVI, MCARI and OSAVI. All three VIs correlated best ( $0.35 < R^2 < 0.5$ ) with the yield of the cultivar that was “on” during each season. It is likely that these VIs are sensitive to differences in some aspect of canopy structure that is related to yield. Specific VIs seem to be best able to estimate yield for specific crop conditions at specific times of the year. Large datasets will be required to determine the exact relationships present and the best time to use them, before VIs can be used to estimate yield in pecans”

**Ms Ncamsile Shongwe (PhD):** “Modelling radiation interception and water use of mature Pecan orchards”

Ms Shongwe began her PhD in January 2021 and will focus on the modelling of radiation interception of mature pecan orchards which can be used to derive orchard specific  $K_c$  values and for modelling soil evaporation.

“The Pecan industry is amongst the economically important industries in South Africa, with production is hugely depended on irrigation. With the current water scarcity in South Africa,

pecan farmers, as with most commercial fruit and nut farmers, are under increasing pressure to ensure sustainability under limited water supply. Therefore, it is important that good water management strategies are implemented in both emerging and established commercial pecan orchards to sustain production and ensure further expansion of the industry within the existing water allocation. Studies have shown that accurate and reliable information and understanding of the dynamics of pecan water use (transpiration and soil evaporation) is important, as substantial water savings can be made by reducing the non-beneficial consumptive water use, i.e. evaporation. Reliable methods to estimate the water use of pecan orchards are expensive, laborious, and often involve complexity with field data collection, hence estimation approaches are often used. Several estimation approaches are available; however, they are faced with challenges: (1) They can be very technical; therefore, their practical implementation can often be limited to academic research, rather than providing a solution to individual users (i.e. farmers). (2) It is not easy to find the balance between accuracy and practicality, since growers are more concerned that the possible reduced accuracy of such approaches should outweigh the benefits of using the expensive, complex, and laborious measurement techniques.

Previous studies on pecan water use in South Africa have indicated that a more realistic estimation approach should integrate all the factors that influence the major variation of water use within pecan orchards. Amongst other factors, canopy size has a major influence on pecan water use. The size of a tree canopy does not only indicate the capability of the canopy to intercept radiation and ultimately the amount of transpiration and soil evaporation that occurs at tree and/or orchard level, but also the differences in orchard management strategies, such as pruning. Therefore, an accurate quantification of the canopy size at any time of the growing season may provide good and convenient estimates of water use. In the current study, a simple radiation interception model of Oyarzun et al., 2007 will be parametrised, validated and used as a potential generic model to estimate canopy size, transpiration, evaporation and ultimately total water use of pecan orchards of different cultivars ('Wichita' and 'Choctaw') grown in two different climatic regions of South Africa. The study orchards are characterised with different tree spacing, canopy cover and zero cover crop between tree rows. The model has been previously used in different fruit and nut crops as a measure of canopy size and/or incorporated in water use models, however, in all the studies, the authors have indicated that acquisition of the canopy porosity using practical and easy methods hugely limits the model's general application in water use studies. The current study presents the use of drone-based images and smart phone applications (VitiCanopy and GLAMA) to estimate the canopy input parameters of the model. This approach does not only put effective tools in the hands of the growers using smartphones and drones, but it also promotes the use of one of the important universal technology in the agricultural sector."



**Mr Robert Godfrey (MSc):** “Environmental and Physiological Control of Transpiration by Pecan Trees”

Mr Godfrey registered for his MSc degree in February 2021 and has focussed on the environmental and physiological control of transpiration in pecan trees to aid in our modelling exercises. He started measurements in February 2021 in the orchard on the Experimental Farm in Pretoria and in the orchards in the Northern Cape. He will make use of the different weather conditions in the three orchards to try and establish the impact of the environment on transpiration of pecan trees. In addition, on the Experimental Farm he will make use of the stress treatments to determine the impact of water stress on tree physiology and transpiration rates. Mr Godfrey finished data collection in December 2022 and is busy compiling his dissertation.

“Pecans are often grown in regions with a high vapor pressure deficit (VPD) which leads to the question if pecans have a physiological mechanism for the control of transpiration and if so what the cause of this physiological control is. As a result, it is important to determine if pecans follow a predominantly isohydric or anisohydric water use strategy. Due to the uncertainty around the physiological control of transpiration, it is also unknown if the crop load has an effect on the physiological control of transpiration and whether the plants incur more stress in order to increase photosynthesis during periods of high assimilate demand, e.g. oil accumulation in the nuts. The arid and semi-arid areas where pecans are cultivated commonly have a high VPD as well as experiencing high temperatures. This can be problematic to the photosynthetic ability of many crops and it is not known what effect high temperatures have on the photosynthetic capacity of pecan trees. This information is also important for determining an upper limit for thermal time accumulation for pecans”

**Ms Amogelang Molamu – (M.Sc. Plant Science)** The use of remote sensing tools to determine water stress in pecan orchards.

Ms Molamu began her studies in January 2023 and will focus on continuing the research started by Mr Pandor.

“There is a pressing need for an effective and reliable water status detection method, specifically designed for pecan trees in South Africa, that can offer timely and accurate information on the water requirements of pecan trees. By monitoring CWSI, farmers can determine the optimal timing of water application to their crops. Therefore, our focus is on the improvement of effective irrigation water management. Research on how to advise farmers on

how to do so in pecan orchards is limited, and the available literature cannot be reproduced because determining methods are site-dependent (Testi et al., 2008), crop-specific, and may even be cultivar-specific (Gardner et al., 1992). Addressing this problem may enable farmers to optimise irrigation practices, conserve water resources, and improve pecan tree growth, and nut yield. In South Africa, currently, the production and expansion of pecan farming is growing exponentially, and there is a great need for monitoring water status and estimating water stress in orchards to 1) realise water-stressed areas before they become problematic, and 2) improve irrigation management of pecan trees in the major production regions, which are located in semi-arid regions in South Africa. UAV bound multispectral and thermal sensors will help us achieve this effectively, because if stress can be monitored on a large scale, over time, we can identify areas of stress individually or separately, and irrigate them accordingly, thus allowing for significant amounts of water to be saved. This may also equip farmers with essential knowledge they may need to adapt to limiting water conditions.”

## **NON-DEGREE PURPOSES**

### **ORGANISATION**

Capacity, in terms of both measurement techniques and modelling, was built at the various institutions, as a result of collaboration between the different organisations, which all have a unique set of skills. These skills included estimation of transpiration through sap flow techniques, estimation of total evapotranspiration using the eddy covariance technique, ecophysiology measurements relating to water relations of the crops and horticultural knowledge of the phenological cycle of the crops. In addition, training of technical personnel within the organisations will be performed. Within this project new skills pertaining to remote sensing were developed within the group at the University of Pretoria.

### **COMMUNITY**

The information obtained in this study has been disseminated to Technical Advisors in the pecan industry in order to ensure that producers can take advantage of the improved understanding of water use of pecan orchards. It is therefore possible to improve the capacity of the broader pecan producing community in terms of irrigation management and scheduling. Continued opportunities together with SAPPA will be explored after the end of the project, together with the dissemination of the Illustrated guide on pecan water use to growers.

## **APPENDIX B – KNOWLEDGE DISSEMINATION AND TECHNOLOGY TRANSFER**

### **Popular articles**

Articles were published in the SA Pecan as follows:

- 2018 Volume 80 pages 27-29 “Quantifying water use of mature pecan orchards in selected irrigation areas of the Northern Cape – research report”
- 2019 Volume 84 pages 14-16 “Quantifying water use of mature pecan orchards in selected irrigation areas of the Northern Cape – research report”
- 2020 Volume 87 pages 12-16 “Quantifying Water Use of Mature Pecan Orchards in selected irrigation areas of the Northern Cape – research report”
- 2021 Volume 90 pages 22-27 “Quantifying water use of mature pecan orchards in selected irrigation areas of the Northern Cape”

### **Presentations at local and international conferences**

The project was introduced to SAPPA members at the SAPPA AGM in Cradock from 9-10 November 2018 by the project leader.

The importance of water use estimates for pecan orchards was also explained to growers at an event organised by GWK in the Douglas region (Die Groentoeer) on 12 March 2019.

The Department of Plant and Soil Sciences hosted a postgrad symposium on 19 September 2019. Three MSc students presented results from the pecan water use project at the symposium. This was a valuable experience for the students and showcased the project to the wider department. It was also a scientific forum, as opposed to the presentations for growers.

- Werner Rossouw “Measuring and modelling water use of mature pecan orchards according to seasonal growth stages”
- Seluleko Kunene “The impact of water stress at key phenological stages on yield and quality of pecan trees (*Carya illinoensis* Wangenh. K.Koch)”
- Mhlonishwa Zwane “Quantifying canopy size and water use of pecan trees”

The SAPPA AGM was held in Modimolle, at the Weesgerus Holiday resort, from 15-16 November 2019. Dr NJ Taylor presented a talk entitled “Quantifying water use of mature pecan orchards in selected irrigation regions of the Northern Cape”. It was an update of project progress.

In February 2020 an update on project progress was provided to growers in Jacobsdal (19 February – approximately 20-30 growers) and Jan Kempdorp (20 February – approximately 40 growers). This was facilitated by SAPPA through Hardus du Toit. A very similar presentation to the one delivered at the AGM was given to the growers. The aim was to show growers that valuable research is being conducted and that in future the research will be applicable to their particular situation.

In May 2021 results from the study were presented at a Pecan Water Management course in Jan Kempdorp from 5-6 May. The presentation was entitled “Water use of Mature Pecan Orchards” and provided growers with feedback from the project in terms of average transpiration and evapotranspiration volumes from research orchards.

In November 2021 results from the project were shared at SAPPA AGM held in Upington from 5-6 November 2021. An update on progress with measurements was provided to the growers and good feedback was received.

In October 2022 results from the project were shared at the SAPPA AGM held in Hartswater from 21-22 October 2022. An update on progress with measurements was provided to the growers and good feedback was received.

Two papers and a poster were presented at the ISHS Xth International Symposium on the Irrigation of Horticultural crops In Stellenbosch from 29 January to 2 February 2023. The first paper title was “Are pecan orchards the best use of irrigation water in semi-arid regions of the Northern Cape province of South Africa?” and was presented by Nicky Taylor. The second paper title was “Estimating solar radiation interception and canopy size in pecan orchards using aerial and ground-based images for water use modelling” and was presented by Ncamsile Shongwe. Mr Seluleko Kunene presented results from his MSc and his poster was entitled “The impact of water stress at key phenological stages on yield and quality of pecans (*Carya illinoensis* Wangenh. K.Koch).

In October 2023 results from the project were shared at the SAPPA AGM held in Rayton from 20-21 October 2023. An update on progress with measurements was provided to the growers and good feedback was received. Nicky Taylor, Ncamsile Shongwe and Amogelang Molamu presented the results.

## **APPENDIX C – DATA STORAGE**

All data from the study is stored on Google drive as facilitated by the University of Pretoria and on external hard drives at the University of Pretoria, Hatfield, Pretoria.